Analysis of a Simply-Supported Thick Composite Beam with Stiffened Lateral Ends

Thesis

M. Sc. in Mechanical Engineering

Submitted by

Abdullah Al Mamun

Roll No. 1009102023F

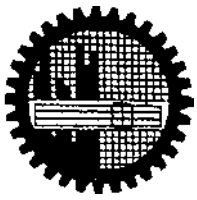

Department of Mechanical Engineering
Bangladesh University of Engineering and Technology (BUET)
Dhaka – 1000, Bangladesh

May 2014

The thesis entitled "**Analysis of a Simply-Supported Thick Composite Beam with Stiffened Lateral Ends**", submitted by **Abdullah Al Mamun**, Roll no: 1009102023F, session October 2009 has been accepted as satisfactory in partial fulfillment of the requirement for the degree of MASTER OF SCIENCE IN MECHANICAL ENGINEERING on May 28, 2014.

BOARD OF EXAMINERS

Dr. Shaikh Reaz Ahmed Professor Department of Mechanical Engineering, BUET Dhaka, Bangladesh	Chairman
Dr. Muhammed Mahbubur Razzaque Professor Department of Mechanical Engineering, BUET Dhaka, Bangladesh	Member
Dr. Md. Abdus Salam Akanda Professor Department of Mechanical Engineering, BUET Dhaka, Bangladesh	Member
Dr. Md. Zahurul Haq Professor & Head Department of Mechanical Engineering, BUET Dhaka, Bangladesh	Member (Ex-officio)
Dr. Khan Mahmud Amanat Professor Department of Civil Engineering, BUET Dhaka, Bangladesh	Member (External)

Acknowledgement

The author would like to express his gratitude to The Almighty Allah's continual mercy and help without which no work would have been possible to accomplish the goal. The author is pleased to acknowledge with gratefulness to his supervisor Dr. Shaikh Reaz Ahmed, Professor, Department of Mechanical Engineering, Bangladesh University of Engineering and Technology, for his guidance, constant support, intuitive suggestions and relentless encouragement, which he found very benevolent for the outcome of the research. The author would like to take the opportunity to thank the members of the examination committee, for their comments and constructive criticism. The author gratefully acknowledges the computing support provided by the Department of Mechanical Engineering.

Candidate’s Declaration

It is hereby declared that no portion of the work contained in this thesis has been submitted elsewhere for any degree or diploma.

Author
Abdullah Al Mamun

Dedicated To

My Father and Mother

Table of Contents

List of Tables

List of Figures

List of Symbols

Notation	Definition
x,y	Rectangular co-ordinates
$\sigma_{xx,}\ \sigma_{yy}$	Normal stress components in x- and y-directions respectively
σ_{xy}	Shear stress component in the xy plane
$u_x\ ,u_y$	Displacement components in x- and y-directions respectively
μ	Poisson's ratio
E	Modulus of elasticity
G	Modulus of rigidity
ψ	Displacement Potential Function
ϕ	Airy's Stress Function
L	Length of the beam
D	Depth or height of the beam
E_1,E_2	Elastic modulus of the material in direction 1 & 2
μ_{12}	Major Poisson's ratio
μ_{21}	Minor Poisson's ratio
G_{12}	In plane shear modulus in the plane 1-2 plane
θ	Angle of fiber
σ_o	Maximum intensity of applied load

Abstract

This thesis deals with the analysis of stress and displacement fields of a mixed boundary-value problem of fiber-reinforced composite materials. More specifically, the elastic field of a thick stiffened simply-supported composite beam is investigated using an efficient analytical scheme based on displacement-potential field formulation.

In the present displacement-potential approach, the elastic problem of composite materials is formulated in terms of a single potential function of space variables, which is defined in terms of the displacement components of plane elasticity. Accordingly, all the parameters associated with the solution, namely stress, strain and displacements are expressed in terms of the same potential function, which eventually reduces the plane problem to the determination of the potential function from a single partial differential equation of equilibrium. The solution of the equilibrium equation is obtained in the form of infinite series, the coefficients of which are determined by appropriately satisfying the boundary conditions at different edges of the beam.

Analytical expressions of the elastic field of the simply-supported beam are derived in terms of the potential function using Fourier series. Solutions are obtained for two different types of stiffeners (axial and lateral stiffeners) at the opposing lateral ends of the beam. Both the isotropic as well as fiber-reinforced composite materials are considered for the present analysis. Some of the practical issues of interest, like the effects of beam aspect ratio and stiffeners are discussed in relation to the composite beam. The analytical scheme is then extended to determine the fiber-orientation dependent stresses in stiffened simply-supported beam. Two limiting cases of fiber orientation (θ = 0^o and 90^o) are considered for a wide range of beam aspect ratio.

In an attempt to verify the reliability and accuracy of the analytical scheme developed, the present potential function solutions are compared with the corresponding solutions obtained by classical beam theory and verified with two standard computational methods of numerical techniques. The four solutions are found to be in excellent agreement with each other for all the cases of stiffeners and fiber orientations considered, which eventually establishes the soundness and appropriateness of the analytical scheme developed.

CHAPTER 1

INTRODUCTION

1.1 Preamble

The use of stiffeners, especially in the construction of marine and aerospace structures is quite extensive. Stiffeners are usually placed along the boundaries of structural components mainly to increase the stiffness of the components, which, in turn, reduces the level of deformation as well as overall weight of the structure. As a result, the subject of analyzing the mechanical behaviour of stiffened structures has received widespread attention. In particular, reliable and accurate analysis of stresses in these structures is of great practical importance as far as the modern design philosophy is concerned.

In the solution of stiffened structures, the physical conditions of stiffeners are usually modelled in terms of a mixed mode of boundary conditions, namely known values of loading (traction) and restraints for the stiffened sections. In general, stiffeners are of directional type, i.e., stiffness of a surface at which they are employed is enhanced in a particular direction, namely normal and tangential directions. As far as the opposing lateral ends of a beam are concerned, stiffeners may primarily be of two types, namely, axial stiffeners and lateral stiffeners. Axial stiffeners are those which prevent axial deflection caused by bending of the beam, but the stiffened section is free to assume any deflection along the lateral direction. On the other hand, lateral stiffeners prevent deflection along the lateral direction, but the section is free to assume any axial deflection.

Now-a-days, the theory of elasticity has found considerable application in the solution of engineering problems. There are many cases where elementary theory is inadequate to give accurate results. The elementary theory is insufficient to give the information regarding local stresses near the load and near the supports/stiffeners of beams as well as in regions of sharp

variation of structure. This led to the emergence of a special trend of physics, i.e., the theory of elasticity to apply to elastic solids. The equations of theory of elasticity are a system of partial differential equations. In cases where a rigorous solution cannot be readily obtained, approximate method, such as, numerical methods have been developed. Numerical methods give approximate results instead of exact solution that can be obtained from analytical method. That is, analytical method is always preferable because results obtained by approximate method are not always reliable and acceptable for some applications where accuracy is important. These are sometimes expensive. Sometimes analytical method is not independently adequate to solve a practical problem and it needs some help from numerical methods.

Due to outstanding advantage of composite materials, they are being increasingly used structural elements in various problems. The response of stiffened composite beams to mechanical loadings largely depends on the fibre orientation. Therefore, the effect of fibre orientation on the distribution of stresses and displacements are required to be analyzed to ensure proper and safe application.

1.2 Literature Review

The theory of elasticity deals mainly with deformation parameters and stress parameters for the solution of two dimensional problems since most of the three-dimensional problems may be resolved to a two dimensional one. If it remains beyond the extent of analytical studies anyway, the problem has to be handled experimentally as a particular case.

Although the theories of elasticity had been established long before, the solutions of practical problems started mainly after the introduction of a stress function by George Biddell Airy [1]. The Airy's stress function is governed by a fourth order partial deferential equation and stress components are related to it through its various second order derivatives. The stress function solutions were initially sought taking polynomial expressions of various degrees and suitably adjusting their coefficients. By this way, a number of practically important problems of long rectangular strips could be solved [2]. But the success of this approach was very limited. Using these polynomial expressions, an elementary derivation of the effect of the shearing force on

the curvature of the deflection curve of beams were made. The problem of stresses in masonry dams is of great practical interest and has been attempted for solution using polynomial expressions for the stress functions [1-2]. But the solutions obtained do not satisfy the conditions at the bottom of the dam where it is connected with the foundation.

Thereafter the use of trigonometric series is considered more fruitful in producing results instead of polynomial expressions. The first application of trigonometric series in the solution of elastic problems using stress function method was given by Ribiere [1]. Further progress in the application of these solutions was made by Filon [1].

A number of works are found with the stress function in this regard [3-6]. Even tough the stress analysis problems are bearing enumerable shortcomings to be addressed yet. The stumbling block of obtaining exact solution using stress function is the inability of managing the physical conditions imposed on them, i.e., management of boundary conditions of practical problems. Boundary restraints specified in terms of the displacement components cannot be satisfactorily imposed on the stress function. Since most of the practical problems in elasticity are of mixed boundary conditions, the approach fails to provide any explicit understanding of the state of stresses at the critical regions of supports and loadings. Moreover, the famous Saint Venant's principle is still applied and its merit is evaluated in solving problems of solid mechanics in which full boundary effects could not be taken into account satisfactorily in the process of solution [7-9]. For complex shapes of boundary, the difficulties of obtaining analytical solutions become formidable. These difficulties were partially avoided by renovating to experimental methods, such as extensometers, strain gauges or photoelastic methods. Using Photoelasticity, Hetengi investigated the stresses in the threads of a bolt and nut fastening. Even now, photoelastic studies are being carried out for classical problems like uniformly loaded beams on two supports mainly because the boundary effects could not be taken into account fully in the analytical method of solutions.

The drawback of Airy's stress function and the difficulties of experimental works led to works for finding ways to solve the engineering problems where boundary conditions are prescribed in terms of displacements. Thus the displacement formulation was introduced for those

problems where boundary restraints exist [10]. This process involves finding of two displacement functions simultaneously from the two second-order elliptic partial differential equations of equilibrium, which is extremely difficult and the problem becomes more serious when the boundary conditions are mixed. The difficulties involved in trying to solve practical stress problems using the existing models have been pointed out by Durelli and Ranganayakamma [11]. The complications associated with the solution of beams, especially short/deep beams, were also brought to light by Rehfield and Murthy [12], Murty [13], Suzuki [14], and Hardy [15].

Since neither the stress function nor the displacement formulation is suitable for solving problems of mixed-boundary conditions, a new mathematical model called displacement potential formulation is used to solve the elastic problems [16-20]. The current modelling approach based on displacement potential formulation reduces the two-dimensional problem to the solution of a single differential equation of equilibrium and also enables the mixed mode of the boundary conditions to be managed appropriately. It is worth mentioning that a number of researchers worked on the advancement of displacement potential approach to handle the structural analysis with different loading and supporting conditions. Ahmed et. al. have developed numerical solution of both ends fixed deep beams based on displacement potential formulation [16]. An investigation of stresses at the fixed end of deep cantilever beams has been carried out by Ahmed et. al.[17]. Akanda et. al. have carried out stress analysis of gear teeth using displacement potential function and finite differences [19]. The potential of the formulation has also been investigated by Ahmed et. al. [18] to design optimum shapes of tire-treads for avoiding lateral slippage between tires and roads. Recently, Ahmed et. al. [18] have proposed a general mathematical formulation for the solution of mixed-boundary-value problems of anisotropic materials. Debnath et. al. have carried out analytical solution of a deep stiffened cantilever beam of orthotropic composite material [21], and stiffened composite struts subjected to eccentric loading [22]. Further, Rahman et. al. have analyzed the stress analysis of cracked stiffened panels under flexural and axial loading [23]

Exact analytical solutions to the elastic field of structural components of composite materials, especially with stiffened beam are hardly available in the literature. This is mainly because of

the lack of suitable mathematical formulations that can model of the problem appropriately, and thus the solutions of such problems are usually investigated through numerical methods [24-27]. On the other hand, the investigation of the effect of fibre orientation on the mechanical behaviour of structural components has now become a key subject in the field of fibre reinforced composite structures, and the corresponding reporting in the literature is quite extensive, some of which are cited as examples in Reference [28-31]. For practical cases, these investigations are also usually found to carry out by numerical approaches, as the exact analytical methods are limited to very ideal cases. Recently, some experimental investigations of the same are also being carried out mainly to validate the numerical approaches [32]. However, a reliable and accurate investigation of the effect of fibre orientation on the critical stresses, especially in a stiffened simply supported beam of fibre-reinforced composites has not been yet conducted.

1.3 Stiffened Structures

Stiffeners are secondary plates or sections which are attached to beam boundaries or webs or flanges to stiffen them against deformations. There are two principal types of stiffener:

- Longitudinal web stiffeners, which are aligned in the span direction
- Transverse stiffeners, which are aligned normal to the span direction.

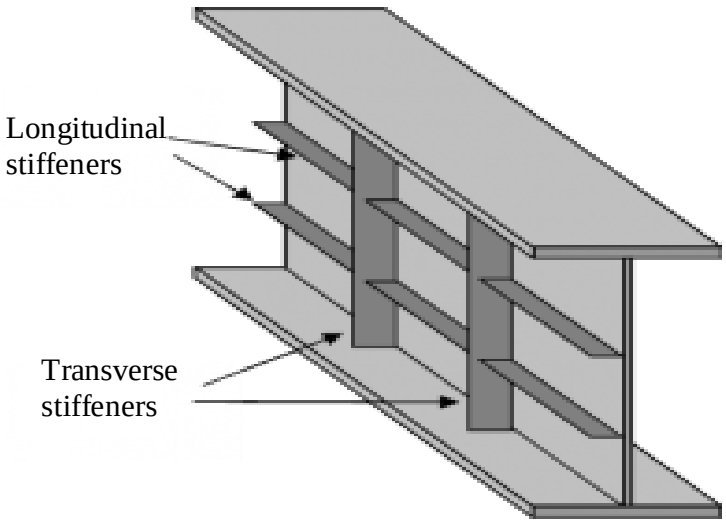

Fig. 1.1: Stiffeners on box griders

Almost all main bridge beams have stiffeners. However, most only have transverse web stiffeners, i.e., vertical stiffeners attached to the web. Thick beams sometimes have longitudinal web stiffeners. Stiffeners are extensively used in marine, aerodynamic and automobile structures. Some of the applications of stiffened structures are shown in Fig. 1.2:

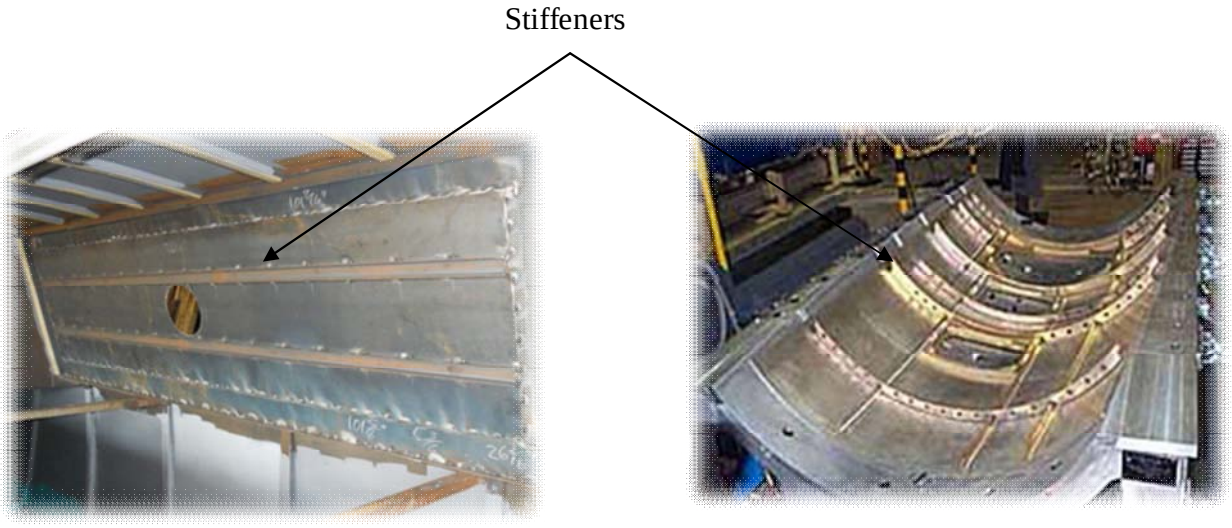

(a) Ship body (b) Air-craft body

Fig. 1.2: Stiffeners used in small ship and air-craft body

In the present research, the proposed stiffening conditions which are used in beam boundaries:

(a) Axial stiffening condition: Prevent axial deflection of the lateral ends, which are however free to assume any deflection along the lateral direction of the beam.

(b) Lateral stiffening condition: Prevent deflection along the lateral directions of the ends, but they are free to assume any deflection along the axial direction of the beam.

1.4 Fiber-reinforced composite

Composite materials are materials made from two or more constituent materials with significantly different physical or chemical properties, that when combined, produce a material with characteristics different from the individual components. The individual components remain separate and distinct within the finished structure. The new material may be preferred for many reasons: common examples include materials which are stronger, lighter or less expensive when compared to traditional materials.

Composite materials are generally used for buildings, bridges and structures such as boat hulls, swimming pool panels, race car bodies, shower stalls, bathtubs, storage tanks, imitation granite and cultured marble sinks and counter tops. The most advanced examples perform routinely on spacecraft in demanding environments.

Typical engineered composite materials include:

- Composite building materials such as cements, concrete
- Reinforced plastics such as fiber-reinforced polymer
- Metal Composites
- Ceramic Composites (composite ceramic and metal matrices)

Among these composite materials, fiber-reinforced composites are made up of individual materials referred to as constituent materials. There are two main categories of constituent materials: matrix and reinforcement. At least one portion of each type is required. The matrix material surrounds and supports the reinforcement materials by maintaining their relative positions. The reinforcements impart their special mechanical and physical properties to enhance the matrix properties. A synergism produces material properties unavailable from the individual constituent materials, while the wide variety of matrix and strengthening materials allows the designer of the product or structure to choose an optimum combination.

Fiber-reinforced composite materials have gained popularity (despite their generally high cost)

in high-performance products that need to be lightweight, yet strong enough to take harsh loading conditions such as aerospace components (tails, wings, fuselages, propellers), boat and scull hulls, bicycle frames, swimming pool panels and racing car bodies. Other uses include fishing rods, storage tanks, swimming pool panels, and baseball bats.

1.5 Analysis of Thick Beams

A beam may be considered as one of the most commonly used structural elements in engineering applications. A beam is said to be a thick beam when the thickness (depth) is comparable to its span. In the field of civil engineering application, the beams are known as deep beams while the same in the area of mechanical engineering is termed as thick or short beam. In this research, in an attempt to analyze the thick beam, the aspect ratio, that is, span to depth ratio (*L/D*) is considered from 1 to 10.

Design of thick beams based on classical Euler bending theory can be seriously erroneous, since the simple theory of flexure takes no account of the effect of normal pressures on the top and bottom edges of the beam caused by the loads and reactions [4]. The effect of normal pressures on the stress distribution in thick beams is such that the distribution of bending stresses on vertical sections is not linear and the distribution of shear stresses is not parabolic. Consequently, a plane transverse section does not remain plane after bending, and the neutral axis does not lie at the mid-depth, which eventually causes the basis of classical theory to be violated. In an attempt to make up the limitation, different theories as well as methods of solution have been reported in the literature [3-5, 13-14].

The use of standard structures, like beams, columns, etc. with stiffeners on part or full of their bounding surfaces is receiving increased importance in order to satisfy precise and strict design criteria in many of the engineering applications. Stiffened boundaries usually help in reducing the level of deformation in the structural elements, which eventually resist the change of the original shape of the bounding surfaces under loading. But structures with stiffened boundaries usually remain away from the scope of analytical solutions, because the physical conditions of

stiffened boundaries need to be mathematically modelled in terms of a mixed mode of boundary conditions.

Again the use of fibre-reinforced composites is found to increase extensively in almost all the areas of structural applications, mainly because of their specific characteristics of light-weight and high-strength. As a result, the analysis of composite structures has now become a key subject in the field of solid mechanics. These analyses are mainly handled by approximate numerical techniques [33-34], as, in most cases, the available mathematical models are found to be inadequate to provide exact analytical solutions to them.

Since the exact analytical solution of mixed-boundary-value elastic problems, especially with fibre reinforced composite materials is beyond the scope of existing mathematical models of elasticity, the use of a new mathematical formulation will be investigated to analyze the elastic behaviour of a stiffened thick beam of fibre reinforced composites under different loading and support arrangements. It would be worth mentioning that, as far as the reporting in the literature is concerned, the author has not come across any reliable study of the present problem, either theoretical or experimental. Therefore, the analytical solution for a stiffened thick beam of orthotropic as well as isotropic composite materials has been chosen as the subject of the present thesis.

1.6 Objectives

The present study is an attempt to extend the capability of the displacement potential formulation in order to address the structural analysis of orthotropic composites materials having mixed boundary conditions. The main objectives of the present research work are summarized as follows:

a. Development of a suitable mathematical scheme for the analysis of thick, simply-supported composite beams with stiffened lateral ends

b. Determination of the elastic field of a stiffened isotropic beam using the analytical scheme developed
c. Investigation the effect of stiffeners at the lateral ends of a stiffened thick simply-supported fibre reinforced composite beam.
d. Investigation of the effect of fibre orientation on the state of deformation as well as stresses in the stiffened composite beam
e. Establishment of credibility of the analytical scheme for the analysis of stiffened beams by comparing the results with those of standard computational technique.

Results of the present analysis are expected to provide a reliable design guide for thick composite beams of the present kind, which will be of significant help for their improved and economic design. More importantly, the present analytical solution will remain as a standard guide for checking reliability and accuracy of approximate solutions of the problem. The study would be particularly important for machine parts under bending, supported on two supports which are placed/inserted in a position that allows no axial deformation of the structural member.

1.7 Study Procedure

In the present study, the elastic behaviour of stiffened thick beams of composite materials are investigated through an analytical procedure based on displacement potential formulation, which is suitable for mixed-boundary-value elastic problems of composite materials. In the displacement potential boundary modelling approach, the plane elastic problem is formulated in terms of a single function of space variables, called as displacement potential function which is defined in terms of displacement components of plane elasticity, which has to satisfy a single fourth-order partial differential equation of equilibrium. The relevant displacement and stress components are derived into infinite series using Fourier integral with coincided boundary conditions along with the physical boundary conditions. The beam is assumed to be simply supported on two supports at the bottom, and the two opposing lateral edges are stiffened for which any change in the axial displacement for axial stiffener and any change in the lateral

displacement for lateral stiffener are restrained. First isotropic material is taken into consideration for the beam material and the respective material chosen is steel. And finally fiber-reinforced orthotropic composite material is considered by taking glass/epoxy material into consideration. The fibres of the orthotropic composite materials are assumed to be situated along the beam length (fiber orientation, 0^0) and along the beam depth (fiber orientation, 90^0). The numerical solution of the composite beam is also obtained by using finite element method and finite difference solution with the help of standard commercial softwares which are used to validate the accuracy of the present potential function solutions.

1.6 Significance of Present Study

The present study has the significant importance in regard to academic interest, design reference and manufacturing engineering. The study presents the application of a new concept, i.e., displacement potential approach for the analysis of stress and displacement in structures for isotropic as well as orthotropic materials under mixed mode of boundary conditions. It is expected to provide some additional aspects to the theory of elasticity, which in turn may encourage academicians and researchers to explore the concept further and eliminate the lack of suitable method for dealing with mixed boundary value problems of complex geometries. In this study a number of problems of stiffened structures are solved by using the present analytical methods and results are presented in the form of graphs. The results may be used as a database and may be helpful to the designers working in the industries of aerospace, shipbuilding and automobile, where numerous composite structures are used. The present study of stiffened beam analysis would be very pertinent for those machine parts where expansion in one dimension is restricted.

CHAPTER 2

THEORETICAL OUTLINE AND FORMULATION

2.1 Preamble

The theory of elasticity sets forth the solution of problem in determining internal forces in a solid elastic body. The internal forces represent interaction between molecules; they insure the external forces applied to body. Under the action of external forces the body deforms, the mutual position of molecules changes and so do the distance between them. The action of external forces that produce deformation gives rise to additional internal forces causing the stress of the body.

Thus structural analysis necessitates the requirements to investigate the state of stresses, strains and displacements at any point due to given body forces and given conditions at the boundary of the body. Most of the cases the requirement is to find the stress distribution in an elastic body. In some cases, it is also required to find the strain distribution of the body. The state of stress, strains and displacement are termed as the elastic field. A complete description of the elastic fields requires specification of forces acting on the elementary body and its surface orientation.

2.2 Equilibrium and Compatibility Conditions

Let us take an infinitesimal cubic element from an elastic body with sides parallel to the coordinate axes. To ensure the equilibrium of the element, six forces will act on the six different faces of the element. The forces acting on each face may be resolved into two types i.e. one perpendicular to the plane of the face and the other parallel to the face. The stress component acting perpendicular to the face is the normal stress and the two stress components acting parallel of the face are the shearing stress as illustrated in Fig. 2.1.

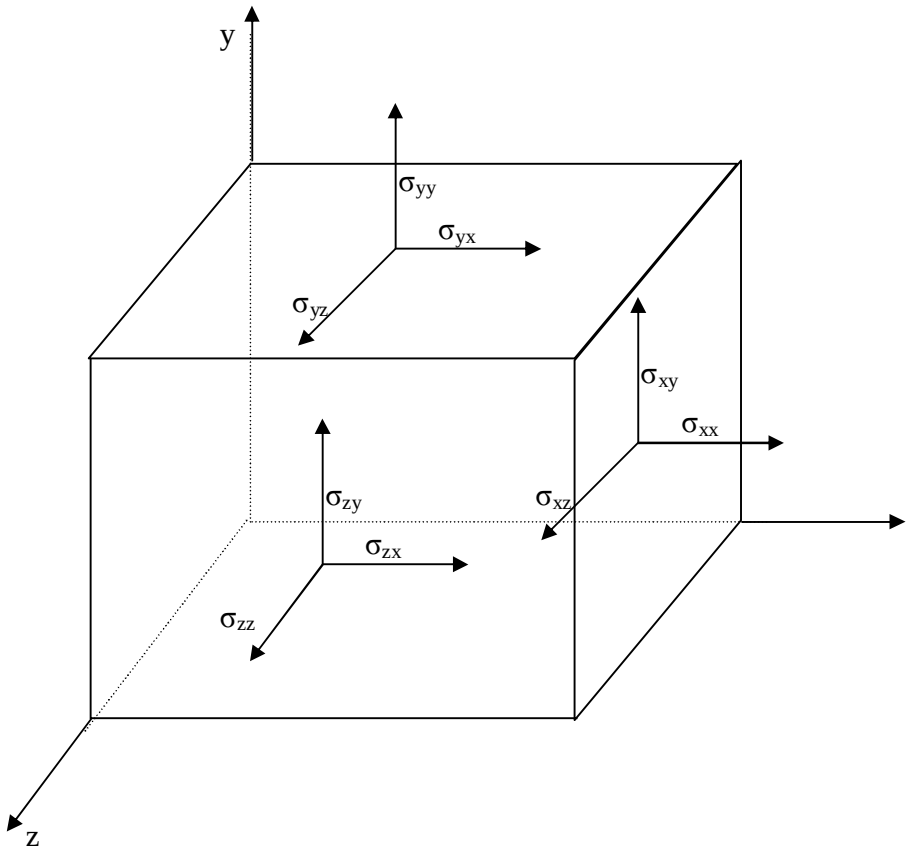

Fig. 2.1 Elementary cubic body

In order to provide complete information of an elastic field, it is necessary to determine nine stress components ($\sigma_{xx}, \sigma_{yy}, \sigma_{zz}, \sigma_{xy}, \sigma_{yx}, \sigma_{yz}, \sigma_{zy}, \sigma_{xz}$ and σ_{zx}) and six strain components ($\varepsilon_{xx}, \varepsilon_{yy}, \varepsilon_{zz}, \gamma_{xr}, \gamma_{yz}$ and γ_{zx}). Instead of strain components, sometimes the displacement components (u_x, u_y and u_z) are determined. It is worthy to mention that the components of strain and displacement can be determined from each other and each set provide the similar information. Therefore, either the components of strain or displacement are sufficient for a particular purpose.

According to general conventions, the normal stress is taken positive when producing tension and negative when producing compression. On any side the direction of the positive shearing

stress coincides with the positive direction of the axis if the outward normal of this side has the positive direction of the corresponding axis. If the outward normal has a direction opposite to positive axis the positive shearing stress will also have the opposite direction of the corresponding axis. The first subscript of the symbol indicates the direction of the normal of the plane on which the stress acting and the second subscript indicates the direction of stress. By a simple consideration of the equilibrium of the element shown in Fig. 2.1, it can be shown that $\sigma_{xy} = \sigma_{yx}$, $\sigma_{zx} = \sigma_{xz}$ and $\sigma_{yz} = \sigma_{zy}$ Thus, the nine components of stress are reduced to six σ_{xx}, σ_{yy}, σ_{zz}, σ_{xy}, σ_{yz} and σ_{zx} [1-2].

From the consideration of an infinitesimal cubic element surrounding a given point in a body, it is found that the static equilibrium of forces requires at this point is to satisfy the followings equations:

$$\left.\begin{aligned} \frac{\partial \sigma_{xx}}{\partial x} + \frac{\partial \sigma_{xy}}{\partial y} + \frac{\partial \sigma_{xz}}{\partial z} + F_x = 0 \\ \frac{\partial \sigma_{yy}}{\partial y} + \frac{\partial \sigma_{xy}}{\partial x} + \frac{\partial \sigma_{yz}}{\partial z} + F_y = 0 \\ \frac{\partial \sigma_{zz}}{\partial z} + \frac{\partial \sigma_{yz}}{\partial y} + \frac{\partial \sigma_{zx}}{\partial x} + F_z = 0 \end{aligned}\right\} \qquad (2.1)$$

These equations are known as the equations of equilibrium, where F_x, F_y and F_z are the components of the body force per unit volume in x, y and z directions respectively [2].

The six stress components satisfy the above mentioned three equations of equilibrium, but it is not practicable to obtain six stress components solving three equations. As such consideration of more relations is the option to have equity in number of variables as well as equations. In this regard, following six relations are defining the three strain components in terms of the three displacement components through partial differentiation [2].

$$\varepsilon_{xx} = \frac{\partial u_x}{\partial x}, \varepsilon_{yy} = \frac{\partial u_y}{\partial y}, \varepsilon_{zz} = \frac{\partial u_z}{\partial z},$$
$$\gamma_{xy} = \frac{\partial u_x}{\partial y} + \frac{\partial u_y}{\partial x}, \gamma_{yz} = \frac{\partial u_y}{\partial z} + \frac{\partial u_z}{\partial y}, \gamma_{zx} = \frac{\partial u_z}{\partial x} + \frac{\partial u_x}{\partial z} \quad (2.2)$$

In addition, the six stress-strain relations are also there. Thus one can have altogether 15 unknowns and 15 equations. This system of equations is generally sufficient for the solution of an elasticity problem.

By differentiation and simple manipulation of Eq. (2.2), the following set of differential equations can be obtained.

$$\frac{\partial^2 \varepsilon_{xx}}{\partial y^2} + \frac{\partial^2 \varepsilon_{yy}}{\partial x^2} = \frac{\partial^2 \gamma_{xy}}{\partial x \partial y}; \quad 2\frac{\partial^2 \varepsilon_{xx}}{\partial y \partial z} = \frac{\partial}{\partial x}\left(-\frac{\partial \gamma_{yz}}{\partial x} + \frac{\partial \gamma_{xz}}{\partial y} + \frac{\partial \gamma_{xy}}{\partial z}\right)$$
$$\frac{\partial^2 \varepsilon_{yy}}{\partial z^2} + \frac{\partial^2 \varepsilon_{zz}}{\partial y^2} = \frac{\partial^2 \gamma_{yz}}{\partial y \partial z}; \quad 2\frac{\partial^2 \varepsilon_{yy}}{\partial x \partial z} = \frac{\partial}{\partial y}\left(\frac{\partial \gamma_{yz}}{\partial x} - \frac{\partial \gamma_{xz}}{\partial y} + \frac{\partial \gamma_{xy}}{\partial z}\right) \quad (2.3)$$
$$\frac{\partial^2 \varepsilon_{zz}}{\partial x^2} + \frac{\partial^2 \varepsilon_{xx}}{\partial z^2} = \frac{\partial^2 \gamma_{xz}}{\partial x \partial z}; \quad 2\frac{\partial^2 \varepsilon_{zz}}{\partial x \partial y} = \frac{\partial}{\partial z}\left(\frac{\partial \gamma_{yz}}{\partial x} + \frac{\partial \gamma_{xz}}{\partial y} - \frac{\partial \gamma_{xy}}{\partial z}\right)$$

These differential relations are called the conditions of compatibility. The solution of an elasticity problem must satisfy the equilibrium i.e. Eq. (2.1) and the compatibility conditions i.e. Eq. (2.3) along with the boundary conditions.

2.3 Hooke's Law

In the simplest approximation the relation between stress and strain is taken to be linear and called Hooke's law named after the 17th century British physicist Robert Hooke. The most general form of linear stress-strain relationship for anisotropic material is given by the following expression [38].

$$\begin{Bmatrix}\sigma_{xx}\\ \sigma_{yy}\\ \sigma_{zz}\\ \sigma_{yz}\\ \sigma_{zx}\\ \sigma_{xy}\\ \sigma_{yx}\\ \sigma_{xz}\\ \sigma_{zy}\end{Bmatrix}=\begin{bmatrix}c_{11} & c_{12} & c_{13} & c_{14} & c_{15} & c_{16} & c_{17} & c_{18} & c_{19}\\ c_{21} & c_{22} & c_{23} & c_{24} & c_{25} & c_{26} & c_{27} & c_{28} & c_{29}\\ c_{31} & c_{32} & c_{33} & c_{34} & c_{35} & c_{36} & c_{37} & c_{38} & c_{39}\\ c_{41} & c_{42} & c_{43} & c_{44} & c_{45} & c_{46} & c_{47} & c_{48} & c_{49}\\ c_{51} & c_{52} & c_{53} & c_{54} & c_{55} & c_{56} & c_{57} & c_{58} & c_{59}\\ c_{61} & c_{62} & c_{63} & c_{64} & c_{65} & c_{66} & c_{67} & c_{68} & c_{69}\\ c_{71} & c_{72} & c_{73} & c_{74} & c_{75} & c_{76} & c_{77} & c_{78} & c_{79}\\ c_{81} & c_{82} & c_{83} & c_{84} & c_{85} & c_{86} & c_{87} & c_{88} & c_{89}\\ c_{91} & c_{92} & c_{93} & c_{94} & c_{95} & c_{96} & c_{97} & c_{98} & c_{99}\end{bmatrix}\begin{Bmatrix}\varepsilon_{xx}\\ \varepsilon_{yy}\\ \varepsilon_{zz}\\ \gamma_{yz}\\ \gamma_{zx}\\ \gamma_{xy}\\ \gamma_{yx}\\ \gamma_{xz}\\ \gamma_{zy}\end{Bmatrix} \tag{2.4}$$

Where the 81 coefficients c_{11},……, c_{99} are called elastic coefficients or stiffness. For the equilibrium condition it is found that $\sigma_{ij}=\sigma_{ji}$ $\gamma_{ij}=\gamma_{ji}$. As such $\sigma_{xy}=\sigma_{yx}$, $\sigma_{zx}=\sigma_{xz}$, $\sigma_{yz}=\sigma_{zy}$, $\gamma_{xy}=\gamma_{yx}$, $\gamma_{zx}=\gamma_{zz}$ and $\gamma_{yz}=\gamma_{zy}$.

Therefore, the stress–strain relation becomes as follows

$$\begin{Bmatrix}\sigma_{xx}\\ \sigma_{yy}\\ \sigma_{zz}\\ \sigma_{yx}\\ \sigma_{zx}\\ \sigma_{xy}\end{Bmatrix}=\begin{bmatrix}c_{11} & c_{12} & c_{13} & c_{14} & c_{15} & c_{16}\\ c_{21} & c_{22} & c_{23} & c_{24} & c_{25} & c_{26}\\ c_{31} & c_{32} & c_{33} & c_{34} & c_{35} & c_{36}\\ c_{41} & c_{42} & c_{43} & c_{44} & c_{45} & c_{46}\\ c_{51} & c_{52} & c_{53} & c_{54} & c_{55} & c_{56}\\ c_{61} & c_{62} & c_{63} & c_{64} & c_{65} & c_{66}\end{bmatrix}\begin{Bmatrix}\varepsilon_{xx}\\ \varepsilon_{yy}\\ \varepsilon_{zz}\\ \gamma_{yz}\\ \gamma_{zx}\\ \gamma_{xy}\end{Bmatrix} \tag{2.5}$$

From the consideration of strain energy density, it can be shown that $c_{ij}=c_{ji}$

Therefore,

$c_{12}=c_{21}$, $c_{13}=c_{31}$, $c_{14}=c_{41}$, $c_{15}=c_{51}$, $c_{16}=c_{61}$
$c_{23}=c_{32}$, $c_{24}=c_{42}$, $c_{25}=c_{52}$, $c_{26}=c_{62}$, $c_{34}=c_{43}$
$c_{35}=c_{53}$, $c_{36}=c_{63}$, $c_{45}=c_{54}$, $c_{46}=c_{64}$, $c_{56}=c_{65}$

Thus, the 36 coefficients of the stiffness matrix in Eq. (2.5) come down to 21 and the stiffness matrix turns to a symmetric matrix as follows.

$$[C_{ij}] = \begin{bmatrix} c_{11} & c_{12} & c_{13} & c_{14} & c_{15} & c_{16} \\ c_{12} & c_{22} & c_{23} & c_{24} & c_{25} & c_{26} \\ c_{13} & c_{23} & c_{33} & c_{34} & c_{35} & c_{36} \\ c_{14} & c_{24} & c_{34} & c_{44} & c_{45} & c_{46} \\ c_{15} & c_{25} & c_{35} & c_{45} & c_{55} & c_{56} \\ c_{16} & c_{26} & c_{36} & c_{46} & c_{56} & c_{66} \end{bmatrix} \tag{2.6}$$

Materials having symmetry with respect to one plane is referred to as monoclinic materials. For such case of material, transformation of axis can be done and found that $c_{14} = c_{15} = c_{24} = c_{25} = c_{34} = c_{35} = c_{44} = c_{56} = 0$ and then the number of elastic coefficient becomes 13 only.

Thus, the stiffness matrix of Eq. (2.6) further reduces to

$$[C_{ij}] = \begin{bmatrix} c_{11} & c_{12} & c_{13} & 0 & 0 & c_{16} \\ c_{12} & c_{22} & c_{23} & 0 & 0 & c_{26} \\ c_{13} & c_{23} & c_{33} & 0 & 0 & c_{36} \\ 0 & 0 & 0 & c_{44} & c_{45} & 0 \\ 0 & 0 & 0 & c_{45} & c_{55} & 0 \\ c_{16} & c_{26} & c_{36} & 0 & 0 & 0 \end{bmatrix} \tag{2.7}$$

Again an orthotropic material has at least two orthogonal planes of symmetry, where material properties are independent of direction within each plane. Normally the reference system of coordinates is selected along the principal planes of material symmetry. Examples of an orthogonal material include a single lamina of continuous fibre composite arranged in a rectangular array, a wooden bar and rolled steel. For such case $c_{16} = c_{26} = c_{36} = c_{45} = 0$ and

then this type of materials require 9 independent variables as elastic constants in their stiffness matrix as follows.

$$[C_{ij}](Orthotropic) = \begin{bmatrix} c_{11} & c_{12} & c_{13} & 0 & 0 & 0 \\ c_{12} & c_{22} & c_{23} & 0 & 0 & 0 \\ c_{13} & c_{23} & c_{33} & 0 & 0 & 0 \\ 0 & 0 & 0 & c_{44} & 0 & 0 \\ 0 & 0 & 0 & 0 & c_{55} & 0 \\ 0 & 0 & 0 & 0 & 0 & c_{66} \end{bmatrix} \tag{2.8}$$

Where

$$c_{11} = \frac{1-\mu_{yz}\mu_{zy}}{E_y E_z \nabla}; \quad c_{12} = \frac{\mu_{xy}+\mu_{zy}\mu_{xz}}{E_x E_z \nabla}$$

$$c_{13} = \frac{\mu_{xz}+\mu_{zy}\mu_{yz}}{E_x E_y \nabla}; \quad c_{22} = \frac{1-\mu_{xz}\mu_{zx}}{E_x E_z \nabla}$$

$$c_{23} = \frac{\mu_{yz}+\mu_{yx}\mu_{xz}}{E_x E_y \nabla}; \quad c_{33} = \frac{1-\mu_{xy}\mu_{yx}}{E_x E_y \nabla}$$

$$c_{44} = G_{yz}; c_{55} = G_{zx}; c_{66} = G_{xy}$$

$$\nabla = \frac{1-\mu_{xy}\mu_{yx}-\mu_{yz}\mu_{zy}-\mu_{zx}\mu_{xz}-2\mu_{yx}\mu_{zy}\mu_{xz}}{E_x E_y E_z}$$

The reciprocal relations are given by

$$\frac{\mu_{ij}}{E_i} = \frac{\mu_{ji}}{E_j}; i, j = x, y, z$$

Most metallic alloys and thermoset polymers are considered isotropic material, where by definition the mechanical properties are independent of direction. In this case there are infinite planes of symmetry. Such materials have only two independent variables i.e. elastic constants in their stiffness matrix as

$$[C_{ij}](Isotropic) = \begin{bmatrix} c_{11} & c_{12} & c_{12} & 0 & 0 & 0 \\ c_{12} & c_{11} & c_{12} & 0 & 0 & 0 \\ c_{12} & c_{12} & c_{11} & 0 & 0 & 0 \\ 0 & 0 & 0 & \frac{c_{11}-c_{12}}{2} & 0 & 0 \\ 0 & 0 & 0 & 0 & \frac{c_{11}-c_{12}}{2} & 0 \\ 0 & 0 & 0 & 0 & 0 & \frac{c_{11}-c_{12}}{2} \end{bmatrix} \quad (2.9)$$

These constants are given by

$$c_{11} = \frac{E(1-\mu)}{(1-2\mu)(1+\mu)};\ c_{12} = \frac{\mu E}{(1-2\mu)(1+\mu)} \text{ and } \quad \frac{c_{11}-c_{12}}{2} = \frac{E}{2(1+2\mu)(1-2\mu)}$$

The summarised form of independent elastic constants for general anisotropic, anisotropic with symmetric stress and strain components or with energy consideration, orthotropic and isotropic materials can be thus presented in Table 2.1 as follows.

Table 2.1 Number of elastic constants

Serial	Material	Condition	No. of constant
1	Anisotropic	General form	81
2	Anisotropic	Equilibrium condition	36
3	Anisotropic	Stain energy consideration	21
4	Monoclinic	Symmetric to a plane	13
5	Orthotropic	Having mutually perpendicular planes of symmetry	09
6	Isotropic	Same elastic properties in all directions (having infinite perpendicular planes of symmetry)	02

2.4 Two-Dimensionalization of the Problem

Although the elastic analysis in general form is of three dimensional, orthotropic and isotropic materials can be analyzed using two dimensions on the consideration of symmetry of planes. For such simplification there are two options, i.e., (i) plane stress condition and (ii) plane strain condition.

Plane stress condition is considered to be a state of stress in which the normal stress σ_{zz} and the shear stresses σ_{xz} and σ_{yz} directed perpendicular to the plane are assumed to be zero (but not the strain). Generally, members that are thin (those with a small *z* dimension compared to the in-plane *x* and *y* dimensions) and whose loads act only in the *x-y* plane can be considered to be under plane stress. Thus, a state of plane stress exists in a thin object loaded in the plane of its largest dimensions. The non-zero stresses σ_{xx}, σ_{yy}, and σ_{xy} lie in the *x-y* plane and do not vary in the *z* direction. A thin beam loaded in its plane and a spur gear tooth are good examples of plane stress problems.

On the other hand plane strain is said to be a state of strain in which the strain normal to the *x-y* plane ε_{zz} and the shear strains $\gamma_{xz \text{ and }} \gamma_{yz}$ are assumed to be zero. The assumptions of the plane strain are realistic for long bodies (saying in the *z* direction) with constant cross-sectional area subjected to loads that act only in the *x* and/or *y* directions and do not vary in the *z* direction.

The option (i), i.e., the plane stress condition has been followed in the present study. Thus

$$\sigma_{zz} = 0;\ \sigma_{zx} = 0;\ \sigma_{yz} = 0 \tag{2.10}$$

At this condition, the equilibrium Eq. (2.1) having no body forces reduces to

$$\frac{\partial \sigma_{xx}}{\partial x} + \frac{\partial \sigma_{xy}}{\partial y} = 0 \tag{2.11a}$$

$$\frac{\partial \sigma_{yy}}{\partial y} + \frac{\partial \sigma_{xy}}{\partial x} = 0 \tag{2.11b}$$

The stresses for a two dimensional element at plane stress condition are shown in Fig. 2.2.

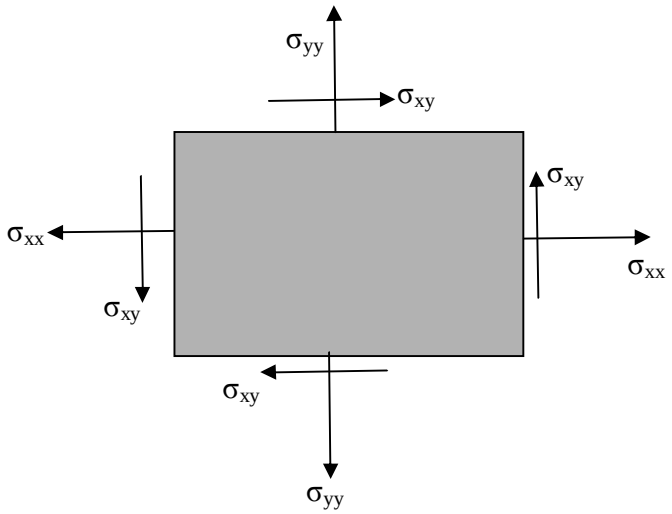

Fig. 2.2 Stress components on a plane

The two equilibrium Eqs. (2.11) contain three unknown stress components. Thus, one more equation is required to obtain an exclusive solution of three unknowns. The third equation is the mathematical formulation of the condition for compatibility, which can be obtained from the strain displacement relations. For two dimensional cases, these relations are:

$$\varepsilon_{xx} = \frac{\partial u_x}{\partial x}, \quad \varepsilon_{yy} = \frac{\partial u_y}{\partial y}, \quad \gamma_{xy} = \frac{\partial u_x}{\partial y} + \frac{\partial u_y}{\partial x} \tag{2.12}$$

Differentiating the first Eq. of (2.12) twice with respective to *y*, the second twice with respect to *x* and the third once with respect to *x* and once with respect to *y*, the expression for condition of compatibility in term of strain then becomes as follows:

$$\frac{\partial^2 \varepsilon_{xx}}{\partial y^2} + \frac{\partial^2 \varepsilon_{yy}}{\partial x^2} = \frac{\partial^2 \gamma_{xy}}{\partial x \partial y} \tag{2.13}$$

But there would have been the necessity of one more equation in terms of stresses; which can be obtained using stiffness matrix in Eq. (2.13). For orthotropic material, while the stiffness matrix is given by Eq. (2.8), the stress-strain relations in the case of plane stress can be reduced to:

$$\begin{bmatrix} \sigma_{xx} \\ \sigma_{yy} \\ \sigma_{xy} \end{bmatrix} = \begin{bmatrix} K_{11} & K_{12} & 0 \\ K_{12} & K_{22} & 0 \\ 0 & 0 & K_{66} \end{bmatrix} \begin{bmatrix} \varepsilon_{xx} \\ \varepsilon_{yy} \\ \gamma_{xy} \end{bmatrix} \tag{2.14}$$

It can be noted that the symbols of elastic constants (c) are replaced conveniently by the symbols *K*'s for the case of plane stress condition so that they can be identified easily, where

$$\left.\begin{aligned} K_{11} &= \frac{E_x}{1-\mu_{xy}\mu_{yx}}; \qquad K_{12} = \frac{\mu_{xy}E_y}{1-\mu_{xy}\mu_{yx}} = \frac{\mu_{yx}E_x}{1-\mu_{xy}\mu_{yx}} \\ K_{22} &= \frac{E_y}{1-\mu_{xy}\mu_{yx}}; \qquad K_{66} = G_{xy} \end{aligned}\right\} \tag{2.15}$$

From the elastic constant K_{12} of Eq. (2.15) the reciprocal relations can be reduced as:

$$\frac{\mu_{xy}}{E_x} = \frac{\mu_{yx}}{E_y} \tag{2.16}$$

Using Eqs. (2.13), (2.14), (2.15) and (2.16), the differential equation for compatibility condition in terms of stresses can be as follows:

$$\left(\frac{1}{E_x}\frac{\partial^2\sigma_{xx}}{\partial y^2} + \frac{1}{E_y}\frac{\partial^2\sigma_{yy}}{\partial x^2}\right) - \frac{\mu_{xy}}{E_x}\left(\frac{\partial^2\sigma_{yy}}{\partial y^2} + \frac{\partial^2\sigma_{xx}}{\partial x^2}\right) = \frac{1}{G_{xy}}\frac{\partial^2\sigma_{xy}}{\partial x\partial y} \tag{2.17}$$

Now Eq. (2.11) and (2.17) are to be solved to obtain elastic fields satisfying the boundary conditions.

2.5 Usual Method for Solution

As per existing mathematical methods, the analytical solution of three simultaneous partial differential equations given by Eq. (2.11) and (2.17) is fairly impossible. However, these equations may be solved numerically. The numerical solution procedure is even complicated and cumbersome for this type of equations. Moreover, it gives only approximate results. As such it continues to remain a challenging job for the researchers to obtain the solution of elastic fields analytically for a composite structural element under mixed mode boundary conditions using traditional formulation. In this study, attention is paid to the theoretical enhancement of suitable and reliable formulation for the solution for elastic fields of orthotropic as well as isotropic composite beams under mixed mode of boundary conditions. The principal viewpoint in this regard is summarized in subsequent paragraphs.

There are mathematical concepts on the reduction in number of unknowns by assuming intermediate functions, which in turn reduces the number of equations for solution. It is noticed that the number of partial differential equations (Eq. 2.11 and 2.17) and the unknown terms can be reduced to two when the stress components of these equations are replaced by displacement components. Using Eqs. (2.12), (2.14) and (2.15) it is possible to get three expressions for three stresses in terms of two displacement components as follows:

$$\sigma_{xx} = \frac{\mathrm{E_x}}{1 - \mu_{xy}\mu_{yx}}\left[\frac{\partial u_x}{\partial x} + \mu_{yx}\frac{\partial u_y}{\partial y}\right] \tag{2.18a}$$

$$\sigma_{yy} = \frac{\mathrm{E_y}}{1 - \mu_{xy}\mu_{yx}}\left[\frac{\partial u_y}{\partial y} + \mu_{yx}\frac{\partial u_x}{\partial x}\right] \tag{2.18b}$$

$$\sigma_{xy} = \mathrm{G_{xy}}\left[\frac{\partial u_x}{\partial y} + \mu_{yx}\frac{\partial u_y}{\partial x}\right] \tag{2.18c}$$

Substituting Eq. (2.16) and (2.18) in to equilibrium Eqs. (2.11) the following two elliptical partial differential equations are obtained.

$$\left(\frac{E_x^2}{E_x-\mu_{xy}^2E_y}\right)\frac{\partial^2 u_x}{\partial x^2}+\left(\frac{\mu_{xy}E_xE_y}{E_x-\mu_{xy}^2E_y}+G_{xy}\right)\frac{\partial^2 u_y}{\partial x\partial y}+G_{xy}\frac{\partial^2 u_x}{\partial y^2}=0 \tag{2.19a}$$

$$\left(\frac{E_xE_y}{E_x-\mu_{xy}^2E_y}\right)\frac{\partial^2 u_y}{\partial y^2}+\left(\frac{\mu_{xy}E_xE_y}{E_x-\mu_{xy}^2E_y}+G_{xy}\right)\frac{\partial^2 u_x}{\partial x\partial y}+G_{xy}\frac{\partial^2 u_y}{\partial x^2}=0 \tag{2.19b}$$

2.6 Stress Function Approach

It may be noted that, in the analytical approach, stress function is being used for long time, since it was introduced by George Biddell Airy, a British astrologer and mathematician, in 1862. Airy's stress function *Φ(x,y)* is defined in terms of stresses as a function of *x* and *y* for which following conditions are met [1-2]:

$$\sigma_{xx}=\frac{\partial^2\phi}{\partial y^2};\quad \sigma_{yy}=\frac{\partial^2\phi}{\partial x^2}\quad ;\quad \sigma_{xy}=-\frac{\partial^2\phi}{\partial x\partial y} \tag{2.20}$$

Stress function satisfies the equilibrium equations and compatibility conditions. After applying the above relations of stresses in terms of *Φ(x,y)* in Eq. (2.17) following expression is obtained.

$$\left\{\frac{1}{E_x}\frac{\partial^2}{\partial y^2}\left(\frac{\partial^2\phi}{\partial y^2}\right)+\frac{1}{E_y}\frac{\partial^2}{\partial x^2}\left(\frac{\partial^2\phi}{\partial x^2}\right)\right\}-\frac{\mu_{xy}}{E_x}\left\{\frac{\partial^2}{\partial y^2}\left(\frac{\partial^2\phi}{\partial x^2}\right)+\frac{\partial^2}{\partial x^2}\left(\frac{\partial^2\phi}{\partial y^2}\right)\right\}=\frac{1}{G_{xy}}\frac{\partial^2}{\partial x\partial y}\left(-\frac{\partial^2\phi}{\partial x\partial y}\right)$$

$$\text{or,}\quad \frac{1}{E_y}\frac{\partial^4\phi}{\partial x^4}+\left(\frac{1}{G_{xy}}-\frac{2\mu_{xy}}{E_x}\right)\frac{\partial^4\phi}{\partial x^2\partial y^2}+\frac{1}{E_x}\frac{\partial^4\phi}{\partial y^4}=0 \tag{2.21}$$

This expression is the bi-harmonic partial differential equation for Airy's stress function. Now Eq. (2.21) is to be solved satisfying the boundary conditions to obtain stress components using Eq. (2.20) and then Hooke's law as well as strain displacement relations are used to obtain the displacement components.

For orthotropic case [Fig. 2.3] the young's moduli E_x and E_y may be replaced by E_1 and E_2 where they are used to denote the Young's modulus in the fibre direction and in perpendicular to the fibre direction respectively. Further G_{xy} is replaced by G_{12} to denote the shear modulus for on-axis orientation.

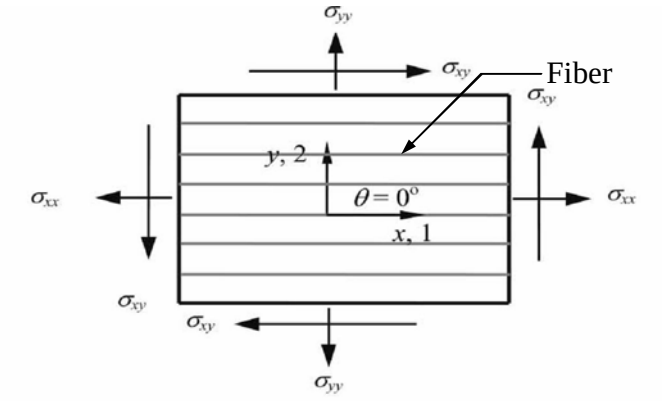

Fig. 2.3 Stress components on a composite plane

In such case, the bi-harmonic governing differential equation for orthotropic composites, on the basis of stress function *Φ(x,y)*, i.e., Eq. (2.21) becomes:

$$\frac{1}{E_2}\frac{\partial^4\phi}{\partial x^4}+\left(\frac{1}{G_{12}}-\frac{2\mu_{12}}{E_1}\right)\frac{\partial^4\phi}{\partial x^2\partial y^2}+\frac{1}{E_1}\frac{\partial^4\phi}{\partial y^4}=0 \tag{2.22}$$

For an isotropic elastic materials under the condition of plane stress $E_x = E_y = E$, $\mu_{xy} = \mu_{yx} = \mu$ and $G_{xy} = G = \frac{E}{2(1+\mu)}$. Substituting these relations in Eq. (2.21) the mathematical model for the isotropic condition is found as:

$$\frac{\partial^4\phi}{\partial x^4}+2\frac{\partial^4\phi}{\partial x^2\partial y^2}+\frac{\partial^4\phi}{\partial y^4}=0 \tag{2.23}$$

Eqs. (2.22) and (2.23) developed basing on Airy's stress function can handle elastic problems of orthotropic and isotropic materials, whose boundary conditions are in terms of stress or load

only. Thus attention is obviously necessary towards the solution of the two elliptical partial differential equations for those problems where the boundary restrains are to be satisfied. Again it is not even easy task to obtain the values of displacement components by the solution of Eqs. (2.19). Consequently, further simplification of the solution method is the necessity.

2.7 Displacement Potential Formulation

Considering the difficulty of solving Eqs. (2.19), a single function $\psi(x, y)$ is taken into consideration [30-33], which has to satisfy a single partial differential equation of equilibrium, somewhat similar in concept to that of Eq. (2.21). It is named as displacement potential function and defined as a function $\psi\,(x,\, y)$ of space variables *x* and *y*, where the displacement components are expressed as follows:

$$u_x = \alpha_1 \frac{\partial^2 \psi}{\partial x^2} + \alpha_2 \frac{\partial^2 \psi}{\partial x \partial y} + \alpha_3 \frac{\partial^2 \psi}{\partial y^2} \tag{2.24a}$$

$$u_y = \alpha_4 \frac{\partial^2 \psi}{\partial x^2} + \alpha_5 \frac{\partial^2 \psi}{\partial x \partial y} + \alpha_6 \frac{\partial^2 \psi}{\partial y^2} \tag{2.24b}$$

Here, $\alpha's$ are unknown material constants.

Using the expressions of Eq. (2.24) in Eq. (2.19a) for fibre orientation θ=0^0 following equation is obtained.

$$\begin{aligned} &\left(\frac{E_x^2}{E_x - \mu_{xy}^2 E_y}\right)\alpha_1 \frac{\partial^4 \psi}{\partial x^4} + \left\{\left(\frac{E_x^2}{E_x - \mu_{xy}^2 E_y}\right)\alpha_2 + \left(\frac{\mu_{xy} E_x E_y}{E_x - \mu_{xy}^2 E_y} + G_{xy}\right)\alpha_4\right\}\frac{\partial^4 \psi}{\partial x^3 \partial y} + \\ &\left\{\left(\frac{E_x^2}{E_x - \mu_{xy}^2 E_y}\right)\alpha_3 + \left(\frac{\mu_{xy} E_x E_y}{E_x - \mu_{xy}^2 E_y} + G_{xy}\right)\alpha_5 + G_{xy}\alpha_1\right\}\frac{\partial^4 \psi}{\partial x^2 \partial y^2} + \\ &\left\{\left(\frac{\mu_{xy} E_x E_y}{E_x - \mu_{xy}^2 E_y} + G_{xy}\right)\alpha_6 + G_{xy}\alpha_2\right\}\frac{\partial^4 \psi}{\partial x \partial y^3} + G_{xy}\alpha_3 \frac{\partial^4 \psi}{\partial y^4} = 0 \end{aligned} \tag{2.25}$$

The material constants α's are chosen in such a way that the Eq. (2.25) is automatically satisfied under all circumstances. This will happen when all of its coefficients are independently zero. In that situation,

$$\left(\frac{E_x^2}{E_x-\mu_{xy}^2E_y}\right)\alpha_1=0$$

$$\left(\frac{E_x^2}{E_x-\mu_{xy}^2E_y}\right)\alpha_2+\left(\frac{\mu_{xy}E_xE_y}{E_x-\mu_{xy}^2E_y}+G_{xy}\right)\alpha_4=0$$

$$\left(\frac{E_x^2}{E_x-\mu_{xy}^2E_y}\right)\alpha_3+\left(\frac{\mu_{xy}E_xE_y}{E_x-\mu_{xy}^2E_y}+G_{xy}\right)\alpha_5+G_{xy}\alpha_1=0$$

$$\left(\frac{\mu_{xy}E_xE_y}{E_x-\mu_{xy}^2E_y}+G_{xy}\right)\alpha_6+G_{xy}\alpha_2=0$$

$$G_{xy}\alpha_3=0$$

Therefore,

$$\left.\begin{aligned}&\alpha_1=\alpha_3=\alpha_5=0\\&\alpha_4=\frac{-E_x^2\alpha_2}{\left\{\mu_{xy}E_xE_y+G_{xy}\left(E_x-\mu_{xy}^2E_y\right)\right\}}\\&\alpha_6=\frac{-G_{xy}\left(E_x-\mu_{xy}^2E_y\right)\alpha_2}{\left\{\mu_{xy}E_xE_y+G_{xy}\left(E_x-\mu_{xy}^2E_y\right)\right\}}\end{aligned}\right\}\qquad(2.26)$$

Again from the Eq. of (2.19b) and Eq. (2.24) it is found that

$$\begin{aligned}&G_{xy}\alpha_4\frac{\partial^4\psi}{\partial x^4}+\left\{\left(\frac{\mu_{xy}E_xE_y}{E_x-\mu_{xy}^2E_y}+G_{xy}\right)\alpha_1+G_{xy}\alpha_5\right\}\frac{\partial^4\psi}{\partial x^3\partial y}+\left\{\left(\frac{E_xE_y}{E_x-\mu_{xy}^2E_y}\right)\alpha_4+\left(\frac{\mu_{xy}E_xE_y}{E_x-\mu_{xy}^2E_y}+G_{xy}\right)\alpha_2+G_{xy}\alpha_6\right\}\\&\frac{\partial^4\psi}{\partial x^2\partial y^2}+\left\{\left(\frac{E_xE_y}{E_x-\mu_{xy}^2E_y}\right)\alpha_5+\left(\frac{\mu_{xy}E_xE_y}{E_x-\mu_{xy}^2E_y}+G_{xy}\right)\alpha_3\right\}\frac{\partial^4\psi}{\partial x\partial y^3}+\left(\frac{E_xE_y}{E_x-\mu_{xy}^2E_y}\right)\alpha_6\frac{\partial^4\psi}{\partial y^4}=0\end{aligned}\qquad(2.27)$$

Now using Eq. (2.26) and (2.27) it is found that

$$E_x G_{xy} \frac{\partial^4 \psi}{\partial x^4} + E_y \left(E_x - 2\mu_{xy} G_{xy}\right) \frac{\partial^4 \psi}{\partial x^2 \partial y^2} + E_y G_{xy} \frac{\partial^4 \psi}{\partial y^4} = 0 \tag{2.28}$$

The above fourth order partial differential Eq. (2.28) is the single governing equation for the solution of the displacement potential function ψ. Once the displacement potential function ψ is known, the components of displacement can be readily found from Eq. (2.24). Thereafter, using the stress displacement relations of Eq. (2.18) can be used for obtaining stress components.

Assuming the value of α_2 is unity, and taking the values of α_1, α_3, α_4, α_5 and α_6 from Eq. (2.26), one can obtain the components of displacement and stress using Eqs. (2.24) and (2.18) respectively as follows:

$$u_x(x, y) = \frac{\partial^2 \psi}{\partial x \partial y} \tag{2.29a}$$

$$u_y(x, y) = \left\{ \frac{-1}{\mu_{xy} E_x E_y + G_{xy}\left(E_x - \mu_{xy}^2 E_y\right)} \right\} \left[E_x^2 \frac{\partial^2 \psi}{\partial x^2} + G_{xy}\left(E_x - \mu_{xy}^2 E_y\right) \frac{\partial^2 \psi}{\partial y^2} \right] \tag{2.29b}$$

$$\sigma_{xx}(x, y) = \left\{ \frac{-E_x G_{xy}}{\mu_{xy} E_x E_y + G_{xy}\left(E_x - \mu_{xy}^2 E_y\right)} \right\} \left[E_x \frac{\partial^3 \psi}{\partial x^2 \partial y} - \mu_{xy} E_y \frac{\partial^2 \psi}{\partial y^2} \right] \tag{2.29c}$$

$$\sigma_{yy}(x, y) = \left\{ \frac{-E_x E_y}{\mu_{xy} E_x E_y + G_{xy}\left(E_x - \mu_{xy}^2 E_y\right)} \right\} \left[\left(\mu_{xy} G_{xy} - E_x\right) \frac{\partial^3 \psi}{\partial x^2 \partial y} - G_{xy} \frac{\partial^3 \psi}{\partial y^3} \right] \tag{2.29d}$$

$$\sigma_{xy}(x, y) = \left\{ \frac{-E_x G_{xy}}{\mu_{xy} E_x E_y + G_{xy}\left(E_x - \mu_{xy}^2 E_y\right)} \right\} \left[E_x \frac{\partial^3 \psi}{\partial x^3} - \mu_{xy} E_y \frac{\partial^3 \psi}{\partial x \partial y^2} \right] \tag{2.29e}$$

Now using the expressions of Eq. (2.24) in Eq. (2.19c) for fibre orientation θ=90^0 following equation is obtained.

$$\left(\frac{E_xE_y}{E_x-\mu_{xy}^2E_y}\right)\alpha_1\frac{\partial^4\psi}{\partial x^4}+\left\{\left(\frac{E_xE_y}{E_x-\mu_{xy}^2E_y}\right)\alpha_2+\left(\frac{\mu_{xy}E_xE_y}{E_x-\mu_{xy}^2E_y}+G_{xy}\right)\alpha_4\right\}\frac{\partial^4\psi}{\partial x^3\partial y}+$$
$$\left\{\left(\frac{E_xE_y}{E_x-\mu_{xy}^2E_y}\right)\alpha_3+\left(\frac{\mu_{xy}E_xE_y}{E_x-\mu_{xy}^2E_y}+G_{xy}\right)\alpha_5+G_{xy}\alpha_1\right\}\frac{\partial^4\psi}{\partial x^2\partial y^2}+ \qquad (2.30)$$
$$\left\{\left(\frac{\mu_{xy}E_xE_y}{E_x-\mu_{xy}^2E_y}+G_{xy}\right)\alpha_6+G_{xy}\alpha_2\right\}\frac{\partial^4\psi}{\partial x\partial y^3}+G_{xy}\alpha_3\frac{\partial^4\psi}{\partial y^4}=0$$

The material constants α's are chosen in such a way that the Eq. (2.30) is automatically satisfied under all circumstances. This will happen when all of its coefficients are independently zero. In that situation,

$$\left(\frac{E_xE_y}{E_x-\mu_{xy}^2E_y}\right)\alpha_1=0$$
$$\left(\frac{E_xE_y}{E_x-\mu_{xy}^2E_y}\right)\alpha_2+\left(\frac{\mu_{xy}E_xE_y}{E_x-\mu_{xy}^2E_y}+G_{xy}\right)\alpha_4=0$$
$$\left(\frac{E_xE_y}{E_x-\mu_{xy}^2E_y}\right)\alpha_3+\left(\frac{\mu_{xy}E_xE_y}{E_x-\mu_{xy}^2E_y}+G_{xy}\right)\alpha_5+G_{xy}\alpha_1=0$$
$$\left(\frac{\mu_{xy}E_xE_y}{E_x-\mu_{xy}^2E_y}+G_{xy}\right)\alpha_6+G_{xy}\alpha_2=0$$
$$G_{xy}\alpha_3=0$$

Therefore,

$$\left.\begin{aligned}
&\alpha_1 = \alpha_3 = \alpha_5 = 0 \\
&\alpha_4 = \frac{-E_x E_y \alpha_2}{\left\{\mu_{xy} E_x E_y + G_{xy}\left(E_x - \mu_{xy}^2 E_y\right)\right\}} \\
&\alpha_6 = \frac{-G_{xy}\left(E_x - \mu_{xy}^2 E_y\right)\alpha_2}{\left\{\mu_{xy} E_x E_y + G_{xy}\left(E_x - \mu_{xy}^2 E_y\right)\right\}}
\end{aligned}\right\} \tag{2.31}$$

Again from the third Eq. of (2.19) and Eq. (2.24) it is found that

$$\begin{aligned}
&G_{xy}\alpha_4 \frac{\partial^4 \psi}{\partial x^4} + \left\{\left(\frac{\mu_{xy} E_x E_y}{E_x - \mu_{xy}^2 E_y} + G_{xy}\right)\alpha_1 + G_{xy}\alpha_5\right\}\frac{\partial^4 \psi}{\partial x^3 \partial y} + \left\{\left(\frac{E_x^2}{E_x - \mu_{xy}^2 E_y}\right)\alpha_4 + \left(\frac{\mu_{xy} E_x E_y}{E_x - \mu_{xy}^2 E_y} + G_{xy}\right)\alpha_2 + G_{xy}\alpha_6\right\} \\
&\frac{\partial^4 \psi}{\partial x^2 \partial y^2} + \left\{\left(\frac{E_x^2}{E_x - \mu_{xy}^2 E_y}\right)\alpha_5 + \left(\frac{\mu_{xy} E_x E_y}{E_x - \mu_{xy}^2 E_y} + G_{xy}\right)\alpha_3\right\}\frac{\partial^4 \psi}{\partial x \partial y^3} + \left(\frac{E_x^2}{E_x - \mu_{xy}^2 E_y}\right)\alpha_6 \frac{\partial^4 \psi}{\partial y^4} = 0
\end{aligned} \tag{2.32}$$

Now using Eq. (2.32) and (2.31) it is found that

$$E_y G_{xy} \frac{\partial^4 \psi}{\partial x^4} + E_y\left(E_x - 2\mu_{xy} G_{xy}\right)\frac{\partial^4 \psi}{\partial x^2 \partial y^2} + E_x G_{xy} \frac{\partial^4 \psi}{\partial y^4} = 0 \tag{2.33}$$

The above fourth order partial differential Eq. (2.33) is single governing equation for the solution of the displacement potential function ψ. Once the displacement potential function ψ is known, the components of displacement can be readily found from Eq. (2.24). Thereafter, using the stress displacement relations of Eq. (2.18) can be used for obtaining stress components.

Assuming the value of α_2 is unity, and taking the values of α_1, α_3, α_4, α_5 and α_6 from Eq. (2.31), one can obtain the components of displacement and stress using Eq. (2.24) and (2.18) respectively as follows:

$$u_x(x,y)=\frac{\partial^2\psi}{\partial x\partial y} \tag{2.34a}$$

$$u_y(x,y)=\left\{\frac{-1}{\mu_{xy}E_xE_y+G_{xy}\left(E_x-\mu_{xy}^2E_y\right)}\right\}\left[E_xE_y\frac{\partial^2\psi}{\partial x^2}+G_{xy}\left(E_x-\mu_{xy}^2E_y\right)\frac{\partial^2\psi}{\partial y^2}\right] \tag{2.34b}$$

$$\sigma_{xx}(x,y)=\left\{\frac{-E_xE_yG_{xy}}{\mu_{xy}E_xE_y+G_{xy}\left(E_x-\mu_{xy}^2E_y\right)}\right\}\left[\frac{\partial^3\psi}{\partial x^2\partial y}-\mu_{xy}\frac{\partial^2\psi}{\partial y^2}\right] \tag{2.34c}$$

$$\sigma_{yy}(x,y)=\left\{\frac{-E_x}{\mu_{xy}E_xE_y+G_{xy}\left(E_x-\mu_{xy}^2E_y\right)}\right\}\left[\left(E_x-\mu_{xy}G_{xy}\right)\frac{\partial^3\psi}{\partial x^2\partial y}+E_xG_{xy}\frac{\partial^3\psi}{\partial y^3}\right] \tag{2.34d}$$

$$\sigma_{xy}(x,y)=\left\{\frac{-E_xE_yG_{xy}}{\mu_{xy}E_xE_y+G_{xy}\left(E_x-\mu_{xy}^2E_y\right)}\right\}\left[\frac{\partial^3\psi}{\partial x^3}-\mu_{xy}\frac{\partial^3\psi}{\partial x\partial y^2}\right] \tag{2.34e}$$

2.7.1 Displacement potential formulation for orthotropic materials

Case-A: θ=0^0 (Fibres are perpendicular to the direction of loading)

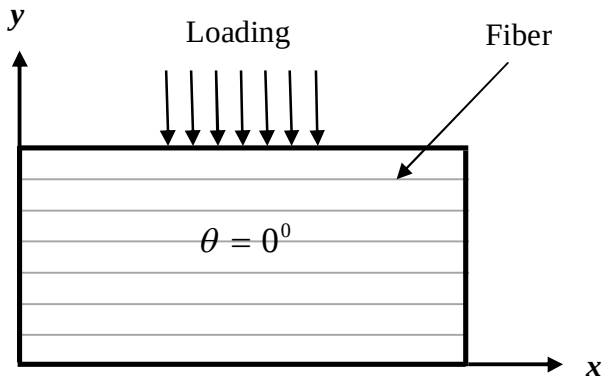

Fig. 2.4 Fibres are perpendicular to the direction of loading

For orthotropic materials with fibre orientation $\theta=0^0$ (Fig. 2.4) the young's moduli E_x and E_y may be replaced by E_1 and E_2 where they are used to denote the Young's modulus in fibre direction and in perpendicular to fiber direction respectively. Further G_{xy} is replaced by G_{12} to denote the shear modulus for on-axis orientation.

Now for fibre orientation $\theta=0^0$, the governing differential equation for the solution of two dimensional orthotropic composite structures becomes:

$$E_1 G_{12} \frac{\partial^4 \psi}{\partial x^4} + E_2 \left(E_1 - 2\mu_{12} G_{12}\right) \frac{\partial^4 \psi}{\partial x^2 \partial y^2} + E_2 G_{12} \frac{\partial^4 \psi}{\partial y^4} = 0 \tag{2.35}$$

Then the components of displacement and stress are:

$$u_x(x,y) = \frac{\partial^2 \psi}{\partial x \partial y} \tag{2.36a}$$

$$u_y(x,y) = -\frac{1}{Z_{11}} \left[E_1^2 \frac{\partial^2 \psi}{\partial x^2} + G_{12} \left(E_1 - \mu_{12}^2 E_2\right) \frac{\partial^2 \psi}{\partial y^2} \right] \tag{2.36b}$$

$$\sigma_{xx}(x,y) = -\frac{E_1 G_{12}}{Z_{11}} \left[E_1 \frac{\partial^3 \psi}{\partial x^2 \partial y} - \mu_{12} E_2 \frac{\partial^2 \psi}{\partial y^2} \right] \tag{2.36c}$$

$$\sigma_{yy}(x,y) = -\frac{E_1 E_2}{Z_{11}} \left[\left(\mu_{12} G_{12} - E_1\right) \frac{\partial^3 \psi}{\partial x^2 \partial y} - G_{12} \frac{\partial^3 \psi}{\partial y^3} \right] \tag{2.36d}$$

$$\sigma_{xy}(x,y) = -\frac{E_1 G_{12}}{Z_{11}} \left[E_1 \frac{\partial^3 \psi}{\partial x^3} - \mu_{12} E_2 \frac{\partial^3 \psi}{\partial x \partial y^2} \right] \tag{2.36e}$$

Where, $Z_{11} = \mu_{12} E_1 E_2 + G_{12} \left(E_1 - \mu_{12}^2 E_2\right)$

Case-B: θ=90^0 (Fibres are parallel to the direction of loading)

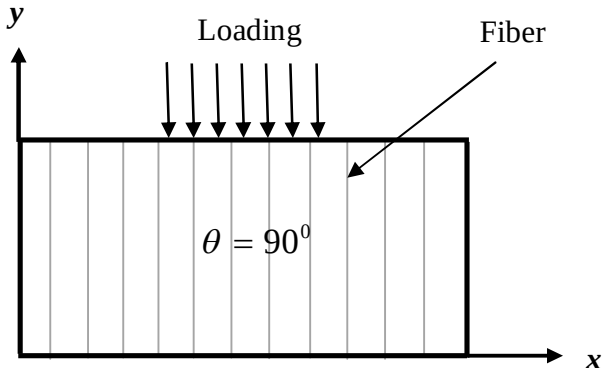

Fig. 2.5 Fibres are parallel to the direction of loading

For orthotropic materials with fibre orientation θ=90^0 (Fig. 2.5), the young's moduli E_x and E_y would be replaced by E_2 and E_1. Further G_{xy} is replaced by G_{12} to denote the shear modulus for on-axis orientation.

In such case the governing differential equation for the solution of two dimensional orthotropic composite structures becomes:

$$E_2 G_{12} \frac{\partial^4 \psi}{\partial x^4} + E_2 \left(E_1 - 2\mu_{12} G_{12}\right) \frac{\partial^4 \psi}{\partial x^2 \partial y^2} + E_1 G_{12} \frac{\partial^4 \psi}{\partial y^4} = 0 \tag{2.37}$$

Then the components of displacement and stress are:

$$u_x(x, y) = \frac{\partial^2 \psi}{\partial x \partial y} \tag{2.38a}$$

$$u_y(x, y) = -\frac{1}{Z_{11}} \left[E_1 E_2 \frac{\partial^2 \psi}{\partial x^2} + G_{12} \left(E_1 - \mu_{12}^2 E_2\right) \frac{\partial^2 \psi}{\partial y^2} \right] \tag{2.38b}$$

$$\sigma_{xx}(x, y) = -\frac{E_1 E_2 G_{12}}{Z_{11}} \left[\frac{\partial^3 \psi}{\partial x^2 \partial y} - \mu_{12} \frac{\partial^2 \psi}{\partial y^2} \right] \tag{2.38c}$$

$$\sigma_{yy}(x,y) = -\frac{E_1}{Z_{11}}\left[E_2(E_1 - \mu_{12}G_{12})\frac{\partial^3\psi}{\partial x^2\partial y} + E_1G_{12}\frac{\partial^3\psi}{\partial y^3} \right] \tag{2.38d}$$

$$\sigma_{xy}(x,y) = -\frac{E_1E_2G_{12}}{Z_{11}}\left[\frac{\partial^3\psi}{\partial x^3} - \mu_{12}\frac{\partial^3\psi}{\partial x\partial y^2} \right] \tag{2.38e}$$

Where, $Z_{11} = \mu_{12}E_1E_2 + G_{12}\left(E_1 - \mu_{12}^2E_2\right)$

2.7.2 Displacement Potential Formulation for isotropic materials

For an isotropic elastic solid under the condition of plane stress $E_x = E_y = E$, $\mu_{xy} = \mu_{yx} = \mu$ and $G_{xy} = G = \frac{E}{2(1+\mu)}$. Then the values of α's of Eq. (2.24) are also obtained as follows:

$$\alpha_1 = \alpha_3 = \alpha_5 = 0; \alpha_2 = 1;\ \alpha_4 = \frac{-2}{1+\mu};\ \alpha_6 = \frac{1-\mu}{1+\mu} \tag{2.39}$$

Then the stress-displacement relations for the plane stress problems are obtained from the Hook's law as follows:

$$\sigma_{xx} = \frac{E}{1-\mu^2}\left[\frac{\partial u_x}{\partial x} + \mu \quad \frac{\partial u_y}{\partial y} \right] \tag{2.40a}$$

$$\sigma_{yy} = \frac{E}{1-\mu^2}\left[\mu\frac{\partial u_x}{\partial x} + \quad \frac{\partial u_y}{\partial y} \right] \tag{2.40b}$$

$$\sigma_{xy} = \frac{E}{2(1+\mu)}\left[\frac{\partial u_x}{\partial y} + \frac{\partial u_y}{\partial x} \right] \tag{2.40c}$$

When the displacement components in Eq. (2.19) are replaced by Eq. (2.24) having values of α as in Eq. (2.37), the single governing equation of equilibrium in partial differential form being satisfied by $\psi(x, y)$ is found for isotropic materials as follows:

$$\frac{\partial^4\psi}{\partial x^4} + 2\frac{\partial^4\psi}{\partial x^2\partial y^2} + \frac{\partial^4\psi}{\partial y^4} = 0 \tag{2.41}$$

Combining Eqs. (2.18), (2.38) and (2.39), the expressions of displacement and stress components in terms of function $\psi(x, y)$ are obtained as follows:

$$u_x(x,y)=\frac{\partial^2\psi}{\partial x\partial y} \tag{2.42a}$$

$$u_y(x,y)=-\frac{1}{1+\mu}\left[2\frac{\partial^2\psi}{\partial x^2}+(1-\mu)\frac{\partial^2\psi}{\partial y^2}\right] \tag{2.42b}$$

$$\sigma_{xx}(x,y)=-\frac{E}{(1+\mu)^2}\left[\frac{\partial^3\psi}{\partial x^2\partial y}-\mu\frac{\partial^2\psi}{\partial y^2}\right] \tag{2.42c)\}$$

$$\sigma_{yy}(x,y)=-\frac{E}{(1+\mu)^2}\left[(2+\mu)\frac{\partial^3\psi}{\partial x^2\partial y}+\frac{\partial^3\psi}{\partial y^3}\right] \tag{2.42d}$$

$$\sigma_{xy}(x,y)=-\frac{E}{(1+\mu)^2}\left[\frac{\partial^3\psi}{\partial x^3}-\mu\frac{\partial^3\psi}{\partial x\partial y^2}\right] \tag{2.42e}$$

2.8 Consideration of Boundary Conditions

The equilibrium Eq. (2.1) has to be satisfied at all points throughout the volume of the solid elastic body. The components of stress may vary over the volume of the body, and at the surface the stresses must be such as to be in equilibrium with external forces acting on the boundary of the body. As such the external forces would have a contribution over the internal stress distribution.

In practical situation, along the edge or boundary of a structure, there are two things to be known, i.e. (i) displacements and (ii) loading or stress. Both the displacements and stresses are identified by their respective components as follows:

a. Normal displacement
b. Tangential displacement
c. Normal stress
d. Tangential stress

The solution of the governing equation requires specific normal and tangential conditions. At any point on the boundary, any 2 components out of 4 are known at a time. Thus there are 6 types of following boundary conditions:

i. Normal displacement + Tangential displacement
ii. Normal displacement + Normal stress
iii. Normal displacement + Tangential stress
iv. Tangential displacement + Normal stress
v. Tangential displacement + Tangential stress
vi. Normal stress + Tangential stress

While both the components are purely normal or purely tangential, the boundary conditions do not practically exist. As such boundary conditions of (ii) and (v) are no longer required to be considered and the remaining four boundary conditions would be considered for solving the physical problems of elastic body. If the shape of the boundary surface is rectangular, the structure may be oriented so that its edges are parallel to the co-ordinate axes. In that case, the normal and the tangential components of displacement and stress at the boundary are the corresponding coordinate components inside the structure. Out of the above mentioned four possible boundaries, only the number (vi) is suitable for Airy's stress function; whereas all four boundary conditions can be dealt with using displacement potential function, ψ.

2.9 Solution Procedure Using Displacement Potential Approach

The concept of structural analysis consists of four essential matters, like any engineering system, such as, proper understanding of physical phenomena, derivation of governing equation, proper application of boundary conditions, and development of routines for the solution and finally the interpretation of solutions. Thus the solution procedure is the uniting of physics and mathematics with a view to potential usefulness in practical problems.

The equilibrium problem is essentially one of describing the steady-state configuration of the physical system. This can usually be achieved by specifying the magnitudes of state variables

like stresses, displacements, pressures, etc. at a finite number of points. In this thesis work, boundary-value problems are dealt with having equilibrium state of affairs. With this pretext a very powerful method of solving boundary-value problems is the so-called trial function or trial solution method.

Attempt is made here to solve the fourth order homogeneous partial differential equations, i.e., Eqs. (2.35) and (2.37) for orthotropic, Eq. (2.41) for isotropic materials through utilization of different trial functions for $\psi(x, y)$. Since the Airy's stress function of similar pattern has been solved using polynomials for quite long time, similar type of functions are considered here at first as trial solutions. It is observed that pure polynomials do not actually help much in this regard. Rather it is seen that various combinations of trigonometric and hyperbolic functions offer suitable choices for analytical functions. If these functions can be expressed as an infinite series, then construction of solutions of differential equations becomes more accurate. In the light of the ubiquitous problems which display aspects of periodic and a discontinuous nature, those infinite series known as Fourier series attain a place of special importance.

The Fourier series is probably the most commonly used of all the series for the solution of physical problems. It is a trigonometric series which can be used for the expansion of an arbitrary function. The usefulness of the Fourier series is due to the fact that certain functions which cannot be expanded in power series form can still be represented by Fourier series. The reason for this is that the coefficients of the power series contain derivatives of the function; hence these derivatives must exist uniquely in order to obtain the power series expansion. Many functions which are not differentiable, including certain types of discontinues function, can be expanded in Fourier series. Thus a much greater degree of generality is attained by taking the function as Fourier series.

Taking all this in mind trial and error operations are done to reach to the possible best displacement potential function to be assumed. In this assumption process, boundary conditions of the two ends should be satisfied automatically. Then the solution can be progressed further to make the boundary conditions of remaining two ends of the beam satisfied.

CHAPTER 3

ANALYSIS OF THE STIFFENED BEAM

The main focus of this chapter is to find the stress and displacement fields of a boundary value problems of elasticity using displacement potential function approach. In this chapter, a stiffened simply supported thick beam of isotropic material is considered for the analysis. The beam is stiffened at its opposing lateral ends by using two different kinds of stiffeners, i.e., axial stiffeners and lateral stiffeners. The beam is loaded transversely at a certain portion on the upper surface of the beam and roller supports are used for certain portions of the lower surface of the beam. The effect of beam aspect ratio on the stress field is also discussed in this chapter.

3.1 Problem Description

A simply supported thick beam of rectangular cross section subjected to a distributed load is considered. The generalised form of such a beam is shown in Fig. 3.1[(a) and (b)]. Since the two opposing lateral ends of this beam are stiffened by some means, it can be considered as stiffened simply supported beam. The support at the bottom surface is inserted over a certain portion of beam length. Beam length, depth and width are denoted by L, D and W, respectively. As a particular enunciation for the development of analytical solution, the load acting over the top surface is considered as uniformly distributed with a magnitude of σ_o acting over 80% of the length. The support of the beam is also considered as uniformly distributed and the effective length for each support is assumed to be 10% of the beam span. The plane stress is assumed here taking unit thickness of the beam. Two different types of stiffeners are considered for the two opposing lateral ends of the beam, which are axial stiffener (Case-1) and lateral stiffener (Case-2).The axial stiffeners prevent axial deflection of the lateral ends which are however free to assume any deflection along the lateral direction. On the other hand, lateral stiffeners prevent deflection along the lateral directions of the ends, but they are free to assume any deflection along the axial direction.

3.2 Boundary Conditions

The physical conditions of the present problem with reference to Fig. 3.1 are to be satisfied along the all four boundaries of the beam. The boundary conditions are considered for the present stiffened composite beam problem can be expressed mathematically as follows:

(a) Loaded boundary, EH:

The loading of the top boundary is modelled by assigning a uniform value to the normal stress component, which is free from any shearing stress. The mathematical expressions of the boundary are

$\sigma_{yy}(x,D)=\sigma_0 \quad [0.1\le x/L\le 0.9]$

$\sigma_{xy}(x,D)=0 \qquad [0.0\le x/L\le 1.0]$

(b) Supporting surface, FG:

The roller supported regions of the bottom surface are modelled by a uniform compressive normal loading and free from shearing stress. At the supports, the total reaction forces should be equal and opposite to the applied loading on the top surface. The reactions are distributed over 20% of the beam span (x/L= 0.0-0.1 and 0.9-1.0).The remaining section of the bottom surface are assumed to be free from loading. Therefore,

Supporting region : $\sigma_{xy}(x,0)=0 \qquad [0.0\le x/L\le 1.0]$

$\sigma_{yy}(x,0)=4\sigma_0 \quad [0.0\le x/L\le 0.1 \;\&\; 0.9\le x/L\le 1.0]$

Free region : $\sigma_{xy}(x,0)=0 \qquad [0.0\le x/L\le 1.0]$

$\sigma_{yy}(x,0)=0 \qquad [0.1< x/L< 0.9]$

(c) Left lateral end, EF:

i. For axial stiffener: The physical condition of the axial stiffener is modelled here by considering no axial displacement and shearing stress. Thus,

$u_x(0,y)=0$

$\sigma_{xy}(0,y)=0 \quad [0.0 \le y/D \le 1.0]$

ii. For lateral stiffener: The physical condition of the lateral stiffener is modelled here by considering the boundary free from lateral displacement and axial normal stress. Thus,

$u_y(0,y)=0$

$\sigma_{xx}(0,y)=0 \quad [0.0 \le y/D \le 1.0]$

(d) Right lateral end, GH:

i. For axial stiffener: The mathematical expressions of this boundary are

$u_x(L,y)=0$

$\sigma_{xy}(L,y)=0 \quad [0.0 \le y/D \le 1.0]$

ii. For lateral stiffener: The mathematical expressions of this boundary are

$u_y(L,y)=0$

$\sigma_{xx}(L,y)=0 \quad [0.0 \le y/D \le 1.0]$

3.3 Analytical Solution

The governing differential equation for the plane beam problem of isotropic materials in terms of the displacement potential function $\psi(x, y$ as follows [Eq. (2.34)]:

$$\frac{\partial^4 \psi}{\partial x^4} + 2\frac{\partial^4 \psi}{\partial x^2 \partial y^2} + \frac{\partial^4 \psi}{\partial y^4} = 0 \tag{3.1}$$

The expressions of displacement and stress components in terms of function $\psi(x, y)$ are also obtained from Eqs. (2.35) as follows:

$$u_x(x,y) = \frac{\partial^2 \psi}{\partial x \partial y} \tag{3.2a}$$

$$u_y(x, y) = -\frac{1}{1+\mu}\left[2\frac{\partial^2 \psi}{\partial x^2} + (1-\mu)\frac{\partial^2 \psi}{\partial y^2}\right] \tag{3.2b}$$

$$\sigma_{xx}(x, y) = -\frac{E}{(1+\mu)^2}\left[\frac{\partial^3\psi}{\partial x^2\partial y} - \mu\frac{\partial^2\psi}{\partial y^2}\right] \tag{3.2c}$$

$$\sigma_{yy}(x, y) = -\frac{E}{(1+\mu)^2}\left[(2+\mu)\frac{\partial^3\psi}{\partial x^2\partial y} + \frac{\partial^3\psi}{\partial y^3}\right] \tag{3.2d}$$

$$\sigma_{xy}(x, y) = -\frac{E}{(1+\mu)^2}\left[\frac{\partial^3\psi}{\partial x^3} - \mu\frac{\partial^3\psi}{\partial x\partial y^2}\right] \tag{3.2e}$$

3.3.1 Beam with axial stiffeners (Case-1)

First, a trial function is assumed for the displacement potential in such a way that the boundary conditions at the two stiffened edges are satisfied instantly. The trial function is assumed in terms of cosine function so that its first and third derivatives with respect to x are obtained in terms of sine function. By this way the requirements of physical conditions of the two opposing stiffened ends are automatically satisfied, i.e., boundary conditions of c(i) and d(i). Considering all these factors the expression for ψ may be approximated as follows

$$\psi(x, y) = \sum_{m=1}^{\infty} Y_m(y)\cos\alpha x + K y^3 \tag{3.3}$$

where, $Y_m = f(y)$, $\alpha = (m\pi / L)$, K is an arbitrary constant and m = 1, 2, 3, ……..∞.

Derivatives of Eq. (3.3) with respect to x and y are

$$\frac{\partial\psi}{\partial x} = -\sum_{m=1}^{\infty} Y_m\alpha\sin\alpha x$$

$$\frac{\partial^2\psi}{\partial x^2} = -\sum_{m=1}^{\infty} Y_m\alpha^2\cos\alpha x$$

$$\frac{\partial^3\psi}{\partial x^3} = \sum_{m=1}^{\infty} Y_m\alpha^3\sin\alpha x$$

$$\frac{\partial^4\psi}{\partial x^4} = \sum_{m=1}^{\infty} Y_m \alpha^4 \cos\alpha x$$

$$\frac{\partial^2\psi}{\partial x \partial y} = -\sum_{m=1}^{\infty} Y_m' \alpha \sin\alpha x$$

$$\frac{\partial^3\psi}{\partial x \partial y^2} = -\sum_{m=1}^{\infty} Y_m'' \alpha \sin\alpha x$$

$$\frac{\partial^3\psi}{\partial x^2 \partial y} = -\sum_{m=1}^{\infty} Y_m' \alpha^2 \cos\alpha x$$

$$\frac{\partial^4\psi}{\partial x^2 \partial y^2} = -\sum_{m=1}^{\infty} Y_m'' \alpha^2 \cos\alpha x$$

$$\frac{\partial\psi}{\partial y} = \sum_{m=1}^{\infty} Y_m' \cos\alpha x + 3Ky^2$$

$$\frac{\partial^2\psi}{\partial y^2} = \sum_{m=1}^{\infty} Y_m'' \cos\alpha x + 6Ky$$

$$\frac{\partial^3\psi}{\partial y^3} = \sum_{m=1}^{\infty} Y_m''' \cos\alpha x + 6K$$

$$\frac{\partial^4\psi}{\partial y^4} = \sum_{m=1}^{\infty} Y_m'''' \cos\alpha x$$

Substituting the expressions of above derivatives in Eq. (3.1) following equation is obtained.

$$\sum_{m=1}^{\infty} Y_m \alpha^4 \cos\alpha x - 2\sum_{m=1}^{\infty} Y_m'' \alpha^2 \cos\alpha x + \sum_{m=1}^{\infty} Y_m'''' \cos\alpha x = 0$$

or, $Y_m'''' - 2\alpha^2 Y_m'' + \alpha^4 Y_m =$ (3.4)

The general solution of the above 4th order ordinary differential equation with constant coefficients [Eq. (3.4)] can be approximated as follows:

$$Y_m = A_m e^{r_1 y} + B_m y e^{r_2 y} + C_m e^{r_3 y} + D_m y e^{r_4 y} \tag{3.5}$$

But the ordinary differential Eq. (3.4) has the complementary function of repeated roots. Thus $r_1 = r_2 = \alpha$ and $r_3 = r_4 = -\alpha$ and the general solution of Eq. (3.4) can be written as

$$Y_m = (A_m + B_m y)e^{\alpha y} + (C_m + D_m y)e^{-\alpha y} \tag{3.6}$$

where A_m, B_m, C_m and D_m are arbitrary constants.

Differentiating Eq. (3.6) following expressions are found

$$Y_m^{'} = (A_m \alpha + B_m \alpha y + B_m)e^{\alpha y} + (-C_m \alpha - D_m \alpha y + D_m)e^{-\alpha y}$$
$$Y_m^{''} = (A_m \alpha^2 + B_m \alpha^2 y + 2B_m \alpha)e^{\alpha y} + (C_m \alpha^2 + D_m \alpha^2 y - 2D_m \alpha)e^{-\alpha y}$$
$$Y_m^{'''} = (A_m \alpha^3 + B_m \alpha^3 y + 3B_m \alpha^3)e^{\alpha y} + (-C_m \alpha^3 - D_m \alpha^3 y + 3D_m \alpha^2)e^{-\alpha y}$$
$$Y_m^{''''} = (A_m \alpha^4 + B_m \alpha^4 y + 4B_m \alpha^3)e^{\alpha y} + (C_m \alpha^4 + D_m \alpha^4 y - 4D_m \alpha^3)e^{-\alpha y}$$

Now substituting the derivatives of ψ and Y_m in the expressions for displacement (3.2) and stresses (3.3), following expressions are found.

$$u_x(x,y) = \frac{\partial^2 \psi}{\partial x \partial y}$$
$$= -\sum_{m=1}^{\infty} Y^{'}{}_m \alpha \sin \alpha x$$
$$= -\sum_{m=1}^{\infty} \left[(A_m \alpha + B_m \alpha y + B_m)e^{\alpha y} + (-C_m \alpha - D_m \alpha y + D_m)e^{-\alpha y} \right] \alpha \sin \alpha x$$
$$= -\sum_{m=1}^{\infty} \left[A_m \alpha e^{\alpha y} + B_m (\alpha y + 1)e^{\alpha y} - C_m \alpha e^{-\alpha y} - D_m (\alpha y - 1)e^{-\alpha y} \right] \alpha \sin \alpha x \tag{3.7a}$$

$$u_y(x,y) = -\frac{1}{(1+\mu)} \left[2 \frac{\partial^2 \psi}{\partial x^2} + (1-\mu) \frac{\partial^2 \psi}{\partial y^2} \right]$$

$$= -\frac{1}{(1+\mu)}\left[2\left\{-\sum_{m=1}^{\infty} Y_m \alpha^2 \cos\alpha x\right\} + (1-\mu)\left\{\sum_{m=1}^{\infty} Y_m'' \cos\alpha x + 6Ky\right\}\right]$$

$$= -\frac{1}{(1+\mu)}\left[\begin{array}{l} -2\sum_{m=1}^{\infty}\left\{(A_m + B_m y)e^{\alpha y} + (C_m + D_m y)e^{-\alpha y}\right\}\alpha^2 \cos\alpha x + (1-\mu) \\ \sum_{m=1}^{\infty}\left\{\begin{array}{l}(A_m\alpha^2 + B_m\alpha^2 y + 2B_m\alpha)e^{\alpha y} + \\ (C_m\alpha^2 + D_m\alpha^2 y - 2D_m\alpha)e^{-\alpha y}\end{array}\right\}\cos\alpha x + 6K(1-\mu)y \end{array}\right]$$

$$= \frac{-1}{(1+\mu)}\left[\sum_{m=1}^{\infty}\left\{\begin{array}{l} -A_m(1+\mu)\alpha^2 e^{\alpha y} + \\ B_m(-\alpha y - \mu\alpha y - 2\mu + 2)\alpha e^{\alpha y} \\ -C_m(1+\mu)\alpha^2 e^{-\alpha y} + \\ D_m(-\alpha y - \mu\alpha y + 2\mu - 2)\alpha e^{-\alpha y}\end{array}\right\}\cos\alpha x + 6K(1-\mu)y\right] \qquad (3.7b)$$

$$\sigma_{xx}(x,y) = \frac{E}{(1+\mu)^2}\left[\frac{\partial^3\psi}{\partial x^2\partial y} - \mu\frac{\partial^3\psi}{\partial y^3}\right]$$

$$= \frac{E}{(1+\mu)^2}\left[\left\{-\sum_{m=1}^{\infty} Y_m'\alpha^2 \cos\alpha x\right\} - \mu\left\{\sum_{m=1}^{\infty} Y_m''' \cos\alpha x + 6K\right\}\right]$$

$$= \frac{-E}{(1+\mu)^2}\left[\begin{array}{l}\sum_{m=1}^{\infty}\left\{(A_m\alpha + B_m\alpha y + B_m)e^{\alpha y} + (-C_m\alpha - D_m\alpha y + D_m)e^{-\alpha y}\right\}\alpha^2 \cos\alpha x \\ +\mu\sum_{m=1}^{\infty}\left\{\begin{array}{l}(A_m\alpha^3 + B_m\alpha^3 y + 3B_m\alpha^2)e^{\alpha y} + \\ (-C_m\alpha^3 - D_m\alpha^3 y + 3D_m\alpha^2)e^{-\alpha y}\end{array}\right\}\cos\alpha x + 6\mu K\end{array}\right]$$

$$= \frac{-E}{(1+\mu)^2}\left[\sum_{m=1}^{\infty}\left\{\begin{array}{l}A_m\alpha(1+\mu)e^{\alpha y} + B_m(\alpha y + \mu\alpha y + 3\mu + 1)e^{\alpha y} \\ -C_m\alpha(1+\mu)e^{-\alpha y} + D_m(-\alpha y - \mu\alpha y + 3\mu + 1)e^{-\alpha y}\end{array}\right\}\alpha^2\cos\alpha x + 6\mu K\right] \qquad (3.7c)$$

$$\sigma_{yy}(x,y) = \frac{-E}{(1+\mu)^2}\left[(2+\mu)\frac{\partial^3\psi}{\partial x^2\partial y} + \frac{\partial^3\psi}{\partial y^3}\right]$$

$$= \frac{-E}{(1+\mu)^2}\left[(2+\mu)\left\{-\sum_{m=1}^{\infty} Y_m'\alpha^2 \cos\alpha x\right\} + \left\{\sum_{m=1}^{\infty} Y_m''' \cos\alpha x + 6K\right\}\right]$$

$$= \frac{-E}{(1+\mu)^2}\left[\begin{array}{l} -(2+\mu)\sum_{m=1}^{\infty}\left\{(A_m\alpha + B_m\alpha y + B_m)e^{\alpha y} + (-C_m\alpha - D_m\alpha y + D_m)e^{-\alpha y}\right\}\alpha^2\cos\alpha x \\ +\sum_{m=1}^{\infty}\left\{\begin{array}{l}(A_m\alpha^3 + B_m\alpha^3 y + 3B_m\alpha^2)e^{\alpha y} + \\ (-C_m\alpha^3 - D_m\alpha^3 y + 3D_m\alpha^2)e^{-\alpha y}\end{array}\right\}\cos\alpha x + 6K \end{array}\right]$$

$$= \frac{-E}{(1+\mu)^2}\left[\sum_{m=1}^{\infty}\left\{\begin{array}{l}A_m\alpha(-1-\mu)e^{\alpha y} + B_m(-\alpha y - \mu\alpha y - \mu + 1)e^{\alpha y} + \\ C_m\alpha(1+\mu)e^{-\alpha y} + D_m(\alpha y + \mu\alpha y - \mu + 1)e^{-\alpha y}\end{array}\right\}\alpha^2\cos\alpha x + 6K\right] \quad (3.7d)$$

$$\sigma_{xy}(x,y) = \frac{-E}{(1+\mu)^2}\left[\frac{\partial^3\psi}{\partial x^3} - \mu\frac{\partial^3\psi}{\partial x\partial y^2}\right]$$

$$= \frac{-E}{(1+\mu)^2}\left[\sum_{m=1}^{\infty}Y_m\alpha^3\sin\alpha x - \mu\left\{-\sum_{m=1}^{\infty}Y_m''\alpha\sin\alpha x\right\}\right]$$

$$= \frac{-E}{(1+\mu)^2}[\sum_{m=1}^{\infty}\left\{(A_m + B_m y)e^{\alpha y} + (C_m + D_m y)e^{-\alpha y}\right\}\alpha^3\sin\alpha x +$$
$$\mu\sum_{m=1}^{\infty}\left\{\begin{array}{l}(A_m\alpha^2 + B_m\alpha^2 y + 2B_m\alpha)e^{\alpha y} + \\ (C_m\alpha^2 + D_m\alpha^2 y - 2D_m\alpha)e^{-\alpha y}\end{array}\right\}\alpha\sin\alpha x]$$

$$= \frac{-E}{(1+\mu)^2}\left[\sum_{m=1}^{\infty}\left\{\begin{array}{l}A_m(1+\mu)\alpha e^{\alpha y} + B_m(\alpha y + \mu\alpha y + 2\mu)e^{\alpha y} \\ +C_m(1+\mu)\alpha e^{-\alpha y} + D_m(\alpha y + \mu\alpha y - 2\mu)e^{-\alpha y}\end{array}\right\}\alpha^2\sin\alpha x\right] \quad (3.7e)$$

Now, the reactions on the bottom boundary (y = 0) are acting over the two supports. It is considered that the supports are located at x=0 to 0.1L and x=0.9L to L respectively. The total length for reaction is 20 percent of beam length, where the load is over the 80 percent. As a result the intensity of reaction is four times of the load intensity. Therefore, the reactions over the beam at the supports can be taken as Fourier series in the following manner:

$$\sigma_{yy}(x,0) = 4\sigma_0 = E_0 + \sum_{m=1}^{\infty}E_m\cos\alpha x \qquad \text{for } x = 0 \text{ to } 0.1L \text{ and } 0.9\text{L to } L \quad (3.8)$$

Here

$$E_0 = \frac{1}{L}\left[\int_0^{L/10}4\sigma_0 dx + \int_{9L/10}^{L}4\sigma_0 dx\right]$$

$$= \frac{4\sigma_0}{L}\left[\frac{L}{10} + L - \frac{9L}{10}\right]$$

$$= \frac{4\sigma_0}{5} \qquad (3.9a)$$

$$E_m = \frac{2}{L}\left[\int_0^{L/10} 4\sigma_0 \cos\alpha x dx + \int_{9L/10}^{L} 4\sigma_0 \cos\alpha x dx\right]$$

$$= \frac{8\sigma_0}{L}\left[\int_0^{L/10} \cos\alpha x dx\right] + \frac{8\sigma_0}{L}\left[\int_{9L/10}^{L} \cos\alpha x dx\right]$$

$$= \frac{8\sigma_0}{L}\left[\frac{\sin\alpha x}{\alpha}\right]_0^{L/10} + \frac{8\sigma_0}{L}\left[\frac{\sin\alpha x}{\alpha}\right]_{9L/10}^{L}$$

$$= \frac{8\sigma_0}{\alpha L}\left\{\sin\left(\frac{\alpha L}{10}\right) + \sin(\alpha L) - \sin\left(\frac{9\alpha L}{10}\right)\right\}$$

$$= \frac{8\sigma_0}{m\pi}\left\{\sin\left(\frac{m\pi}{10}\right) + \sin(m\pi) - \sin\left(\frac{9m\pi}{10}\right)\right\}; \qquad m = 1,2,3, \ldots. \infty \qquad (3.9b)$$

The compressive load on the edge $y = D$ acting over $x = 0.1L$ to $0.9L$ can also be given by a Fourier series as follows

$$\sigma_{yy}(x,0) = \sigma_0 = I_0 + \sum_{m=1}^{\infty} I_m \cos\alpha x \qquad \text{for } x = 0.1L \text{ to } 0.9L \qquad (3.10)$$

Here

$$I_0 = \frac{1}{L}\left[\int_{L/10}^{9L/10} \sigma_0 dx\right]$$

$$= \frac{\sigma_0}{L}\left[\frac{9L}{10} - \frac{L}{10}\right]$$

$$= \frac{4\sigma_0}{5} \qquad (3.11a)$$

$$I_m = \frac{2}{L}\left[\int_{L/10}^{9L/10} \sigma_0 \cos\alpha x dx\right]$$

$$= \frac{2\sigma_0}{L}\left[\frac{\sin \alpha x}{\alpha}\right]_{l/10}^{9L/10}$$

$$= \frac{2\sigma_0}{\alpha L}\left\{\sin\left(\frac{9\alpha L}{10}\right) - \sin\left(\frac{\alpha L}{10}\right)\right\}$$

$$= \frac{2\sigma_0}{m\pi}\left\{\sin\left(\frac{9m\pi}{10}\right) - \sin\left(\frac{m\pi}{10}\right)\right\}; \qquad m = 1,2,3, \ldots\ldots \infty \tag{3.11b}$$

The loading considerations of Eqs. (3.8) and (3.9a) are to satisfy the boundary conditions at the bottom and top boundaries of the beam. Using boundary condition $\sigma_{xy}(x,0) = 0$ at the edge of $y = 0$, it is found that

$$\frac{-E}{(1+\mu)^2}\left[\sum_{m=1}^{\infty}(A_m + C_m)\alpha^3 \sin \alpha x + \mu\sum_{m=1}^{\infty}\left\{\begin{matrix}(A_m\alpha^2 + 2B_m\alpha) + \\ (C_m\alpha^2 - 2D_m\alpha)\end{matrix}\right\}\alpha \sin \alpha x\right] = 0$$

or, $$\frac{-E}{(1+\mu)^2}\left[(A_m + C_m)\alpha^3 + \mu\left\{(A_m\alpha^2 + 2B_m\alpha) + (C_m\alpha^2 - 2D_m\alpha)\right\}\alpha\right] = 0$$

or, $$\frac{-E}{(1+\mu)^2}\left[(1+\mu)\alpha^3 A_m + 2B_m\mu\alpha^2 + (1+\mu)\alpha^3 C_m - 2\mu\alpha^2 D_m\right] = 0$$

or, $$\frac{-E\alpha^2}{(1+\mu)^2}\left[(1+\mu)\alpha A_m + 2\mu B_m + (1+\mu)\alpha C_m - 2\mu D_m\right] = 0 \tag{3.12a}$$

Using boundary condition $\sigma_{xy}(x,D) = 0$ at the edge of $y = D$

$$\frac{-E}{(1+\mu)^2}\left[\begin{matrix}\sum_{m=1}^{\infty}\left\{(A_m + B_m D)e^{\alpha D} + (C_m + D_m D)e^{-\alpha D}\right\}\alpha^3 \sin \alpha x + \\ \mu\sum_{m=1}^{\infty}\left\{\begin{matrix}(A_m\alpha^2 + B_m\alpha^2 D + 2B_m\alpha)e^{\alpha D} + \\ (C_m\alpha^2 + D_m\alpha^2 D - 2D_m\alpha)e^{-\alpha D}\end{matrix}\right\}\alpha \sin \alpha x\end{matrix}\right] = 0$$

or, $$\frac{-E}{(1+\mu)^2}\left[\begin{matrix}\left\{(A_m + B_m D)e^{\alpha D} + (C_m + D_m D)e^{-\alpha D}\right\}\alpha^3 + \\ \mu\left\{\begin{matrix}(A_m\alpha^2 + B_m\alpha^2 D + 2B_m\alpha)e^{\alpha D} + \\ (C_m\alpha^2 + D_m\alpha^2 D - 2D_m\alpha)e^{-\alpha D}\end{matrix}\right\}\alpha\end{matrix}\right] = 0$$

$$\text{or, } \frac{-E\alpha^2}{(1+\mu)^2}\begin{bmatrix} A_m(1+\mu)\alpha e^{\alpha D} + B_m(\alpha D + \mu\alpha D + 2\mu)e^{\alpha D} + \\ C_m(1+\mu)\alpha e^{-\alpha D} + D_m(\alpha D + \mu\alpha D - 2\mu)e^{-\alpha D} \end{bmatrix} = 0 \tag{3.12b}$$

Using boundary condition $\sigma_{yy}(x,0) = 4\sigma_0$ at the edge of $y=0$

$$\frac{-E}{(1+\mu)^2}\begin{bmatrix} -(2+\mu)\sum_{m=1}^{\infty}\{(A_m\alpha + B_m) + (-C_m\alpha + D_m)\}\alpha^2\cos\alpha x \\ +\sum_{m=1}^{\infty}\begin{Bmatrix}(A_m\alpha^3 + 3B_m\alpha^2) + \\ (-C_m\alpha^3 + 3D_m\alpha^2)\end{Bmatrix}\cos\alpha x + 6K \end{bmatrix} = \sum_{m=1}^{\infty} E_m\cos\alpha x + E_o \tag{3.13a}$$

Therefore,

$$\frac{E\alpha^2}{(1+\mu)^2}\begin{bmatrix}(2+\mu)\{(A_m\alpha + B_m) + (-C_m\alpha + D_m)\} \\ -(A_m\alpha + 3B_m) - (-C_m\alpha + 3D_m)\end{bmatrix} = E_m$$

$$\text{or, } \frac{E\alpha^2}{(1+\mu)^2}[A_m(1+\mu)\alpha + B_m(-1+\mu) - C_m(1+\mu)\alpha + D_m(-1+\mu)] = E_m \tag{3.13b}$$

Using boundary condition $\sigma_{yy}(x,D) = \sigma_0$ at the edge of $y = D$

$$\frac{-E}{(1+\mu)^2}\begin{bmatrix} -(2+\mu)\sum_{m=1}^{\infty}\begin{Bmatrix}(A_m\alpha + B_m\alpha D + B_m)e^{\alpha D} + \\ (-C_m\alpha - D_m\alpha D + D_m)e^{-\alpha D}\end{Bmatrix}\alpha^2\cos\alpha x \\ +\sum_{m=1}^{\infty}\begin{Bmatrix}(A_m\alpha^3 + B_m\alpha^3 D + 3B_m\alpha^2)e^{\alpha D} + \\ (-C_m\alpha^3 - D_m\alpha^3 D + 3D_m\alpha^2)e^{-\alpha D}\end{Bmatrix}\cos\alpha x + 6K \end{bmatrix} = \sum_{m=1}^{\infty} I_m\cos\alpha x + I_o \tag{3.14a}$$

Therefore,

$$\frac{E}{(1+\mu)^2}\begin{bmatrix}(2+\mu)\{(A_m\alpha + B_m\alpha D + B_m)e^{\alpha D} + (-C_m\alpha - D_m\alpha D + D_m)e^{-\alpha D}\}\alpha^2 \\ -\{(A_m\alpha^3 + B_m\alpha^3 D + 3B_m\alpha^2)e^{\alpha D} + (-C_m\alpha^3 - D_m\alpha^3 D + 3D_m\alpha^2)e^{-\alpha D}\}\end{bmatrix} = I_m$$

$$\text{or, } \frac{E\alpha^2}{(1+\mu)^2}\left[\begin{matrix} A_m(1+\mu)\alpha e^{\alpha D} + B_m(\mu\alpha D + \alpha D + \mu - 1)e^{\alpha D} - \\ C_m(1+\mu)\alpha e^{-\alpha D} - D_m(\mu\alpha D + \alpha D - \mu + 1)e^{-\alpha D} \end{matrix}\right] = I_m \tag{3.14b}$$

and using Eq. (3.9a) and Eq. (3.13a) the arbitrary constant K can be obtained as follows:

$$\frac{-E}{(1+\mu)^2}6K = E_0 = \frac{4\sigma_0}{5}$$

$$\text{or, } K = \frac{-2\sigma_0(1+\mu)^2}{15E} \tag{3.15}$$

The simultaneous Eqs. (3.12a), (3.12b), (3.13b) and (3.14b) can be realized in a simplified matrix form for the solution of unknown coefficients like A_m, B_m, C_m and D_m as follows:

$$\begin{bmatrix} DD_1 & DD_2 & DD_3 & DD_4 \\ FF_1 & FF_2 & FF_3 & FF_4 \\ HH_1 & HH_2 & HH_3 & HH_4 \\ KK_1 & KK_2 & KK_3 & KK_4 \end{bmatrix}\begin{bmatrix} A_m \\ B_m \\ C_m \\ D_m \end{bmatrix} = \begin{bmatrix} 0 \\ 0 \\ E_m \\ I_m \end{bmatrix} \tag{3.16}$$

Where

$$DD_1 = Z_{11}(1+\mu)\alpha$$
$$DD_2 = 2\mu Z_{11}$$
$$DD_3 = Z_{11}(1+\mu)\alpha$$
$$DD_4 = -2\mu Z_{11}$$

$$FF_1 = Z_{11}(1+\mu)\alpha e^{\alpha D}$$
$$FF_2 = Z_{11}\{(1+\mu)\alpha D + 2\mu\}e^{\alpha D}$$
$$FF_3 = Z_{11}(1+\mu)\alpha e^{-\alpha D}$$
$$FF_4 = Z_{11}\{(1+\mu)\alpha D - 2\mu\}e^{-\alpha D}$$

$$HH_1 = -Z_{11}(1+\mu)\alpha$$
$$HH_2 = -Z_{11}(-1+\mu)$$
$$HH_3 = Z_{11}(1+\mu)\alpha$$
$$HH_4 = -Z_{11}(-1+\mu)$$

$$KK_1 = -Z_{11}(1+\mu)\alpha e^{\alpha D}$$

$$KK_2 = -Z_{11}\{(1+\mu)\alpha D + \mu - 1\}e^{\alpha D}$$
$$KK_3 = Z_{11}(1+\mu)\alpha e^{-\alpha D}$$
$$KK_4 = Z_{11}\{(1+\mu)\alpha D - \mu + 1\}e^{-\alpha D}$$

$$Z_{11} = \frac{-E\alpha^2}{(1+\mu)^2}$$

Once the matrix Eq. (3.16) or four algebraic Eqs. (3.12a), (3.12b), (3.13b) and (3.14b) are solved simultaneously and the values of four unknowns, namely, A_m, B_m, C_m and D_m, are obtained, Eqs. of (3.7) are then used for subsequent finding of stress and displacement components of the beam at various points.

3.3.2 Beam with lateral stiffeners (Case-2)

In this case, the trial function is assumed in terms of sine function so that its first and third derivatives with respect to x can be found in terms of a sine function. The displacement potential function ψ for the case of lateral stiffener is assumed as

$$\psi = \sum_{m=1}^{\infty} Y_m \sin\alpha x \tag{3.17}$$

where $Y_m = f(y)$, $\alpha = \frac{m\pi}{L}$ and K = Arbitrary constant and m = 1, 2, 3, …….. ∞ .

Derivatives of Eq. (3.14) with respect to x and y are

$$\frac{\partial\psi}{\partial x} = \sum_{m=1}^{\infty} Y_m \alpha \cos\alpha x$$
$$\frac{\partial^2\psi}{\partial x^2} = -\sum_{m=1}^{\infty} Y_m \alpha^2 \sin\alpha x$$
$$\frac{\partial^3\psi}{\partial x^3} = -\sum_{m=1}^{\infty} Y_m \alpha^3 \cos\alpha x$$

$$\frac{\partial^4 \psi}{\partial x^4} = \sum_{m=1}^{\infty} Y_m \alpha^4 \sin \alpha x$$

$$\frac{\partial^2 \psi}{\partial x \partial y} = \sum_{m=1}^{\infty} Y_m' \alpha \cos \alpha x$$

$$\frac{\partial^3 \psi}{\partial x \partial y^2} = \sum_{m=1}^{\infty} Y_m'' \alpha \cos \alpha x$$

$$\frac{\partial^3 \psi}{\partial x^2 \partial y} = -\sum_{m=1}^{\infty} Y_m' \alpha^2 \sin \alpha x$$

$$\frac{\partial^4 \psi}{\partial x^2 \partial y^2} = -\sum_{m=1}^{\infty} Y_m'' \alpha^2 \sin \alpha x$$

$$\frac{\partial \psi}{\partial y} = \sum_{m=1}^{\infty} Y_m' \sin \alpha x$$

$$\frac{\partial^2 \psi}{\partial y^2} = \sum_{m=1}^{\infty} Y_m'' \sin \alpha x$$

$$\frac{\partial^3 \psi}{\partial y^3} = \sum_{m=1}^{\infty} Y_m''' \sin \alpha x$$

$$\frac{\partial^4 \psi}{\partial y^4} = \sum_{m=1}^{\infty} Y_m'''' \sin \alpha x$$

Substituting the expressions of above derivatives in Eq. (3.1) following equation is obtained.

$$\sum_{m=1}^{\infty} Y_m \alpha^4 \sin \alpha x - 2\sum_{m=1}^{\infty} Y_m'' \alpha^2 \sin \alpha x + \sum_{m=1}^{\infty} Y_m'''' \sin \alpha x = 0$$

or, $Y_m'''' - 2\alpha^2 Y_m'' + Y_m = 0$ (3.18)

The solution of the above 4th order ordinary differential equation with constant coefficients [Eq. (3.18)] can normally be approximated as follows:

$$Y_m = L_m e^{r_1 y} + M_m y e^{r_2 y} + N_m e^{r_3 y} + O_m y e^{r_4 y} \tag{3.19}$$

But the ordinary differential Eq. (3.18) has the complementary function of repeated roots. Thus $r_1 = r_2 = \alpha$ and $r_3 = r_4 = -\alpha$ and the general solution of Eq. (3.18) can be written as

$$Y_m = (L_m + M_m y)e^{\alpha y} + (N_m + O_m y)e^{-\alpha y} \tag{3.20}$$

Where, L_m, M_m, N_m and O_m are arbitrary constants.

Differentiating Eq. (3.20) following expressions are found

$$Y_m' = (L_m \alpha + M_m \alpha y + M_m)e^{\alpha y} + (-N_m \alpha - O_m \alpha y + O_m)e^{-\alpha y}$$
$$Y_m'' = (L_m \alpha^2 + M_m \alpha^2 y + 2M_m \alpha)e^{\alpha y} + (N_m \alpha^2 + O_m \alpha^2 y - 2O_m \alpha)e^{-\alpha y}$$
$$Y_m''' = (L_m \alpha^3 + M_m \alpha^3 y + 3N_m \alpha^2)e^{\alpha y} + (-N_m \alpha^3 - O_m \alpha^3 y + 3O_m \alpha^2)e^{-\alpha y}$$
$$Y_m'''' = (L_m \alpha^4 + M_m \alpha^4 y + 4M_m \alpha^3)e^{\alpha y} + (N_m \alpha^4 + O_m \alpha^4 y - 4O_m \alpha^3)e^{-\alpha y}$$

Now substituting the derivatives of ψ and Y_m in the expressions for displacement (3.2) and stresses (3.3), following expressions are found.

$$u_x(x,y) = \frac{\partial^2 \psi}{\partial x \partial y}$$

$$= \sum_{m=1}^{\infty} Y'_m \alpha \cos \alpha x$$

$$= \sum_{m=1}^{\infty} \left[(L_m \alpha + M_m \alpha y + M_m)e^{\alpha y} + (-N_m \alpha - O_m \alpha y + O_m)e^{-\alpha y} \right] \alpha \cos \alpha x$$

$$= \sum_{m=1}^{\infty} \left[L_m \alpha e^{\alpha y} + M_m (\alpha y + 1)e^{\alpha y} - N_m \alpha e^{-\alpha y} - O_m (\alpha y - 1)e^{-\alpha y} \right] \alpha \cos \alpha x \tag{3.21a}$$

$$u_y(x,y) = -\frac{1}{(1+\mu)}\left[2\frac{\partial^2\psi}{\partial x^2} + (1-\mu)\frac{\partial^2\psi}{\partial y^2}\right]$$

$$= -\frac{1}{(1+\mu)}\left[2\left\{-\sum_{m=1}^{\infty} Y_m\alpha^2\sin\alpha x\right\} + (1-\mu)\left\{\sum_{m=1}^{\infty} Y_m''\sin\alpha x\right\}\right]$$

$$= -\frac{1}{(1+\mu)}\left[\begin{array}{l} -2\sum_{m=1}^{\infty}\left\{(L_m + M_m y)e^{\alpha y} + (N_m + O_m y)e^{-\alpha y}\right\}\alpha^2\sin\alpha x + (1-\mu) \\ \sum_{m=1}^{\infty}\left\{\begin{array}{l}(L_m\alpha^2 + M_m\alpha^2 y + 2M_m\alpha)e^{\alpha y} + \\ (N_m\alpha^2 + O_m\alpha^2 y - 2O_m\alpha)e^{-\alpha y}\end{array}\right\}\sin\alpha x \end{array}\right]$$

$$= \frac{-1}{(1+\mu)}\left[\sum_{m=1}^{\infty}\left\{\begin{array}{l} -L_m(1+\mu)\alpha^2 e^{\alpha y} + \\ M_m(-\alpha y - \mu\alpha y - 2\mu + 2)\alpha e^{\alpha y} \\ -N_m(1+\mu)\alpha^2 e^{-\alpha y} + \\ O_m(-\alpha y - \mu\alpha y + 2\mu - 2)\alpha e^{-\alpha y}\end{array}\right\}\sin\alpha x\right] \qquad (3.21b)$$

$$\sigma_{xx}(x,y) = \frac{E}{(1+\mu)^2}\left[\frac{\partial^3\psi}{\partial x^2\partial y} - \mu\frac{\partial^3\psi}{\partial y^3}\right]$$

$$= \frac{E}{(1+\mu)^2}\left[\left\{-\sum_{m=1}^{\infty} Y_m'\alpha^2\sin\alpha x\right\} - \mu\left\{\sum_{m=1}^{\infty} Y_m'''\sin\alpha x\right\}\right]$$

$$= \frac{-E}{(1+\mu)^2}\left[\begin{array}{l}\sum_{m=1}^{\infty}\left\{(L_m\alpha + M_m\alpha y + M_m)e^{\alpha y} + (-N_m\alpha - O_m\alpha y + O_m)e^{-\alpha y}\right\}\alpha^2\sin\alpha x \\ +\mu\sum_{m=1}^{\infty}\left\{\begin{array}{l}(L_m\alpha^3 + M_m\alpha^3 y + 3M_m\alpha^2)e^{\alpha y} + \\ (-N_m\alpha^3 - O_m\alpha^3 y + 3O_m\alpha^2)e^{-\alpha y}\end{array}\right\}\sin\alpha x\end{array}\right]$$

$$= \frac{-E}{(1+\mu)^2}\left[\sum_{m=1}^{\infty}\left\{\begin{array}{l}L_m\alpha(1+\mu)e^{\alpha y} + M_m(\alpha y + \mu\alpha y + 3\mu + 1)e^{\alpha y} \\ -N_m\alpha(1+\mu)e^{-\alpha y} + O_m(-\alpha y - \mu\alpha y + 3\mu + 1)e^{-\alpha y}\end{array}\right\}\alpha^2\sin\alpha x\right] \qquad (3.21c)$$

$$\sigma_{yy}(x,y) = \frac{-E}{(1+\mu)^2}\left[(2+\mu)\frac{\partial^3\psi}{\partial x^2\partial y} + \frac{\partial^3\psi}{\partial y^3}\right]$$

$$= \frac{-E}{(1+\mu)^2}\left[(2+\mu)\left\{-\sum_{m=1}^{\infty} Y_m'\alpha^2\sin\alpha x\right\} + \left\{\sum_{m=1}^{\infty} Y_m'''\sin\alpha x\right\}\right]$$

$$= \frac{-E}{(1+\mu)^2}\left[\begin{array}{l} -(2+\mu)\sum_{m=1}^{\infty}\left\{(L_m\alpha + M_m\alpha y + N_m)e^{\alpha y} + (-N_m\alpha - O_m\alpha y + O_m)e^{-\alpha y}\right\}\alpha^2 \sin\alpha x \\ +\sum_{m=1}^{\infty}\left\{\begin{array}{l}(L_m\alpha^3 + M_m\alpha^3 y + 3M_m\alpha^2)e^{\alpha y} + \\ (-N_m\alpha^3 - O_m\alpha^3 y + 3O_m\alpha^2)e^{-\alpha y}\end{array}\right\}\sin\alpha x \end{array}\right]$$

$$= \frac{-E}{(1+\mu)^2}\left[\sum_{m=1}^{\infty}\left\{\begin{array}{l} L_m\alpha(-1-\mu)e^{\alpha y} + M_m(-\alpha y - \mu\alpha y - \mu + 1)e^{\alpha y} + \\ N_m\alpha(1+\mu)e^{-\alpha y} + O_m(\alpha y + \mu\alpha y - \mu + 1)e^{-\alpha y}\end{array}\right\}\alpha^2 \sin\alpha x\right] \tag{3.21d}$$

$$\sigma_{xy}(x,y) = \frac{-E}{(1+\mu)^2}\left[\frac{\partial^3\psi}{\partial x^3} - \mu\frac{\partial^3\psi}{\partial x\partial y^2}\right]$$

$$= \frac{-E}{(1+\mu)^2}\left[-\sum_{m=1}^{\infty}Y_m\alpha^3\cos\alpha x - \mu\left\{-\sum_{m=1}^{\infty}Y_m^{"}\alpha\cos\alpha x\right\}\right]$$

$$= \frac{E}{(1+\mu)^2}[\sum_{m=1}^{\infty}\left\{(L_m + M_m y)e^{\alpha y} + (N_m + O_m y)e^{-\alpha y}\right\}\alpha^3\cos\alpha x +$$
$$\mu\sum_{m=1}^{\infty}\left\{\begin{array}{l}(L_m\alpha^3 + M_m\alpha^2 y + 2M_m\alpha)e^{\alpha y} + \\ (N_m\alpha^3 + O_m\alpha^2 y - 2O_m\alpha)e^{-\alpha y}\end{array}\right\}\alpha\cos\alpha x]$$

$$= \frac{E}{(1+\mu)^2}\left[\sum_{m=1}^{\infty}\left\{\begin{array}{l} L_m(1+\mu)\alpha e^{\alpha y} + M_m(\alpha y + \mu\alpha y + 2\mu)e^{\alpha y} \\ +N_m(1+\mu)\alpha e^{-\alpha y} + O_m(\alpha y + \mu\alpha y - 2\mu)e^{-\alpha y}\end{array}\right\}\alpha^2\cos\alpha x\right] \tag{3.21e}$$

Now, the reactions on the bottom boundary ($y = 0$) are acting over the two supports. Therefore, the reactions over the beam at the supports can be taken as Fourier series in the following manner:

$$\sigma_{yy}(x,0) = 4\sigma_0 = E_0 + \sum_{m=1}^{\infty}E_m\sin\alpha x \qquad \text{for } x = 0 \text{ to } 0.1L \text{ and } 0.9L \text{ to } L \tag{3.22}$$

Here

$$E_0 = 0 \tag{3.23a}$$

$$E_m = \frac{2}{L}\left[\int_0^{L/10} 4\sigma_0 \sin\alpha x dx + \int_{9L/10}^{L} 4\sigma_0 \sin\alpha x dx\right]$$

$$= \frac{8\sigma_0}{L}\left[\int_0^{L/10} \sin\alpha x dx\right] + \frac{8\sigma_0}{L}\left[\int_{9L/10}^{L} \sin\alpha x dx\right]$$

$$= -\frac{8\sigma_0}{L}\left[\frac{\cos\alpha x}{\alpha}\right]_0^{L/10} + \frac{8\sigma_0}{L}\left[-\frac{\cos\alpha x}{\alpha}\right]_{9L/10}^{L}$$

$$= -\frac{8\sigma_0}{\alpha L}\left\{\cos\left(\frac{\alpha L}{10}\right) - 1 + \cos(\alpha L) - \cos\left(\frac{9\alpha L}{10}\right)\right\}$$

$$= -\frac{8\sigma_0}{m\pi}\left\{\cos\left(\frac{m\pi}{10}\right) - 1 + \cos(m\pi) - \cos\left(\frac{9m\pi}{10}\right)\right\}; \qquad m = 1,2,3, \ldots. \infty \qquad (3.23b)$$

The compressive load on the edge $y = D$ acting over $x = 0.1L$ to $0.9L$ can also be given by a Fourier series as follows

$$\sigma_{yy}(x,0) = \sigma_0 = I_0 + \sum_{m=1}^{\infty} I_m \sin\alpha x \qquad \text{for } x = 0.1L \text{ to } 0.9L \qquad (3.24)$$

Here

$$I_0 = 0 \qquad (3.25a)$$

$$I_m = \frac{2}{L}\left[\int_{L/10}^{9L/10} \sigma_0 \sin\alpha x dx\right]$$

$$= -\frac{2\sigma_0}{L}\left[\frac{\cos\alpha x}{\alpha}\right]_{l/10}^{9L/10}$$

$$= -\frac{2\sigma_0}{m\pi}\left\{\cos\left(\frac{9m\pi}{10}\right) - \cos\left(\frac{m\pi}{10}\right)\right\}; \qquad m = 1,2,3, \ldots\ldots. \infty \qquad (3.25b)$$

The loading considerations of Eqns. (3.22) and (3.23a) are to satisfy the boundary conditions at the bottom and top boundaries of the beam. Using boundary condition $\sigma_{xy}(x,0) = 0$ at the edge of y=0, it is found that

$$\frac{E}{(1+\mu)^2}\left[\sum_{m=1}^{\infty}(L_m+M_m)\alpha^3\sin\alpha x+\mu\sum_{m=1}^{\infty}\left\{\begin{matrix}(L_m\alpha^2+2M_m\alpha)+\\(N_m\alpha^2-2O_m\alpha)\end{matrix}\right\}\alpha\cos\alpha x\right]=0$$

or, $$\frac{E}{(1+\mu)^2}\left[(L_m+M_m)\alpha^3+\mu\{(L_m\alpha^2+2M_m\alpha)+(N_m\alpha^2-2O_m\alpha)\}\alpha\right]=0$$

or, $$\frac{E\alpha^2}{(1+\mu)^2}\left[(1+\mu)\alpha L_m+2\mu M_m+(1+\mu)\alpha N_m-2\mu O_m\right]=0 \qquad (3.26a)$$

Using boundary condition $\sigma_{xy}(x,D)=0$ at the edge of $y=D$

$$\frac{E}{(1+\mu)^2}\left[\begin{matrix}\sum_{m=1}^{\infty}\{(L_m+M_mD)e^{\alpha D}+(N_m+O_mD)e^{-\alpha D}\}\alpha^3\sin\alpha x+\\ \mu\sum_{m=1}^{\infty}\left\{\begin{matrix}(L_m\alpha^2+M_m\alpha^2D+2M_m\alpha)e^{\alpha D}+\\(N_m\alpha^2+O_m\alpha^2D-2O_m\alpha)e^{-\alpha D}\end{matrix}\right\}\alpha\sin\alpha x\end{matrix}\right]=0$$

or, $$\frac{E}{(1+\mu)^2}\left[\begin{matrix}\{(L_m+M_mD)e^{\alpha D}+(N_m+O_mD)e^{-\alpha D}\}\alpha^3+\\ \mu\left\{\begin{matrix}(L_m\alpha^2+M_m\alpha^2D+2N_m\alpha)e^{\alpha D}+\\(N_m\alpha^2+O_m\alpha^2D-2O_m\alpha)e^{-\alpha D}\end{matrix}\right\}\alpha\end{matrix}\right]=0$$

or, $$\frac{E\alpha^2}{(1+\mu)^2}\left[\begin{matrix}L_m(1+\mu)\alpha e^{\alpha D}+M_m(\alpha D+\mu\alpha D+2\mu)e^{\alpha D}+\\N_m(1+\mu)\alpha e^{-\alpha D}+O_m(\alpha D+\mu\alpha D-2\mu)e^{-\alpha D}\end{matrix}\right]=0 \qquad (3.26b)$$

Using boundary condition $\sigma_{yy}(x,0)=4\sigma_0$ at the edge of $y=0$

$$\frac{-E}{(1+\mu)^2}\left[\begin{matrix}-(2+\mu)\sum_{m=1}^{\infty}\{(L_m\alpha+M_m)+(-N_m\alpha+O_m)\}\alpha^2\sin\alpha x\\ +\sum_{m=1}^{\infty}\left\{\begin{matrix}(L_m\alpha^3+3M_m\alpha^2)+\\(-N_m\alpha^3+3O_m\alpha^2)\end{matrix}\right\}\sin\alpha x\end{matrix}\right]=\sum_{m=1}^{\infty}E_m\sin\alpha x+E_o \qquad (3.27a)$$

Therefore,

$$\frac{E\alpha^2}{(1+\mu)^2}\begin{bmatrix}(2+\mu)\{(L_m\alpha+M_m)+(-N_m\alpha+O_m)\}\\-(L_m\alpha+3M_m)-(-N_m\alpha+3O_m)\end{bmatrix}=E_m$$

$$\text{or, } \frac{E\alpha^2}{(1+\mu)^2}\left[L_m(1+\mu)\alpha+M_m(-1+\mu)-N_m(1+\mu)\alpha+O_m(-1+\mu)\right]=E_m \qquad (3.27b)$$

Using boundary condition $\sigma_{yy}(x,D)=\sigma_0$ at the edge of $y=D$

$$\frac{-E}{(1+\mu)^2}\begin{bmatrix}-(2+\mu)\sum_{m=1}^{\infty}\left\{\begin{matrix}(L_m\alpha+M_m\alpha D+M_m)e^{\alpha D}+\\(-N_m\alpha-O_m\alpha D+O_m)e^{-\alpha D}\end{matrix}\right\}\alpha^2\sin\alpha x\\+\sum_{m=1}^{\infty}\left\{\begin{matrix}(L_m\alpha^3+M_m\alpha^3D+3N_m\alpha^2)e^{\alpha D}+\\(-O_m\alpha^3-O_m\alpha^3D+3O_m\alpha^2)e^{-\alpha D}\end{matrix}\right\}\sin\alpha x\end{bmatrix}=\sum_{m=1}^{\infty}I_m\sin\alpha x+I_o \qquad (3.28a)$$

$$\text{or, } \frac{E}{(1+\mu)^2}\begin{bmatrix}(2+\mu)\{(L_m\alpha+M_m\alpha D+M_m)e^{\alpha D}+(-N_m\alpha-O_m\alpha D+O_m)e^{-\alpha D}\}\alpha^2\\-\{(L_m\alpha^3+M_m\alpha^3D+3M_m\alpha^2)e^{\alpha D}+(-N_m\alpha^3-O_m\alpha^3D+3O_m\alpha^2)e^{-\alpha D}\}\end{bmatrix}=I_m$$

$$\text{or, } \frac{E\alpha^2}{(1+\mu)^2}\begin{bmatrix}L_m(1+\mu)\alpha e^{\alpha D}+M_m(\mu\alpha D+\alpha D+\mu-1)e^{\alpha D}-\\N_m(1+\mu)\alpha e^{-\alpha D}-O_m(\mu\alpha D+\alpha D-\mu+1)e^{-\alpha D}\end{bmatrix}=I_m \qquad (3.28b)$$

The simultaneous Eqs. (3.26a), (3.26b), (3.27b) and (3.28b) can be realized in a simplified matrix form for the solution of unknown terms like L_m, M_m, N_m and O_m as follows:

$$\begin{bmatrix}EE_1 & EE_2 & EE_3 & EE_4\\GG_1 & GG_2 & GG_3 & GG_4\\II_1 & II_2 & II_3 & II_4\\JJ_1 & JJ_2 & JJ_3 & JJ_4\end{bmatrix}\begin{bmatrix}L_m\\M_m\\N_m\\O_m\end{bmatrix}=\begin{bmatrix}0\\0\\E_m\\I_m\end{bmatrix} \qquad (3.29)$$

Where,

$$EE_1 = Z_{11}(1+\mu)\alpha$$
$$EE_2 = 2\mu Z_{11}$$
$$EE_3 = Z_{11}(1+\mu)\alpha$$
$$EE_4 = -2\mu Z_{11}$$

$$GG_1 = Z_{11}(1+\mu)\alpha e^{\alpha D}$$
$$GG_2 = Z_{11}\{(1+\mu)\alpha D + 2\mu\}e^{\alpha D}$$
$$GG_3 = Z_{11}(1+\mu)\alpha e^{-\alpha D}$$
$$GG_4 = Z_{11}\{(1+\mu)\alpha D - 2\mu\}e^{-\alpha D}$$

$$II_1 = -Z_{11}(1+\mu)\alpha$$
$$II_2 = -Z_{11}(-1+\mu)$$
$$II_3 = Z_{11}(1+\mu)\alpha$$
$$II_4 = -Z_{11}(-1+\mu)$$

$$JJ_1 = -Z_{11}(1+\mu)\alpha e^{\alpha D}$$
$$JJ_2 = -Z_{11}\{(1+\mu)\alpha D + \mu - 1\}e^{\alpha D}$$
$$JJ_3 = Z_{11}(1+\mu)\alpha e^{-\alpha D}$$
$$JJ_4 = Z_{11}\{(1+\mu)\alpha D - \mu + 1\}e^{-\alpha D}$$
$$Z_{11} = \frac{E\alpha^2}{(1+\mu)^2}$$

Once the matrix Eq. (3.29) or four algebraic Eqs. (3.26a), (3.26b), (3.27b) and (3.28b) are solved simultaneously and the values of four unknowns, namely, L_m, M_m, N_m and O_m, are obtained, Eqs. of (3.21) are then used for subsequent finding of stress and displacement components of the beam at various points.

3.4 Results of Displacement Potential Solution

The analytical solutions of displacement and stress components are obtained using displacement potential function for various aspect ratios (*L/D*) of the stiffened deep beam taking steel material into consideration both for axial stiffeners (Case-1) and lateral stiffeners (Case-2) .The properties of the material considered for solutions are as follows:

Table 3.1 Properties of the isotropic material used in the present study

Material	E (MPa)	G (MPa)	μ
Steel	209000	4500	0.3

At first by considering axial stiffener (Case-1) the result of a stiffened beam of steel material having aspect ratio three (L/D = 3) and the uniform loading parameter, σ_o= 40 N/mm on the top edge is presented in sequence of axial displacement (u_x), lateral displacement (u_y), bending stress (σ_{xx}), normal stress (σ_{yy}) and shearing stress (σ_{xy}). The same procedure is then used for the results of the beam with lateral stiffener (Case-2). Thereafter, the effects of change of aspect ratio and on the elastic fields are observed from the solution.

3.4.1 Solution of the beam with axial stiffeners (Case-1)

Axial displacements (u_x) are found zero at the mid section of span, at the lateral stiffened boundaries and over the mid-horizontal plane [Fig. 3.2(a) and (b)]. Zero value of u_x at the stiffened boundaries confirms the satisfaction of boundary condition of those ends. Axial displacements are found to be symmetric about the mid-vertical plane. The magnitudes of axial displacement at the top half are quite less than those of bottom half of the beam. The values of u_x are negative for sections $0<x/L< 0.5$ and positive for $0.5<x/L<1.0$. The maximum magnitude of u_x/L=0.0016 is observed at sections x/L = 0.1 and 0.9 of the bottom surface, where the loads terminate from both sides of the beam.

Lateral displacements (u_y) near the two lateral ends are found to take positive value because of the supports at the bottom boundary, and for the region $0.2<x/L<0.8$, displacements are negative [Fig. 3.3(a) and (b)]. In the present problem, there is no restriction on the lateral displacement other than the loading at the top edge and balanced at the bottom corners of the beam to bring the equilibrium condition. The result confirms this physical condition being pushed the corners up and mid-region down. The positive and negative maximum lateral displacements are $u_y/D=0.000225$ and $u_y/D= -0.00017$, respectively. The positive maximum value is observed at the two ends on the lowest fibre and the negative maximum value is found on the top fibre at the mid section of the beam.

Fig. 3.4 presents the deformed shape of the beam together with the original shape with the magnification of 500 times of displacement. The stiffened ends have gone up and at the same time centre region of the beam have gone down. The deformation of the top edge is uniform throughout the length of beam with the uniformly distributed loading. The bottom edge is also deformed uniformly except the support region, where there is very little non-uniformity of deformation. However, the overall vertical sliding type deformation is again in excellent agreement with the applied loading and support of the beam.

Bending stress distribution is more or less non-linear over the whole span [Fig. 3.5(a) and (b)]. This non-linearity increases towards the stiffened ends. The stress (σ_{xx}) maximizes at the top and bottom edges of the beam but carries opposite sign. The maximum normalized values at the top and bottom fibre are 3.368 and -5.243 respectively. Near the stiffened ends, σ_{xx} is positive for the upper half and negative for the lower half of the beam, but the opposite is observed for sections away from the support.

Fig. 3.6 reveals that the lateral stress (σ_{yy}) gets its highest value around the position of supports on the bottom edge. As per the loading configuration, the uniform load is distributed over 80% of beam length (from $x/L= 0.1$ to $x/L=0.9$) and support reaction is distributed over 20% of beam length ($x/L= 0.0$ to 0.1 and $x/L=0.9$ to 1.0). Therefore, the reaction at each support is four times of the load density. From the solution of displacement potential approach it is comprehensible

that the normalized value of the lateral stress is zero where load is absent at the top layer and unity in the loaded region. The magnitude of the normalized value is four at the bottom layer of the support region and zero in the free region. This is in full agreement with the applied loading as well as boundary condition.

Four edges and mid-span section of the stiffened beam are found free from shearing stress [Fig. 3.7(a) and (b)]. The distributions of shearing stress (σ_{xy}) conform to the standard parabolic profile except that at sections x/L= 0.1 and 0.9, *i.e.*, the termination point of loading [Fig. 3.1]. The maximum shear stress is observed at y/D=0.2 of sections x/L=0.1 (σ_{xy}/σ_0 = - 1.512) and x/L=0.9 (σ_{xy}/σ_0 =1.512).

3.4.2 Solution of the beam with lateral stiffeners (Case-2)

Axial displacements (u_x) are found zero at the mid section of span and positive or negative at the lateral stiffened boundaries [Fig. 3.8(a) and (b)]. Positive or negative values of u_x at the stiffened boundaries confirm the satisfaction of boundary condition of those ends. Axial displacements are found to be symmetric about the mid-vertical plane. The significant values of u_x are negative for beam depths $0<y/D<0.5$ and positive for $0.5<y/D<1.0$. The maximum magnitude of u_x/L=3.2708 is observed on bottom fibre at the sections of x/L = 0.1 and 0.9, where the loads terminate from both sides of the beam.

Lateral displacements (u_y) near the two lateral ends are found zero and for the rest of region $0.0<x/L<1.0$, displacements are negative [Fig. 3.9(a) and (b)]. In the present problem, there is no restriction on the axial displacement other than the loading at the top edge and balanced at the bottom corners of the beam to bring the equilibrium condition. The result confirms this physical condition being pushed the supporting portions up and mid-region down. The negative maximum lateral displacement is u_y/D= -0.00078028 and it is observed immediate lowest fibre at the mid section of the beam.

Fig. 3.10 presents the deformed shape of the isotropic beam for lateral stiffener along with its original shape at the magnification of 500 times of displacement. The stiffened ends are displaced in the axial direction and at the same time loading portion is displaced down from original shape of the beam. However, the overall axial sliding type deformation is in excellent agreement with the physical condition of applied loading and support of the stiffened beam.

Bending stress distribution is more or less non-linear over the whole span [Fig. 3.11(a) and (b)]. This non-linearity becomes zero towards the stiffened ends. The stress (σ_{xx}) maximizes at the top and bottom edges of the beam but carries opposite sign. The maximum normalized values at the top and bottom fibre are 5.5898 and -5.5720 respectively. At the stiffened ends, σ_{xx} is zero for both the upper half and lower half of the beam, whereas it is positive for upper half and negative for lower half of the beam if we advanced towards the mid section of the beam from stiffened ends.

Fig. 3.12 reveals that the lateral stress (σ_{yy}) gets its highest value around the position of supports on the bottom edge and becomes zero at a the stiffened ends. As per the loading configuration, the uniform load is distributed over 80% of beam length (from x/L= 0.1 to x/L=0.9) and support reaction is distributed over 20% of beam length (x/L= 0.0 to 0.1 and x/L=0.9 to 1.0). Therefore, the reaction at each support is four times of the load density. From the solution of displacement potential approach it is comprehensible that the normalized value of the lateral stress is zero where load is absent at the bottom layer and unity in the loaded region. The magnitude of the normalized value is four at the bottom layer of the support region and zero in the free region. This is a full agreement with the applied loading as well as boundary condition.

Four edges of the stiffened beam experience non zero shearing stress whereas mid-span section of the beam is found free from shearing stress [Fig. 3.13(a) and (b)]. The distributions of shearing stress (σ_{xy}) conform to the standard parabolic profile except that at sections x/L= 0.1 and 0.9, *i.e.*, the termination point of loading [Fig. 3.1]. The maximum shear stress is observed at y/D=0.4 of sections x/L=0.15 (σ_{xy}/σ_0 = - 1.516) and x/L=0.9 (σ_{xy}/σ_0 =1.512).

3.5 Effect of Beam Aspect ratio on the Stress fields

The effect of the aspect ratio (*L/D*) on the stress components are discussed in this chapter. The stress components are observed with respect to beam depth (*y/D*) for both axial and lateral stiffening conditions and also for various *L/D* ratios from 1 to 4 at different sections of the beam.

3.5.1 Beam with axial stiffeners (Case-1)

The bending stresses for various aspect ratios (*L/D*=1 to 4) at different sections of the beam are observed as shown in Fig. 3.14 (a) and (b). It is seen that the nonlinearity of bending stress is highest at the stiffened end, while aspect ratio is one and it gets reduced with the increase of aspect ratio. For higher *L/D* ratio at the mid region (*x/L*=0.4 to 0.6) of the beam, the bending stress distribution is quite linear [Fig. 3.14(b)], whereas it is still nonlinear for aspect ratio one or two. However, the maximum magnitude of bending stress is increasing with the increase of *L/D* ratio.

The lateral stress distributions for *L/D*=1 to 4 at sections from stiffened end to middle of the span (*x/L*=0.0 to 0.5) are shown in Fig. 3.15 (a) and (b). As appeared from the figures that lateral stresses in all *L/D* ratios follow the loading pattern. With the increase of *L/D* ratio the nonlinearity reduces, but some degree of nonlinearity remains. Lateral stress at the guided ends as shown in Fig. 3.15(a) indicates that the distribution pattern changes while the length depth ratio is changed. This pattern changing phenomenon is less with respect to sections moving away from the guide. At the mid sections it is almost insignificant.

Shear stress is zero at the stiffened ends and at the mid span for all *L/D* ratios. Therefore, the results at *x/L*=0.1 to 0.4 (4 sections) are shown in Fig. 3.16 (a) and (b), where the shearing stress distribution patterns for *L/D*=1 are found quite different from others. With the rise of

length depth ratio parabolic pattern of shear stress distribution is observed with higher value of maximum shear stress magnitude. The accuracy of parabolic pattern becomes finer at the sections away from the stiffened ends.

3.5.2 Beam with lateral stiffeners (Case-2)

The bending stress distribution is zero at the stiffened end of the beam for various aspect ratios. That's why section x/L=0.1 and mid span section is considered in Fig. 3.17(a) and (b) for various aspect ratios (L/D=1-4). At section x/L=0.1, all the bending stress distribution is non linear and maximum non linearity is observed for lower aspect ratio L/D=1.0. Now advancing towards the midsection of the beam x/L=0.5, the nonlinearity is still observed for lower aspect ratio L/D=1, whereas it is almost linear for higher aspect ratio L/D=4.

Again section x/L=0.1 is considered instead of stiffened end in Fig. 3.18(a) and (b), because the lateral stress distributions at the stiffened end is zero. At Fig. 3.18(a), maximum non linearity is observed at lower aspect ratio L/D=1. Now advancing towards the higher aspect ratio, this non linearity decreases and lowest non linearity is observed at aspect ratio L/D=4. Now to get the overall idea of lateral stress, mid span section x/L=0.5 is considered for L/D=1 to 4 in Fig. 3.18(b) and it is observed that the change of lateral stress distribution is insignificant with respect to beam aspect ratio.

Fig. 3.19(a) and (b) describe the shearing stress distribution at section x/L=0.1 and 0.4 for different beam aspect ratios (L/D=1-4). Stiffened end section (x/L=0) and mid span section (x/L=0.5) is not considered because the shearing stress distribution is zero at those sections. At section x/L=0.1, the value of shear stress is maximum within beam depth $0 \leq y/D \leq 0.05$ and the difference between these values with respect to beam aspect ratio is too small. Now by advancing towards section x/L=0.4, the distribution pattern becomes parabolic and the difference between the shear stress increases with the increase of beam aspect ratio.

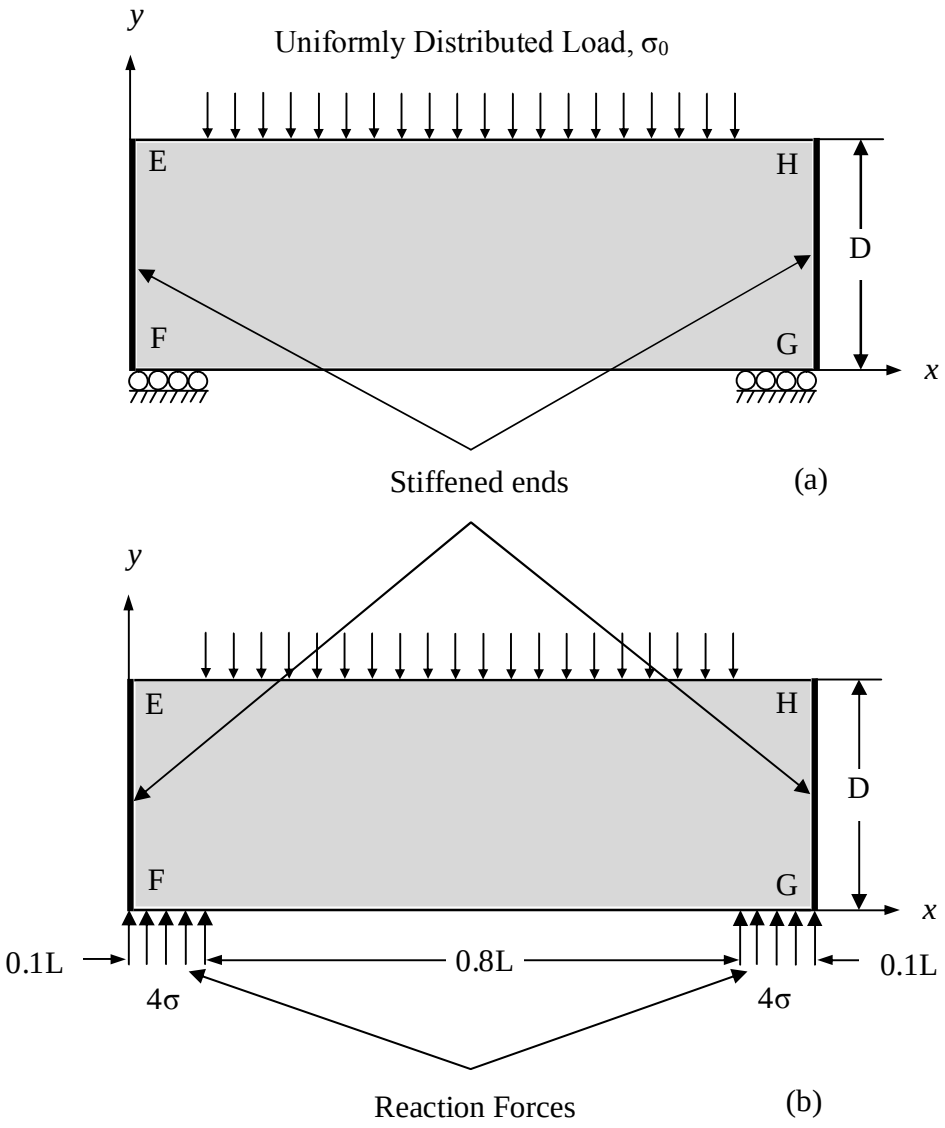

Fig. 3.1 A stiffened simply-supported beam of isotropic material:
(a) Physical model, (b) Analytical model

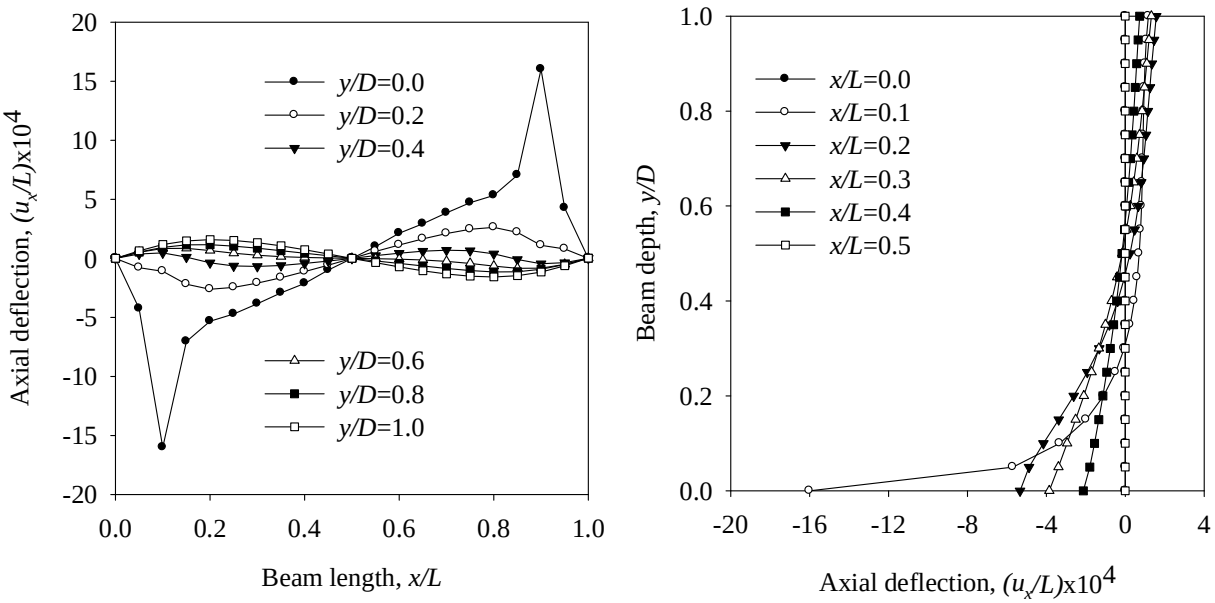

(a) along beam span (b) along beam depth

Fig. 3.2 Distribution of normalized axial displacement components at different sections of the beam with axial stiffener (L/D=3): (a) along beam span, (b) along beam depth

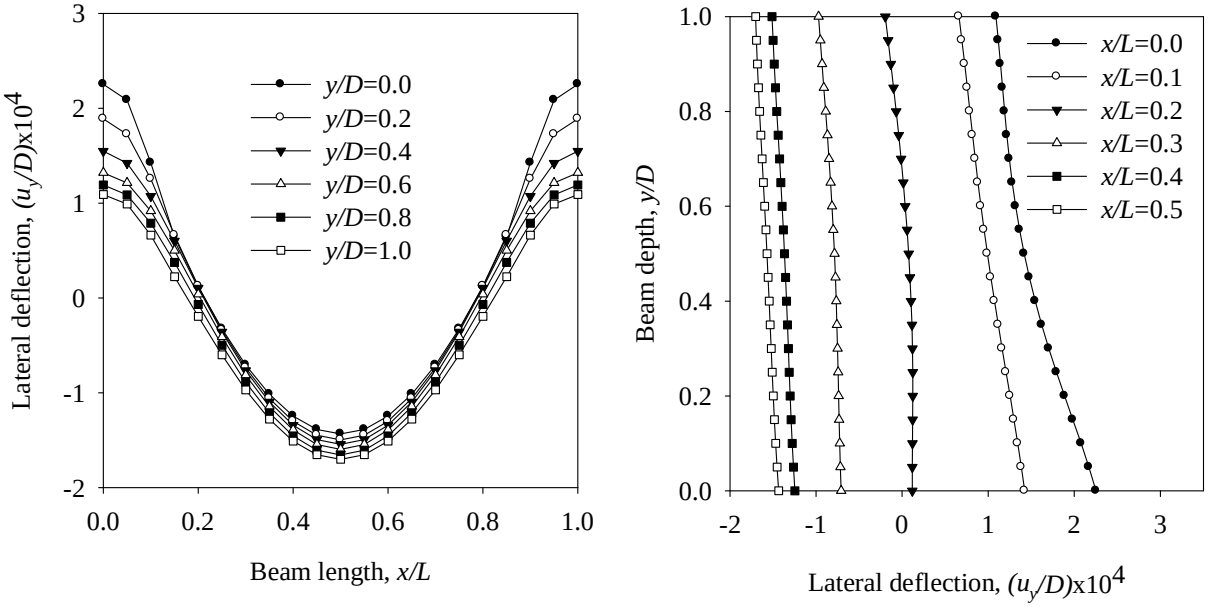

(a) along beam span

(b) along beam depth

Fig. 3.3 Distribution of normalized lateral displacement components at different sections of the beam with axial stiffener (L/D=3): (a) along beam span, (b) along beam depth

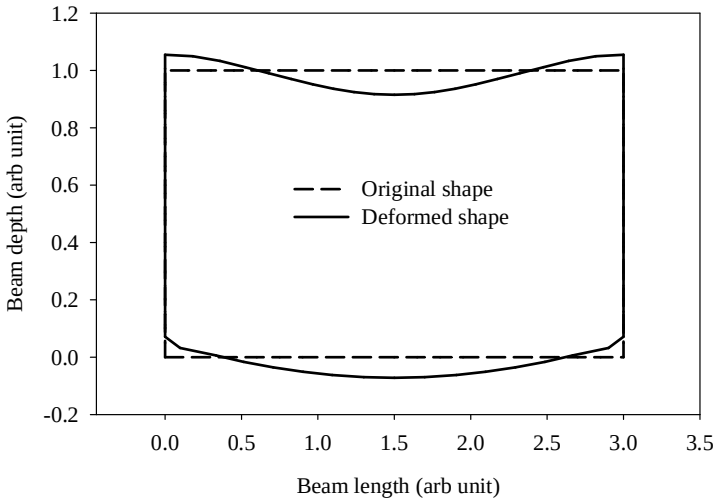

Fig. 3.4 Deformed shape of the stiffened (axial) isotropic thick beam, $L/D = 3$ (magnification factor ×500)

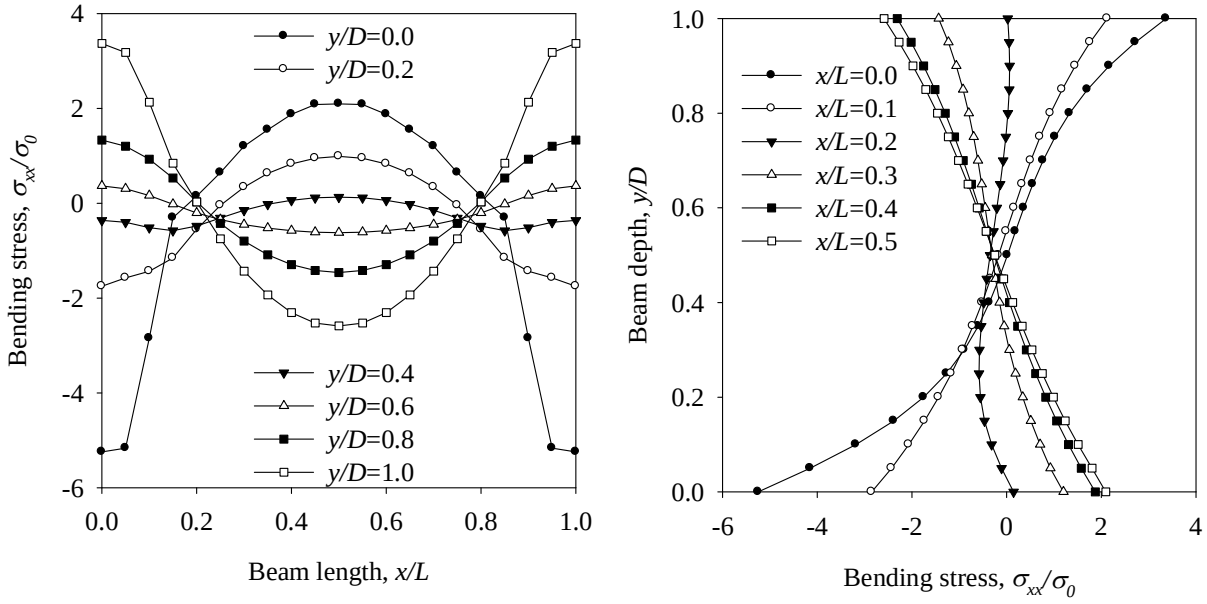

(a) along beam span

(b) along beam depth

Fig. 3.5 Distribution of normalized bending stress components at different sections of the beam with axial stiffener (L/D=3): (a) along beam span, (b) along beam depth

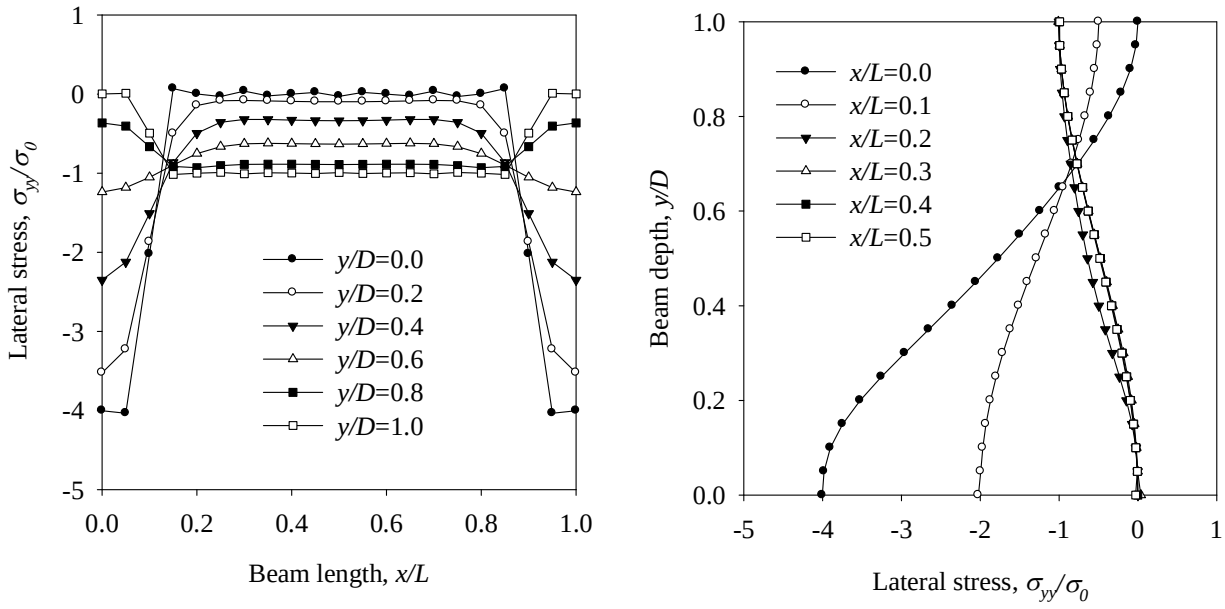

(a) along beam span (b) along beam depth

Fig. 3.6 Distribution of normalized lateral stress components at different sections of the beam with axial stiffener (L/D=3): (a) along beam span, (b) along beam depth

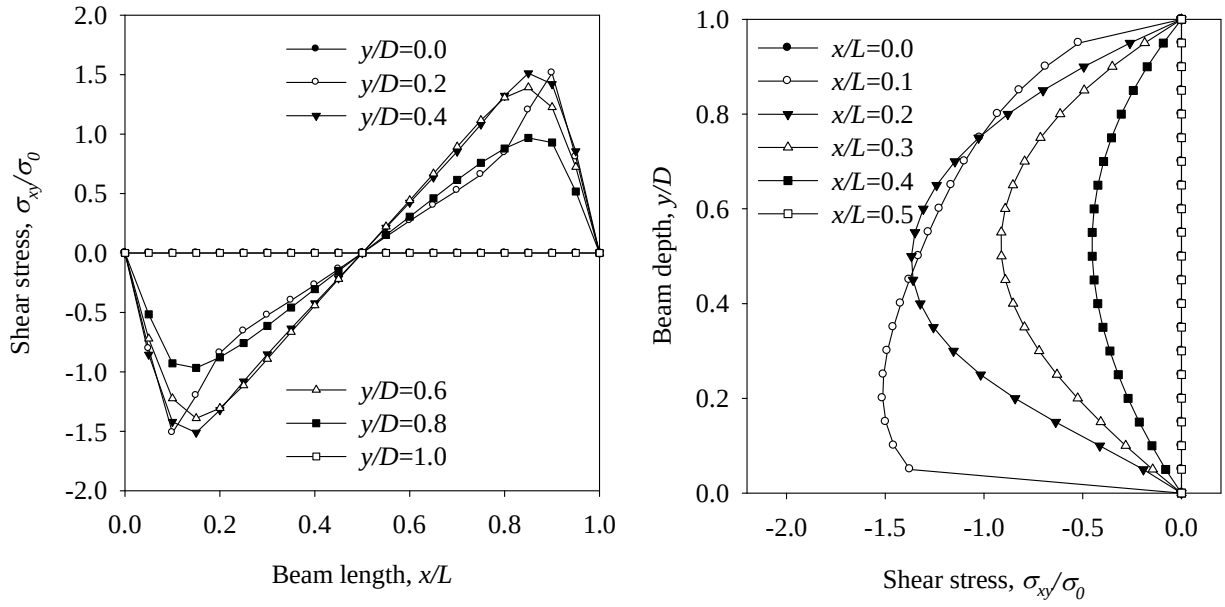

(a) along beam span

(b) along beam depth

Fig. 3.7 Distribution of normalized shear stress components at different sections of the beam with axial stiffener (L/D=3): (a) along beam span, (b) along beam depth

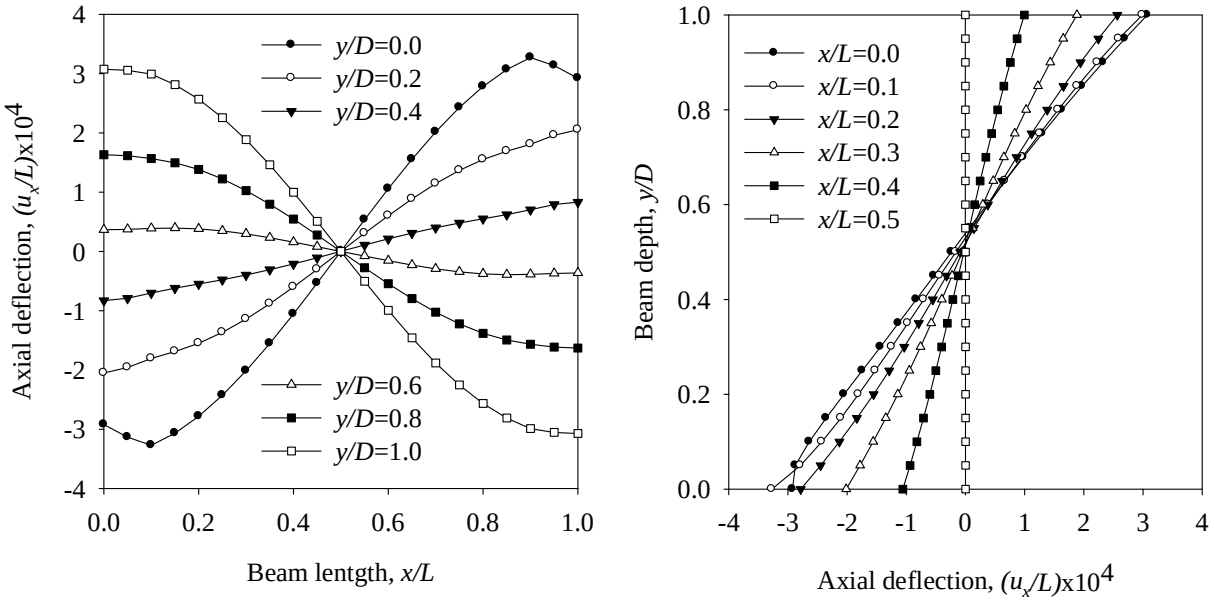

(a) along beam span

(b) along beam depth

Fig. 3.8 Distribution of normalized axial displacement components at different sections of the beam with lateral stiffener (L/D=3): (a) along beam span, (b) along beam depth

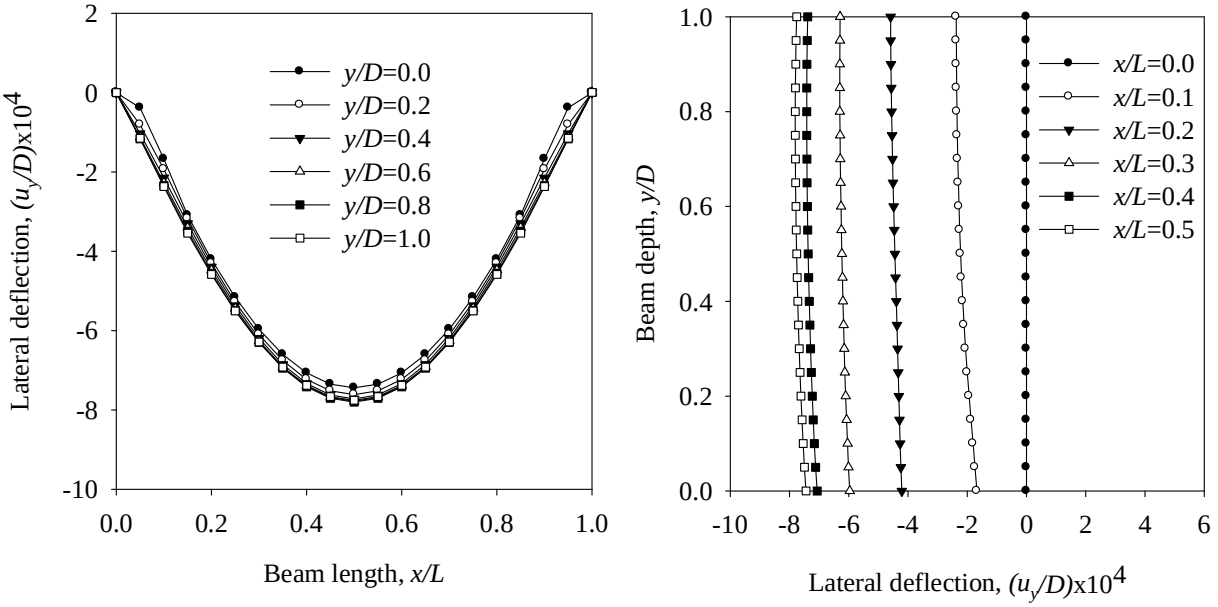

(a) along beam span

(b) along beam depth

Fig. 3.9 Distribution of normalized lateral displacement components at different sections of the beam with lateral stiffener (L/D=3): (a) along beam span, (b) along beam depth

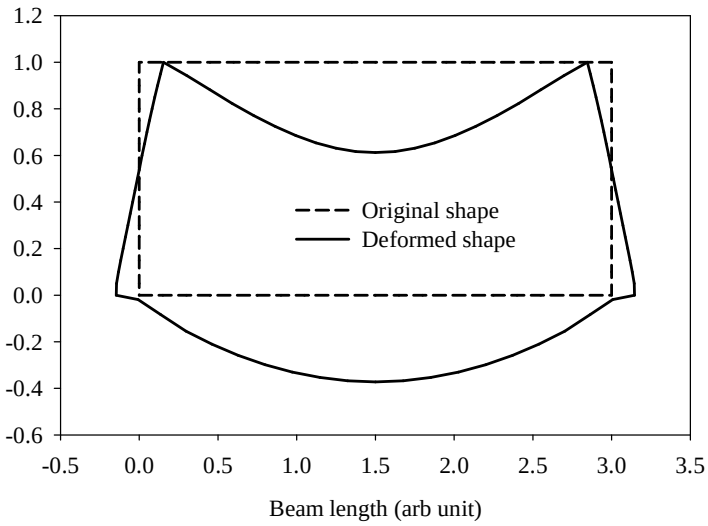

Fig. 3.10 Deformed shape of the stiffened (lateral) isotropic thick beam, $L/D = 3$ (magnification factor ×500)

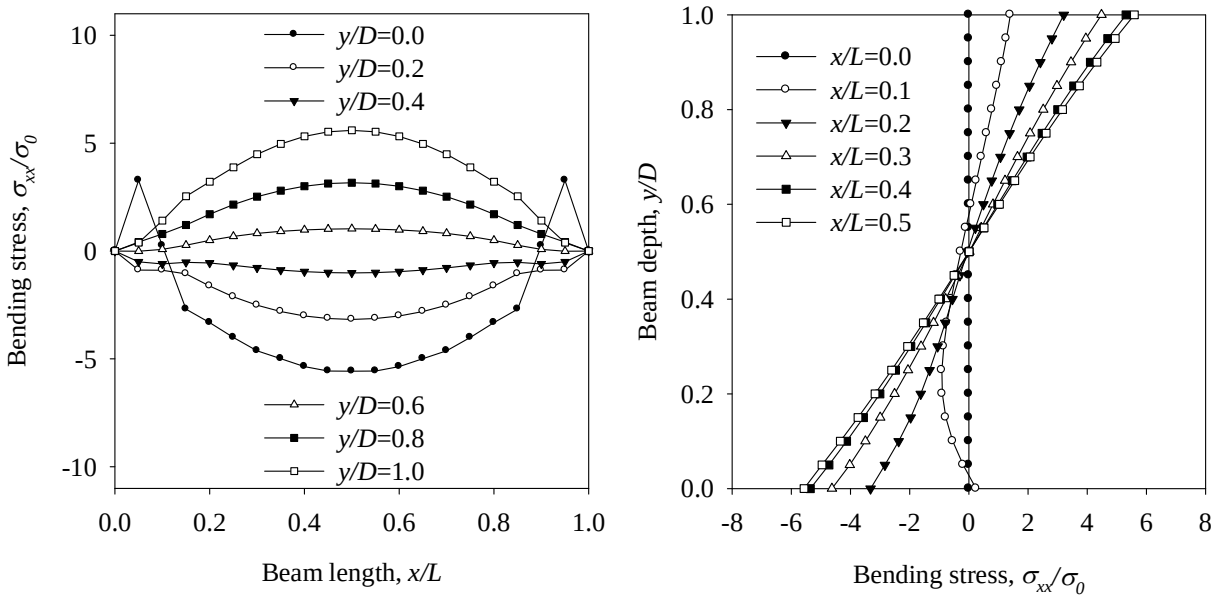

(a) along beam span

(b) along beam depth

Fig. 3.11 Distribution of normalized bending stress components at different sections of the beam with lateral stiffener (L/D=3): (a) along beam span, (b) along beam depth

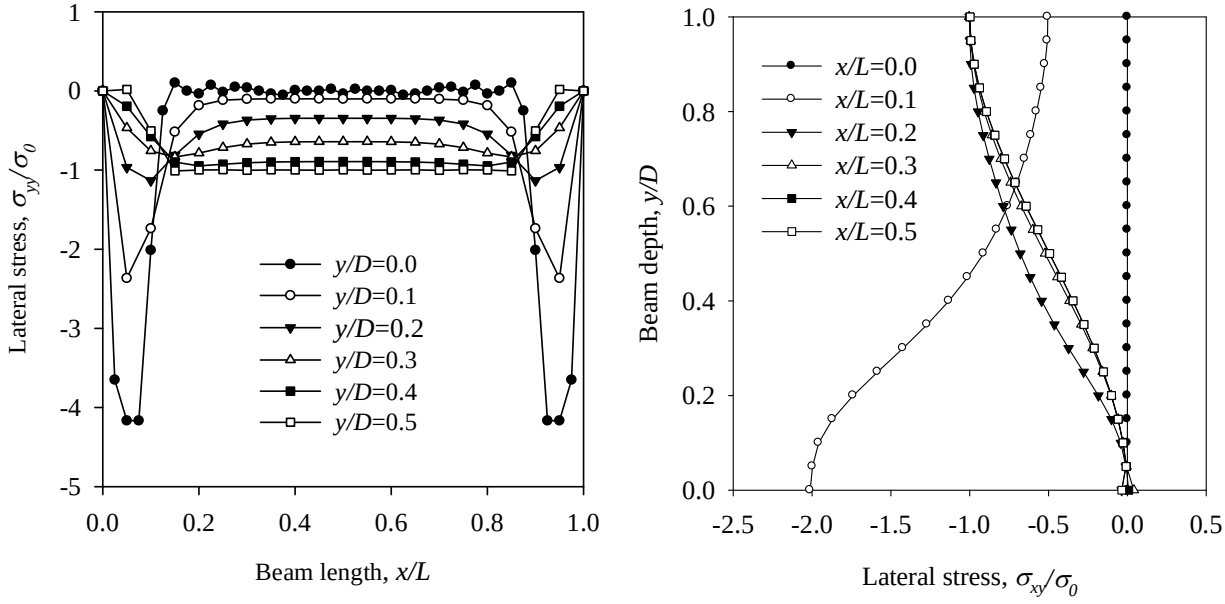

(a) along beam span

(b) along beam depth

Fig. 3.12 Distribution of normalized lateral stress components at different sections of the beam with lateral stiffener (L/D=3): (a) along beam span, (b) along beam depth

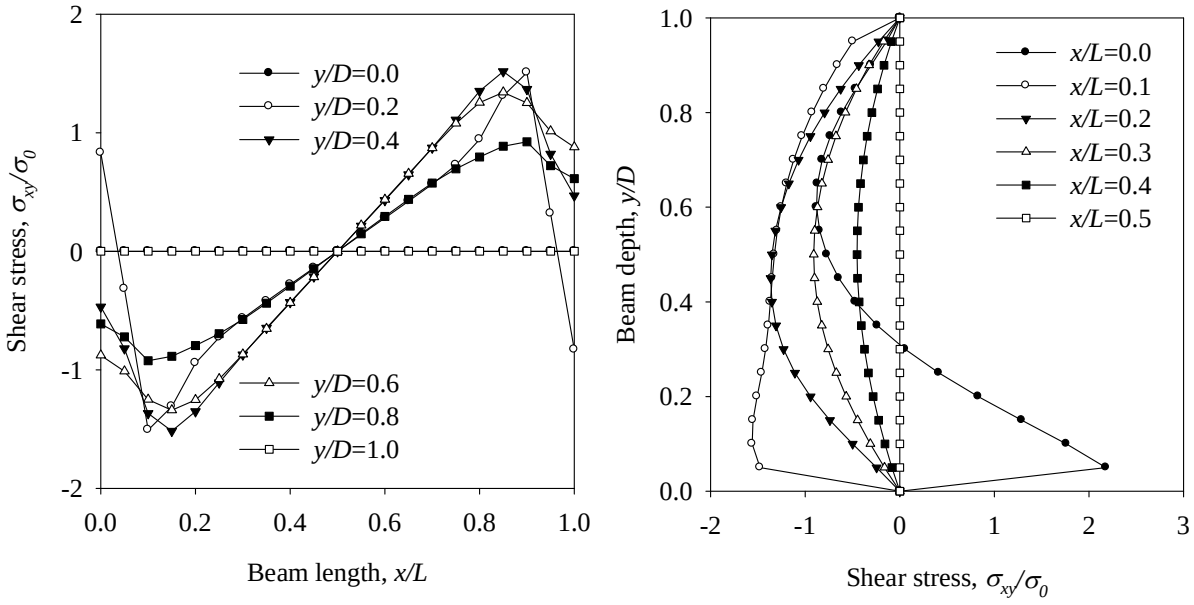

(a) along beam span

(b) along beam depth

Fig. 3.13 Distribution of normalized shear stress components at different sections of the beam with lateral stiffener (L/D=3): (a) along beam span, (b) along beam depth

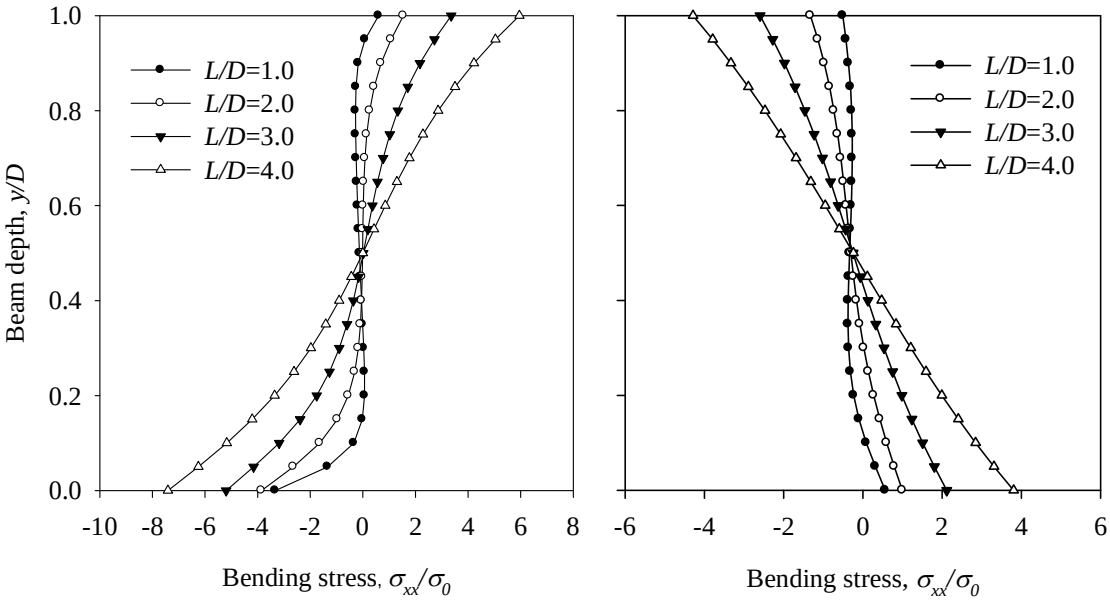

(a) at left lateral end (b) at mid-span section

Fig. 3.14 Distribution of bending stress components at different sections of the stiffened (axial) beam for different aspect ratios: (a) at left lateral end, (b) at mid-span section

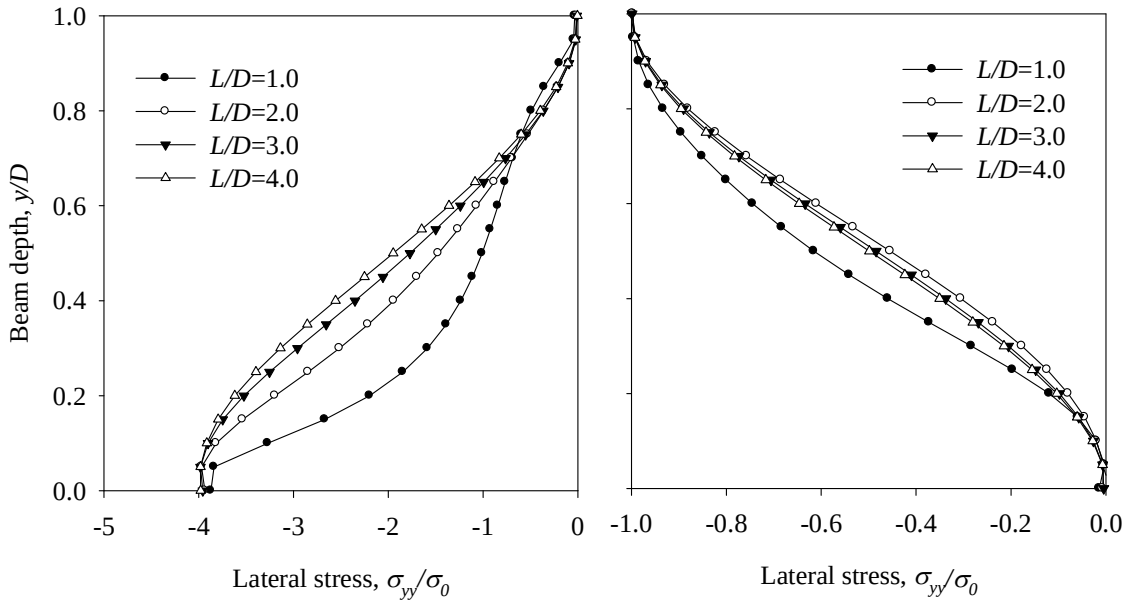

(a) at left lateral end

(b) at mid-span section

Fig. 3.15 Distribution of lateral stress at different sections of the stiffened (axial) beam for different aspect ratios: (a) at left lateral end, (b) at mid-span section

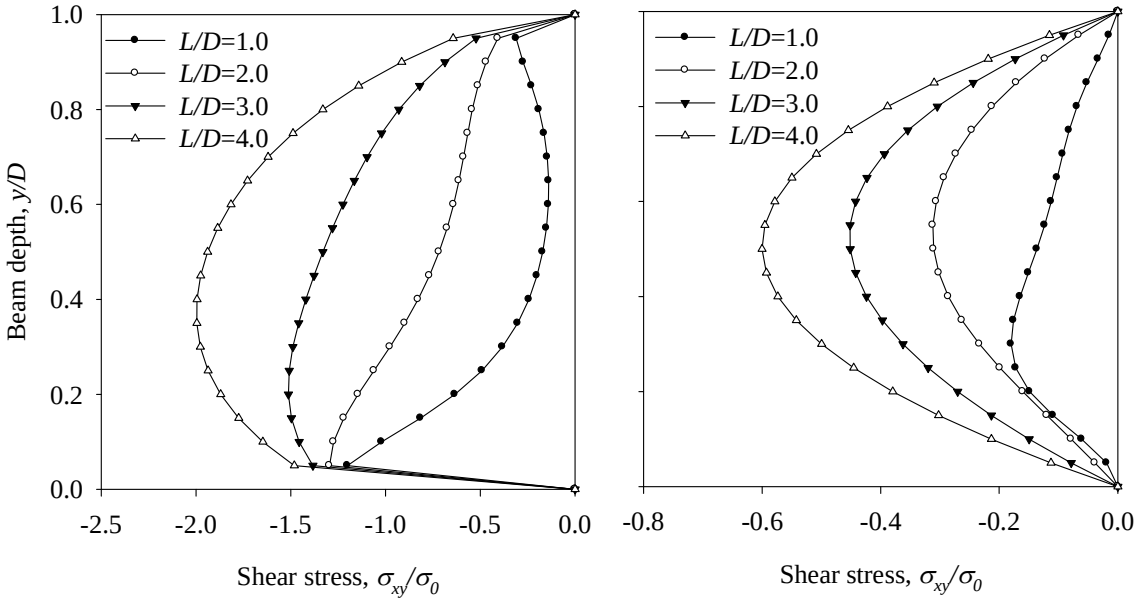

(a) at section x/L=0.1

(b) at section x/L=0.4

Fig. 3.16 Distribution of shear stress at different sections of the stiffened (axial) beam for different aspect ratios: (a) at section x/L=0.1, (b) at section x/L=0.4

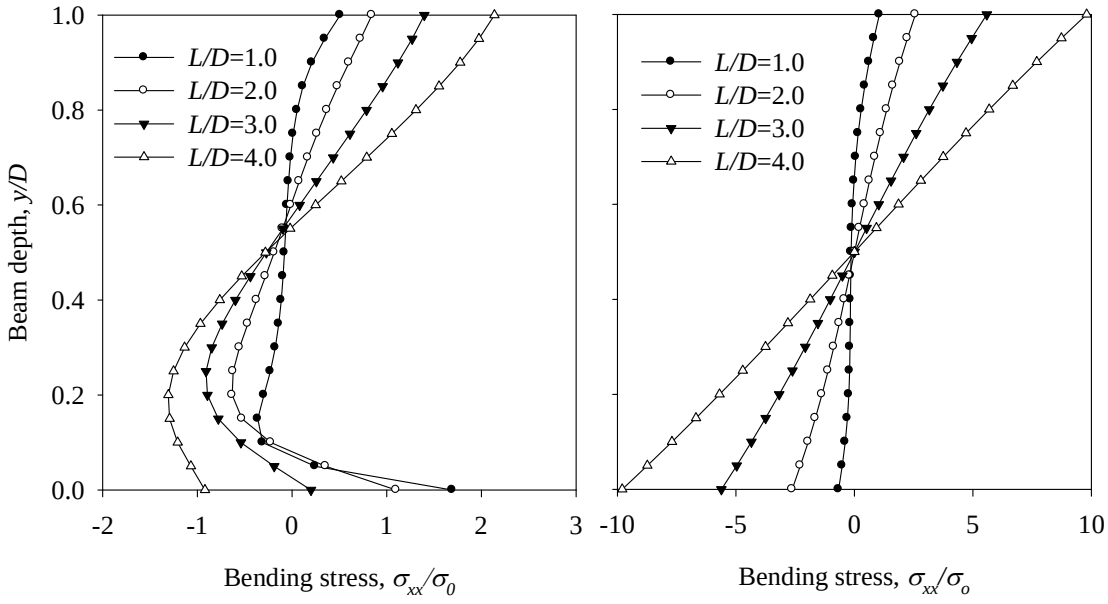

(a) at section x/L=0.1 (b) at mid-span section

Fig. 3.17 Distribution of bending stress at different sections of the stiffened (lateral) beam for different aspect ratios: (a) at section x/L=0.1, (b) at mid-span section

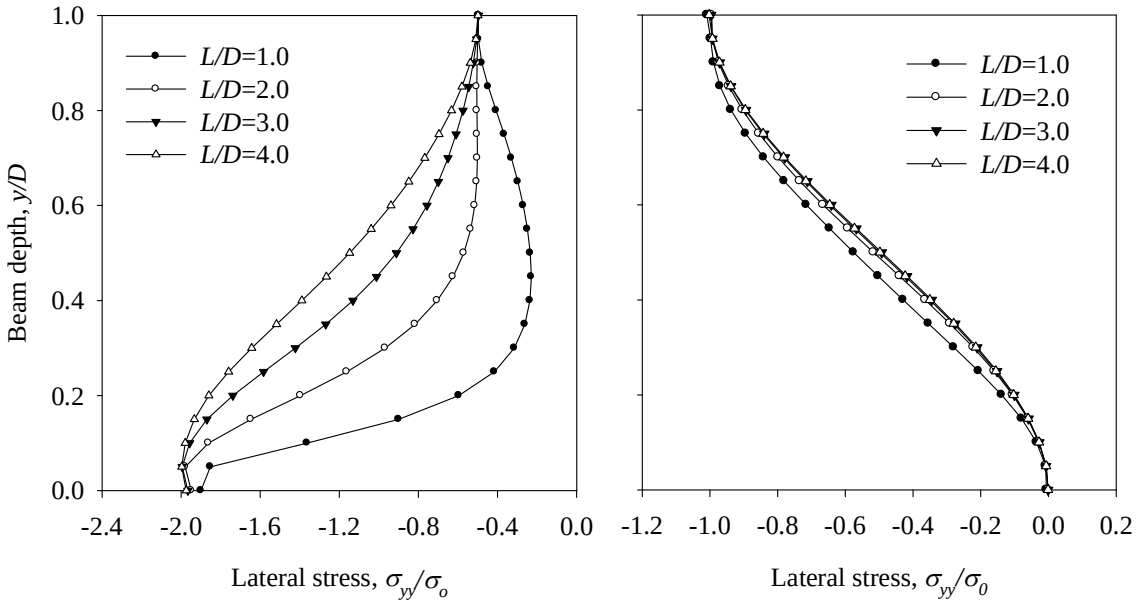

(a) at section x/L=0.1 (b) at mid-span section

Fig. 3.18 Distribution of lateral stress at different sections of the stiffened (lateral) beam for different aspect ratios: (a) at section x/L=0.1, (b) at mid-span section

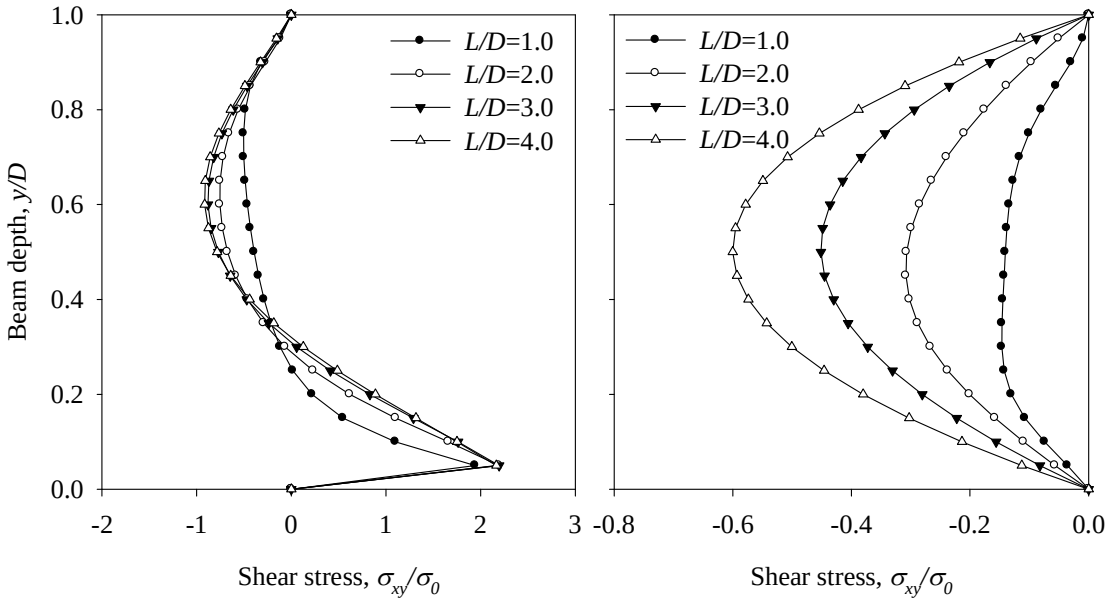

(a) at section x/L=0.1 (b) at section x/L=0.4

Fig. 3.19 Distribution of shear stress at different sections of the stiffened (lateral) beam for different aspect ratios: (a) at section x/L=0.1, (b) at section x/L=0.4

CHAPTER 4

ANALYSIS OF A STIFFENED FIBER REINFORCED COMPOSITE BEAM

The main focus of this chapter is to investigate the effect of stiffeners on the elastic field of a mixed boundary value problem using displacement potential function approach. In this chapter, a stiffened simply supported thick beam of orthotropic composite material is considered for the analysis. The beam is stiffened at its opposing lateral ends by using two different kinds of stiffeners, i.e., axial stiffeners and lateral stiffeners. The beam is loaded transversely at a certain portion on its upper surface and roller supports are used at certain portions of the lower surface of the beam. The effect of beam aspect ratio on the stress field is also discussed in a comparative fashion for both kinds of stiffeners.

4.1 Problem Description

A uniform rectangular composite beam of length L, depth D and thickness W is considered for the present analysis. The beam is subjected to a uniformly distributed load at its upper surface and is simply supported at the two extreme regions of the bottom surface. The beam is in equilibrium with a uniform loading σ_0 acting over 80% of its span (from $0.1L$ to $0.9L$) at the upper surface ($y = D$), and distributed reactions from $x = 0$ to $0.1L$ and $x = 0.9L$ to L at the bottom surface ($y = 0$), as shown in Fig. 4.1. It is noted that the chosen analytical model of the beam is similar to those treated by Chow [3, 4] and Hardy and Pipelzadeh [15]. The lateral ends of the beam, EF and HG are assumed to be stiffened with rigid stiffeners. Two different types of stiffeners are considered for the opposing lateral ends of the beam, which are axial stiffener (Case-1) and lateral stiffener (Case-2). The beam is considered to be of unit thickness and the fibers are assumed to be oriented along the length of the beam (x-axis, Fig. 4.1).

4.2 Boundary Conditions

The physical conditions of the present problem with reference to Fig. 4.1 [(a) and (b)] are to be satisfied along the all four boundaries of the beam can be expressed mathematically as follows:

(a) Loaded boundary, EH ($y = D$):

The loading at the upper boundary is modelled by assigning a uniform value to the normal stress component, which is also free from any shearing stress. The corresponding mathematical expressions of the conditions are

$$\sigma_{yy}(x, D) = \begin{cases} -\sigma_0 & [0.1 \le x/L \le 0.9] \\ 0 & [\text{otherwise}] \end{cases}$$

$$\sigma_{xy}(x, D) = 0 \quad [0.0 \le x/L \le 1.0]$$

(b) Supporting surface, FG ($y = 0$):

The roller supported regions of the bottom surface are modelled by a uniform distribution of normal loading which is free from shearing stress. At the supports, the total reaction forces are considered to be equal and opposite to the loading applied at the top surface. The reactions are distributed over 20% of the beam span (*i.e.*, x/L = 0.0-0.1 and 0.9-1.0). The remaining section of the bottom surface is assumed to be free from loading.

$$\sigma_{xy}(x, 0) = 0 \qquad [0.0 \le x/L \le 1.0]$$

$$\sigma_{yy}(x, 0) = \begin{cases} -4\sigma_0 & [0.0 \le x/L \le 0.1;\ 0.9 \le x/L \le 1.0] \\ 0 & [\text{otherwise}] \end{cases}$$

(c) Left lateral end, EF ($x = 0$):

Axial stiffener (Case-1): The physical condition of the rigid axial stiffener is modelled here by assigning zero values to both the axial displacement and the associated tangential stress components along the end. Thus,

$$\left.\begin{aligned} u_x(0, y) &= 0 \\ \sigma_{xy}(0, y) &= 0 \end{aligned}\right\} \quad [0.0 \le y/D \le 1.0]$$

Lateral stiffener (Case-2): The physical condition of the rigid lateral stiffener is modelled here by considering the boundary free from lateral displacement and axial normal stress. Thus,

$$\left.\begin{aligned} u_y\,(0,\,y)\;&=0\\ \sigma_{xx}\,(0,y)&=0\end{aligned}\right\} \qquad [0.0 \le y/D \le 1.0]$$

(d) Right lateral end, GH ($x = L$):

Axial stiffener (Case-1): Likewise the case of left lateral end, the corresponding mathematical expressions for the conditions of rigid axial stiffener at this boundary are

$$\left.\begin{aligned} u_x\,(L,\,y)\;&=0\\ \sigma_{xy}\,(L,y)&=0\end{aligned}\right\} \qquad [0.0 \le y/D \le 1.0]$$

Lateral stiffener (Case-2): The conditions of rigid lateral stiffener at the right lateral end are modelled by the following expressions:

$$\left.\begin{aligned} u_y\,(L,\,y)\;&=0\\ \sigma_{xx}\,(L,y)&=0\end{aligned}\right\} \qquad [0.0 \le y/D \le 1.0]$$

4.3 Analytical Solution

4.3.1 Approach

Based on the potential-function formulation, an analytical scheme is developed for the analysis of the stiffened simply-supported beams. In the present scheme, a trial solution to the potential function ψ is first assumed as a function of coordinate parameters (x, y) in the form of an infinite series. More specifically, the solution is expressed as an infinite series of combinations of two independent functions of x and y, which assumes a form like, $\psi(x,y) = \sum_m g_m(x)\, h_m(y)$.

A suitable form of the function is determined in a trial and error fashion so that it can automatically satisfy the prescribed physical conditions of the two opposing lateral ends of the

beam. Substitution of the trial solution into the governing differential equation results in a fourth-order ordinary differential equation. A general solution to the ordinary differential equation is then assumed in terms of four arbitrary constants. These four constants are determined by satisfying the remaining four physical conditions associated with the top and bottom surfaces of the beam. By knowing the values of the four arbitrary constants the trial solution assumed for the beam problem is explicitly known. Once the appropriate potential function for the beam is explicitly determined, all the parameters of interest of the elastic field can readily be obtained, as in the present potential-function formulation, they are expressed as the summation of different derivatives of the function, ψ.

4.3.2 Solution procedure

The governing differential equation for the present composite beam is expressed in terms of the potential function, ψ through the following partial differential equation of equilibrium [Eq. (2.30)]:

$$E_1 G_{12} \frac{\partial^4 \psi}{\partial x^4} + E_2 \left(E_1 - 2\mu_{12} G_{12}\right) \frac{\partial^4 \psi}{\partial x^2 \partial y^2} + E_2 G_{12} \frac{\partial^4 \psi}{\partial y^4} = 0 \tag{4.1}$$

In this case the displacement and stress components are also obtained from Eq. (2.29) as follows:

$$u_x(x,y) = \frac{\partial^2 \psi}{\partial x \partial y} \tag{4.2a}$$

$$u_y(x,y) = -\frac{1}{Z_{11}} \left[E_1^2 \frac{\partial^2 \psi}{\partial x^2} + G_{12} \left(E_1 - \mu_{12}^2 E_2\right) \frac{\partial^2 \psi}{\partial y^2} \right] \tag{4.2b}$$

$$\sigma_{xx}(x,y) = \frac{E_1 G_{12}}{Z_{11}} \left[E_1 \frac{\partial^3 \psi}{\partial x^2 \partial y} - \mu_{12} E_2 \frac{\partial^3 \psi}{\partial y^3} \right] \tag{4.2c}$$

$$\sigma_{yy}(x,y) = \frac{E_1 E_2}{Z_{11}} \left[\left(\mu_{12} G_{12} - E_1\right) \frac{\partial^3 \psi}{\partial x^2 \partial y} - G_{12} \frac{\partial^3 \psi}{\partial y^3} \right] \tag{4.2d}$$

$$\sigma_{xy}(x,y) = -\frac{E_1 G_{12}}{Z_{11}}\left[E_1 \frac{\partial^3 \psi}{\partial x^3} - \mu_{12} E_2 \frac{\partial^3 \psi}{\partial x \partial y^2}\right] \tag{4.2e}$$

Where $Z_{11} = \mu_{12} E_1 E_2 + G_{12}\left(E_1 - \mu_{12}^2 E_2\right)$

4.3.3 Beam with axial stiffeners (Case-1)

The trial function for the present problem is assumed in terms of a cosine function so that its first and third derivatives with respect to *x* are obtained in terms of a sine function. It is observed that such a trial solution is capable of satisfying the necessary physical conditions associated with the two opposing lateral ends automatically, which are given by the conditions of 'c' and 'd' of section 4.2. Considering all these factors, the potential function, ψ for the present problem is approximated as follows:

$$\psi = \sum_{m=1}^{\infty} Y_m \cos \alpha x + K y^3 \tag{4.3}$$

where $Y_m = f(y)$, $\alpha = \dfrac{m\pi}{L}$ and K = Arbitrary constant and m = 1, 2, 3, …….. ∞.

Derivatives of Eq. (4.3) with respect to x and y are

$$\frac{\partial \psi}{\partial x} = -\sum_{m=1}^{\infty} Y_m \alpha \sin \alpha x$$

$$\frac{\partial^2 \psi}{\partial x^2} = -\sum_{m=1}^{\infty} Y_m \alpha^2 \cos \alpha x$$

$$\frac{\partial^3 \psi}{\partial x^3} = \sum_{m=1}^{\infty} Y_m \alpha^3 \sin \alpha x$$

$$\frac{\partial^4 \psi}{\partial x^4} = \sum_{m=1}^{\infty} Y_m \alpha^4 \cos \alpha x$$

$$\frac{\partial^2\psi}{\partial x\partial y} = -\sum_{m=1}^{\infty} Y_m^{'}\alpha \sin\alpha x$$

$$\frac{\partial^3\psi}{\partial x\partial y^2} = -\sum_{m=1}^{\infty} Y_m^{''}\alpha \sin\alpha x$$

$$\frac{\partial^3\psi}{\partial x^2\partial y} = -\sum_{m=1}^{\infty} Y_m^{'}\alpha^2 \cos\alpha x$$

$$\frac{\partial^4\psi}{\partial x^2\partial y^2} = -\sum_{m=1}^{\infty} Y_m^{''}\alpha^2 \cos\alpha x$$

$$\frac{\partial\psi}{\partial y} = \sum_{m=1}^{\infty} Y_m^{'} \cos\alpha x + 3Ky^2$$

$$\frac{\partial^2\psi}{\partial y^2} = \sum_{m=1}^{\infty} Y_m^{''} \cos\alpha x + 6Ky$$

$$\frac{\partial^3\psi}{\partial y^3} = \sum_{m=1}^{\infty} Y_m^{'''} \cos\alpha x + 6K$$

$$\frac{\partial^4\psi}{\partial y^4} = \sum_{m=1}^{\infty} Y_m^{''''} \cos\alpha x$$

Using the derivatives of Eq. (4.3), Eq. (4.1) yields

$$E_1G_{12}\sum_{m=1}^{\infty} Y_m\alpha^4 \cos\alpha x - E_2\left(E_1 - 2\mu_{12}G_{12}\right)\sum_{m=1}^{\infty} Y_m^{''}\alpha^2 \cos\alpha x + E_2G_{12}\sum_{m=1}^{\infty} Y_m^{''''} \cos\alpha x = 0$$

$$\text{or, } E_2G_{12}\sum_{m=1}^{\infty}\left[Y_m^{''''} - \frac{E_2\left(E_1 - 2\mu_{12}G_{12}\right)}{E_2G_{12}}Y_m^{''}\alpha^2 + \frac{E_1G_{12}}{E_2G_{12}}Y_m\alpha^4\right]\cos\alpha x = 0$$

$$\text{or, } Y_m^{''''} - \left(\frac{E_1}{G_{12}} - 2\mu_{12}\right)Y_m^{''}\alpha^2 + \frac{E_1}{E_2}Y_m\alpha^4 = 0 \qquad (4.4)$$

Eq. (4.4) is a fourth-order ordinary differential equation. The general solution of the differential equation can be written as

$$Y_m = A_m e^{r_1 y} + B_m e^{r_2 y} + C_m e^{r_3 y} + D_m e^{r_4 y} \tag{4.5}$$

where A_m, B_m, C_m and D_m are arbitrary constants, and r_1, r_2, r_3 and r_4 are the corresponding roots which are given below

$$r_1, r_2 = \frac{\alpha}{\sqrt{2}}\left[\left(\frac{E_1}{G_2} - 2\mu_{12}\right) \pm \sqrt{\left(\frac{E_1}{G_2} - 2\mu_{12}\right)^2 - 4\frac{E_1}{E_2}}\right]^{\frac{1}{2}} \tag{4.6a}$$

$$r_3, r_4 = -\frac{\alpha}{\sqrt{2}}\left[\left(\frac{E_1}{G_2} - 2\mu_{12}\right) \pm \sqrt{\left(\frac{E_1}{G_2} - 2\mu_{12}\right)^2 - 4\frac{E_1}{E_2}}\right]^{\frac{1}{2}} \tag{4.6b}$$

Now substituting the derivatives of ψ and Y_m as obtained from Eq. (4.3) and (4.5), respectively, in the expressions for displacement and stresses (4.2a, 4.2b, 4.2c, 4.2d and 4.2e).

$$u_x(x,y) = \frac{\partial^2 \psi}{\partial x \partial y}$$

$$= -\sum_{m=1}^{\infty} Y'_m \alpha \sin \alpha x$$

$$= -\sum_{m=1}^{\infty} \left(A_m r_1 e^{r_1 y} + B_m r_2 e^{r_2 y} + C_m r_3 e^{r_3 y} + D_m r_4 e^{r_4 y}\right) \alpha \sin \alpha x \tag{4.7a}$$

$$u_y(x,y) = -\frac{1}{Z_{11}}\left[E_1^2 \frac{\partial^2 \psi}{\partial x^2} + G_{12}\left(E_1 - \mu_{12}^2 E_2\right)\frac{\partial^2 \psi}{\partial y^2}\right]$$

$$= -\frac{1}{Z_{11}}\left[E_1^2\left\{-\sum_{m=1}^{\infty} Y_m \alpha^2 \cos \alpha x\right\} + G_{12}\left(E_1 - \mu_{12}^2 E_2\right)\left\{\sum_{m=1}^{\infty} Y''_m \cos \alpha x + 6Ky\right\}\right]$$

$$= -\frac{1}{Z_{11}}\begin{bmatrix} E_1^2\left\{-\sum_{m=1}^{\infty}\left(A_m e^{r_1 y} + B_m e^{r_2 y} + C_m e^{r_3 y} + D_m e^{r_4 y}\right)\alpha^2 \cos\alpha x\right\} + G_{12}\left(E_1 - \mu_{12}^2 E_2\right) \\ \left\{\sum_{m=1}^{\infty}\left(A_m r_1^2 e^{r_1 y} + B_m r_2^2 e^{r_2 y} + C_m r_3^2 e^{r_3 y} + D_m r_4^2 e^{r_4 y}\right)\cos\alpha x + 6Ky\right\} \end{bmatrix}$$

$$= \frac{1}{Z_{11}}\begin{bmatrix} \sum_{m=1}^{\infty}\begin{Bmatrix}\left(E_1^2\alpha^2 - E_1 G_{12} r_1^2 + \mu_{12}^2 E_2 G_{12} r_1^2\right)e^{r_1 y} A_m + \left(E_1^2\alpha^2 - E_1 G_{12} r_2^2 + \mu_{12}^2 E_2 G_{12} r_2^2\right)e^{r_2 y} B_m + \\ \left(E_1^2\alpha^2 - E_1 G_{12} r_3^2 + \mu_{12}^2 E_2 G_{12} r_3^2\right)e^{r_3 y} C_m + \left(E_1^2\alpha^2 - E_1 G_{12} r_4^2 + \mu_{12}^2 E_2 G_{12} r_4^2\right)e^{r_4 y} D_m \end{Bmatrix} \\ \cos\alpha x - \left(E_1 G_{12} - \mu_{12}^2 E_2 G_{12}\right)6Ky \end{bmatrix} \quad (4.7b)$$

$$\sigma_{xx}(x,y) = \frac{E_1 G_{12}}{Z_{11}}\left[E_1 \frac{\partial^3\psi}{\partial x^2 \partial y} - \mu_{12} E_2 \frac{\partial^3\psi}{\partial y^3}\right]$$

$$= \frac{E_1 G_{12}}{Z_{11}}\left[E_1\left\{-\sum_{m=1}^{\infty} Y_m' \alpha^2 \cos\alpha x\right\} - \mu_{12} E_2\left\{\sum_{m=1}^{\infty} Y_m''' \cos\alpha x + 6K\right\}\right]$$

$$= -\frac{E_1 G_{12}}{Z_{11}}[E_1\left\{\sum_{m=1}^{\infty}\left(A_m r_1 e^{r_1 y} + B_m r_2 e^{r_2 y} + C_m r_3 e^{r_3 y} + D_m r_4 e^{r_4 y}\right)\alpha^2 \cos\alpha x\right\} +$$

$$\mu_{12} E_2\left\{\sum_{m=1}^{\infty}\left(A_m r_1^3 e^{r_1 y} + B_m r_2^3 e^{r_2 y} + C_m r_3^3 e^{r_3 y} + D_m r_4^3 e^{r_4 y}\right)\cos\alpha x + 6K\right\}]$$

$$= -\frac{E_1 G_{12}}{Z_{11}}[\sum_{m=1}^{\infty}\{\left(E_1 r_1 e^{r_1 y}\alpha^2 + \mu_{12} E_2 r_1^3 e^{r_1 y}\right)A_m + \left(E_1 r_2 e^{r_{21} y}\alpha^2 + \mu_{12} E_2 r_2^3 e^{r_2 y}\right)B_m +$$

$$\left(E_1 r_3 e^{r_3 y}\alpha^2 + \mu_{12} E_2 r_3^3 e^{r_3 y}\right)C_m + \left(E_1 r_4 e^{r_4 y}\alpha^2 + \mu_{12} E_2 r_4^3 e^{r_4 y}\right)D_m\}\cos\alpha x + 6K\mu_{12} E_2] \quad (4.7c)$$

$$\sigma_{yy}(x,y) = \frac{E_1 E_2}{Z_{11}}\left[\left(\mu_{12} G_{12} - E_1\right)\frac{\partial^3\psi}{\partial x^2 \partial y} - G_{12}\frac{\partial^3\psi}{\partial y^3}\right]$$

$$= \frac{E_1 E_2}{Z_{11}}\left[\left(\mu_{12} G_{12} - E_1\right)\left\{-\sum_{m=1}^{\infty} Y_m' \alpha^2 \cos\alpha x\right\} - G_{12}\left\{\sum_{m=1}^{\infty} Y_m''' \cos\alpha x + 6K\right\}\right]$$

$$= -\frac{E_1 E_2}{Z_{11}}[\left(\mu_{12} G_{12} - E_1\right)\{\sum_{m=1}^{\infty}\left(A_m r_1 e^{r_1 y} + B_m r_2 e^{r_2 y} + C_m r_3 e^{r_3 y} + D_m r_4 e^{r_4 y}\right)\alpha^2 \cos\alpha x\} +$$

$$G_{12}\{\sum_{m=1}^{\infty}\left(A_m r_1^3 e^{r_1 y} + B_m r_2^3 e^{r_2 y} + C_m r_3^3 e^{r_3 y} + D_m r_4^3 e^{r_4 y}\right)\cos\alpha x + 6K\}]$$

$$= -\frac{E_1 E_2}{Z_{11}} \sum_{m=1}^{\infty} \{ \left(\mu_{12} G_{12} r_1 e^{r_1 y} \alpha^2 - E_1 r_1 e^{r_1 y} \alpha^2 + G_{12} r_1^3 e^{r_1 y} \right) A_m + \left(\mu_{12} G_{12} r_2 e^{r_{21} y} \alpha^2 - E_1 r_2 e^{r_{21} y} \alpha^2 + G_{12} r_2^3 e^{r_2 y} \right) B_m$$
$$+ \left(\mu_{12} G_{12} r_3 e^{r_3 y} \alpha^2 - E_1 r_3 e^{r_3 y} \alpha^2 + G_{12} r_3^3 e^{r_3 y} \right) C_m +$$
$$\left(\mu_{12} G_{12} r_4 e^{r_4 y} \alpha^2 - E_1 r_4 e^{r_4 y} \alpha^2 + G_{12} r_4^3 e^{r_4 y} \right) D_m \} \cos \alpha x + 6KG_{12} \qquad (4.7d)$$

$$\sigma_{xy}(x, y) = -\frac{E_1 G_{12}}{Z_{11}} \left[E_1 \frac{\partial^3 \psi}{\partial x^3} - \mu_{12} E_2 \frac{\partial^3 \psi}{\partial x \partial y^2} \right]$$

$$= -\frac{E_1 G_{12}}{Z_{11}} \{ E_1 \sum_{m=1}^{\infty} \left(A_m e^{r_1 y} + B_m e^{r_2 y} + C_m e^{r_3 y} + D_m e^{r_4 y} \right) \alpha^3 \sin \alpha x + \mu_{12} E_2$$
$$\sum_{m=1}^{\infty} \left(A_m r_1^2 e^{r_1 y} + B_m r_2^2 e^{r_2 y} + C_m r_3^2 e^{r_3 y} + D_m r_4^2 e^{r_4 y} \right) \alpha \sin \alpha x \}$$

$$= -\frac{E_1 G_{12}}{Z_{11}} \sum_{m=1}^{\infty} \left\{ \begin{array}{l} \left(E_1 e^{r_1 y} \alpha^3 + \mu_{12} E_2 r_1^2 e^{r_1 y} \alpha \right) A_m + \left(E_1 e^{r_{21} y} \alpha^3 + \mu_{12} E_2 r_2^2 e^{r_2 y} \alpha \right) B_m + \\ \left(E_1 e^{r_3 y} \alpha^3 + \mu_{12} E_2 r_3^2 e^{r_3 y} \alpha \right) C_m + \left(E_1 e^{r_4 y} \alpha^3 + \mu_{12} E_2 r_4^2 e^{r_4 y} \alpha \right) D_m \end{array} \right\} \sin \alpha x \qquad (4.7e)$$

From the expressions of (4.7a) and (4.7e) it is evident that the boundary conditions associated with the left and right lateral ends are automatically satisfied. Thus the next requirement is to satisfy the remaining boundary conditions associated with the upper and bottom boundary surfaces.

Now the reactions acting at the two extreme regions of the supporting surface, $y = 0$ may be expressed in terms of Fourier series as follows:

$$\sigma_{yy}(x,0) = 4\sigma_0 = E_0 + \sum_{m=1}^{\infty} E_m \cos \alpha x \qquad \text{for } x=0 \text{ to } 0.1L \text{ and } 0.9L \text{ to } L \qquad (4.8a)$$

Here

$$E_0 = \frac{1}{L} \left[\int_0^{L/10} 4\sigma_0 dx + \int_{9L/10}^{L} 4\sigma_0 dx \right]$$

$$= \frac{4\sigma_0}{L}\left[\frac{L}{10} - 0 + L - \frac{9L}{10}\right]$$

$$= \frac{4\sigma_0}{5} \tag{4.8b}$$

$$E_m = \frac{2}{L}\left[\int_0^{L/10} 4\sigma_0 \cos\alpha x dx + \int_{9L/10}^{L} 4\sigma_0 \cos\alpha x dx\right]$$

$$= \frac{8\sigma_{yy}^0}{L}\left[\frac{\sin\alpha x}{\alpha}\right]_0^{L/10} + \frac{8\sigma_{yy}^0}{L}\left[\frac{\sin\alpha x}{\alpha}\right]_{9L/10}^{L}$$

$$= \frac{8\sigma_0}{m\pi}\left\{\sin\left(\frac{m\pi}{10}\right) + \sin(m\pi) - \sin\left(\frac{9m\pi}{10}\right)\right\} \tag{4.8c}$$

The applied loading on the top surface, $y = D$ can also be expressed in terms of Fourier series as follows

$$\sigma_{yy}(x,0) = \sigma_0 = I_0 + \sum_{m=1}^{\infty} I_m \cos\alpha x \qquad \text{for } x = 0.1L \text{ to } 0.9L \tag{4.9a}$$

Here

$$I_0 = \frac{1}{L}\left[\int_{L/10}^{9L/10} \sigma_0 dx\right]$$

$$= \frac{\sigma_0}{L}\left[\frac{9L}{10} - \frac{L}{10}\right]$$

$$= \frac{4\sigma_0}{5} \tag{4.9b}$$

$$I_m = \frac{2}{L}\left[\int_{L/10}^{9L/10} \sigma_0 \cos\alpha x dx\right]$$

$$= \frac{2\sigma_0}{L}\left[\frac{\sin\alpha x}{\alpha}\right]_{l/10}^{9L/10}$$

$$= \frac{2\sigma_0}{m\pi}\left\{\sin\left(\frac{9m\pi}{10}\right) - \sin\left(\frac{m\pi}{10}\right)\right\} \tag{4.9c}$$

Using boundary condition $\sigma_{xy}(x,0) = 0$ at the edge of $y = 0$

$$-\frac{E_1 G_{12}}{Z_{11}}\left[\sum_{m=1}^{\infty}\left\{\begin{matrix}\left(E_1\alpha^3 + \mu_{12}E_2 r_1^2\alpha\right)A_m + \left(E_1\alpha^3 + \mu_{12}E_2 r_2^2\alpha\right)B_m + \\ \left(E_1 e^{r_3 y}\alpha^3 + \mu_{12}E_2 r_3^2\alpha\right)C_m + \left(E_1 e^{r_4 y}\alpha^3 + \mu_{12}E_2 r_4^2\alpha\right)D_m\end{matrix}\right\}\sin\alpha x\right] = 0$$

$$\text{or, } -\frac{E_1 G_{12}}{Z_{11}}\left\{\begin{matrix}\left(E_1\alpha^3 + \mu_{12}E_2 r_1^2\alpha\right)A_m + \left(E_1\alpha^3 + \mu_{12}E_2 r_2^2\alpha\right)B_m + \\ \left(E_1\alpha^3 + \mu_{12}E_2 r_3^2\alpha\right)C_m + \left(E_1\alpha^3 + \mu_{12}E_2 r_4^2\alpha\right)D_m\end{matrix}\right\} = 0 \tag{4.10a}$$

Using boundary condition $\sigma_{xy}(x,D) = 0$ at the edge of $y = D$

$$-\frac{E_1 G_{12}}{Z_{11}}\left[\sum_{m=1}^{\infty}\left\{\begin{matrix}\left(E_1 e^{r_1 D}\alpha^3 + \mu_{12}E_2 r_1^2 e^{r_1 D}\alpha\right)A_m + \left(E_1 e^{r_{21} D}\alpha^3 + \mu_{12}E_2 r_2^2 e^{r_2 D}\alpha\right)B_m + \\ \left(E_1 e^{r_3 D}\alpha^3 + \mu_{12}E_2 r_3^2 e^{r_3 D}\alpha\right)C_m + \left(E_1 e^{r_4 D}\alpha^3 + \mu_{12}E_2 r_4^2 e^{r_4 D}\alpha\right)D_m\end{matrix}\right\}\sin\alpha x\right] = 0$$

$$\text{or, } -\frac{E_1 G_{12}}{Z_{11}}\left\{\begin{matrix}\left(E_1 e^{r_1 D}\alpha^3 + \mu_{12}E_2 r_1^2 e^{r_1 D}\alpha\right)A_m + \left(E_1 e^{r_2 D}\alpha^3 + \mu_{12}E_2 r_2^2 e^{r_2 D}\alpha\right)B_m + \\ \left(E_1 e^{r_3 D}\alpha^3 + \mu_{12}E_2 r_3^2 e^{r_3 D}\alpha\right)C_m + \left(E_1 e^{r_4 D}\alpha^3 + \mu_{12}E_2 r_4^2 e^{r_4 D}\alpha\right)D_m\end{matrix}\right\} = 0 \tag{4.10b}$$

Using boundary condition $\sigma_{yy}(x,0) = 4\sigma_0$ at the edge of $y = 0$

$$-\frac{E_1 E_2}{Z_{11}}\left[\sum_{m=1}^{\infty}\left\{\begin{matrix}\left(\mu_{12}G_{12}r_1\alpha^2 - E_1 r_1\alpha^2 + G_{12}r_1^3\right)A_m + \\ \left(\mu_{12}G_{12}r_2\alpha^2 - E_1 r_2\alpha^2 + G_{12}r_2^3\right)B_m + \\ \left(\mu_{12}G_{12}r_3\alpha^2 - E_1 r_3\alpha^2 + G_{12}r_3^3\right)C_m + \\ \left(\mu_{12}G_{12}r_4\alpha^2 - E_1 r_4\alpha^2 + G_{12}r_4^3\right)D_m\end{matrix}\right\}\cos\alpha x + 6KG_{12}\right] = \sum_{m=1}^{\infty}E_m\cos\alpha x + E_0$$

Therefore,

$$-\frac{E_1E_2}{Z_{11}}\begin{Bmatrix}\left(\mu_{12}G_{12}r_1\alpha^2-E_1r_1\alpha^2+G_{12}r_1^3\right)A_m+\\ \left(\mu_{12}G_{12}r_2\alpha^2-E_1r_2\alpha^2+G_{12}r_2^3\right)B_m+\\ \left(\mu_{12}G_{12}r_3\alpha^2-E_1r_3\alpha^2+G_{12}r_3^3\right)C_m+\\ \left(\mu_{12}G_{12}r_4\alpha^2-E_1r_4\alpha^2+G_{12}r_4^3\right)D_m\end{Bmatrix}=E_m \tag{4.10c}$$

Using boundary condition $\sigma_{yy}(x,D)=\sigma_0$ at the edge of $y = D$

$$-\frac{E_1E_2}{Z_{11}}\left[\sum_{m=1}^{\infty}\begin{Bmatrix}\left(\mu_{12}G_{12}r_1e^{r_1D}\alpha^2-E_1r_1e^{r_1D}\alpha^2+G_{12}r_1^3e^{r_1D}\right)A_m+\\ \left(\mu_{12}G_{12}r_2e^{r_2D}\alpha^2-E_1r_2e^{r_2D}\alpha^2+G_{12}r_2^3e^{r_2D}\right)B_m+\\ \left(\mu_{12}G_{12}r_3e^{r_3D}\alpha^2-E_1r_3e^{r_3D}\alpha^2+G_{12}r_3^3e^{r_3D}\right)C_m+\\ \left(\mu_{12}G_{12}r_4e^{r_4D}\alpha^2-E_1r_4e^{r_4D}\alpha^2+G_{12}r_4^3e^{r_4D}\right)D_m\end{Bmatrix}\cos\alpha x+6KG_{12}\right]=\sum_{m=1}^{\infty}I_m\cos\alpha x+I_0$$

Therefore,

$$-\frac{E_1E_2}{Z_{11}}\begin{Bmatrix}\left(\mu_{12}G_{12}r_1e^{r_1D}\alpha^2-E_1r_1e^{r_1D}\alpha^2+G_{12}r_1^3e^{r_1D}\right)A_m+\\ \left(\mu_{12}G_{12}r_2e^{r_2D}\alpha^2-E_1r_2e^{r_2D}\alpha^2+G_{12}r_2^3e^{r_2D}\right)B_m+\\ \left(\mu_{12}G_{12}r_3e^{r_3D}\alpha^2-E_1r_3e^{r_3D}\alpha^2+G_{12}r_3^3e^{r_3D}\right)C_m+\\ \left(\mu_{12}G_{12}r_4e^{r_4D}\alpha^2-E_1r_4e^{r_4D}\alpha^2+G_{12}r_4^3e^{r_4D}\right)D_m\end{Bmatrix}=I_m \tag{4.10d}$$

From Eqns. (4.7d) and (4.8) or (4.9), the arbitrary constant *K* can be obtained as follows:

$$-\frac{6E_1E_2KG_{12}}{Z_{11}}=E_0=I_0=\frac{4\sigma_0}{5}$$

$$\text{or, } K=-\frac{2Z_{11}\sigma_0}{15E_1E_2G_{12}} \tag{4.11}$$

The simultaneous Eqs. (4.10a), (4.10b), (4.10c) and (4.10d) can be realized in a simplified matrix form for solution of the unknown terms of arbitrary constants like A_m, B_m, C_m and D_m as follows:

$$\begin{bmatrix} F_1 & F_2 & F_3 & F_4 \\ H_1 & H_2 & H_3 & H_4 \\ R_1 & R_2 & R_3 & R_4 \\ S_1 & S_2 & S_3 & S_4 \end{bmatrix} \begin{bmatrix} A_m \\ B_m \\ C_m \\ D_m \end{bmatrix} = \begin{bmatrix} 0 \\ 0 \\ \overline{E}_m \\ \overline{I}_m \end{bmatrix} \tag{4.12}$$

Where

$$\left.\begin{aligned} F_i &= E_1\alpha^3 + \mu_{12}E_2 r_i^2\alpha \\ H_i &= E_1 e^{r_i D}\alpha^3 + \mu_{12}E_2 r_1^2 e^{r_i D}\alpha \\ R_i &= \mu_{12}G_{12}r_i\alpha^2 - E_1 r_i\alpha^2 + G_{12}r_i^3 \\ S_i &= \mu_{12}G_{12}r_i e^{r_i D}\alpha^2 - E_1 r_i e^{r_i D}\alpha^2 + G_{12}r_i^3 e^{r_i D} \end{aligned}\right\} \quad i=1, 2, 3, 4$$

$$\overline{E}_m = -\frac{Z_{11}E_m}{E_1E_2}$$

$$\overline{I}_m = -\frac{Z_{11}I_m}{E_1E_2}$$

$$Z_{11} = \mu_{12}E_1E_2 + G_{12}\left(E_1 - \mu_{12}^2E_2\right)$$

Eqns. 4.7 are used for finding the stress and displacement components at various points of the beam and the appropriate values of E_m and I_m are determined to get the values of four unknowns constant, namely A_m, B_m, C_m and D_m by using either the matrix (4.12) or the four algebraic simultaneous Eqs. (4.10a), (4.10b), (4.10c) and (4.10d).

4.3.4 Beam with lateral stiffeners (Case-2)

In this case the trial function is assumed in terms of sine function so that its first and third derivatives with respect to x can be found in terms of cosine function. The displacement potential function ψ for the case of lateral stiffener is assumed as:

$$\psi = \sum_{m=1}^{\infty} Y_m \sin \alpha x \tag{4.13}$$

where $Y_m = f(y)$, $\alpha = \dfrac{m\pi}{L}$ and K = Arbitrary constant and m = 1, 2, 3, …….. ∞.

Derivatives of Eq. (4.13) with respect to x and y are

$$\frac{\partial \psi}{\partial x} = \sum_{m=1}^{\infty} Y_m \alpha \cos \alpha x$$

$$\frac{\partial^2 \psi}{\partial x^2} = -\sum_{m=1}^{\infty} Y_m \alpha^2 \sin \alpha x$$

$$\frac{\partial^3 \psi}{\partial x^3} = -\sum_{m=1}^{\infty} Y_m \alpha^3 \cos \alpha x$$

$$\frac{\partial^4 \psi}{\partial x^4} = \sum_{m=1}^{\infty} Y_m \alpha^4 \sin \alpha x$$

$$\frac{\partial^2 \psi}{\partial x \partial y} = \sum_{m=1}^{\infty} Y_m' \alpha \cos \alpha x$$

$$\frac{\partial^3 \psi}{\partial x \partial y^2} = \sum_{m=1}^{\infty} Y_m'' \alpha \cos \alpha x$$

$$\frac{\partial^3 \psi}{\partial x^2 \partial y} = -\sum_{m=1}^{\infty} Y_m^{'} \alpha^2 \sin \alpha x$$

$$\frac{\partial^4 \psi}{\partial x^2 \partial y^2} = -\sum_{m=1}^{\infty} Y_m^{''} \alpha^2 \sin \alpha x$$

$$\frac{\partial \psi}{\partial y} = \sum_{m=1}^{\infty} Y_m^{'} \sin \alpha x$$

$$\frac{\partial^2 \psi}{\partial y^2} = \sum_{m=1}^{\infty} Y_m^{''} \sin \alpha x$$

$$\frac{\partial^3 \psi}{\partial y^3} = \sum_{m=1}^{\infty} Y_m^{'''} \sin \alpha x$$

$$\frac{\partial^4 \psi}{\partial y^4} = \sum_{m=1}^{\infty} Y_m^{''''} \sin \alpha x$$

Using the derivatives of Eq. (4.13), Eq. (4.11) yields

$$E_1 G_{12} \sum_{m=1}^{\infty} Y_m \alpha^4 \cos \alpha x - E_2 \left(E_1 - 2\mu_{12} G_{12}\right) \sum_{m=1}^{\infty} Y_m^{''} \alpha^2 \sin \alpha x + E_2 G_{12} \sum_{m=1}^{\infty} Y_m^{''''} \sin \alpha x = 0$$

$$\text{or, } Y_m^{''''} - \left(\frac{E_1}{G_{12}} - 2\mu_{12}\right) Y_m^{''} \alpha^2 + \frac{E_1}{E_2} Y_m \alpha^4 = 0 \qquad (4.14)$$

The general solution of ordinary differential equation be

$$Y_m = L_m e^{r_1 y} + M_m e^{r_2 y} + N_m e^{r_3 y} + O_m e^{r_4 y} \qquad (4.15)$$

where L_m, M_m, N_m and O_m are arbitrary constants, and r_1, r_2, r_3 and r_4 are the corresponding roots which are given below

$$r_1, r_2 = \frac{\alpha}{\sqrt{2}}\left[\left(\frac{E_1}{G_2} - 2\mu_{12}\right) \pm \sqrt{\left(\frac{E_1}{G_2} - 2\mu_{12}\right)^2 - 4\frac{E_1}{E_2}}\right]^{\frac{1}{2}} \tag{4.16a}$$

$$r_3, r_4 = -\frac{\alpha}{\sqrt{2}}\left[\left(\frac{E_1}{G_2} - 2\mu_{12}\right) \pm \sqrt{\left(\frac{E_1}{G_2} - 2\mu_{12}\right)^2 - 4\frac{E_1}{E_2}}\right]^{\frac{1}{2}} \tag{4.16b}$$

Now substituting the derivatives of ψ and Y_m by using Eq. (4.13) and (4.15) respectively in the expressions for displacement and stresses (4.2a, 4.2b, 4.2c, 4.2d and 4.2e).

$$u_x(x,y) = \frac{\partial^2 \psi}{\partial x \partial y}$$

$$= \sum_{m=1}^{\infty}\left(L_m r_1 e^{r_1 y} + M_m r_2 e^{r_2 y} + N_m r_3 e^{r_3 y} + O_m r_4 e^{r_4 y}\right)\alpha \cos \alpha x \tag{4.17a}$$

$$u_y(x,y) = -\frac{1}{Z_{11}}\left[E_1^2 \frac{\partial^2 \psi}{\partial x^2} + G_{12}\left(E_1 - \mu_{12}^2 E_2\right)\frac{\partial^2 \psi}{\partial y^2}\right]$$

$$= -\frac{1}{Z_{11}}\left[-E_1^2\left\{\sum_{m=1}^{\infty} Y_m \alpha^2 \sin \alpha x\right\} + G_{12}\left(E_1 - \mu_{12}^2 E_2\right)\left\{\sum_{m=1}^{\infty} Y_m'' \sin \alpha x\right\}\right]$$

$$= \frac{1}{Z_{11}}\left[\sum_{m=1}^{\infty}\left\{\begin{array}{l}\left(E_1^2\alpha^2 - E_1 G_{12} r_1^2 + \mu_{12}^2 E_2 G_{12} r_1^2\right)e^{r_1 y} L_m + \left(E_1^2\alpha^2 - E_1 G_{12} r_2^2 + \mu_{12}^2 E_2 G_{12} r_2^2\right)e^{r_2 y} M_m + \\ \left(E_1^2\alpha^2 - E_1 G_{12} r_3^2 + \mu_{12}^2 E_2 G_{12} r_3^2\right)e^{r_3 y} N_m + \left(E_1^2\alpha^2 - E_1 G_{12} r_4^2 + \mu_{12}^2 E_2 G_{12} r_4^2\right)e^{r_4 y} O_m\end{array}\right\}\sin \alpha x\right] \tag{4.17b}$$

$$\sigma_{xx}(x,y) = \frac{E_1 G_{12}}{Z_{11}}\left[E_1 \frac{\partial^3 \psi}{\partial x^2 \partial y} - \mu_{12} E_2 \frac{\partial^3 \psi}{\partial y^3}\right]$$

$$= \frac{E_1 G_{12}}{Z_{11}}\left[E_1\left\{-\sum_{m=1}^{\infty} Y_m' \alpha^2 \sin \alpha x\right\} - \mu_{12} E_2\left\{\sum_{m=1}^{\infty} Y_m''' \sin \alpha x\right\}\right]$$

$$= -\frac{E_1 G_{12}}{Z_{11}}[\sum_{m=1}^{\infty}\{\left(E_1 r_1 e^{r_1 y}\alpha^2 + \mu_{12}E_2 r_1^3 e^{r_1 y}\right)L_m + \left(E_1 r_2 e^{r_{21} y}\alpha^2 + \mu_{12}E_2 r_2^3 e^{r_2 y}\right)M_m +$$

$$\left(E_1 r_3 e^{r_3 y}\alpha^2 + \mu_{12}E_2 r_3^3 e^{r_3 y}\right)N_m + \left(E_1 r_4 e^{r_4 y}\alpha^2 + \mu_{12}E_2 r_4^3 e^{r_4 y}\right)O_m\}\sin\alpha x] \qquad (4.17c)$$

$$\sigma_{yy}(x,y) = \frac{E_1 E_2}{Z_{11}}\left[(\mu_{12}G_{12} - E_1)\frac{\partial^3\psi}{\partial x^2 \partial y} - G_{12}\frac{\partial^3\psi}{\partial y^3}\right]$$

$$= \frac{E_1 E_2}{Z_{11}}\left[(\mu_{12}G_{12} - E_1)\left\{-\sum_{m=1}^{\infty} Y_m^{'}\alpha^2 \sin\alpha x\right\} - G_{12}\left\{\sum_{m=1}^{\infty} Y_m^{'''}\sin\alpha x\right\}\right]$$

$$= -\frac{E_1 E_2}{Z_{11}}\sum_{m=1}^{\infty}\{\left(\mu_{12}G_{12}r_1 e^{r_1 y}\alpha^2 - E_1 r_1 e^{r_1 y}\alpha^2 + G_{12}r_1^3 e^{r_1 y}\right)L_m + \left(\mu_{12}G_{12}r_2 e^{r_{21} y}\alpha^2 - E_1 r_2 e^{r_{21} y}\alpha^2 + G_{12}r_2^3 e^{r_2 y}\right)M_m$$
$$+ \left(\mu_{12}G_{12}r_3 e^{r_3 y}\alpha^2 - E_1 r_3 e^{r_3 y}\alpha^2 + G_{12}r_3^3 e^{r_3 y}\right)N_m +$$
$$\left(\mu_{12}G_{12}r_4 e^{r_4 y}\alpha^2 - E_1 r_4 e^{r_4 y}\alpha^2 + G_{12}r_4^3 e^{r_4 y}\right)O_m\}\sin\alpha x \qquad (4.17d)$$

$$\sigma_{xy}(x,y) = -\frac{E_1 G_{12}}{Z_{11}}\left[E_1\frac{\partial^3\psi}{\partial x^3} - \mu_{12}E_2\frac{\partial^3\psi}{\partial x \partial y^2}\right]$$

$$= \frac{E_1 G_{12}}{Z_{11}}\{E_1\sum_{m=1}^{\infty}\left(L_m e^{r_1 y} + M_m e^{r_2 y} + N_m e^{r_3 y} + O_m e^{r_4 y}\right)\alpha^3\cos\alpha x + \mu_{12}E_2$$
$$\sum_{m=1}^{\infty}\left(L_m r_1^2 e^{r_1 y} + M_m r_2^2 e^{r_2 y} + N_m r_3^2 e^{r_3 y} + O_m r_4^2 e^{r_4 y}\right)\alpha\cos\alpha x\}$$

$$= \frac{E_1 G_{12}}{Z_{11}}\sum_{m=1}^{\infty}\left\{\begin{matrix}\left(E_1 e^{r_1 y}\alpha^3 + \mu_{12}E_2 r_1^2 e^{r_1 y}\alpha\right)L_m + \left(E_1 e^{r_{21} y}\alpha^3 + \mu_{12}E_2 r_2^2 e^{r_2 y}\alpha\right)M_m + \\ \left(E_1 e^{r_3 y}\alpha^3 + \mu_{12}E_2 r_3^2 e^{r_3 y}\alpha\right)N_m + \left(E_1 e^{r_4 y}\alpha^3 + \mu_{12}E_2 r_4^2 e^{r_4 y}\alpha\right)O_m\end{matrix}\right\}\cos\alpha x \qquad (4.17e)$$

From the expressions of (4.17a) and (4.17e) it is evident that the boundary conditions associated with the left and right lateral ends are automatically satisfied. Thus the next requirement is to satisfy the remaining boundary conditions associated with the upper and bottom boundary surfaces.

Now the compressive load exerted at the two corners on the edge $y = 0$ may be taken as Fourier function in the following manner:

$$\sigma_{yy}(x,0) = 4\sigma_0 = E_0 + \sum_{m=1}^{\infty} E_m \cos \alpha x \quad \text{for } x\text{=0 to } 0.1L \text{ and } 0.9L \text{ to } L \tag{4.18a}$$

Here

$$E_0 = 0 \tag{4.18b}$$

$$E_m = \frac{2}{L}\left[\int_0^{L/10} 4\sigma_0 \sin \alpha x dx + \int_{9L/10}^{L} 4\sigma_0 \sin \alpha x dx\right]$$

$$= \frac{8\sigma_{yy}^0}{L}\left[\frac{-\cos \alpha x}{\alpha}\right]_0^{L/10} + \frac{8\sigma_{yy}^0}{L}\left[\frac{-\cos \alpha x}{\alpha}\right]_{9L/10}^{L}$$

$$= -\frac{8\sigma_0}{m\pi}\left\{\cos\left(\frac{m\pi}{10}\right) - 1 + \cos(m\pi) - \cos\left(\frac{9m\pi}{10}\right)\right\} \tag{4.18c}$$

The compressive load on the edge $y = D$ can also be given by a Fourier series as follows

$$\sigma_{yy}(x,0) = \sigma_0 = I_0 + \sum_{m=1}^{\infty} I_m \sin \alpha x \qquad \text{for } x\text{= } 0.1L \text{ to } 0.9L \tag{4.19a}$$

Here

$$I_0 = 0 \tag{4.19b}$$

$$I_m = \frac{2}{L}\left[\int_{L/10}^{9L/10} \sigma_0 \sin \alpha x dx\right]$$

$$= -\frac{2\sigma_0}{L}\left[\frac{\cos \alpha x}{\alpha}\right]_{l/10}^{9L/10}$$

$$= \frac{2\sigma_0}{m\pi}\left\{\cos\left(\frac{9m\pi}{10}\right) - \cos\left(\frac{m\pi}{10}\right)\right\} \tag{4.19c}$$

Using boundary condition $\sigma_{xy}(x,0)=0$ at the edge of $y=0$

$$\frac{E_1G_{12}}{Z_{11}}\left[\sum_{m=1}^{\infty}\begin{Bmatrix}\left(E_1\alpha^3+\mu_{12}E_2r_1^2\alpha\right)L_m+\left(E_1\alpha^3+\mu_{12}E_2r_2^2\alpha\right)M_m+\\ \left(E_1e^{r_3y}\alpha^3+\mu_{12}E_2r_3^2\alpha\right)N_m+\left(E_1e^{r_4y}\alpha^3+\mu_{12}E_2r_4^2\alpha\right)O_m\end{Bmatrix}\cos\alpha x\right]=0$$

$$\text{or, } \frac{E_1G_{12}}{Z_{11}}\begin{Bmatrix}\left(E_1\alpha^3+\mu_{12}E_2r_1^2\alpha\right)L_m+\left(E_1\alpha^3+\mu_{12}E_2r_2^2\alpha\right)M_m+\\ \left(E_1\alpha^3+\mu_{12}E_2r_3^2\alpha\right)N_m+\left(E_1\alpha^3+\mu_{12}E_2r_4^2\alpha\right)O_m\end{Bmatrix}=0 \qquad (4.20a)$$

Using boundary condition $\sigma_{xy}(x,D)=0$ at the edge of $y=D$

$$\frac{E_1G_{12}}{Z_{11}}\left[\sum_{m=1}^{\infty}\begin{Bmatrix}\left(E_1e^{r_1D}\alpha^3+\mu_{12}E_2r_1^2e^{r_1D}\alpha\right)L_m+\left(E_1e^{r_{21}D}\alpha^3+\mu_{12}E_2r_2^2e^{r_2D}\alpha\right)M_m+\\ \left(E_1e^{r_3D}\alpha^3+\mu_{12}E_2r_3^2e^{r_3D}\alpha\right)N_m+\left(E_1e^{r_4D}\alpha^3+\mu_{12}E_2r_4^2e^{r_4D}\alpha\right)O_m\end{Bmatrix}\cos\alpha x\right]=0$$

$$\text{or, } \frac{E_1G_{12}}{Z_{11}}\begin{Bmatrix}\left(E_1e^{r_1D}\alpha^3+\mu_{12}E_2r_1^2e^{r_1D}\alpha\right)L_m+\left(E_1e^{r_2D}\alpha^3+\mu_{12}E_2r_2^2e^{r_2D}\alpha\right)M_m+\\ \left(E_1e^{r_3D}\alpha^3+\mu_{12}E_2r_3^2e^{r_3D}\alpha\right)N_m+\left(E_1e^{r_4D}\alpha^3+\mu_{12}E_2r_4^2e^{r_4D}\alpha\right)O_m\end{Bmatrix}=0 \qquad (4.20b)$$

Using boundary condition $\sigma_{yy}(x,0)=4\sigma_0$ at the edge of $y=0$

$$-\frac{E_1E_2}{Z_{11}}\left[\sum_{m=1}^{\infty}\begin{Bmatrix}\left(\mu_{12}G_{12}r_1\alpha^2-E_1r_1\alpha^2+G_{12}r_1^3\right)L_m+\\ \left(\mu_{12}G_{12}r_2\alpha^2-E_1r_2\alpha^2+G_{12}r_2^3\right)M_m+\\ \left(\mu_{12}G_{12}r_3\alpha^2-E_1r_3\alpha^2+G_{12}r_3^3\right)N_m+\\ \left(\mu_{12}G_{12}r_4\alpha^2-E_1r_4\alpha^2+G_{12}r_4^3\right)O_m\end{Bmatrix}\sin\alpha x\right]=\sum_{m=1}^{\infty}E_m\sin\alpha x+E_0$$

Therefore,

$$-\frac{E_1E_2}{Z_{11}}\begin{Bmatrix}\left(\mu_{12}G_{12}r_1\alpha^2-E_1r_1\alpha^2+G_{12}r_1^3\right)L_m+\\ \left(\mu_{12}G_{12}r_2\alpha^2-E_1r_2\alpha^2+G_{12}r_2^3\right)M_m+\\ \left(\mu_{12}G_{12}r_3\alpha^2-E_1r_3\alpha^2+G_{12}r_3^3\right)N_m+\\ \left(\mu_{12}G_{12}r_4\alpha^2-E_1r_4\alpha^2+G_{12}r_4^3\right)O_m\end{Bmatrix}=E_m \qquad (4.20c)$$

Using boundary condition $\sigma_{yy}(x,D)=\sigma_0$ at the edge of $y=D$

$$-\frac{E_1E_2}{Z_{11}}\left[\sum_{m=1}^{\infty}\begin{Bmatrix}\left(\mu_{12}G_{12}r_1e^{r_1D}\alpha^2-E_1r_1e^{r_1D}\alpha^2+G_{12}r_1^3e^{r_1D}\right)L_m+\\ \left(\mu_{12}G_{12}r_2e^{r_2D}\alpha^2-E_1r_2e^{r_2D}\alpha^2+G_{12}r_2^3e^{r_2D}\right)M_m+\\ \left(\mu_{12}G_{12}r_3e^{r_3D}\alpha^2-E_1r_3e^{r_3D}\alpha^2+G_{12}r_3^3e^{r_3D}\right)N_m+\\ \left(\mu_{12}G_{12}r_4e^{r_4D}\alpha^2-E_1r_4e^{r_4D}\alpha^2+G_{12}r_4^3e^{r_4D}\right)O_m\end{Bmatrix}\sin\alpha x\right]=\sum_{m=1}^{\infty}I_m\sin\alpha x+I_0$$

Therefore,

$$-\frac{E_1E_2}{Z_{11}}\begin{Bmatrix}\left(\mu_{12}G_{12}r_1e^{r_1D}\alpha^2-E_1r_1e^{r_1D}\alpha^2+G_{12}r_1^3e^{r_1D}\right)L_m+\\ \left(\mu_{12}G_{12}r_2e^{r_2D}\alpha^2-E_1r_2e^{r_2D}\alpha^2+G_{12}r_2^3e^{r_2D}\right)M_m+\\ \left(\mu_{12}G_{12}r_3e^{r_3D}\alpha^2-E_1r_3e^{r_3D}\alpha^2+G_{12}r_3^3e^{r_3D}\right)N_m+\\ \left(\mu_{12}G_{12}r_4e^{r_4D}\alpha^2-E_1r_4e^{r_4D}\alpha^2+G_{12}r_4^3e^{r_4D}\right)O_m\end{Bmatrix}=I_m \qquad (4.20d)$$

From Eqs. (4.17d) and (4.19) or (4.20)

$E_0=I_0=0$

The simultaneous Eqs. (4.20a), (4.20b), (4.20c) and (4.20d) can be realized in a simplified matrix form for solution of the unknown terms of arbitrary constants like L_m, M_m, N_m and O_m as follows:

$$\begin{bmatrix}P_1&P_2&P_3&P_4\\Q_1&Q_2&Q_3&Q_4\\T_1&T_2&T_3&T_4\\U_1&U_2&U_3&U_4\end{bmatrix}\begin{bmatrix}L_m\\M_m\\N_m\\O_m\end{bmatrix}=\begin{bmatrix}0\\0\\\overline{E}_m\\\overline{I}_m\end{bmatrix} \qquad (4.21)$$

where

$$P_i = E_1\alpha^3 + \mu_{12}E_2 r_i^2\alpha$$

$$Q_i = E_1 e^{r_i D}\alpha^3 + \mu_{12}E_2 r_1^2 e^{r_i D}\alpha$$

$$T_i = \mu_{12}G_{12}r_i\alpha^2 - E_1 r_i\alpha^2 + G_{12}r_i^3$$

$$U_i = \mu_{12}G_{12}r_i e^{r_i D}\alpha^2 - E_1 r_i e^{r_i D}\alpha^2 + G_{12}r_i^3 e^{r_i D}$$

} i=1, 2, 3, 4

$$\overline{E}_m = -\frac{Z_{11}E_m}{E_1E_2}$$

$$\overline{I}_m = -\frac{Z_{11}I_m}{E_1E_2}$$

$$Z_{11} = \mu_{12}E_1E_2 + G_{12}\left(E_1 - \mu_{12}^2E_2\right)$$

Eqs. 4.17 are used for finding the stress and displacement components at various points of the beam and the appropriate values of E_m and I_m are determined to get the values of four unknowns constant, namely L_m, M_m, N_m and O_m by using either the matrix (4.21) or the four algebraic simultaneous Eqs. (4.20a), (4.20b), (4.20c) and (4.20d).

4.4 Results of Composite Beam

In this section, numerical results of the analytical solution of the composite beams are presented in the form of graphs. First, the distributions of different displacement and stress components at different sections of a thick beam (L/D = 3) are discussed. The effects of stiffeners at the lateral ends and beam aspect ratio on the elastic field are then investigated. Although the analytical method developed can be applied to any composite material of interest, a glass-epoxy composite beam is chosen as an example in the present study, the effective mechanical properties of which are listed in Table 4.1. The value of the maximum intensity of the normal loading assumed to calculate the present results is σ_0 = 40 N/mm.

Table 4.1: Mechanical properties used for the Glass-Epoxy composite

Material	Mechanical Property	Symbol (unit)	Value
Glass-Epoxy	Elastic modulus	E_1 (GPa)	43.0
		E_2 (GPa)	8.9
	Shear modulus	G_{12} (GPa)	4.5
	Poisson's ratio	ν_{12}	0.27
		ν_{21}	0.0559

4.4.1 Displacement field

The variations in the normalized axial and lateral displacement components (u_x/L, u_y/D) along the span (x/L) of a glass-epoxy beam (L/D = 3) with axial stiffeners at the lateral ends are shown in Fig. 4.2. Axial displacements (u_x/L) are found to be of nearly anti-symmetric nature about the mid-span section of the beam. The displacements are found to be zero at the mid-span section as well as the lateral stiffened ends [Fig. 4.2(a)], which, in turn, verifies the proper modeling of the boundary conditions at the stiffened ends. The maximum magnitudes of axial displacement are observed at the bottom surface of the beam, particularly at the sections x/L = 0.1 and 0.9.

Lateral displacements (u_y/D) are found to assume positive value (upward displacement) around the two supporting regions near the lateral ends, and negative value (downward displacement) for the region $0.2 < x/L < 0.8$, which is in good conformity with the distributions of loading at the top and bottom surfaces as well as with the boundary conditions of the lateral ends [Fig. 4.2(b)]. The distributions are symmetric about the mid-span section of the beam. The maximum and minimum downward displacements are found to occur at the bottom and top surfaces of the beam, respectively. A comparison of the results shown in Figs. 4.2(a) and (b) reveals that the maximum lateral displacement is nearly three times higher than the maximum axial displacement occurred for the present stiffened composite beam, $L/D = 3$.

4.4.2 Stress field

The distributions of normalized bending stress component σ_{xx}/σ_0 with respect to beam depth, y/D at different sections of the beam are illustrated in Fig. 4.3(a). Bending stress distributions are observed to be non-linear over the whole span, although the beam length is three times higher than its depth. The degree of nonlinearity increases with the decrease of distances from the stiffened ends. In general, maximum values of bending stresses are observed at the top and bottom surfaces of the beam with opposite sign. The maximum normalized values of the stress at the top and bottom surfaces are found to be nearly 4.8 and –9.0, respectively. These maximum bending stresses are found to occur at the stiffened ends of the beam, which, in turn, identifies the stiffened lateral ends of the beam as the most critical section in term of axial stresses, which is, however, the most dominating stress components among the others. Bending stress is found to be positive (tensile) for the upper half and negative (compressive) for the lower half for sections close to the stiffened ends, but opposite characteristics are observed for sections in the region, $0.1<x/L<0.9$. The bending stress distribution at the mid-span section of the present composite beam (L/D=3) is found to be still highly nonlinear which is in contrast with the case of unstiffened beam, as the distribution was verified to be almost linear at the mid-span section of an unstiffened beam of L/D=2 [9].

As appears from Fig. 4.3(b), the lateral stress (σ_{yy}/σ_0) is of higher concentration around the regions of supports at the bottom surface. The applied uniform load is distributed over 80% of beam-span (from x/L= 0.1 to x/L=0.9) and support reactions are distributed over 20% of the beam-span (x/L= 0.0 to 0.1 and 0.9 to 1.0). A simple quantitative analysis shows that the intensity of the reactions is four times the applied load intensity. From the present displacement-potential solution it is revealed that the normalized value of lateral stress varies from zero to unity at the bottom and top surfaces, respectively, for sections within the loaded region ($0.1<x/L<0.9$), and the corresponding values at the stiffened ends vary from −4 to zero, which is in excellent agreement with the applied loading as well as other boundary conditions of the beam. When the distributions of lateral stress are analyzed in the perspective of the beam-depth, they are found to be highly nonlinear, particularly for sections near the stiffened ends. This nonlinearity is found to decrease as the distance from the stiffened end is increased. It can be noted that for sections around the mid-span section of the beam (L/D=3), the distributions are found to be still nonlinear, which is, however, in contrast to the case of an equivalent un-stiffened beam.

From the distributions of shear stress at different sections of the beam it is observed that the entire top and bottom surfaces and the two stiffened ends as well as the mid-span section are completely free from shear stress (see Fig.4.3(c)), which is in conformity with the physical characteristics of the present beam. Maximum shear stress is found to occur at the load transition section, x/L= 0.1 and 0.9, specifically at the vicinity of the bottom surface, which is in contrast with the standard parabolic profile. The shear stress distributions are found to assume the parabolic profile in a gradual fashion as we move towards the mid-span section. Distributions are symmetric about the mid-span section of the beam. The maximum shear stress developed at section x/L= 0.1 of the present beam is found to be nearly 1.8 times the intensity of the applied loading, σ_0.

4.4.3 Effect of stiffeners at the opposing lateral ends

This section describes the effect of different types of stiffeners at the opposing lateral ends of the beam on the state of stresses. More specifically, the distributions of stresses obtained with axial and lateral stiffeners at the ends are compared with those of the unstiffened beam. Fig. 4.4 compares the bending stress distributions at sections x/L= 0 and 0.5 for three different cases of stiffeners at the lateral ends. At the lateral ends, the bending stresses are basically zero for both the cases of lateral and no stiffeners, whereas for the case of axial stiffeners, the lateral ends are identified as the most critical sections in terms of the bending stress. The maximum stress is developed for the case of axial stiffeners at the bottom surface of the beam, which is more than eight times the intensity of the applied loading. When the corresponding solution of bending stress at the mid-span section are compared, it is observed that the lateral stiffeners at the two opposing lateral ends do not cause much change in the mid-span bending stress distribution from the corresponding case of no stiffeners. However, the axial stiffeners at the lateral ends have significant influence on the mid-span bending stress compared to the case of lateral stiffeners, as the corresponding magnitude of the stress is found to be nearly half of that of the unstiffened beam.

Fig. 4.5 illustrates the comparison of distribution of lateral stresses at the lateral ends (x/L= 0) and mid-span section (x/L= 0.5) of the beam is subjected to axial and lateral stiffeners as well as of an unstiffened beam. The lateral ends of the beam with lateral stiffeners are free from normal stress, σ_{yy}, whereas the remaining two cases are close to each other in terms of magnitude and shape with slight discrepancy only at the left and right corner points of the bottom surface. The three distributions are found to be almost identical when the section concerned is the mid-span section of the beam, which vary from zero at the bottom surface to unity at the top surface. However, the distributions are found to be slightly nonlinear even at the mid-span section of the beam, L/D =3.

The comparison of shear stress distributions at two different sections of the beam with and without stiffeners is presented in Fig. 4.6. It is observed that the effect of stiffeners at the lateral

ends on shear stress distribution is not that significant, when the section concerned is away from the lateral ends [Fig.4.6(b)], as the three distributions are found to assume nearly the similar parabolic profile. On the other hand, the lateral ends of the beam subjected to lateral stiffeners are identified to be the most critical sections of the beam in terms of shear stress, while the ends of the other two cases are free from shear stress, which is, however, in complete conformity with the given end conditions. Shear stress at the lateral ends for the case of lateral stiffeners assumes negative value for the upper 70% of the depth and for the lower 30% of the depth; it increases gradually with positive value and eventually assumes its maximum value near the bottom surface.

In attempt to demonstrate the overall deformation of the beam under the influence of stiffeners at the lateral ends, the corresponding deformed shapes of a beam (L/D =3) are compared with the original undeformed shape in Fig. 4.7. The conditions of the two types of stiffeners are clearly reflected through the corresponding deformed shapes of the beam.

4.4.4 Effect of beam aspect ratio

The effects of the aspect ratio (L/D) on the components of stress are also analyzed for both the axial and lateral stiffening conditions at the lateral ends. Figs. 4.8(a.1) and (b.1) represent the distribution of bending stresses at mid span section (x/L=0.5) of the beam for different L/D ratios for the cases of axial and lateral stiffeners, respectively. For both the cases, stress level increases with the increase of L/D ratio, although the stress level itself is much higher for the case of lateral stiffeners. Another important observation is, the axial stiffeners at the lateral ends make the distribution of bending stress more nonlinear (warping) than those caused by the lateral stiffeners. The distributions for the case of lateral stiffener are found to be similar to those of unstiffened beam in terms of both magnitude and nature of variation. Further Figs. 4.8(a.2) and (b.2) present the analysis of critical bending stresses at the stiffened and the mid-span sections in the perspective of beam aspect ratio for the cases of axial and lateral stiffeners, respectively, where a wide range of L/D ratio has been covered. For the case of axial and lateral stiffeners, the lateral ends and the mid-span sections, respectively, are found to be the most

critical sections in terms of bending stress, which are observed to be the functions of beam aspect ratio. For the entire range of *L/D* ratio considered, the critical bending stresses are found to increase with the increase of *L/D* ratio.

The effect of ratio on the magnitude and distribution of shear stresses in the stiffened beams is illustrated in Fig.4.9. The distributions of shear stress along the beam depth are presented in Figs. 4.9(a.1) and (b.1) for various *L/D* ratios of the beam with axial and lateral stiffeners, respectively. The overall magnitude of the stress increases with the increase of beam aspect ratio. For lower aspect ratios, the distributions are different from the standard parabolic profile, which is mainly because of short beam effect. For the beam with *L/D* =4, the shear stress distributions are found to assume nearly the parabolic profile for both the cases of stiffeners considered. The comparison of distributions of shear stress for the two kinds of stiffeners reveals that distributions are hardly effected by the stiffeners at the two opposing lateral ends. Again, the maximum shear stresses at the critical sections, namely, *x/L*= 0 and 0.1 are also analyzed in the perspective of beam aspect ratio for both the stiffeners, in Figs. 4.9(a.2) and (b.2). Although the stiffened ends (axial stiffener) are free from shearing stresses, those with lateral stiffeners are found to experience a significant level of shear stress, the maximum value of which is however found to be nearly independent of beam aspect ratio, as shown in Fig. 4.9(b.2). The increase in the maximum value of shear stress at the load changing section (*x/L*= 0.1), with the increase of *L/D* ratio are identified to be nearly similar for both the cases of stiffeners.

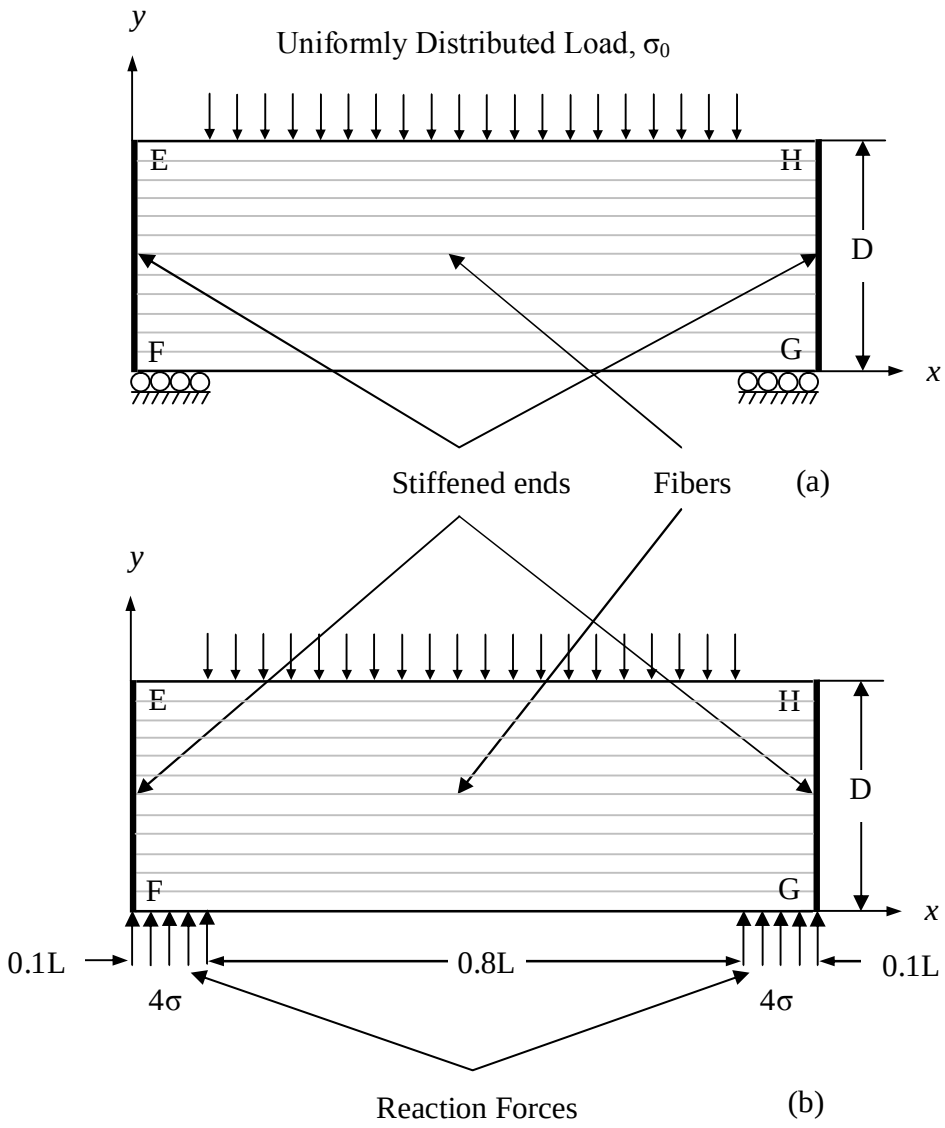

Fig. 4.1 A stiffened simply-supported beam of fiber-reinforced composite material: (a) Physical model, (b) Analytical model

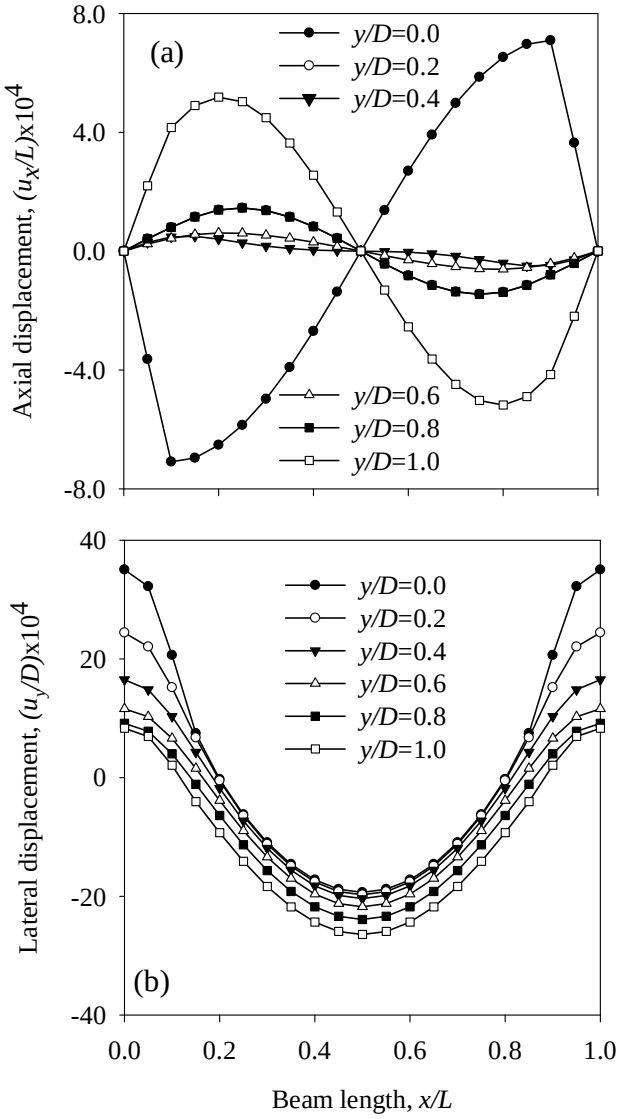

Fig. 4.2 Distribution of displacement components at different sections of the stiffened (axial) composite beam, L/D = 3

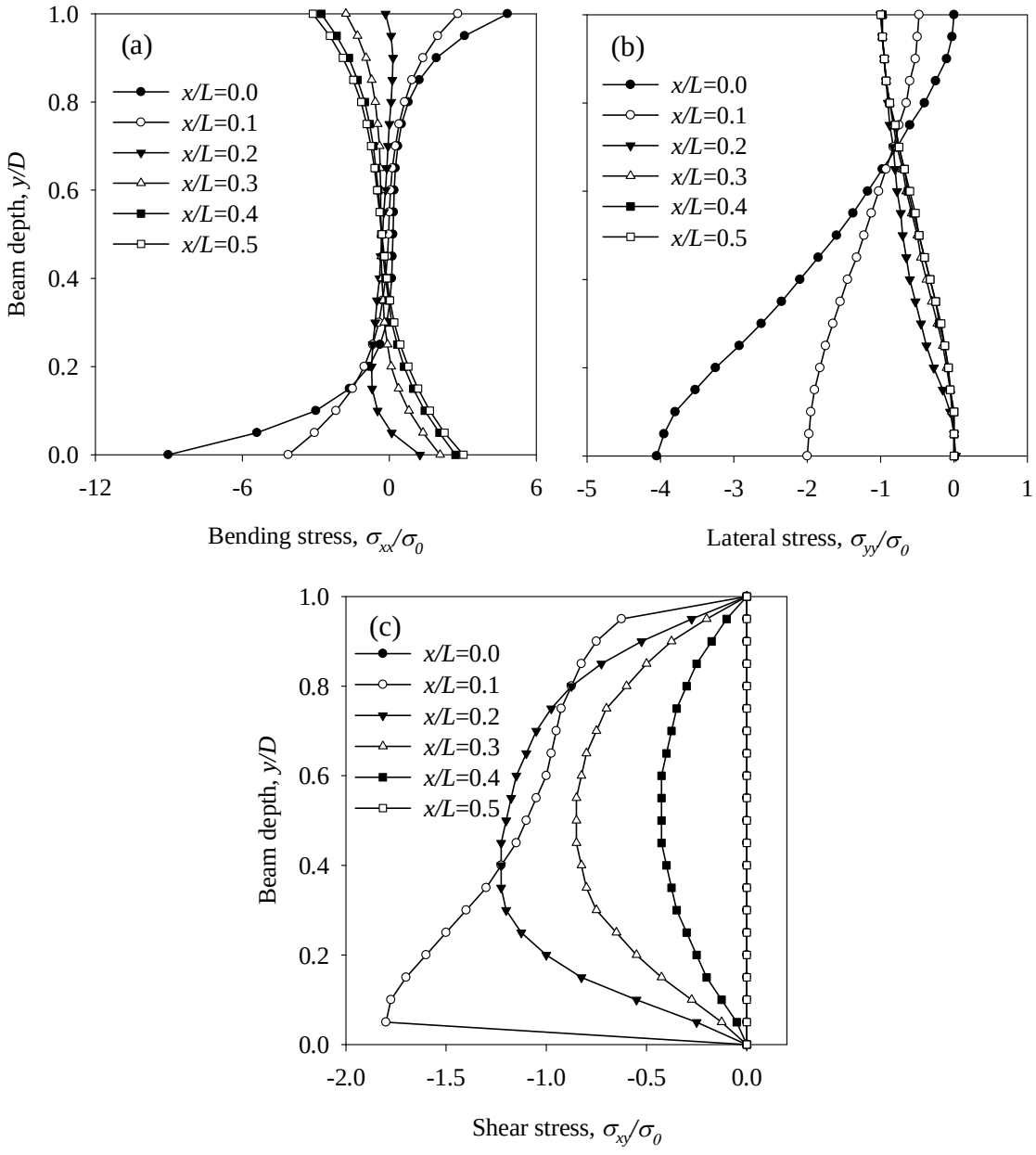

Fig. 4.3 Distribution of stress components at different sections of the stiffened (axial) composite beam, L/D = 3

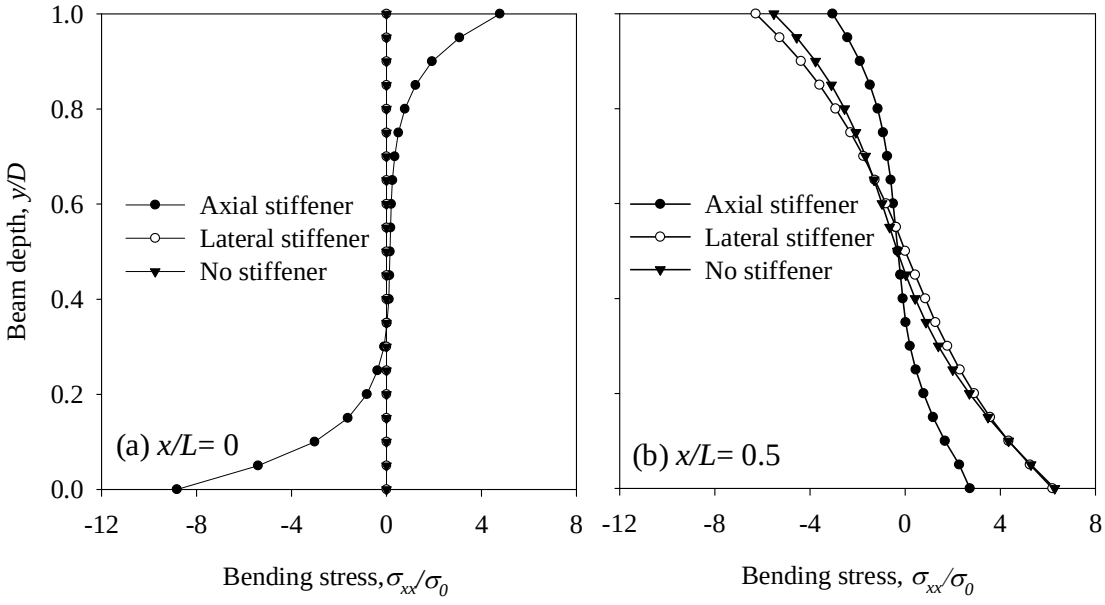

Fig. 4.4 Distribution of bending stress components at different sections of the composite beam (L/D = 3) with different types of stiffeners

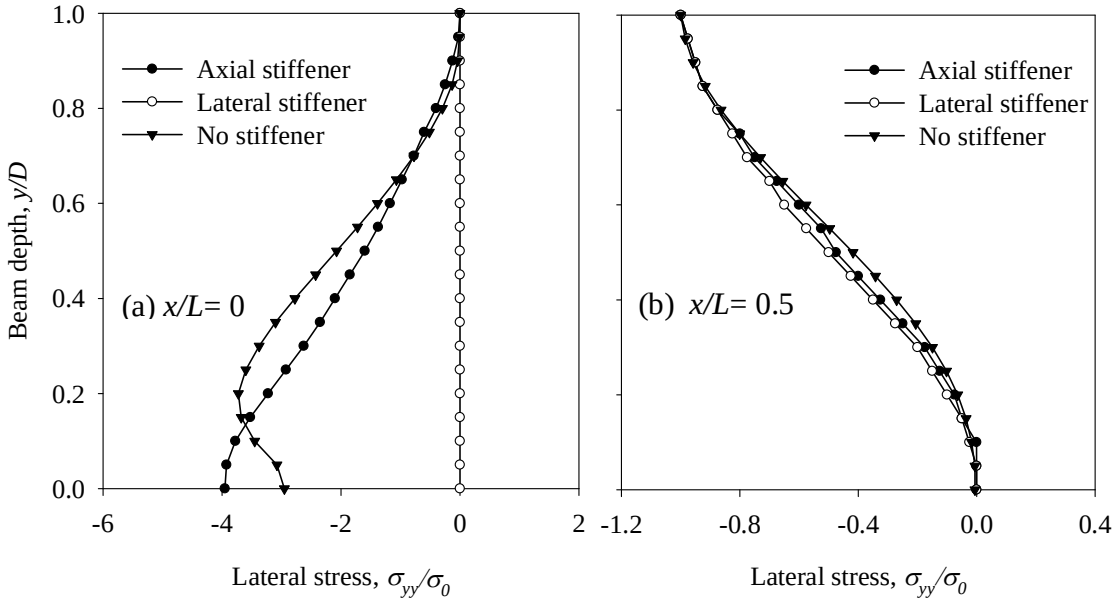

Fig. 4.5 Distribution of lateral stress components at different sections of the composite beam (L/D = 3) with different types of stiffeners

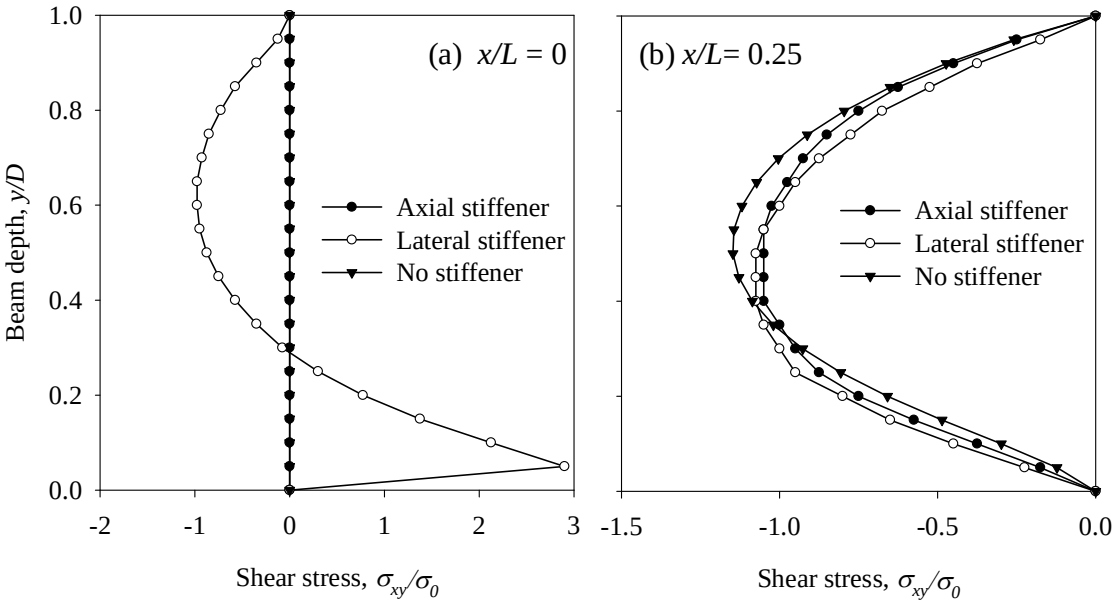

Fig. 4.6 Distribution of shear stress components at different sections of the composite beam (L/D = 3) with different types of stiffeners

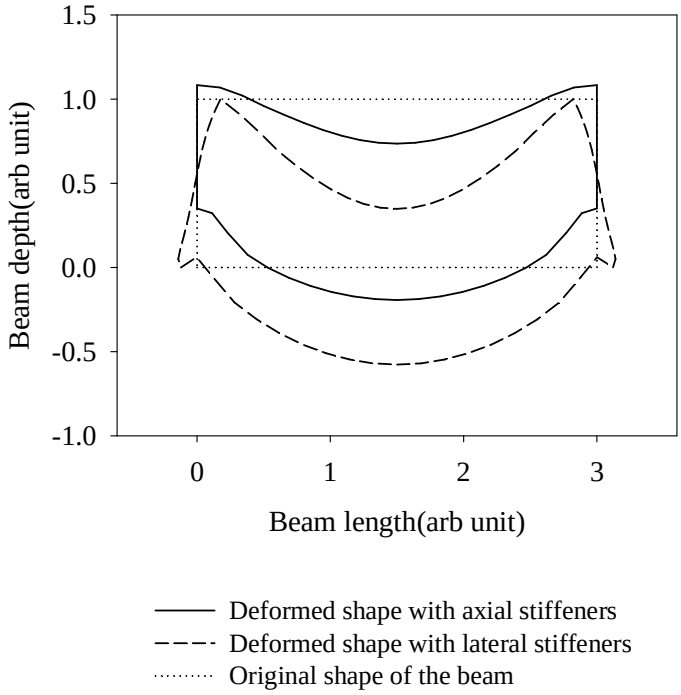

Fig. 4.7 Deformed shapes of the stiffened composite beam, $L/D = 3$ (magnification factor, $\times 200$)

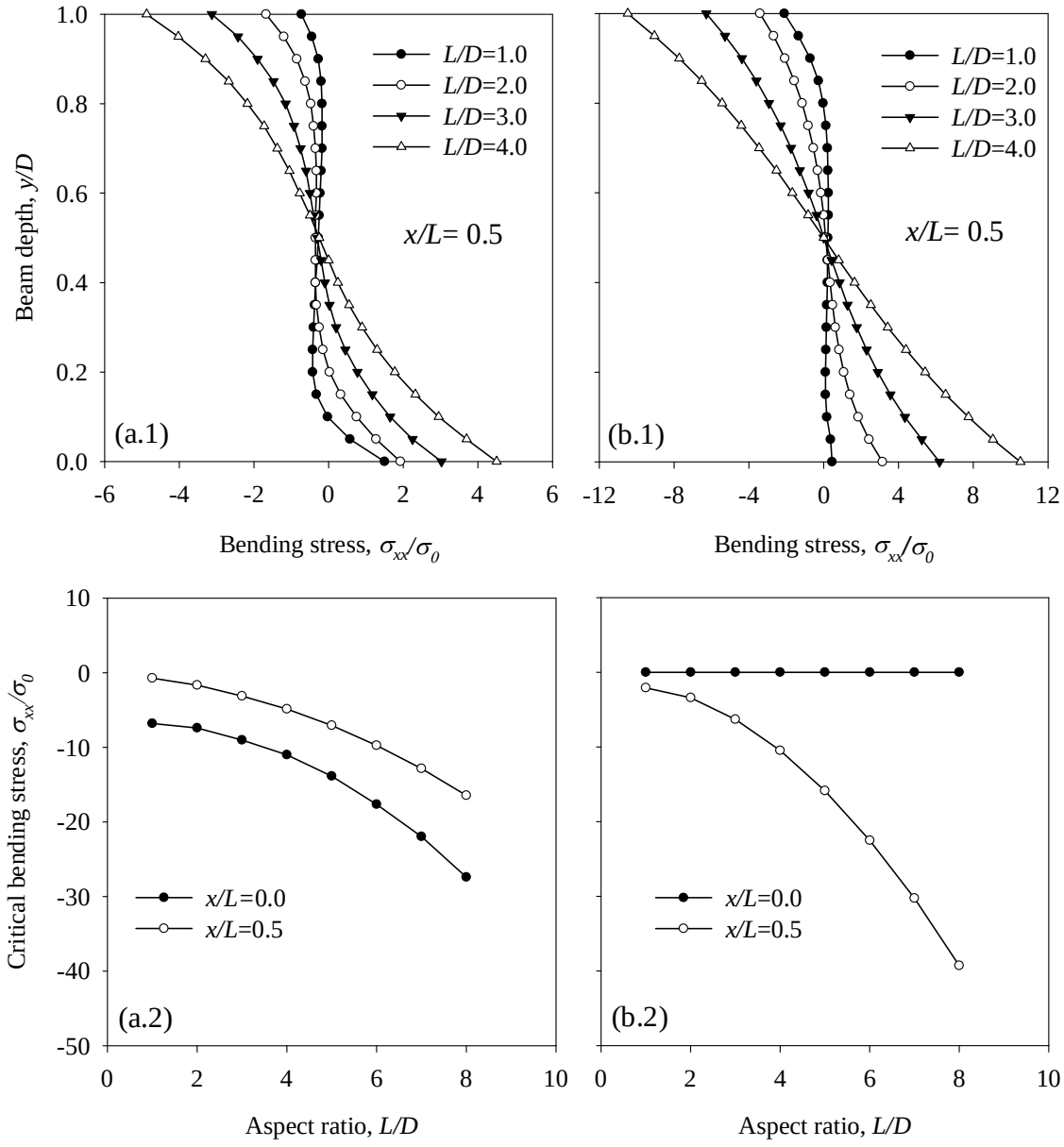

Fig. 4.8 Effect of aspect ratio on bending stress components in the stiffened composite beam: a) axial stiffener, b) lateral stiffener

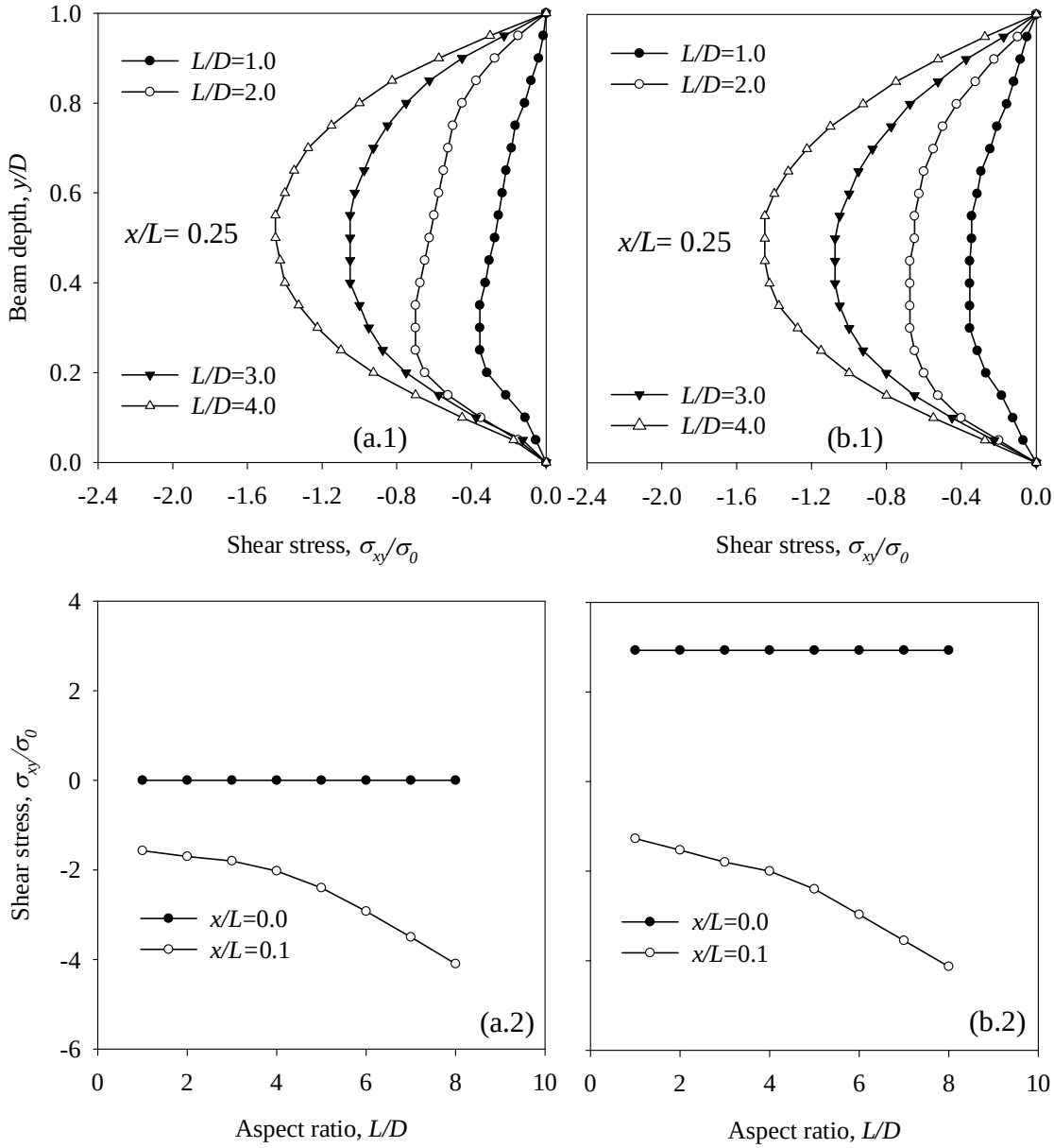

Fig. 4.9 Effect of aspect ratio on shear stress components in the stiffened composite beam: a) axial stiffener, b) lateral stiffener

CHAPTER 5

EFFECT OF FIBER ORIENTATION ON THE ELASTIC FIELD

In the previous chapter, the effect of stiffeners on the elastic field of a simply supported orthotropic beam was investigated with fibre orientation $\theta=0^0$. The main focus in this chapter is to investigate the effect of fibre orientation on the elastic field of the stiffened simply supported orthotropic beam. For this purpose, the stress and displacement fields of the simply supported beam with fibre orientation $\theta=90^0$ and $\theta=0^0$ are obtained for both the axial and lateral stiffening conditions, and then the effect of fibre orientation is described for both with respect to stress and displacement fields. All the solutions of stresses and displacements are analyzed for different beam aspect ratios.

5.1 Problem Description

A uniform rectangular composite beam of length L, depth D and thickness W is considered for the present analysis. The beam is subjected to a uniformly distributed load at its upper surface and is simply supported at the two extreme regions of the bottom surface. The beam is in equilibrium with a uniform loading σ_0 acting over 80% of its span (from $0.1L$ to $0.9L$) at the upper surface ($y = D$), and distributed reactions from $x = 0$ to $0.1L$ and $x = 0.9L$ to L at the bottom surface ($y = 0$), as shown in Fig. 5.1. The lateral ends of the beam, EF and HG are assumed to be stiffened with rigid stiffeners. Two different types of stiffeners are considered for the opposing lateral ends of the beam, which are axial stiffener and lateral stiffener. The beam is considered to be of unit thickness and the fibres are assumed to be oriented along the depth of the beam ($\theta=90^0$, Fig. 5.1(a)) as well as along the length of the beam ($\theta=0^0$, Fig. 5.1(b)).

5.2 Boundary Conditions

The physical conditions of the present problem with reference to Fig. 5.1 are to be satisfied along the all four boundaries of the beam can be expressed mathematically as follows:

(a) Loaded boundary, EH ($y = D$):

The loading at the upper boundary is modelled by assigning a uniform value to the normal stress component, which is also free from any shearing stress. The corresponding mathematical expressions of the conditions are

$$\sigma_{yy}(x, D) = \begin{cases} -\sigma_0 & [0.1 \le x/L \le 0.9] \\ 0 & [\text{otherwise}] \end{cases}$$

$$\sigma_{xy}(x, D) = 0 \quad [0.0 \le x/L \le 1.0]$$

(b) Supporting surface, FG ($y = 0$):

The roller supported regions of the bottom surface are modelled by a uniform distribution of normal loading which is free from shearing stress. At the supports, the total reaction forces are considered to be equal and opposite to the loading applied at the top surface. The reactions are distributed over 20% of the beam span (*i.e.*, x/L = 0.0-0.1 and 0.9-1.0). The remaining section of the bottom surface is assumed to be free from loading.

$$\sigma_{xy}(x, 0) = 0 \qquad [0.0 \le x/L \le 1.0]$$

$$\sigma_{yy}(x, 0) = \begin{cases} -4\sigma_0 & [0.0 \le x/L \le 0.1;\ 0.9 \le x/L \le 1.0] \\ 0 & [\text{otherwise}] \end{cases}$$

(c) Left lateral end, EF ($x = 0$):

Axial stiffener (Case-1): The physical condition of the rigid axial stiffener is modelled here by assigning zero values to both the axial displacement and the associated tangential stress components along the end. Thus,

$$\left.\begin{aligned} u_x(0, y) &= 0 \\ \sigma_{xy}(0, y) &= 0 \end{aligned}\right\} \quad [0.0 \le y/D \le 1.0]$$

Lateral stiffener (Case-2): The physical condition of the rigid lateral stiffener is modelled here by considering the boundary free from lateral displacement and axial normal stress. Thus,

$$\left.\begin{aligned} u_y\,(0,\,y) &= 0 \\ \sigma_{xx}\,(0,y) &= 0 \end{aligned}\right\} \qquad [0.0 \le y/D \le 1.0]$$

(d) Right lateral end, GH ($x = L$):

Axial stiffener (Case-1): Likewise the case of left lateral end, the corresponding mathematical expressions for the conditions of rigid axial stiffener at this boundary are

$$\left.\begin{aligned} u_x\,(L,\,y) &= 0 \\ \sigma_{xy}\,(L,y) &= 0 \end{aligned}\right\} \qquad [0.0 \le y/D \le 1.0]$$

Lateral stiffener (Case-2): The conditions of rigid lateral stiffener at the right lateral end are modelled by the following expressions:

$$\left.\begin{aligned} u_y\,(L,\,y) &= 0 \\ \sigma_{xx}\,(L,y) &= 0 \end{aligned}\right\} \qquad [0.0 \le y/D \le 1.0]$$

5.3 Analytical Solution

Mathematical model here is the partial differential equation derived from the equations of equilibrium and equations of compatibility based on Displacement Potential Function $\psi(x,y)$ obtained from Eq. (2.30) as follows.

$$E_2 G_{12} \frac{\partial^4 \psi}{\partial x^4} + E_2\left(E_1 - 2\mu_{12} G_{12}\right)\frac{\partial^4 \psi}{\partial x^2 \partial y^2} + E_1 G_{12} \frac{\partial^4 \psi}{\partial y^4} = 0 \qquad (5.1)$$

In this case the displacement and stress components are also obtained from Eq. (2.29) as follows:

$$u_x(x,y)=\frac{\partial^2\psi}{\partial x\partial y} \tag{5.2a}$$

$$u_y(x,y)=-\frac{1}{Z_{11}}\left[E_1E_2\frac{\partial^2\psi}{\partial x^2}+G_{12}\left(E_1-\mu_{12}^2E_2\right)\frac{\partial^2\psi}{\partial y^2}\right] \tag{5.2b}$$

$$\sigma_{xx}(x,y)=\frac{E_1E_2G_{12}}{Z_{11}}\left[\frac{\partial^3\psi}{\partial x^2\partial y}-\mu_{12}\frac{\partial^3\psi}{\partial y^3}\right] \tag{5.2c}$$

$$\sigma_{yy}(x,y)=-\frac{E_1}{Z_{11}}\left[E_1G_{12}\frac{\partial^3\psi}{\partial y^3}+E_2\left(E_1-\mu_{12}G_{12}\right)\frac{\partial^3\psi}{\partial x^2\partial y}\right] \tag{5.2d}$$

$$\sigma_{xy}(x,y)=\frac{E_1E_2G_{12}}{Z_{11}}\left[\mu_{12}\frac{\partial^3\psi}{\partial x\partial y^2}-\frac{\partial^3\psi}{\partial x^3}\right] \tag{5.2e}$$

Where $Z_{11}=\mu_{12}E_1E_2+G_{12}\left(E_1-\mu_{12}^2E_2\right)$

The solution of the beam is obtained with fibre orientation, θ=90^0 (case-A) and θ=0^0 (case-B) for both axial and lateral stiffening conditions.

5.3.1 Case-A (Fiber orientation, $\theta = 90^0$)

Case-1: Beam with axial stiffeners

The trial function for the present problem is assumed in terms of a cosine function so that its first and third derivatives with respect to x are obtained in terms of a sine function. It is observed that such a trial solution is capable of satisfying the necessary physical conditions associated with the two opposing lateral ends automatically, which are given by the conditions of ‘c’ and ‘d’ of section 5.2. Considering all these factors, the potential function, ψ for the present problem is approximated as follows:

$$\psi = \sum_{m=1}^{\infty} Y_m \cos \alpha x + Ky^3 \tag{5.3}$$

where $Y_m = f(y)$, $\alpha = \dfrac{m\pi}{L}$ and K = Arbitrary constant and m = 1, 2, 3, …….. ∞.

Derivatives of Eq. (5.3) with respect to x and y are

$$\frac{\partial \psi}{\partial x} = -\sum_{m=1}^{\infty} Y_m \alpha \sin \alpha x$$

$$\frac{\partial^2 \psi}{\partial x^2} = -\sum_{m=1}^{\infty} Y_m \alpha^2 \cos \alpha x$$

$$\frac{\partial^3 \psi}{\partial x^3} = \sum_{m=1}^{\infty} Y_m \alpha^3 \sin \alpha x$$

$$\frac{\partial^4 \psi}{\partial x^4} = \sum_{m=1}^{\infty} Y_m \alpha^4 \cos \alpha x$$

$$\frac{\partial^2 \psi}{\partial x \partial y} = -\sum_{m=1}^{\infty} Y_m' \alpha \sin \alpha x$$

$$\frac{\partial^3 \psi}{\partial x \partial y^2} = -\sum_{m=1}^{\infty} Y_m'' \alpha \sin \alpha x$$

$$\frac{\partial^3 \psi}{\partial x^2 \partial y} = -\sum_{m=1}^{\infty} Y_m' \alpha^2 \cos \alpha x$$

$$\frac{\partial^4 \psi}{\partial x^2 \partial y^2} = -\sum_{m=1}^{\infty} Y_m'' \alpha^2 \cos \alpha x$$

$$\frac{\partial \psi}{\partial y} = \sum_{m=1}^{\infty} Y_m' \cos \alpha x + 3Ky^2$$

$$\frac{\partial^2 \psi}{\partial y^2} = \sum_{m=1}^{\infty} Y_m^{''} \cos \alpha x + 6Ky$$

$$\frac{\partial^3 \psi}{\partial y^3} = \sum_{m=1}^{\infty} Y_m^{'''} \cos \alpha x + 6K$$

$$\frac{\partial^4 \psi}{\partial y^4} = \sum_{m=1}^{\infty} Y_m^{''''} \cos \alpha x$$

Using the derivatives of Eq. (5.3), equation (5.1) yields

$$E_2 G_{12} \sum_{m=1}^{\infty} Y_m \alpha^4 \cos \alpha x - E_2 \left(E_1 - 2\mu_{12} G_{12}\right) \sum_{m=1}^{\infty} Y_m^{''} \alpha^2 \cos \alpha x + E_1 G_{12} \sum_{m=1}^{\infty} Y_m^{''''} \cos \alpha x = 0$$

$$\text{or, } E_1 G_{12} \sum_{m=1}^{\infty} \left[Y_m^{''''} - \frac{E_2 \left(E_1 - 2\mu_{12} G_{12}\right)}{E_1 G_{12}} Y_m^{''} \alpha^2 + \frac{E_2 G_{12}}{E_1 G_{12}} Y_m \alpha^4 \right] \cos \alpha x = 0$$

$$\text{or, } Y_m^{''''} - \frac{E_2 \left(E_1 - 2\mu_{12} G_{12}\right)}{E_1 G_{12}} Y_m^{''} \alpha^2 + \frac{E_2 G_{12}}{E_1 G_{12}} Y_m \alpha^4 = 0$$

$$\text{or, } Y_m^{''''} - \left(\frac{E_2}{G_{12}} - 2\mu_{12} \frac{E_2}{E_1} \right) Y_m^{''} \alpha^2 + \frac{E_2}{E_1} Y_m \alpha^4 = 0 \qquad (5.4)$$

The general solution of ordinary differential equation will be

$$Y_m = A_m e^{r_1 y} + B_m e^{r_2 y} + C_m e^{r_3 y} + D_m e^{r_4 y} \qquad (5.5)$$

where A_m, B_m, C_m and D_m are arbitrary constants and r_1, r_2, r_3 and r_4 are the corresponding roots which are given below

$$r_1, r_2 = \frac{\alpha}{\sqrt{2}}\left[\left(\frac{E_2}{G_2} - 2\mu_{12}\frac{E_2}{E_1}\right) \pm \sqrt{\left(\frac{E_2}{G_{12}} - 2\mu_{12}\frac{E_2}{E_1}\right)^2 - 4\frac{E_2}{E_1}}\right]^{\frac{1}{2}} \tag{5.6a}$$

$$r_3, r_4 = -\frac{\alpha}{\sqrt{2}}\left[\left(\frac{E_2}{G_{12}} - 2\mu_{12}\frac{E_2}{E_1}\right) \pm \sqrt{\left(\frac{E_2}{G_{12}} - 2\mu_{12}\frac{E_2}{E_1}\right)^2 - 4\frac{E_2}{E_1}}\right]^{\frac{1}{2}} \tag{5.6b}$$

Now substituting the derivative of ψ and Y_m by using Eq. (5.3) and (5.5) respectively in the expressions for displacement and stresses (5.2a, 5.2b, 5.2c, 5.2d and 5.2e).

$$u_x(x,y) = \frac{\partial^2 \psi}{\partial x \partial y}$$

$$= -\sum_{m=1}^{\infty} Y'_m \alpha \sin \alpha x$$

$$= -\sum_{m=1}^{\infty}\left(A_m r_1 e^{r_1 y} + B_m r_2 e^{r_2 y} + C_m r_3 e^{r_3 y} + D_m r_4 e^{r_4 y}\right)\alpha \sin \alpha x \tag{5.7a}$$

$$u_y(x,y) = -\frac{1}{Z_{11}}\left[E_1 E_2 \frac{\partial^2 \psi}{\partial x^2} + G_{12}\left(E_1 - \mu_{12}^2 E_2\right)\frac{\partial^2 \psi}{\partial y^2}\right]$$

$$= -\frac{1}{Z_{11}}\left[E_1 E_2\left\{-\sum_{m=1}^{\infty} Y_m \alpha^2 \cos \alpha x\right\} + G_{12}\left(E_1 - \mu_{12}^2 E_2\right)\left\{\sum_{m=1}^{\infty} Y''_m \cos \alpha x + 6Ky\right\}\right]$$

$$= -\frac{1}{Z_{11}}\left[\begin{array}{l} E_1 E_2\left\{-\sum_{m=1}^{\infty}\left(A_m e^{r_1 y} + B_m e^{r_2 y} + C_m e^{r_3 y} + D_m e^{r_4 y}\right)\alpha^2 \cos \alpha x\right\} + G_{12}\left(E_1 - \mu_{12}^2 E_2\right) \\ \left\{\sum_{m=1}^{\infty}\left(A_m r_1^2 e^{r_1 y} + B_m r_2^2 e^{r_2 y} + C_m r_3^2 e^{r_3 y} + D_m r_4^2 e^{r_4 y}\right)\cos \alpha x + 6Ky\right\} \end{array}\right]$$

$$= \frac{1}{Z_{11}}\left[\begin{array}{l} \sum_{m=1}^{\infty}\left\{\begin{array}{l}\left(E_1 E_2 \alpha^2 - E_1 G_{12} r_1^2 + \mu_{12}^2 E_2 G_{12} r_1^2\right)e^{r_1 y} A_{m2} + \left(E_1 E_2 \alpha^2 - E_1 G_{12} r_2^2 + \mu_{12}^2 E_2 G_{12} r_2^2\right)e^{r_2 y} B_{m2} + \\ \left(E_1 E_2 \alpha^2 - E_1 G_{12} r_3^2 + \mu_{12}^2 E_2 G_{12} r_3^2\right)e^{r_3 y} C_{m2} + \left(E_1 E_2 \alpha^2 - E_1 G_{12} r_4^2 + \mu_{12}^2 E_2 G_{12} r_4^2\right)e^{r_4 y} D_{m2}\end{array}\right\} \\ \cos \alpha x - \left(E_1 G_{12} - \mu_{12}^2 E_2 G_{12}\right)6Ky \end{array}\right] \tag{5.7b}$$

$$\sigma_{xx}(x,y)=\frac{E_1E_2G_{12}}{Z_{11}}\left[\frac{\partial^3\psi}{\partial x^2\partial y}-\mu_{12}\frac{\partial^3\psi}{\partial y^3}\right]$$

$$=\frac{E_1G_{12}}{Z_{11}}\left[E_2\left\{-\sum_{m=1}^{\infty}Y_m^{'}\alpha^2\cos\alpha x\right\}-\mu_{12}E_2\left\{\sum_{m=1}^{\infty}Y_m^{'''}\cos\alpha x+6K\right\}\right]$$

$$=-\frac{E_1G_{12}}{Z_{11}}[E_2\left\{\sum_{m=1}^{\infty}\left(A_{m2}r_1e^{r_1y}+B_{m2}r_2e^{r_2y}+C_{m2}r_3e^{r_3y}+D_{m2}r_4e^{r_4y}\right)\alpha^2\cos\alpha x\right\}+$$

$$\mu_{12}E_2\left\{\sum_{m=1}^{\infty}\left(A_{m2}r_1^3e^{r_1y}+B_{m2}r_2^3e^{r_2y}+C_{m2}r_3^3e^{r_3y}+D_{m2}r_4^3e^{r_4y}\right)\cos\alpha x+6K\right\}]$$

$$=-\frac{E_1G_{12}}{Z_{11}}[\sum_{m=1}^{\infty}\{\left(E_2r_1e^{r_1y}\alpha^2+\mu_{12}E_2r_1^3e^{r_1y}\right)A_m+\left(E_2r_2e^{r_{21}y}\alpha^2+\mu_{12}E_2r_2^3e^{r_2y}\right)B_m+$$

$$\left(E_2r_3e^{r_3y}\alpha^2+\mu_{12}E_2r_3^3e^{r_3y}\right)C_m+\left(E_2r_4e^{r_4y}\alpha^2+\mu_{12}E_2r_4^3e^{r_4y}\right)D_m\}\cos\alpha x+6K\mu_{12}E_2] \quad (5.7c)$$

$$\sigma_{yy}(x,y)=-\frac{E_1}{Z_{11}}\left[E_2\left(E_1-\mu_{12}G_{12}\right)\frac{\partial^3\psi}{\partial x^2\partial y}+G_{12}E_1\frac{\partial^3\psi}{\partial y^3}\right]$$

$$=\frac{E_1}{Z_{11}}\left[E_2\left(\mu_{12}G_{12}-E_1\right)\left\{-\sum_{m=1}^{\infty}Y_m^{'}\alpha^2\cos\alpha x\right\}-G_{12}E_1\left\{\sum_{m=1}^{\infty}Y_m^{'''}\cos\alpha x+6K\right\}\right]$$

$$=-\frac{E_1}{Z_{11}}[E_2\left(\mu_{12}G_{12}-E_1\right)\{\sum_{m=1}^{\infty}\left(A_mr_1e^{r_1y}+B_mr_2e^{r_2y}+C_mr_3e^{r_3y}+D_mr_4e^{r_4y}\right)\alpha^2\cos\alpha x\}+$$

$$G_{12}E_1\{\sum_{m=1}^{\infty}\left(A_mr_1^3e^{r_1y}+B_mr_2^3e^{r_2y}+C_mr_3^3e^{r_3y}+D_mr_4^3e^{r_4y}\right)\cos\alpha x+6K\}]$$

$$=-\frac{E_1}{Z_{11}}\sum_{m=1}^{\alpha}\left[\left\{\begin{array}{l}\left(E_2\mu_{12}G_{12}r_1e^{r_1y}\alpha^2-E_1E_2r_1e^{r_1y}\alpha^2+E_2G_{12}r_1^3e^{r_1y}\right)A_m\\+\left(E_2\mu_{12}G_{12}r_2e^{r_2y}\alpha^2-E_1E_2r_2e^{r_2y}\alpha^2+E_2G_{12}r_2^3e^{r_2y}\right)B_m\\+\left(E_2\mu_{12}G_{12}r_3e^{r_3y}\alpha^2-E_1E_2r_3e^{r_3y}\alpha^2+E_2G_{12}r_3^3e^{r_3y}\right)C_m\\+\left(E_2\mu_{12}G_{12}r_4e^{r_4y}\alpha^2-E_1E_2r_4e^{r_4y}\alpha^2+E_2G_{12}r_4^3e^{r_4y}\right)D_m\end{array}\right\}\cos\alpha x+6KG_{12}E_1\right] \quad (5.7d)$$

$$\sigma_{xy}(x,y) = -\frac{E_1 E_2 G_{12}}{Z_{11}}\left[\frac{\partial^3 \psi}{\partial x^3} - \mu_{12}\frac{\partial^3 \psi}{\partial x \partial y^2}\right]$$

$$= -\frac{E_1 G_{12}}{Z_{11}}\{E_2 \sum_{m=1}^{\infty}\left(A_m e^{r_1 y} + B_m e^{r_2 y} + C_m e^{r_3 y} + D_m e^{r_4 y}\right)\alpha^3 \sin \alpha x + \mu_{12} E_2$$

$$\sum_{m=1}^{\infty}\left(A_m r_1^2 e^{r_1 y} + B_m r_2^2 e^{r_2 y} + C_m r_3^2 e^{r_3 y} + D_m r_4^2 e^{r_4 y}\right)\alpha \sin \alpha x\}$$

$$= -\frac{E_1 G_{12}}{Z_{11}}\sum_{m=1}^{\infty}\left\{\begin{matrix}\left(E_2 e^{r_1 y}\alpha^3 + \mu_{12} E_2 r_1^2 e^{r_1 y}\alpha\right)A_m + \left(E_2 e^{r_{21} y}\alpha^3 + \mu_{12} E_2 r_2^2 e^{r_2 y}\alpha\right)B_m + \\ \left(E_2 e^{r_3 y}\alpha^3 + \mu_{12} E_2 r_3^2 e^{r_3 y}\alpha\right)C_m + \left(E_2 e^{r_4 y}\alpha^3 + \mu_{12} E_2 r_4^2 e^{r_4 y}\alpha\right)D_m\end{matrix}\right\}\sin \alpha x \qquad (5.7e)$$

From the expressions of (5.7a) and (5.7e) it is evident that the boundary conditions associated with the left and right lateral ends are automatically satisfied. Thus the next requirement is to satisfy the remaining boundary conditions associated with the upper and bottom boundary surfaces.

Now the reactions acting at the two extreme regions of the supporting surface, $y = 0$ may be expressed in terms of Fourier series as follows:

$$\sigma_{yy}(x,0) = 4\sigma_0 = E_0 + \sum_{m=1}^{\infty} E_m \cos \alpha x \quad \text{for } x=0 \text{ to } 0.1L \text{ and } 0.9L \text{ to } L \qquad (5.8a)$$

Here

$$E_0 = \frac{1}{L}\left[\int_0^{L/10} 4\sigma_0 dx + \int_{9L/10}^{L} 4\sigma_0 dx\right]$$

$$= \frac{4\sigma_0}{L}\left[\frac{L}{10} - 0 + L - \frac{9L}{10}\right]$$

$$= \frac{4\sigma_0}{5} \qquad (5.8b)$$

$$E_m = \frac{2}{L}\left[\int_0^{L/10} 4\sigma_0 \cos\alpha x dx + \int_{9L/10}^{L} 4\sigma_0 \cos\alpha x dx\right]$$

$$= \frac{8\sigma_{yy}^0}{L}\left[\frac{\sin\alpha x}{\alpha}\right]_0^{L/10} + \frac{8\sigma_{yy}^0}{L}\left[\frac{\sin\alpha x}{\alpha}\right]_{9L/10}^{L}$$

$$= \frac{8\sigma_0}{\alpha L}\left\{\sin\left(\frac{\alpha L}{10}\right) - 0 + \sin(\alpha L) - \sin\left(\frac{9\alpha L}{10}\right)\right\}$$

$$= \frac{8\sigma_0}{m\pi}\left\{\sin\left(\frac{m\pi}{10}\right) + \sin(m\pi) - \sin\left(\frac{9m\pi}{10}\right)\right\} \qquad (5.8c)$$

The compressive load on the edge $y = D$ can also be given by a Fourier series as follows

$$\sigma_{yy}(x,0) = \sigma_0 = I_0 + \sum_{m=1}^{\infty} I_m \cos\alpha x \qquad \text{for } x = 0.1L \text{ to } 0.9L \qquad (5.9a)$$

Here

$$I_0 = \frac{1}{L}\left[\int_{L/10}^{9L/10} \sigma_0 dx\right]$$

$$= \frac{\sigma_0}{L}\left[\frac{9L}{10} - \frac{L}{10}\right]$$

$$= \frac{4\sigma_0}{5} \qquad (5.9b)$$

$$I_m = \frac{2}{L}\left[\int_{L/10}^{9L/10} \sigma_0 \cos\alpha x dx\right]$$

$$= \frac{2\sigma_0}{L}\left[\frac{\sin\alpha x}{\alpha}\right]_{l/10}^{9L/10}$$

$$= \frac{2\sigma_0}{\alpha L}\left\{\sin\left(\frac{9\alpha L}{10}\right) - \sin\left(\frac{\alpha L}{10}\right)\right\}$$

$$= \frac{2\sigma_0}{m\pi}\left\{\sin\left(\frac{9m\pi}{10}\right) - \sin\left(\frac{m\pi}{10}\right)\right\} \tag{5.9c}$$

Using boundary condition $\sigma_{xy}(x,0) = 0$ at the edge of $y = 0$

$$-\frac{E_1 G_{12}}{Z_{11}}\left[\sum_{m=1}^{\infty}\begin{Bmatrix}\left(E_2\alpha^3 + \mu_{12}E_2 r_1^2\alpha\right)A_m + \left(E_2\alpha^3 + \mu_{12}E_2 r_2^2\alpha\right)B_m + \\ \left(E_2 e^{r_3 y}\alpha^3 + \mu_{12}E_2 r_3^2\alpha\right)C_m + \left(E_2 e^{r_4 y}\alpha^3 + \mu_{12}E_2 r_4^2\alpha\right)D_m\end{Bmatrix}\sin\alpha x\right] = 0$$

$$\text{or, } -\frac{E_1 G_{12}}{Z_{11}}\begin{Bmatrix}\left(E_2\alpha^3 + \mu_{12}E_2 r_1^2\alpha\right)A_m + \left(E_2\alpha^3 + \mu_{12}E_2 r_2^2\alpha\right)B_m + \\ \left(E_2\alpha^3 + \mu_{12}E_2 r_3^2\alpha\right)C_m + \left(E_2\alpha^3 + \mu_{12}E_2 r_4^2\alpha\right)D_m\end{Bmatrix} = 0 \tag{5.10a}$$

Using boundary condition $\sigma_{xy}(x,D) = 0$ at the edge of $y = D$

$$-\frac{E_1 G_{12}}{Z_{11}}\left[\sum_{m=1}^{\infty}\begin{Bmatrix}\left(E_2 e^{r_1 D}\alpha^3 + \mu_{12}E_2 r_1^2 e^{r_1 D}\alpha\right)A_m + \left(E_2 e^{r_{21} D}\alpha^3 + \mu_{12}E_2 r_2^2 e^{r_2 D}\alpha\right)B_m + \\ \left(E_2 e^{r_3 D}\alpha^3 + \mu_{12}E_2 r_3^2 e^{r_3 D}\alpha\right)C_m + \left(E_2 e^{r_4 D}\alpha^3 + \mu_{12}E_2 r_4^2 e^{r_4 D}\alpha\right)D_m\end{Bmatrix}\sin\alpha x\right] = 0$$

$$\text{or, } -\frac{E_1 G_{12}}{Z_{11}}\begin{Bmatrix}\left(E_2 e^{r_1 D}\alpha^3 + \mu_{12}E_2 r_1^2 e^{r_1 D}\alpha\right)A_m + \left(E_2 e^{r_2 D}\alpha^3 + \mu_{12}E_2 r_2^2 e^{r_2 D}\alpha\right)B_m + \\ \left(E_2 e^{r_3 D}\alpha^3 + \mu_{12}E_2 r_3^2 e^{r_3 D}\alpha\right)C_m + \left(E_2 e^{r_4 D}\alpha^3 + \mu_{12}E_2 r_4^2 e^{r_4 D}\alpha\right)D_m\end{Bmatrix} = 0 \tag{5.10b}$$

Using boundary condition $\sigma_{yy}(x,0) = 4\sigma_0$ at the edge of $y = 0$

$$-\frac{E_1}{Z_{11}}\left[\sum_{m=1}^{\infty}\begin{Bmatrix}\left(E_2\mu_{12}G_{12}r_1\alpha^2 - E_1E_2r_1\alpha^2 + E_1G_{12}r_1^3\right)A_m + \\ \left(E_2\mu_{12}G_{12}r_2\alpha^2 - E_1E_2r_2\alpha^2 + E_1G_{12}r_2^3\right)B_m + \\ \left(E_2\mu_{12}G_{12}r_3\alpha^2 - E_1E_2r_3\alpha^2 + E_1G_{12}r_3^3\right)C_m + \\ \left(E_2\mu_{12}G_{12}r_4\alpha^2 - E_1E_2r_4\alpha^2 + E_1G_{12}r_4^3\right)D_m\end{Bmatrix}\cos\alpha x + 6KG_{12}E_1\right] = \sum_{m=1}^{\infty}E_m\cos\alpha x + E_0$$

Therefore,

$$-\frac{E_1}{Z_{11}}\begin{Bmatrix}\left(E_2\mu_{12}G_{12}r_1\alpha^2-E_1E_2r_1\alpha^2+E_1G_{12}r_1^3\right)A_m+\\ \left(E_2\mu_{12}G_{12}r_2\alpha^2-E_1E_2r_2\alpha^2+E_1G_{12}r_2^3\right)B_m+\\ \left(E_2\mu_{12}G_{12}r_3\alpha^2-E_1E_2r_3\alpha^2+E_1G_{12}r_3^3\right)C_m+\\ \left(E_2\mu_{12}G_{12}r_4\alpha^2-E_1E_2r_4\alpha^2+E_1G_{12}r_4^3\right)D_m\end{Bmatrix}=E_m \tag{5.10c}$$

Using boundary condition $\sigma_{yy}(x,D)=\sigma_0$ at the edge of $y=D$

$$-\frac{E_1}{Z_{11}}\left[\sum_{m=1}^{\infty}\begin{Bmatrix}\left(E_2\mu_{12}G_{12}r_1e^{r_1D}\alpha^2-E_1E_2r_1e^{r_1D}\alpha^2+E_1G_{12}r_1^3e^{r_1D}\right)A_m+\\ \left(E_2\mu_{12}G_{12}r_2e^{r_2D}\alpha^2-E_1E_2r_2e^{r_2D}\alpha^2+E_1G_{12}r_2^3e^{r_2D}\right)B_m+\\ \left(E_2\mu_{12}G_{12}r_3e^{r_3D}\alpha^2-E_1E_2r_3e^{r_3D}\alpha^2+E_1G_{12}r_3^3e^{r_3D}\right)C_m+\\ \left(E_2\mu_{12}G_{12}r_4e^{r_4D}\alpha^2-E_1E_2r_4e^{r_4D}\alpha^2+E_1G_{12}r_4^3e^{r_4D}\right)D_m\end{Bmatrix}\cos\alpha x+6KG_{12}E_1\right]=\sum_{m=1}^{\infty}I_m\cos\alpha x+I_0$$

Therefore,

$$-\frac{E_1}{Z_{11}}\begin{Bmatrix}\left(E_2\mu_{12}G_{12}r_1e^{r_1D}\alpha^2-E_1E_2r_1e^{r_1D}\alpha^2+E_1G_{12}r_1^3e^{r_1D}\right)A_m+\\ \left(E_2\mu_{12}G_{12}r_2e^{r_2D}\alpha^2-E_1E_2r_2e^{r_2D}\alpha^2+E_1G_{12}r_2^3e^{r_2D}\right)B_m+\\ \left(E_2\mu_{12}G_{12}r_3e^{r_3D}\alpha^2-E_1E_2r_3e^{r_3D}\alpha^2+E_1G_{12}r_3^3e^{r_3D}\right)C_m+\\ \left(E_2\mu_{12}G_{12}r_4e^{r_4D}\alpha^2-E_1E_2r_4e^{r_4D}\alpha^2+E_1G_{12}r_4^3e^{r_4D}\right)D_m\end{Bmatrix}=I_m \tag{5.10d}$$

From Eqs. (5.7d) and (5.8) or (5.9), the arbitrary constant *K* can be obtained as follows:

$$-\frac{6E_1^2KG_{12}}{Z_{11}}=E_0=I_0=\frac{4\sigma_0}{5}$$

$$\text{or, } K=-\frac{2Z_{11}\sigma_0}{15E_1^2G_{12}} \tag{5.11}$$

The simultaneous Eqs. (4.10a), (4.10b), (4.10c) and (4.10d) can be realized in a simplified matrix form for solution of the unknown terms of arbitrary constants like A_m, B_m, C_m and D_m as follows:

$$\begin{bmatrix} F_1 & F_2 & F_3 & F_4 \\ H_1 & H_2 & H_3 & H_4 \\ R_1 & R_2 & R_3 & R_4 \\ S_1 & S_2 & S_3 & S_4 \end{bmatrix} \begin{bmatrix} A_m \\ B_m \\ C_m \\ D_m \end{bmatrix} = \begin{bmatrix} 0 \\ 0 \\ \overline{E}_m \\ \overline{I}_m \end{bmatrix} \tag{5.12}$$

where

$$\left.\begin{aligned} F_i &= E_2\alpha^3 + \mu_{12}E_2 r_i^2\alpha \\ H_i &= E_2 e^{r_i D}\alpha^3 + \mu_{12}E_2 r_1^2 e^{r_i D}\alpha \\ R_i &= E_2\mu_{12}G_{12}r_i\alpha^2 - E_1E_2 r_i\alpha^2 + E_1G_{12}r_i^3 \\ S_i &= E_2\mu_{12}G_{12}r_i e^{r_i D}\alpha^2 - E_1E_2 r_i e^{r_i D}\alpha^2 + E_1G_{12}r_i^3 e^{r_i D} \end{aligned}\right\} \quad i=1, 2, 3, 4$$

$$\overline{E}_m = -\frac{Z_{11}E_{m2}}{E_1}$$

$$\overline{I}_m = -\frac{Z_{11}I_{m2}}{E_1}$$

$$Z_{11} = \mu_{12}E_1E_2 + G_{12}\left(E_1 - \mu_{12}^2 E_2\right)$$

Eqs. 5.7 are used for finding the stress and displacement components at various points of the beam and the appropriate values of E_m and I_m are determined to get the values of four unknowns constant, namely A_m, B_m, C_m and D_m by using either the matrix (5.12) or the four algebraic simultaneous Eqs. (5.10a), (5.10b), (5.10c) and (5.10d).

Case-2: Beam with lateral stiffeners

In this case the trial function is assumed in terms of sine function so that its first and third derivatives with respect to x can be found in terms of cosine function. The displacement potential function ψ for the case of lateral stiffener is assumed as:

$$\psi = \sum_{m=1}^{\infty} Y_m \sin \alpha x \tag{5.13}$$

where $Y_m = f(y)$, $\alpha = \dfrac{m\pi}{L}$ and K = Arbitrary constant and m = 1, 2, 3, …….. ∞.

Derivatives of Eq. (4.14) with respect to x and y are

$$\frac{\partial \psi}{\partial x} = \sum_{m=1}^{\infty} Y_m \alpha \cos \alpha x$$

$$\frac{\partial^2 \psi}{\partial x^2} = -\sum_{m=1}^{\infty} Y_m \alpha^2 \sin \alpha x$$

$$\frac{\partial^3 \psi}{\partial x^3} = -\sum_{m=1}^{\infty} Y_m \alpha^3 \cos \alpha x$$

$$\frac{\partial^4 \psi}{\partial x^4} = \sum_{m=1}^{\infty} Y_m \alpha^4 \sin \alpha x$$

$$\frac{\partial^2 \psi}{\partial x \partial y} = \sum_{m=1}^{\infty} Y_m' \alpha \cos \alpha x$$

$$\frac{\partial^3 \psi}{\partial x \partial y^2} = \sum_{m=1}^{\infty} Y_m'' \alpha \cos \alpha x$$

$$\frac{\partial^3 \psi}{\partial x^2 \partial y} = -\sum_{m=1}^{\infty} Y_m^{'} \alpha^2 \sin \alpha x$$

$$\frac{\partial^4 \psi}{\partial x^2 \partial y^2} = -\sum_{m=1}^{\infty} Y_m^{''} \alpha^2 \sin \alpha x$$

$$\frac{\partial \psi}{\partial y} = \sum_{m=1}^{\infty} Y_m^{'} \sin \alpha x$$

$$\frac{\partial^2 \psi}{\partial y^2} = \sum_{m=1}^{\infty} Y_m^{''} \sin \alpha x$$

$$\frac{\partial^3 \psi}{\partial y^3} = \sum_{m=1}^{\infty} Y_m^{'''} \sin \alpha x$$

$$\frac{\partial^4 \psi}{\partial y^4} = \sum_{m=1}^{\infty} Y_m^{''''} \sin \alpha x$$

Using the derivatives of Eq. (5.13), Eq. (5.1) yields

$$E_2 G_{12} \sum_{m=1}^{\infty} Y_m \alpha^4 \cos \alpha x + E_2 \left(E_1 - 2\mu_{12} G_{12}\right) \sum_{m=1}^{\infty} Y_m^{''} \alpha^2 \sin \alpha x + E_1 G_{12} \sum_{m=1}^{\infty} Y_m^{''''} \sin \alpha x = 0$$

$$\text{or, } E_1 G_{12} \sum_{m=1}^{\infty} \left[Y_m^{''''} - \frac{E_2 \left(E_1 - 2\mu_{12} G_{12}\right)}{E_1 G_{12}} Y_m^{''} \alpha^2 + \frac{E_2 G_{12}}{E_1 G_{12}} Y_m \alpha^4 \right] \sin \alpha x = 0$$

$$\text{or, } Y_m^{''''} - \frac{E_2 \left(E_1 - 2\mu_{12} G_{12}\right)}{E_1 G_{12}} Y_m^{''} \alpha^2 + \frac{E_2 G_{12}}{E_1 G_{12}} Y_m \alpha^4 = 0$$

$$\text{or, } Y_m^{''''} - \left(\frac{E_2}{G_{12}} - 2\mu_{12} \frac{E_2}{E_1} \right) Y_m^{''} \alpha^2 + \frac{E_2}{E_1} Y_m \alpha^4 = 0 \qquad (5.14)$$

The general solution of ordinary differential equation will be

$$Y_m = L_m e^{r_1 y} + M_m e^{r_2 y} + N_m e^{r_3 y} + O_m e^{r_4 y} \tag{5.15}$$

Where L_m, M_m, N_m and O_m are arbitrary constants and r_1, r_2, r_3 and r_4 are the corresponding roots which are given below

$$r_1, r_2 = \frac{\alpha}{\sqrt{2}}\left[\left(\frac{E_2}{G_{12}} - 2\mu_{12}\frac{E_2}{E_1}\right) \pm \sqrt{\left(\frac{E_2}{G_{12}} - 2\mu_{12}\frac{E_2}{E_1}\right)^2 - 4\frac{E_2}{E_1}}\right]^{\frac{1}{2}} \tag{5.16a}$$

$$r_3, r_4 = -\frac{\alpha}{\sqrt{2}}\left[\left(\frac{E_2}{G_{12}} - 2\mu_{12}\frac{E_2}{E_1}\right) \pm \sqrt{\left(\frac{E_2}{G_{12}} - 2\mu_{12}\frac{E_2}{E_1}\right)^2 - 4\frac{E_2}{E_1}}\right]^{\frac{1}{2}} \tag{5.16b}$$

Now substituting the derivatives of ψ and Y_m by using Eqs. (5.13) and (5.15) respectively in the expressions for displacement and stresses (5.2a, 5.2b, 4.13c, 4.13d and 4.13e).

$$u_x(x,y) = \frac{\partial^2 \psi}{\partial x \partial y}$$

$$= \sum_{m=1}^{\infty} Y'_m \alpha \cos \alpha x$$

$$= \sum_{m=1}^{\infty} \left(L_m r_1 e^{r_1 y} + M_m r_2 e^{r_2 y} + N_m r_3 e^{r_3 y} + O_m r_4 e^{r_4 y}\right) \alpha \cos \alpha x \tag{5.17a}$$

$$u_y(x,y) = -\frac{1}{Z_{11}}\left[E_1 E_2 \frac{\partial^2 \psi}{\partial x^2} + G_{12}\left(E_1 - \mu_{12}^2 E_2\right)\frac{\partial^2 \psi}{\partial y^2}\right]$$

$$= -\frac{1}{Z_{11}}\left[-E_1 E_2 \left\{\sum_{m=1}^{\infty} Y_m \alpha^2 \sin \alpha x\right\} + G_{12}\left(E_1 - \mu_{12}^2 E_2\right)\left\{\sum_{m=1}^{\infty} Y''_m \sin \alpha x\right\}\right]$$

$$= -\frac{1}{Z_{11}}\begin{bmatrix} E_1 E_2\left\{-\sum_{m=1}^{\infty}\left(L_m e^{r_1 y} + M_m e^{r_2 y} + N_m e^{r_3 y} + O_m e^{r_4 y}\right)\alpha^2 \sin\alpha x\right\} + G_{12}\left(E_1 - \mu_{12}^2 E_2\right) \\ \left\{\sum_{m=1}^{\infty}\left(L_m r_1^2 e^{r_1 y} + M_m r_2^2 e^{r_2 y} + N_m r_3^2 e^{r_3 y} + O_m r_4^2 e^{r_4 y}\right)\sin\alpha x\right\} \end{bmatrix}$$

$$= \frac{1}{Z_{11}}\left[\sum_{m=1}^{\infty}\begin{Bmatrix}\left(E_1 E_2\alpha^2 - E_1 G_{12} r_1^2 + \mu_{12}^2 E_2 G_{12} r_1^2\right)e^{r_1 y} L_m + \left(E_1 E_2\alpha^2 - E_1 G_{12} r_2^2 + \mu_{12}^2 E_2 G_{12} r_2^2\right)e^{r_2 y} M_m + \\ \left(E_1 E_2\alpha^2 - E_1 G_{12} r_3^2 + \mu_{12}^2 E_2 G_{12} r_3^2\right)e^{r_3 y} N_m + \left(E_1 E_2\alpha^2 - E_1 G_{12} r_4^2 + \mu_{12}^2 E_2 G_{12} r_4^2\right)e^{r_4 y} O_m \end{Bmatrix}\sin\alpha x\right] \quad (5.17b)$$

$$\sigma_{xx}(x,y) = \frac{E_1 E_2 G_{12}}{Z_{11}}\left[\frac{\partial^3\psi}{\partial x^2\partial y} - \mu_{12}\frac{\partial^3\psi}{\partial y^3}\right]$$

$$= \frac{E_1 E_2 G_{12}}{Z_{11}}\left[\left\{-\sum_{m=1}^{\infty} Y_m^{'}\alpha^2 \sin\alpha x\right\} - \mu_{12}\left\{\sum_{m=1}^{\infty} Y_m^{'''}\sin\alpha x\right\}\right]$$

$$= -\frac{E_1 E_2 G_{12}}{Z_{11}}[\left\{\sum_{m=1}^{\infty}\left(A_m r_1 e^{r_1 y} + B_m r_2 e^{r_2 y} + C_m r_3 e^{r_3 y} + D_m r_4 e^{r_4 y}\right)\alpha^2 \sin\alpha x\right\} +$$
$$\mu_{12}\left\{\sum_{m=1}^{\infty}\left(A_m r_1^3 e^{r_1 y} + B_m r_2^3 e^{r_2 y} + C_m r_3^3 e^{r_3 y} + D_m r_4^3 e^{r_4 y}\right)\sin\alpha x\right\}]$$

$$= -\frac{E_1 G_{12}}{Z_{11}}[\sum_{m=1}^{\infty}\{\left(E_2 r_1 e^{r_1 y}\alpha^2 + \mu_{12} E_2 r_1^3 e^{r_1 y}\right)L_m + \left(E_2 r_2 e^{r_{21} y}\alpha^2 + \mu_{12} E_2 r_2^3 e^{r_2 y}\right)M_m +$$
$$\left(E_2 r_3 e^{r_3 y}\alpha^2 + \mu_{12} E_2 r_3^3 e^{r_3 y}\right)N_m + \left(E_2 r_4 e^{r_4 y}\alpha^2 + \mu_{12} E_2 r_4^3 e^{r_4 y}\right)O_m\}\sin\alpha x] \quad (5.17c)$$

$$\sigma_{yy}(x,y) = -\frac{E_1}{Z_{11}}\left[E_2\left(E_1 - \mu_{12} G_{12}\right)\frac{\partial^3\psi}{\partial x^2\partial y} + G_{12} E_1\frac{\partial^3\psi}{\partial y^3}\right]$$

$$= \frac{E_1}{Z_{11}}\left[E_2\left(\mu_{12} G_{12} - E_1\right)\left\{-\sum_{m=1}^{\infty} Y_m^{'}\alpha^2 \sin\alpha x\right\} - G_{12} E_1\left\{\sum_{m=1}^{\infty} Y_m^{'''}\sin\alpha x\right\}\right]$$

$$= -\frac{E_1}{Z_{11}}[E_2\left(\mu_{12} G_{12} - E_1\right)\{\sum_{m=1}^{\infty}\left(L_m r_1 e^{r_1 y} + M_m r_2 e^{r_2 y} + N_m r_3 e^{r_3 y} + O_m r_4 e^{r_4 y}\right)\alpha^2 \sin\alpha x\} +$$
$$G_{12} E_1\{\sum_{m=1}^{\infty}\left(L_m r_1^3 e^{r_1 y} + M_m r_2^3 e^{r_2 y} + N_m r_3^3 e^{r_3 y} + O_m r_4^3 e^{r_4 y}\right)\sin\alpha x\}]$$

$$= -\frac{E_1}{Z_{11}} \sum_{m=1}^{\alpha} \left[\begin{Bmatrix} \left(E_2 \mu_{12} G_{12} r_1 e^{r_1 y} \alpha^2 - E_1 E_2 r_1 e^{r_1 y} \alpha^2 + E_2 G_{12} r_1^3 e^{r_1 y}\right) L_m \\ + \left(E_2 \mu_{12} G_{12} r_2 e^{r_2 y} \alpha^2 - E_1 E_2 r_2 e^{r_2 y} \alpha^2 + E_2 G_{12} r_2^3 e^{r_2 y}\right) M_m \\ + \left(E_2 \mu_{12} G_{12} r_3 e^{r_3 y} \alpha^2 - E_1 E_2 r_3 e^{r_3 y} \alpha^2 + E_2 G_{12} r_3^3 e^{r_3 y}\right) N_m \\ + \left(E_2 \mu_{12} G_{12} r_4 e^{r_4 y} \alpha^2 - E_1 E_2 r_4 e^{r_4 y} \alpha^2 + E_2 G_{12} r_4^3 e^{r_4 y}\right) O_m \end{Bmatrix} \sin \alpha x \right] \quad (5.17d)$$

$$\sigma_{xy}(x, y) = -\frac{E_1 E_2 G_{12}}{Z_{11}} \left[\frac{\partial^3 \psi}{\partial x^3} - \mu_{12} \frac{\partial^3 \psi}{\partial x \partial y^2} \right]$$

$$= \frac{E_1 E_2 G_{12}}{Z_{11}} \{ \sum_{m=1}^{\infty} \left(L_m e^{r_1 y} + M_m e^{r_2 y} + N_m e^{r_3 y} + O_m e^{r_4 y} \right) \alpha^3 \cos \alpha x + \mu_{12}$$

$$\sum_{m=1}^{\infty} \left(L_m r_1^2 e^{r_1 y} + M_m r_2^2 e^{r_2 y} + N_m r_3^2 e^{r_3 y} + O_m r_4^2 e^{r_4 y} \right) \alpha \cos \alpha x \}$$

$$= \frac{E_1 G_{12}}{Z_{11}} \sum_{m=1}^{\infty} \begin{Bmatrix} \left(E_2 e^{r_1 y} \alpha^3 + \mu_{12} E_2 r_1^2 e^{r_1 y} \alpha\right) L_m + \left(E_2 e^{r_{21} y} \alpha^3 + \mu_{12} E_2 r_2^2 e^{r_2 y} \alpha\right) M_m + \\ \left(E_2 e^{r_3 y} \alpha^3 + \mu_{12} E_2 r_3^2 e^{r_3 y} \alpha\right) N_m + \left(E_2 e^{r_4 y} \alpha^3 + \mu_{12} E_2 r_4^2 e^{r_4 y} \alpha\right) O_m \end{Bmatrix} \cos \alpha x \quad (5.17e)$$

Now the reactions acting at the two extreme regions of the supporting surface, $y = 0$ may be expressed in terms of Fourier series as follows:

$$\sigma_{yy}(x,0) = 4\sigma_0 = E_0 + \sum_{m=1}^{\infty} E_m \cos \alpha x \text{ for } x = 0 \text{ to } 0.1L \text{ and } 0.9L \text{ to } L \quad (5.18a)$$

Here

$$E_0 = 0 \quad (5.18b)$$

$$E_m = \frac{2}{L} \left[\int_0^{L/10} 4\sigma_0 \sin \alpha x dx + \int_{9L/10}^{L} 4\sigma_0 \sin \alpha x dx \right]$$

$$= \frac{8\sigma_{yy}^0}{L} \left[\frac{-\cos \alpha x}{\alpha} \right]_0^{L/10} + \frac{8\sigma_{yy}^0}{L} \left[\frac{-\cos \alpha x}{\alpha} \right]_{9L/10}^{L}$$

$$= -\frac{8\sigma_0}{\alpha L} \left\{ \cos\left(\frac{\alpha L}{10}\right) - 1 + \cos(\alpha L) - \cos\left(\frac{9\alpha L}{10}\right) \right\}$$

$$= -\frac{8\sigma_0}{m\pi}\left\{\cos\left(\frac{m\pi}{10}\right) - 1 + \cos(m\pi) - \cos\left(\frac{9m\pi}{10}\right)\right\} \tag{5.18c}$$

The compressive load on the edge $y = D$ can also be given by a Fourier series as follows

$$\sigma_{yy}(x,0) = \sigma_0 = I_0 + \sum_{m=1}^{\infty} I_m \sin \alpha x \qquad \text{for } x = 0.1L \text{ to } 0.9L \tag{5.19a}$$

Here

$$I_0 = 0 \tag{5.19b}$$

$$I_m = \frac{2}{L}\left[\int_{L/10}^{9L/10} \sigma_0 \sin \alpha x dx\right]$$

$$= -\frac{2\sigma_0}{L}\left[\frac{\cos \alpha x}{\alpha}\right]_{l/10}^{9L/10}$$

$$= \frac{2\sigma_0}{m\pi}\left\{\cos\left(\frac{9m\pi}{10}\right) - \cos\left(\frac{m\pi}{10}\right)\right\} \tag{5.19c}$$

Using boundary condition $\sigma_{xy}(x,0) = 0$ at the edge of $y = 0$

$$\frac{E_1 G_{12}}{Z_{11}}\left[\sum_{m=1}^{\infty}\left\{\begin{matrix}\left(E_2\alpha^3 + \mu_{12}E_2 r_1^2\alpha\right)L_m + \left(E_2\alpha^3 + \mu_{12}E_2 r_2^2\alpha\right)M_m + \\ \left(E_2 e^{r_3 y}\alpha^3 + \mu_{12}E_2 r_3^2\alpha\right)N_m + \left(E_2 e^{r_4 y}\alpha^3 + \mu_{12}E_2 r_4^2\alpha\right)O_m\end{matrix}\right\}\cos \alpha x\right] = 0$$

$$\text{or, } \frac{E_1 G_{12}}{Z_{11}}\left\{\begin{matrix}\left(E_2\alpha^3 + \mu_{12}E_2 r_1^2\alpha\right)L_m + \left(E_2\alpha^3 + \mu_{12}E_2 r_2^2\alpha\right)M_m + \\ \left(E_2\alpha^3 + \mu_{12}E_2 r_3^2\alpha\right)N_m + \left(E_2\alpha^3 + \mu_{12}E_2 r_4^2\alpha\right)O_m\end{matrix}\right\} = 0 \tag{5.20a}$$

Using boundary condition $\sigma_{xy}(x,D)=0$ at the edge of $y=D$

$$\frac{E_1G_{12}}{Z_{11}}\left[\sum_{m=1}^{\infty}\begin{Bmatrix}\left(E_2e^{r_1D}\alpha^3+\mu_{12}E_2r_1^2e^{r_1D}\alpha\right)L_m+\left(E_2e^{r_{21}D}\alpha^3+\mu_{12}E_2r_2^2e^{r_2D}\alpha\right)M_m+\\ \left(E_2e^{r_3D}\alpha^3+\mu_{12}E_2r_3^2e^{r_3D}\alpha\right)N_m+\left(E_2e^{r_4D}\alpha^3+\mu_{12}E_2r_4^2e^{r_4D}\alpha\right)O_m\end{Bmatrix}\cos\alpha x\right]=0$$

$$\text{or, }\frac{E_1G_{12}}{Z_{11}}\begin{Bmatrix}\left(E_2e^{r_1D}\alpha^3+\mu_{12}E_2r_1^2e^{r_1D}\alpha\right)L_m+\left(E_2e^{r_2D}\alpha^3+\mu_{12}E_2r_2^2e^{r_2D}\alpha\right)M_m+\\ \left(E_2e^{r_3D}\alpha^3+\mu_{12}E_2r_3^2e^{r_3D}\alpha\right)N_m+\left(E_2e^{r_4D}\alpha^3+\mu_{12}E_2r_4^2e^{r_4D}\alpha\right)O_m\end{Bmatrix}=0 \qquad (5.20b)$$

Using boundary condition $\sigma_{yy}(x,0)=4\sigma_0$ at the edge of $y=0$

$$-\frac{E_1}{Z_{11}}\left[\sum_{m=1}^{\infty}\begin{Bmatrix}\left(E_2\mu_{12}G_{12}r_1\alpha^2-E_1E_2r_1\alpha^2+G_{12}E_1r_1^3\right)L_m+\\ \left(E_2\mu_{12}G_{12}r_2\alpha^2-E_1E_2r_2\alpha^2+G_{12}E_1r_2^3\right)M_m+\\ \left(E_2\mu_{12}G_{12}r_3\alpha^2-E_1E_2r_3\alpha^2+G_{12}E_1r_3^3\right)N_m+\\ \left(E_2\mu_{12}G_{12}r_4\alpha^2-E_1E_2r_4\alpha^2+G_{12}E_1r_4^3\right)O_m\end{Bmatrix}\sin\alpha x\right]=\sum_{m=1}^{\infty}E_m\sin\alpha x+E_0$$

Therefore,

$$-\frac{E_1}{Z_{11}}\begin{Bmatrix}\left(E_2\mu_{12}G_{12}r_1\alpha^2-E_1E_2r_1\alpha^2+G_{12}E_1r_1^3\right)L_m+\\ \left(E_2\mu_{12}G_{12}r_2\alpha^2-E_1E_2r_2\alpha^2+G_{12}E_1r_2^3\right)M_m+\\ \left(E_2\mu_{12}G_{12}r_3\alpha^2-E_1E_2r_3\alpha^2+G_{12}E_1r_3^3\right)N_m+\\ \left(E_2\mu_{12}G_{12}r_4\alpha^2-E_1E_2r_4\alpha^2+G_{12}E_1r_4^3\right)O_m\end{Bmatrix}=E_m \qquad (5.20c)$$

Using boundary condition $\sigma_{yy}(x,D)=\sigma_0$ at the edge of $y=D$

$$-\frac{E_1}{Z_{11}}\left[\sum_{m=1}^{\infty}\begin{Bmatrix}\left(E_2\mu_{12}G_{12}r_1e^{r_1D}\alpha^2-E_1E_2r_1e^{r_1D}\alpha^2+G_{12}E_1r_1^3e^{r_1D}\right)L_m+\\ \left(E_2\mu_{12}G_{12}r_2e^{r_2D}\alpha^2-E_1E_2r_2e^{r_2D}\alpha^2+G_{12}E_1r_2^3e^{r_2D}\right)M_m+\\ \left(E_2\mu_{12}G_{12}r_3e^{r_3D}\alpha^2-E_1E_2r_3e^{r_3D}\alpha^2+G_{12}E_1r_3^3e^{r_3D}\right)N_m+\\ \left(E_2\mu_{12}G_{12}r_4e^{r_4D}\alpha^2-E_1E_2r_4e^{r_4D}\alpha^2+G_{12}E_1r_4^3e^{r_4D}\right)O_m\end{Bmatrix}\sin\alpha x\right]=\sum_{m=1}^{\infty}I_m\sin\alpha x+I_0$$

Therefore,

$$-\frac{E_1}{Z_{11}}\begin{Bmatrix}\left(E_2\mu_{12}G_{12}r_1e^{r_1D}\alpha^2-E_1E_2r_1e^{r_1D}\alpha^2+G_{12}E_1r_1^3e^{r_1D}\right)L_m+\\ \left(E_2\mu_{12}G_{12}r_2e^{r_2D}\alpha^2-E_1E_2r_2e^{r_2D}\alpha^2+G_{12}E_1r_2^3e^{r_2D}\right)M_m+\\ \left(E_2\mu_{12}G_{12}r_3e^{r_3D}\alpha^2-E_1E_2r_3e^{r_3D}\alpha^2+G_{12}E_1r_3^3e^{r_3D}\right)N_m+\\ \left(E_2\mu_{12}G_{12}r_4e^{r_4D}\alpha^2-E_1E_2r_4e^{r_4D}\alpha^2+G_{12}E_1r_4^3e^{r_4D}\right)O_m\end{Bmatrix}=I_m \qquad (5.20d)$$

From Eqs. (5.17d) and (5.18) or (5.19)

$$E_0 = I_0 = 0$$

The simultaneous Eqs. (5.20a), (5.20b), (5.20c) and (5.20d) can be realized in a simplified matrix form for solution of the unknown terms of arbitrary constants like L_m, M_m, N_m and O_m as follows:

$$\begin{bmatrix}P_1 & P_2 & P_3 & P_4\\ Q_1 & Q_2 & Q_3 & Q_4\\ T_1 & T_2 & T_3 & T_4\\ U_1 & U_2 & U_3 & U_4\end{bmatrix}\begin{bmatrix}L_m\\ M_m\\ N_m\\ O_m\end{bmatrix}=\begin{bmatrix}0\\ 0\\ \overline{E}_m\\ \overline{I}_m\end{bmatrix} \qquad (5.21)$$

where

$$\left.\begin{aligned}P_i &= E_1\alpha^3+\mu_{12}E_2r_i^2\alpha\\ Q_i &= E_1e^{r_iD}\alpha^3+\mu_{12}E_2r_1^2e^{r_iD}\alpha\\ T_i &= \mu_{12}G_{12}r_i\alpha^2-E_1r_i\alpha^2+G_{12}r_i^3\\ U_i &= \mu_{12}G_{12}r_ie^{r_iD}\alpha^2-E_1r_ie^{r_iD}\alpha^2+G_{12}r_i^3e^{r_iD}\end{aligned}\right\} \quad i=1, 2, 3, 4$$

$$\overline{E}_m = -\frac{Z_{11}E_{m2}}{E_1}$$

$$\overline{I}_m = -\frac{Z_{11}I_{m2}}{E_1}$$

$$Z_{11} = \mu_{12}E_1E_2 + G_{12}\left(E_1 - \mu_{12}^2E_2\right)$$

Eqs. 5.17 are used for finding the stress and displacement components at various points of the beam and the appropriate values of E_m and I_m are determined to get the values of four unknowns constant, namely L_m, M_m, N_m and O_m by using either the matrix (5.22) or the four algebraic simultaneous Eqs. (5.20a), (5.20b), (5.20c) and (5.20d).

5.3.2 Case-B (Fiber orientation, $\theta = 0^0$)

Fiber orientation, $\theta = 0^0$ is already discussed in previous chapter for both stiffening conditions, i.e., beam with axial stiffeners and beam with lateral stiffeners. So, a brief discussion is given below to facilitate the whole understanding of fiber orientation.

Case-1: Beam with axial stiffeners

By utilizing the same assumed potential function in Eqs. (2.19a) and (2.19b), the fourth order ordinary differential equation will be

$$Y_m'''' - \left(\frac{E_1}{G_{12}} - 2\mu_{12}\right)Y_m''\alpha^2 + \frac{E_1}{E_2}Y_m\alpha^4 = 0 \tag{5.22}$$

The general solution of the differential equation can be written as

$$Y_m(y) = A_m e^{r_1 y} + B_m e^{r_2 y} + C_m e^{r_3 y} + D_m e^{r_4 y} \tag{5.23}$$

Where

$$r_1, r_2 = \frac{\alpha}{\sqrt{2}}\left[\left(\frac{E_1}{G_{12}} - 2\mu_{12}\right) \pm \sqrt{\left(\frac{E_1}{G_{12}} - 2\mu_{12}\right)^2 - 4\frac{E_1}{E_2}}\right]^{\frac{1}{2}}$$

$$r_3, r_4 = -\frac{\alpha}{\sqrt{2}}\left[\left(\frac{E_1}{G_{12}} - 2\mu_{12}\right) \pm \sqrt{\left(\frac{E_1}{G_{12}} - 2\mu_{12}\right)^2 - 4\frac{E_1}{E_2}}\right]^{\frac{1}{2}}$$

and A_m, B_m, C_m and D_m are arbitrary constants

Now substituting Eqs. (5.3) and (5.23) in the expressions for displacements and stresses as given by Eqs. (2.36a), (2.36b), (2.36c), (2.36d) and (2.36e), one obtains

$$u_x(x,y) = -\sum_{m=1}^{\infty}\left(A_m r_1 e^{r_1 y} + B_m r_2 e^{r_2 y} + C_m r_3 e^{r_3 y} + D_m r_4 e^{r_4 y}\right)\alpha \sin \alpha x \tag{5.24}$$

$$u_y(x,y) = \frac{1}{Z_{11}}\left[\sum_{m=1}^{\infty}\left\{\begin{matrix}\left(E_1^2\alpha^2 - E_1 G_{12} r_1^2 + \mu_{12}^2 E_2 G_{12} r_1^2\right)e^{r_1 y} A_m + \\ \left(E_1^2\alpha^2 - E_1 G_{12} r_2^2 + \mu_{12}^2 E_2 G_{12} r_2^2\right)e^{r_2 y} B_m + \\ \left(E_1^2\alpha^2 - E_1 G_{12} r_3^2 + \mu_{12}^2 E_2 G_{12} r_3^2\right)e^{r_3 y} C_m + \\ \left(E_1^2\alpha^2 - E_1 G_{12} r_4^2 + \mu_{12}^2 E_2 G_{12} r_4^2\right)e^{r_4 y} D_m\end{matrix}\right\}\cos \alpha x - 6\left(E_1 G_{12} - \mu_{12}^2 E_2 G_{12}\right)ky\right] \tag{5.25}$$

$$\sigma_{xx}(x,y) = -\frac{E_1 G_{12}}{Z_{11}}\left[\sum_{m=1}^{\infty}\left\{\begin{matrix}\left(E_1 r_1 e^{r_1 y}\alpha^2 + \mu_{12} E_2 r_1^3 e^{r_1 y}\right)A_m + \\ \left(E_1 r_2 e^{r_2 y}\alpha^2 + \mu_{12} E_2 r_2^3 e^{r_2 y}\right)B_m + \\ \left(E_1 r_3 e^{r_3 y}\alpha^2 + \mu_{12} E_2 r_3^3 e^{r_3 y}\right)C_m + \\ \left(E_1 r_4 e^{r_4 y}\alpha^2 + \mu_{12} E_2 r_4^3 e^{r_4 y}\right)D_m\end{matrix}\right\}\cos \alpha x + 6k\mu_{12} E_2\right] \tag{5.26}$$

$$\sigma_{yy}(x,y) = -\frac{E_1 E_2}{Z_{11}}\left[\sum_{m=1}^{\infty}\left\{\begin{matrix}\left(\mu_{12} G_{12} r_1 e^{r_1 y}\alpha^2 - E_1 r_1 e^{r_1 y}\alpha^2 + G_{12} r_1^3 e^{r_1 y}\right)A_m + \\ \left(\mu_{12} G_{12} r_2 e^{r_2 y}\alpha^2 - E_1 r_2 e^{r_2 y}\alpha^2 + G_{12} r_2^3 e^{r_2 y}\right)B_m + \\ \left(\mu_{12} G_{12} r_3 e^{r_3 y}\alpha^2 - E_1 r_3 e^{r_3 y}\alpha^2 + G_{12} r_3^3 e^{r_3 y}\right)C_m + \\ \left(\mu_{12} G_{12} r_4 e^{r_4 y}\alpha^2 - E_1 r_4 e^{r_4 y}\alpha^2 + G_{12} r_4^3 e^{r_4 y}\right)D_m\end{matrix}\right\}\cos \alpha x - 6\,k\,G_{12}\right] \tag{5.27}$$

$$\sigma_{xy}(x,y) = -\frac{E_1 G_{12}}{Z_{11}} \sum_{m=1}^{\infty} \begin{Bmatrix} \left(E_1 e^{r_1 y}\alpha^3 + \mu_{12} E_2 r_1^2 e^{r_1 y}\alpha\right)A_m + \\ \left(E_1 e^{r_2 y}\alpha^3 + \mu_{12} E_2 r_2^2 e^{r_2 y}\alpha\right)B_m + \\ \left(E_1 e^{r_3 y}\alpha^3 + \mu_{12} E_2 r_3^2 e^{r_3 y}\alpha\right)C_m + \\ \left(E_1 e^{r_4 y}\alpha^3 + \mu_{12} E_2 r_4^2 e^{r_4 y}\alpha\right)D_m \end{Bmatrix} \sin \alpha x \tag{5.28}$$

The loading parameters (E_0, I_0, E_m, I_m) obtained by the use of Fourier series for the case of axial stiffening condition with fiber orientation $\theta = 0^0$ are same as those obtained for axial stiffening condition with fiber orientation $\theta = 90^0$.

Using boundary condition, $\sigma_{xy}(x, y) = 0$ and $\sigma_{yy}(x, y)$, at the surfaces, $y = 0$ and $y = D$, the following equations are obtained

$$\begin{Bmatrix} \left(E_1\alpha^3 + \mu_{12} E_2 r_1^2 \alpha\right)A_m + \left(E_1\alpha^3 + \mu_{12} E_2 r_2^2 \alpha\right)B_m + \\ \left(E_1\alpha^3 + \mu_{12} E_2 r_3^2 \alpha\right)C_m + \left(E_1\alpha^3 + \mu_{12} E_2 r_4^2 \alpha\right)D_m \end{Bmatrix} = 0 \tag{5.29}$$

$$\begin{Bmatrix} \left(E_1 e^{r_1 D}\alpha^3 + \mu_{12} E_2 r_1^2 e^{r_1 D}\alpha\right)A_m + \left(E_1 e^{r_2 D}\alpha^3 + \mu_{12} E_2 r_2^2 e^{r_2 D}\alpha\right)B_m + \\ \left(E_1 e^{r_3 D}\alpha^3 + \mu_{12} E_2 r_3^2 e^{r_3 D}\alpha\right)C_m + \left(E_1 e^{r_4 D}\alpha^3 + \mu_{12} E_2 r_4^2 e^{r_4 D}\alpha\right)D_m \end{Bmatrix} = 0 \tag{5.30}$$

$$\begin{Bmatrix} \left(\mu_{12} G_{12} r_1 \alpha^2 - E_1 r_1 \alpha^2 + G_{12} r_1^3\right)A_m + \\ \left(\mu_{12} G_{12} r_2 \alpha^2 - E_1 r_2 \alpha^2 + G_{12} r_2^3\right)B_m + \\ \left(\mu_{12} G_{12} r_3 \alpha^2 - E_1 r_3 \alpha^2 + G_{12} r_3^3\right)C_m + \\ \left(\mu_{12} G_{12} r_4 \alpha^2 - E_1 r_4 \alpha^2 + G_{12} r_4^3\right)D_m \end{Bmatrix} = -\frac{Z_{11} E_m}{E_1 E_2} \tag{5.31}$$

$$\begin{Bmatrix} \left(\mu_{12} G_{12} r_1 e^{r_1 D}\alpha^2 - E_1 r_1 e^{r_1 D}\alpha^2 + G_{12} r_1^3 e^{r_1 D}\right)A_m + \\ \left(\mu_{12} G_{12} r_2 e^{r_2 D}\alpha^2 - E_1 r_2 e^{r_2 D}\alpha^2 + G_{12} r_2^3 e^{r_2 D}\right)B_m + \\ \left(\mu_{12} G_{12} r_3 e^{r_3 D}\alpha^2 - E_1 r_3 e^{r_3 D}\alpha^2 + G_{12} r_3^3 e^{r_3 D}\right)C_m + \\ \left(\mu_{12} G_{12} r_4 e^{r_4 D}\alpha^2 - E_1 r_4 e^{r_4 D}\alpha^2 + G_{12} r_4^3 e^{r_4 D}\right)D_m \end{Bmatrix} = -\frac{Z_{11} I_m}{E_1 E_2} \tag{5.32}$$

By using Eqs. (5.27) and (5.8a) or (5.9a), the value of k is determined as

$$k = -\frac{2Z_{11}\sigma_0}{15E_1E_2G_{12}}$$

Eqs. (5.24)-(5.28) are used for finding of stress and displacement components at various points of the beam and the appropriate values of E_m and I_m are determined to get the values of four unknowns constant (A_m, B_m, C_m and D_m).

Case-2: Beam with lateral stiffeners

In this case, by assuming the same assumed potential function in Eq. (5.22), the general expressions for the relevant displacement and stress components are obtained in terms of the four arbitrary constants, as follows:

$$u_x(x,y) = \sum_{m=1}^{\infty}\left(L_m r_1 e^{r_1 y} + M_m r_2 e^{r_2 y} + N_m r_3 e^{r_3 y} + O_m r_4 e^{r_4 y}\right)\alpha\cos\alpha x \tag{5.33}$$

$$u_y(x,y) = \frac{1}{Z_{11}}\left[\sum_{m=1}^{\infty}\begin{Bmatrix}\left(E_1^2\alpha^2 - E_1G_{12}r_1^2 + \mu_{12}^2E_2G_{12}r_1^2\right)e^{r_1 y}L_m + \\ \left(E_1^2\alpha^2 - E_1G_{12}r_2^2 + \mu_{12}^2E_2G_{12}r_2^2\right)e^{r_2 y}M_m + \\ \left(E_1^2\alpha^2 - E_1G_{12}r_3^2 + \mu_{12}^2E_2G_{12}r_3^2\right)e^{r_3 y}N_m + \\ \left(E_1^2\alpha^2 - E_1G_{12}r_4^2 + \mu_{12}^2E_2G_{12}r_4^2\right)e^{r_4 y}O_m\end{Bmatrix}\sin\alpha x\right] \tag{5.34}$$

$$\sigma_{xx}(x,y) = -\frac{E_1G_{12}}{Z_{11}}\left[\sum_{m=1}^{\infty}\begin{Bmatrix}\left(E_1r_1e^{r_1 y}\alpha^2 + \mu_{12}E_2r_1^3e^{r_1 y}\right)L_m + \\ \left(E_1r_2e^{r_2 y}\alpha^2 + \mu_{12}E_2r_2^3e^{r_2 y}\right)M_m + \\ \left(E_1r_3e^{r_3 y}\alpha^2 + \mu_{12}E_2r_3^3e^{r_3 y}\right)N_m + \\ \left(E_1r_4e^{r_4 y}\alpha^2 + \mu_{12}E_2r_4^3e^{r_4 y}\right)O_m\end{Bmatrix}\sin\alpha x\right] \tag{5.35}$$

$$\sigma_{yy}(x,y) = -\frac{E_1 E_2}{Z_{11}}\left[\sum_{m=1}^{\infty}\begin{Bmatrix}\left(\mu_{12}\,G_{12}r_1 e^{r_1 y}\alpha^2 - E_1 r_1 e^{r_1 y}\alpha^2 + G_{12}r_1^3 e^{r_1 y}\right)L_m + \\ \left(\mu_{12}G_{12}r_2 e^{r_2 y}\alpha^2 - E_1 r_2 e^{r_2 y}\alpha^2 + G_{12}r_2^3 e^{r_2 y}\right)M_m + \\ \left(\mu_{12}G_{12}r_3 e^{r_3 y}\alpha^2 - E_1 r_3 e^{r_3 y}\alpha^2 + G_{12}r_3^3 e^{r_3 y}\right)N_m + \\ \left(\mu_{12}G_{12}r_4 e^{r_4 y}\alpha^2 - E_1 r_4 e^{r_4 y}\alpha^2 + G_{12}r_4^3 e^{r_4 y}\right)O_m\end{Bmatrix}\sin\alpha x\right] \tag{5.36}$$

$$\sigma_{xy}(x,y) = -\frac{E_1\,G_{12}}{Z_{11}}\sum_{m=1}^{\infty}\begin{Bmatrix}\left(E_1 e^{r_1 y}\alpha^3 + \mu_{12}E_2 r_1^2 e^{r_1 y}\alpha\right)L_m + \\ \left(E_1 e^{r_2 y}\alpha^3 + \mu_{12}E_2 r_2^2 e^{r_2 y}\alpha\right)M_m + \\ \left(E_1 e^{r_3 y}\alpha^3 + \mu_{12}E_2 r_3^2 e^{r_3 y}\alpha\right)N_m + \\ \left(E_1 e^{r_4 y}\alpha^3 + \mu_{12}E_2 r_4^2 e^{r_4 y}\alpha\right)O_m\end{Bmatrix}\cos\alpha x \tag{5.37}$$

The obtained loading parameters (E_0, I_0, E_m, I_m) associated with the case of lateral stiffeners with fiber orientation $\theta = 0^0$ are as like as those obtained for lateral stiffeners with fiber orientation $\theta = 90^0$. Once the four unknown constants (L_m, M_m , N_m and O_m) in the evaluation are determined with the appropriate values of loading parameters (E_0, I_0, E_m, I_m) then Eqs. (5.33)-(5.37) will give the explicit expressions of the elastic field of the simply-supported composite beam with lateral stiffeners at the opposing lateral ends.

5.4 Results of Composite Beam

In this section, the effects of fibre orientation on the components of stress at different sections of a thick beam are discussed both for axial and lateral stiffening conditions. This discussion or the numerical results of the analytical solution of the composite beams are presented in the form of graphs by considering varying beam aspect ratios, L/D=1-4. Then this effect is further investigated as a manner the influence of fibre orientation by considering axial, lateral and no stiffening conditions. Since the central objective of the present chapter is to investigate the effect of fiber orientation on the elastic field of the beam, results of all the parameters of interest are presented in a comparative fashion for the two cases of fiber orientation, $\theta = 0^o$ and 90^o. The glass/epoxy composite is considered as the beam material, the effective mechanical properties of which are listed in Table 4.1. The magnitude of the compressive stress, σ_0 assumed to generate the numerical results is 40.0 MPa.

5.4.1 Stress field

The distributions of bending stress components σ_{xx}/σ_0 with respect to beam depth, y/D at the stiffened end section x/L=0 for axial stiffening condition are illustrated in Fig. 5.2. Bending stress distributions are observed to be non linear over the whole span of the beam for both fiber orientations. Maximum values of bending stresses are observed at the top and bottom surfaces of the beam with opposite sign. The maximum normalized values of the stress at the top and bottom surfaces are found to be nearly 7 and 11 times the applied intensity of loading for fiber orientation θ=0^0 as well as 6 and 6 times for fiber orientation θ=90^0, respectively. These maximum bending stresses are found to occur at the stiffened ends of the beam with aspect ratio L/D=4, which, in turn, identifies the stiffened lateral ends of the beam as the most critical section in term of axial stresses, which is, however, the most dominating stress components among the others. On the other hand, the minimum values of stress at the top and bottom surfaces are found to be nearly 0.5 and 6.2 times of the applied intensity of the loading for fiber orientation θ=0^0 as well as 0.2, 1.8 times of the applied intensity of loading for fiber orientation θ=90^0. These minimum values of bending stress are also found to occur at the stiffened ends of the beam with aspect ratio L/D=1. For most of the sections, bending stresses are found to be positive (tensile) for upper half and negative (compressive) for lower half of the beam. Now from the distributions it is verified that the fiber orientations has a significant effect on the lower surface of the beam for different beam aspect ratios. Because at the bottom surface of the beam, the difference between the stresses due to fiber orientations are decreasing by increasing the beam aspect ratio, whether, at the upper surface of the beam, this difference is too small with respect to the beam aspect ratio.

The load transition section x/L=0.1 is also considered in Fig. 5.3 to get the overall idea about the distribution of bending stress components σ_{xx}/σ_0. These components are figured out with respect to beam depth y/D for axial stiffening condition at different beam aspect ratios, L/D=1-4. For all the considered beam aspect ratios, the distribution patterns are almost non linear for both fiber orientations and the maximum non linearity is observed for fiber orientation θ=0^0 than θ=90^0. At both fiber orientations (θ= 0^0 and 90^0), the values of maximum bending stresses

are observed 0.7 and 2.8 times the applied intensity of loading for lower beam aspect ratio (L/D=1) and 4 and 6 times the applied intensity of loading for higher beam aspect ratio (L/D=4). All these stresses are developed at the lower surface of the beam and on the other hand, at the upper surface of the beam, the difference between the stresses for both fiber orientations is insignificant. So, it can be said that the degree of non linearity increases and individual value of stress decreases at both fiber orientations by increasing the beam aspect ratio.

From Fig. 5.4, the distributions of bending stress σ_{xx}/σ_0 components with respect to beam depth, y/D are observed by considering mid section (x/L=0.5) of the beam for axial stiffening condition. The degree of non linearity decreases with the increase of section from the stiffened ends, that's why mid section is considered for observation. In this case the bending stress distributions pattern are also non linear over the whole span of the beam for both fiber orientations. The upper surface and lower surface of the beam contain positive and negative values of bending stress like section x/L=0.The maximum values of bending stress at the upper and lower surfaces of the beam are nearly 3 and 4 times the applied intensity of loading for fiber orientation $\theta=90^0$ as well as 4 and 4.5 times the applied intensity of loading for fiber orientation $\theta=0^0$. On the other hand the minimum values of bending stress at the upper and lower surfaces are nearly 0.2 and 0.5 times the applied intensity of loading for fiber orientation $\theta=90^0$ as well as 0.5 and 1.5 times the applied intensity of loading for fiber orientation $\theta=0^0$ .These maximum and minimum values of bending stresses are obtained for beam aspect ratio, L/D=4 and 1. From these values it is verified that the effect of fiber orientation is decreasing by increasing the section from stiffened ends. At the upper and lower surfaces of the beam the difference between the stresses for two fiber orientations is also decreasing by increasing the beam aspect ratios. So, it can be said that the fiber orientation has a high effect on bending stresses for short beam.

For axial stiffening condition, the shear stress σ_{xy}/σ_0 distribution of left lateral end is zero. So, the shear stress distributions at section x/L=0.10 is investigated in Fig. 5.5 with respect to beam depth, y/D. From the distributions of shear stress it is observed that the entire top and bottom

surfaces and the two stiffened ends as well as the mid section are completely free from shear stress, which is in conformity with the physical characteristics of the present beam. Maximum shear stress is found to occur at the load transition section for fiber orientation $\theta=0^0$, especially, at the vicinity of the bottom surface, which is in contrast with the standard parabolic profile. The shear stress distributions are found to assume the parabolic profile in a gradual fashion as we move towards the higher beam aspect ratios for both fiber orientations, especially, it is shown at beam aspect ratio, L/D=4.0. As this aspect ratio, the maximum shear stress is found to be nearly 2 times the intensity of the applied loading for both fiber orientations. On the other hand the minimum values of shear stresses are found nearly 1.5 and 0.8 times the intensity of applied loading and both are developed for fiber orientations, $\theta=0^0$ as well as 90^0 respectively. So, the values of shear stress are increasing by increasing the beam aspect ratios.

At left lateral end, the bending stress σ_{xx}/σ_0 distribution with respect to beam depth, y/D is zero for lateral stiffening condition. That is why section x/L=0.1 is considered in Fig. 5.6 to describe the bending stress distribution at different beam aspect ratios, L/D= 1-4 for lateral stiffening condition. From these figures it is observed that the distributions are non linear over the whole span and non-symmetric with respect to the mid section of the beam depth. Maximum non linearity is observed at the bottom surface of the beam for fiber orientation $\theta=0^0$ and this non linearity exists within beam depth $0\leq y/D\leq 0.2$ for all beam aspect ratios. After this portion of beam depth, this non linearity pattern is similar and at the top surface of the beam the difference of non linearity between two fiber orientations is too small for all beam aspect ratios. The maximum values bending stresses are found nearly 4 and 0.5 for both fiber orientations ($\theta=0^0$ and 90^0) and these stresses are developed at the bottom surface of the beam for aspect ratio, L/D=1.0. Now advancing towards higher beam aspect ratio, the value of shear stress is decreasing for fiber orientation $\theta=0^0$ and increasing for fiber orientation $\theta=90^0$. At beam aspect ratio, L/D=4 the observed maximum bending stresses for both fiber orientations ($\theta=0^0$ and 90^0) are -1 and 1. So, it can be concluded that the fiber orientation has a small effect on long beam.

Now the bending stress distribution σ_{xx}/σ_0 is observed in Fig. 5.7 by advancing towards the midsection, x/L=0.5 of the beam for lateral stiffening condition. From these distributions of

bending stresses at different beam aspect ratios, L/D=1-4 it is observed that the distributions pattern are symmetric about the mid section of the beam depth for both fiber orientations, only exception is observed for fiber orientation $\theta=0^0$ at beam aspect ratio, L/D=1.0. Most bending stress is found to be positive (tensile) for upper half and negative (compressive) for lower half of the beam. At higher beam aspect ratio, L/D=4 the maximum values of bending stresses are found for both fiber orientations, $\theta=0^0$ and 90^0 are nearly 10.5 and 10 times the applied intensity of loading and these values are developed at both the top and bottom surface of the beam. On the other hand for lower beam aspect ratio, L/D=1 again the maximum values of bending stresses are found for both fiber orientations ($\theta=0^0$ and 90^0) are nearly 1.8 and 0.5 times the applied intensity of loading and these values are developed at the top surface of the beam. From these values it is verified that by increasing the beam aspect ratio the difference between the stresses for both fiber orientations is decreasing, which identifies the fiber orientation has a small effect on long beam.

As it appears from Fig. 5.8, the shear stress σ_{xy}/σ_0 stress distributions pattern almost same shape at different beam aspect ratios for both fiber orientations. Here the beam is stiffened with lateral stiffener and stiffened end section, x/L=0 is considered for explanation. From these distributions it is observed that the upper surface and lower surface of the beam are free from shear stress, which is in conformity with the physical characteristics of the beam. Maximum developed shear stress is approximately 3 times the applied intensity of loading for fiber orientation, $\theta=90^0$ and 1 time the applied intensity of loading for fiber orientation, $\theta=0^0$. Both these stresses are developed within beam depth, $0\leq y/D\leq 0.025$ and beyond these portion of beam depth, the magnitudes of shear stresses are decreasing by increasing the beam depth, y/D until it becomes zero. Another most important observation is that the fiber orientation has no effect on shear stress distributions for considering section because the values of shear stress are remain unchanged with respect to beam depth at different beam aspect ratios.

Load transition section, x/L=0 is considered in Fig. 5.9 to describe the shear stress distributions at different beam aspect ratios, L/D=1-4 for both fibre orientations. Midsection is not considered because the shear stress distribution is zero at this section. From this distribution it

is observed that magnitude of shear stress is zero at the top and bottom surfaces of the beam for both fibre orientations. At fibre orientation, $\theta=90^0$ the values of shear stresses become maximum within the beam depth $0\leq y/D\leq 0.02$ and maximum value of shear stress is increasing by increasing the beam aspect ratios. The maximum value of shear stress is found two times the applied intensity of loading and this stress is developed at the beam aspect ratio, $L/D=4$. Now for fibre orientation, $\theta=0^0$ the shear stress distributions patterns are as like as standard parabolic profile if we move towards the higher beam aspect ratio. In this case the maximum value of shear stress is found at the mid position of beam depth and this value is also two times the applied intensity of loading.

5.4.2 Influence of fibre orientation

The influence of fibre orientation on the components of stress and displacement is also analyzed for axial, lateral and no stiffening conditions at the lateral ends. Figs. 5.10-5.12 represent the distribution of bending stresses σ_{xx}/σ_0 at mid span section ($x/L=0.5$) and lower surface ($y/D=0$) of the beam with respect to different L/D ratios. For all the cases of stiffening conditions, the distributions values are positive, distributions pattern are almost similar shape and stress level increases with the increase of L/D ratios, although the individual stress level is much higher for both the cases of lateral and no stiffening conditions than axial stiffening condition. Another important observation is, the influence of fibre orientation is more at lower aspect ratios for both axial and no stiffening conditions than that of lateral stiffening condition. Now, to get the overall idea of fibre orientation, the stiffened end ($x/L=0$) section as well as section $x/L=0.1$ is also considered at lower surface ($y/D=0$) of the beam for axial stiffening condition. In these figures, the distribution of bending stresses is negative and influence of fibre orientation is more at lower aspect ratios. This influence decreases with the increase of aspect ratios, but still the effect is more significant at the lower surface of the beam than the upper surface.

The distributions of maximum shear stress σ_{xy}/σ_0 along the beam depth are presented in Figs. 5.13-5.15 for various L/D ratios of the beam with axial, lateral and no stiffeners, respectively.

At section x/L=0.1, the shear stress distributions pattern are almost similar shape and the magnitude of the maximum shear stress increases with the increase of beam aspect ratios. For lower aspect ratios, i.e., up to L/D=4 for axial and lateral stiffeners as well as up to L/D=3 for no stiffeners, the influence of fibre orientation is maximum and this influence increases with the increase of beam aspect ratios. Beyond the considered beam aspect ratios, the influence of fiber orientation is still significant, but it is less than the considered lower aspect ratios. Now the distributions of maximum shear stresses at the stiffened end for lateral stiffening condition is considered to describe the overall idea of shear stresses. The value of maximum shear stress is almost similar with respect to the beam aspect ratios for both fibre orientations. Only exception is observed for L/D=1, which is due to the effect of short beam. Another important observation is the influence of fibre orientation is more at $\theta=90^0$ than that of $\theta=0^0$.

In Figs. 5.16-5.18, the distribution of lateral displacement u_y/D component is considered at mid span section (x/L=0.5) and lower surface of the beam (y/D=0) with respect to the beam aspect ratios for axial, lateral and no stiffeners, respectively. Here the distribution patterns are almost similar shape, lateral displacement increases with the increase of beam aspect ratios and fibre orientation effect is more at $\theta=90^0$ than $\theta=0^0$ for all the cases of stiffening conditions. Maximum displacement is observed at no stiffening condition for both fibre orientations, because no restriction is provided at any direction. Then, due to the restriction of displacement at lateral direction, maximum displacement is found for lateral stiffening condition and finally, lowest displacement is found for axial stiffening condition, where, restriction of displacement is provided at axial direction for both fibre orientations.

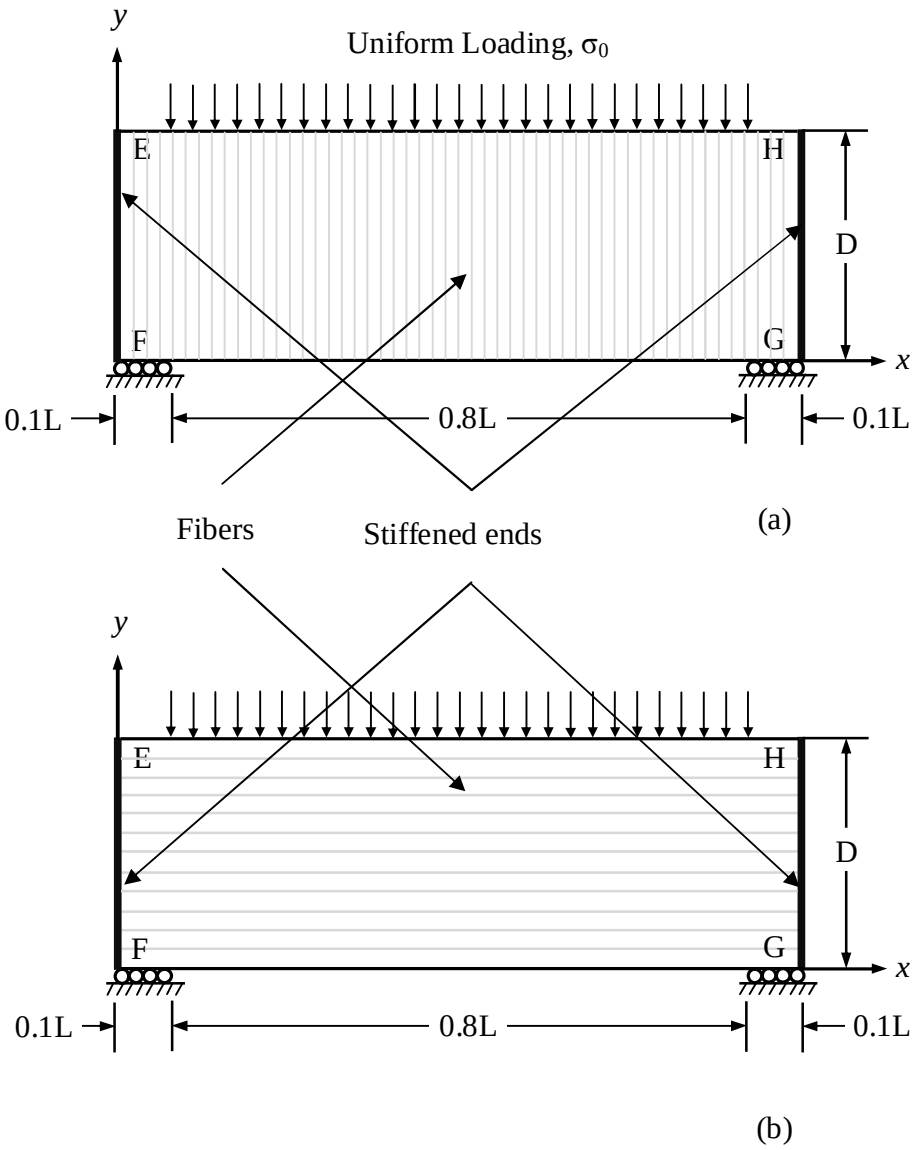

Fig. 5.1 Physical model of a simply-supported beam of composite material with stiffened lateral ends and fiber orientation (a) $\theta=90^0$, (b) $\theta=0^0$

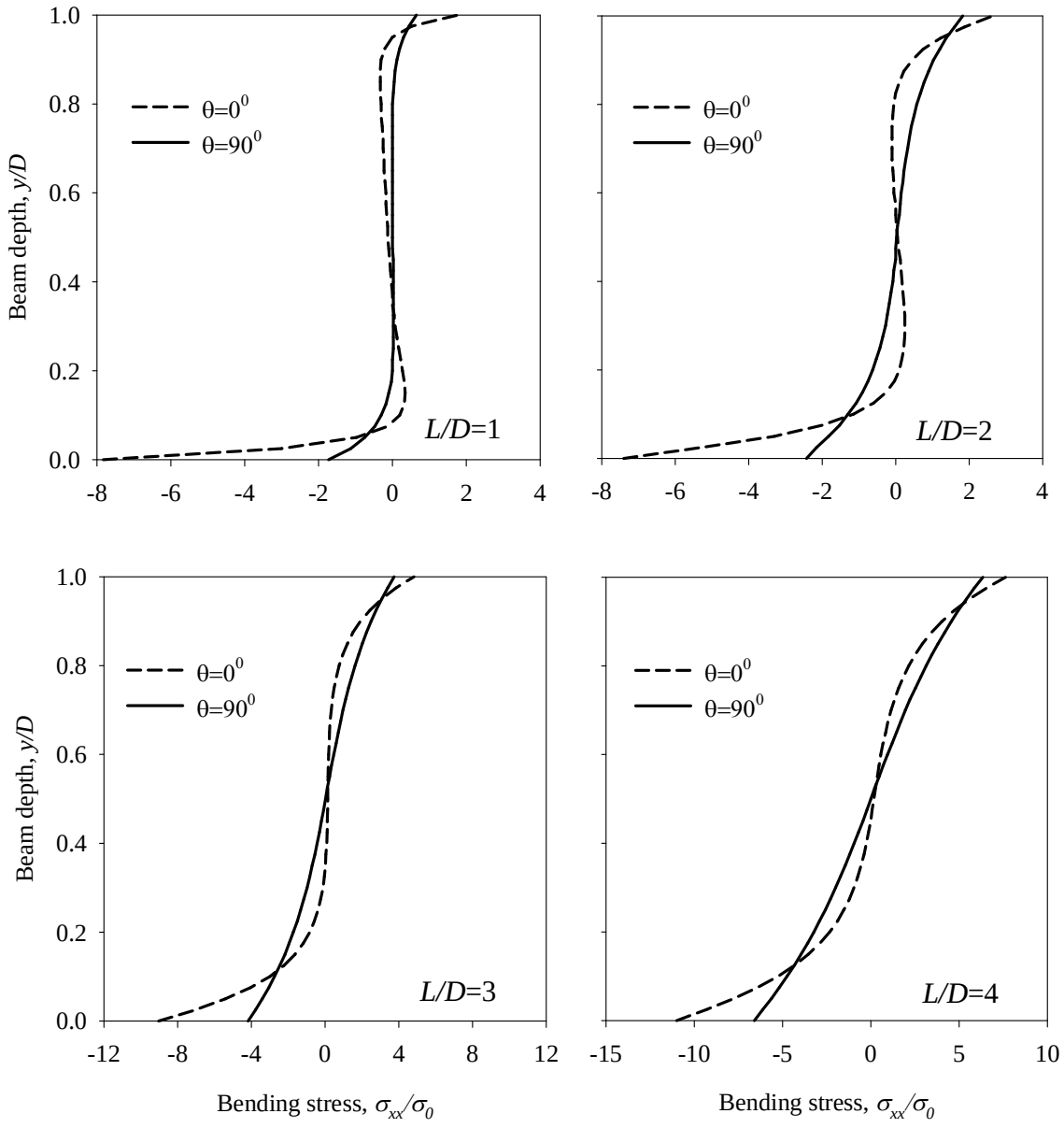

Fig. 5.2 Effect of fiber orientation on bending stress components at the stiffened end section *(x/L*=0) of the composite beam with axial stiffeners for different aspect ratios

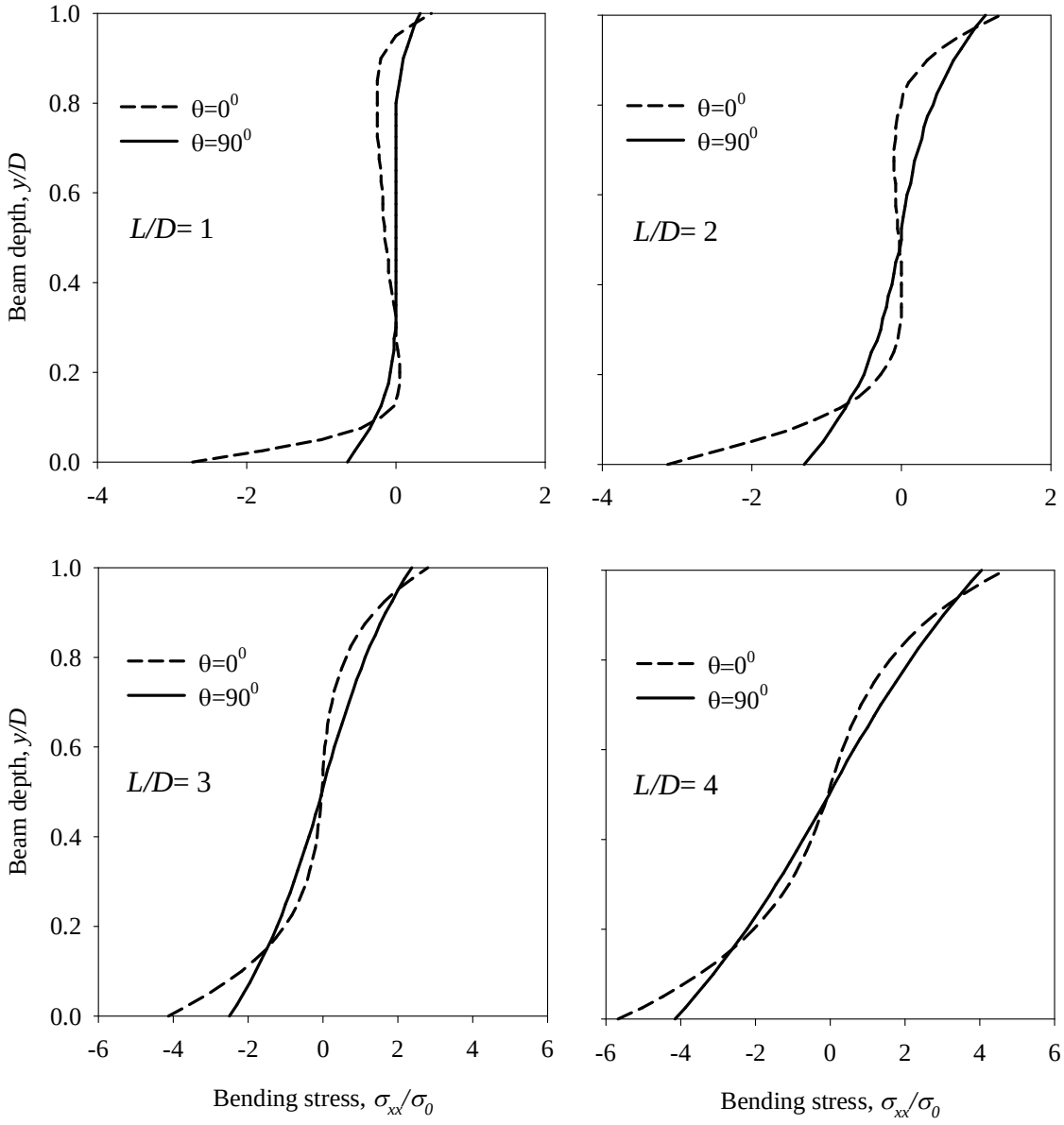

Fig. 5.3 Effect of fiber orientation on bending stress components at the section (*x/L*=0.1) of the composite beam with axial stiffeners for different aspect ratios

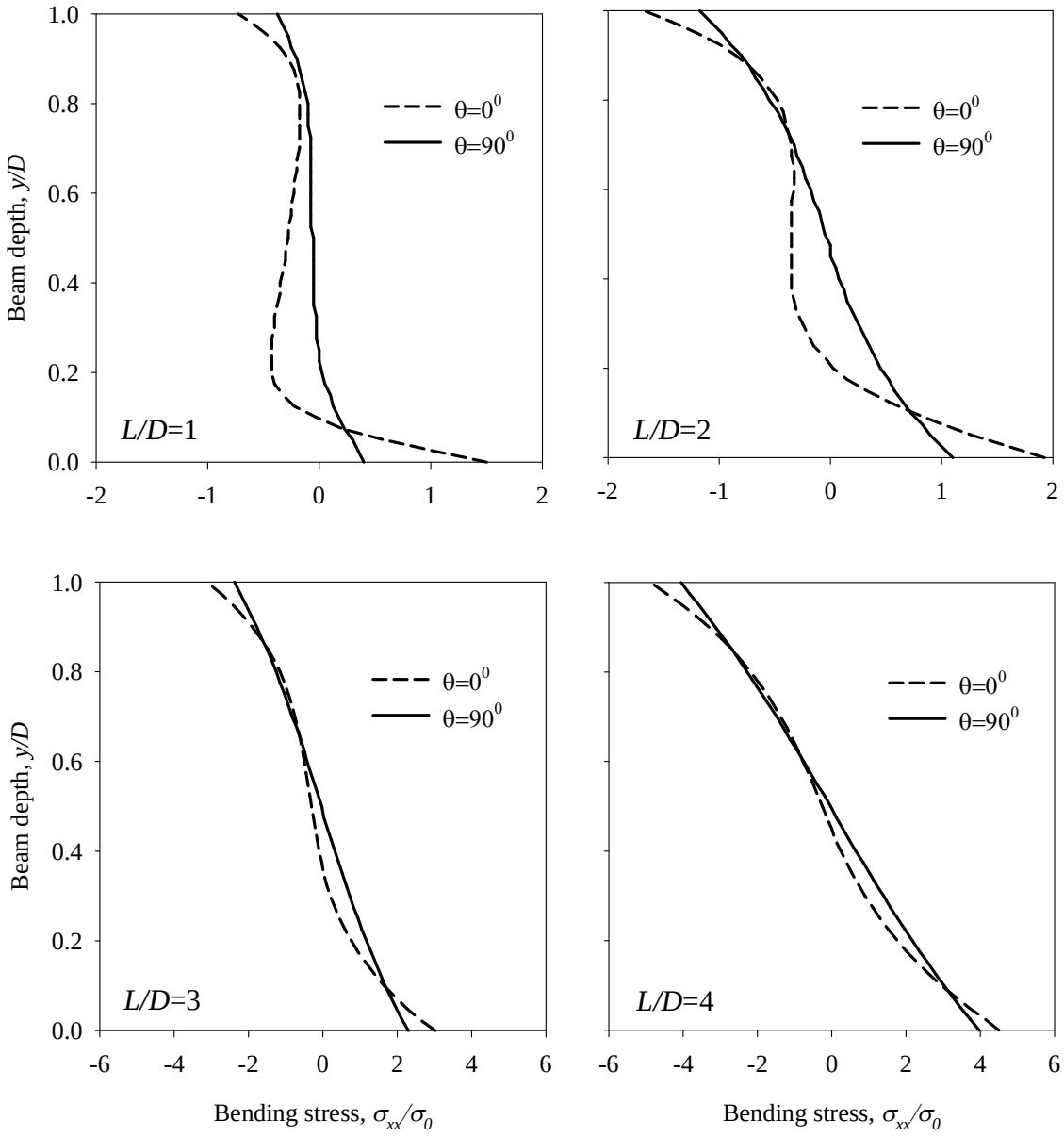

Fig. 5.4 Effect of fiber orientation on bending stress components at the mid section (*x/L*=0.5) of the composite beam with lateral stiffeners for different aspect ratios

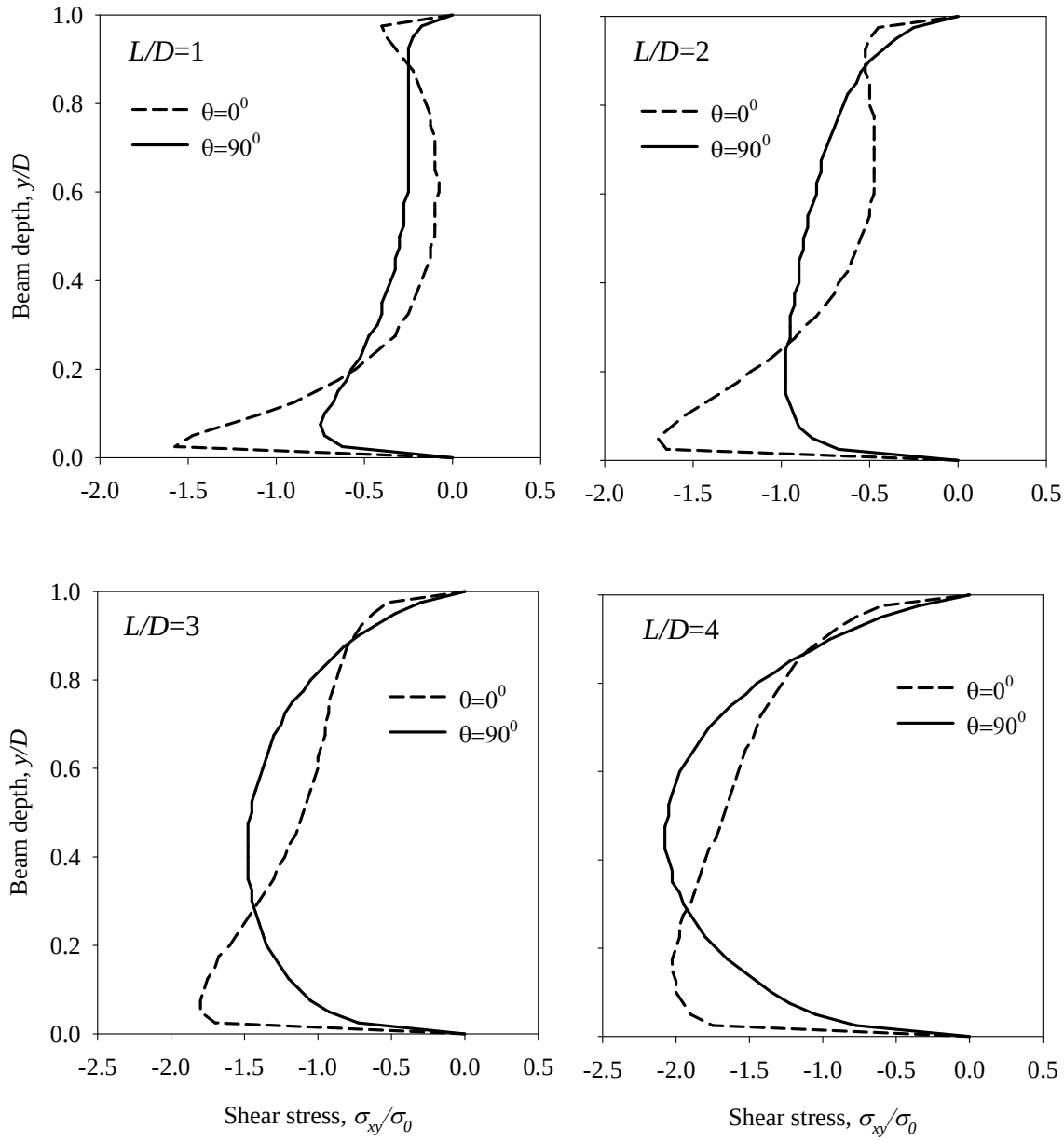

Fig. 5.5 Effect of fiber orientation on shear stress components at the section (*x/L*=0.1) of the composite beam with axial stiffeners for different aspect ratios

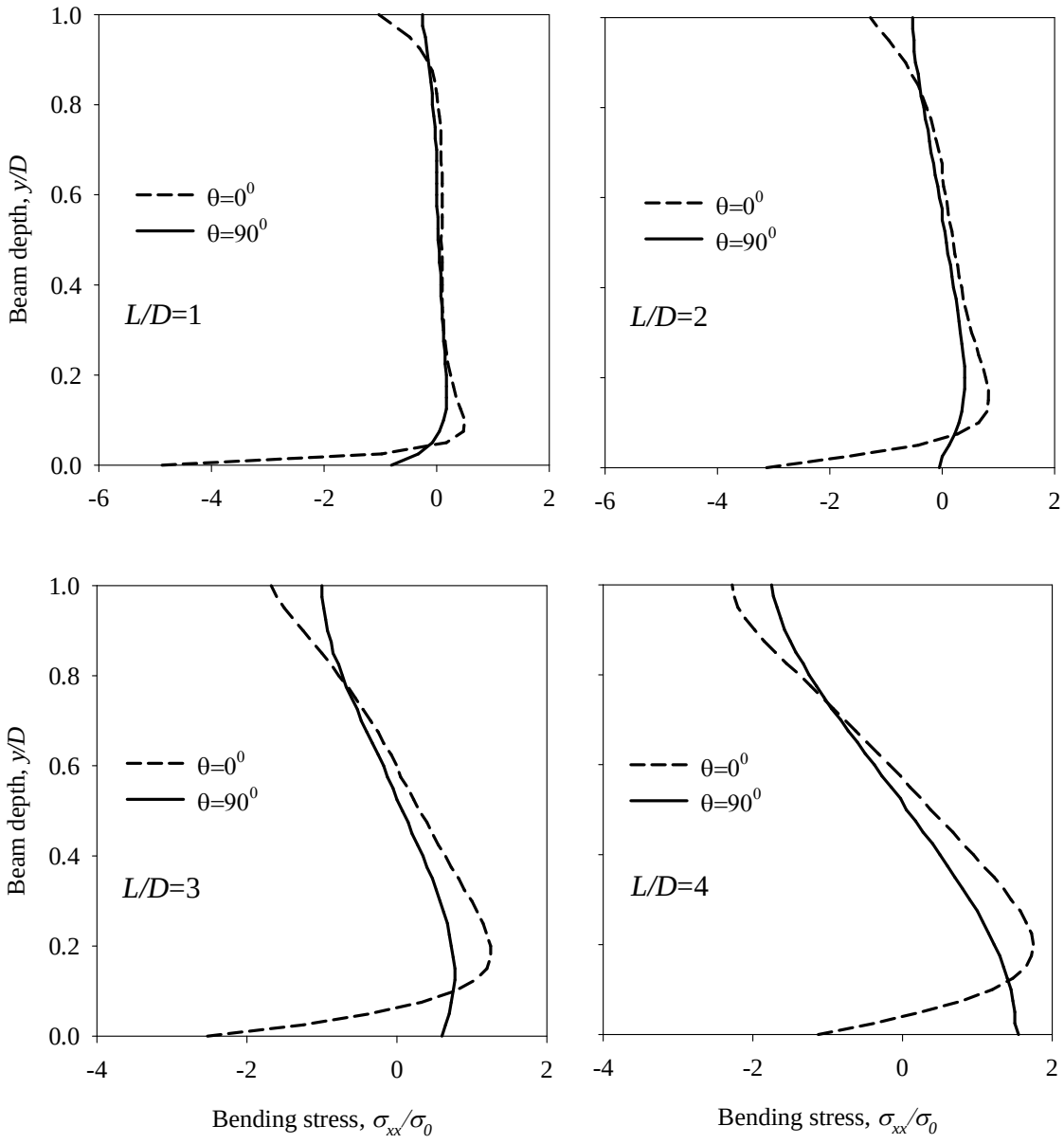

Fig. 5.6 Effect of fiber orientation on bending stress components at the section *(x/L*=0.1) of the composite beam with lateral stiffeners for different aspect ratios

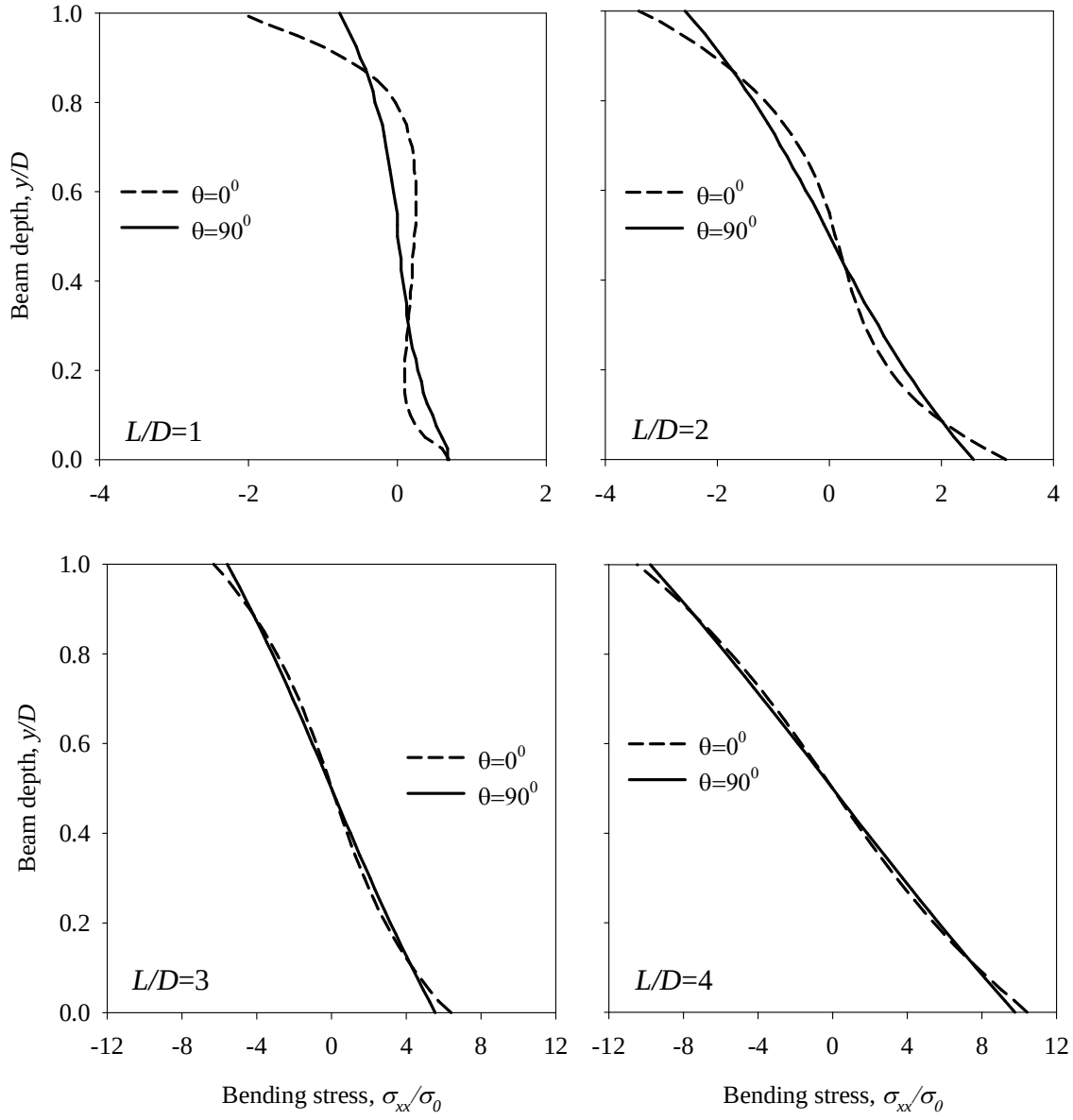

Fig. 5.7 Effect of fiber orientation on bending stress components at the mid section (*x/L*=0.5) of the composite beam with lateral stiffeners for different aspect ratios

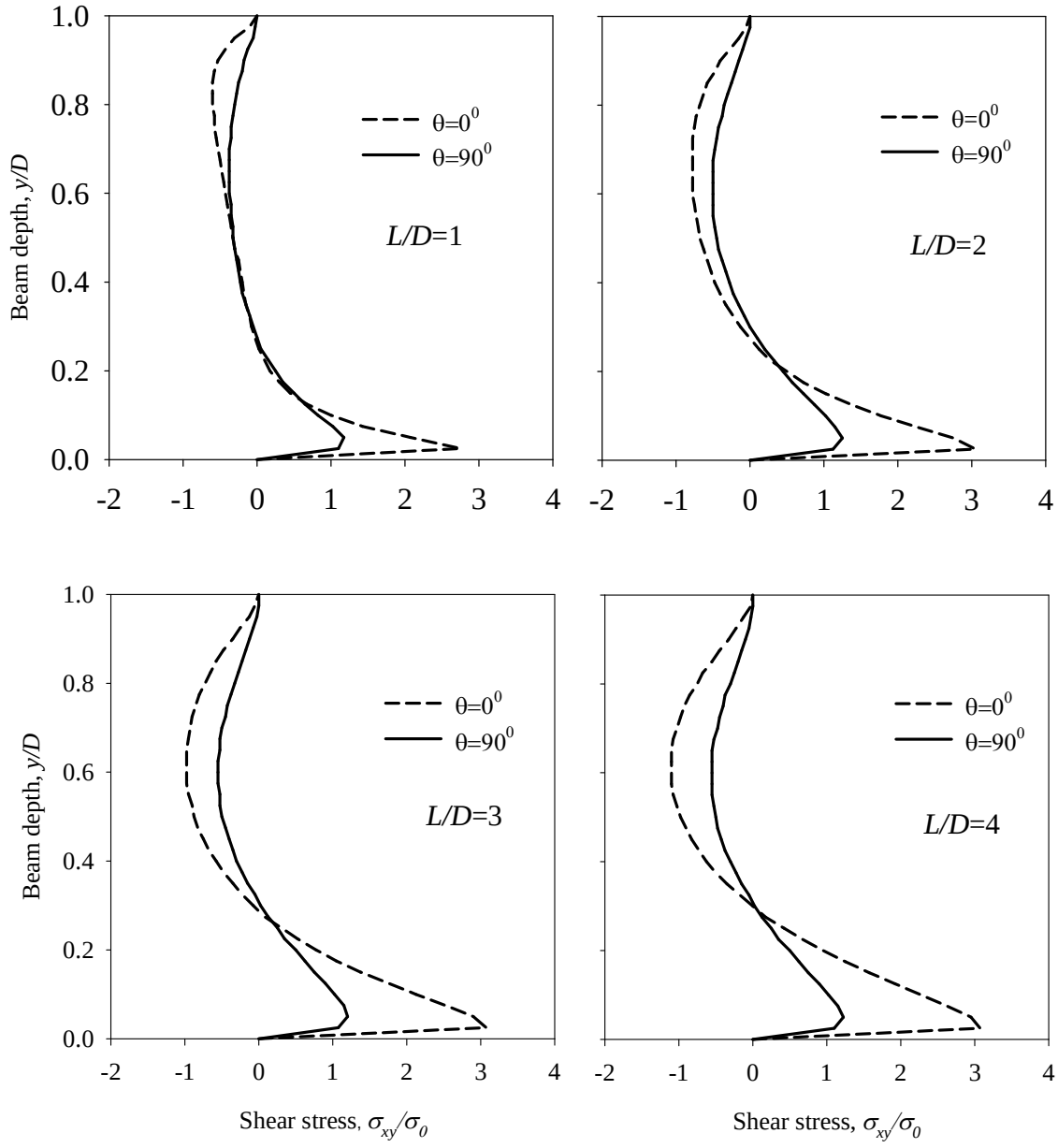

Fig. 5.8 Effect of fiber orientation on shear stress components at the stiffened end section *(x/L*=0) of the composite beam with lateral stiffeners for different aspect ratios

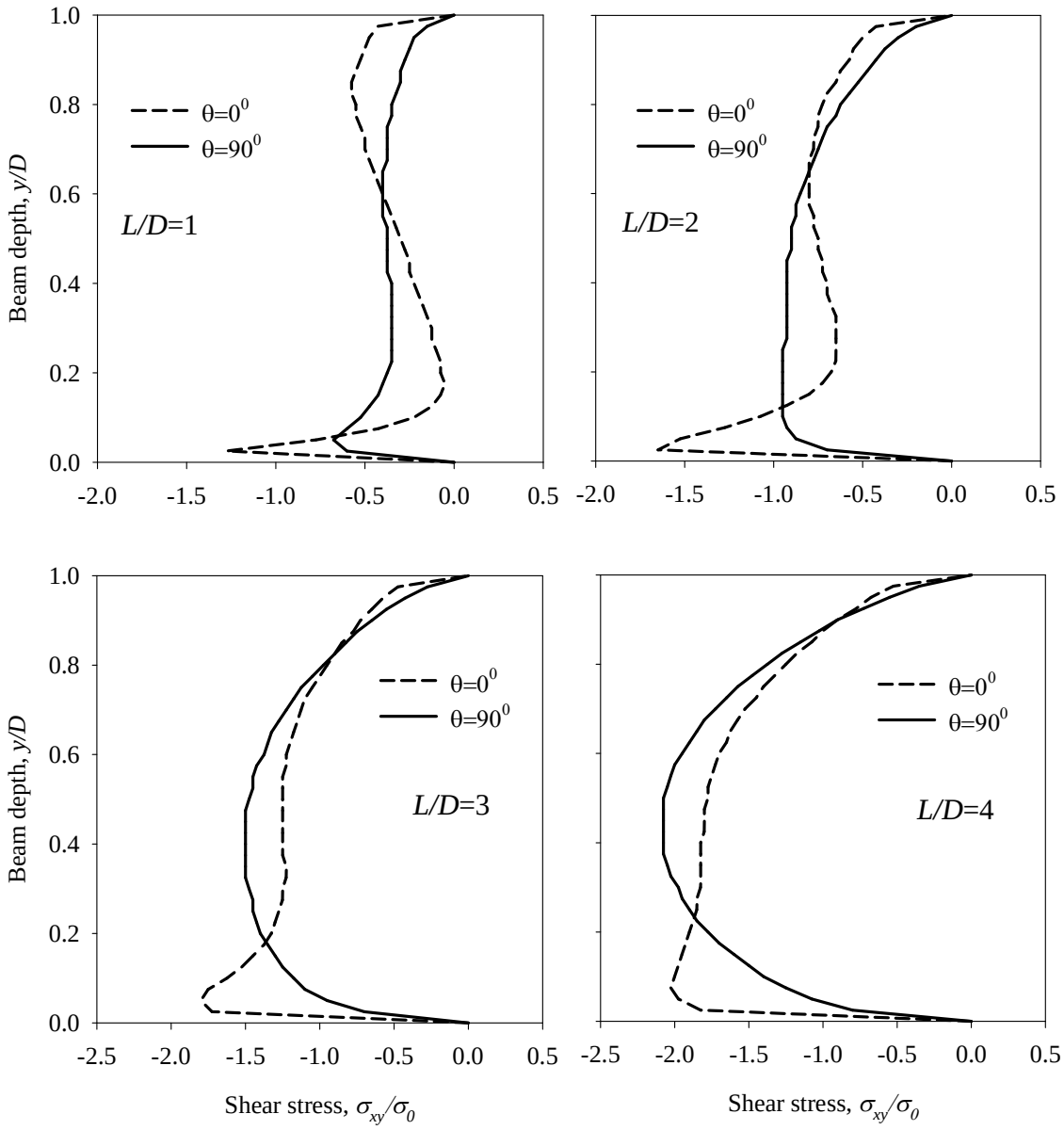

Fig. 5.9 Effect of fiber orientation on shear stress components at the section *(x/L*=0.1) of the composite beam with lateral stiffeners for different aspect ratios

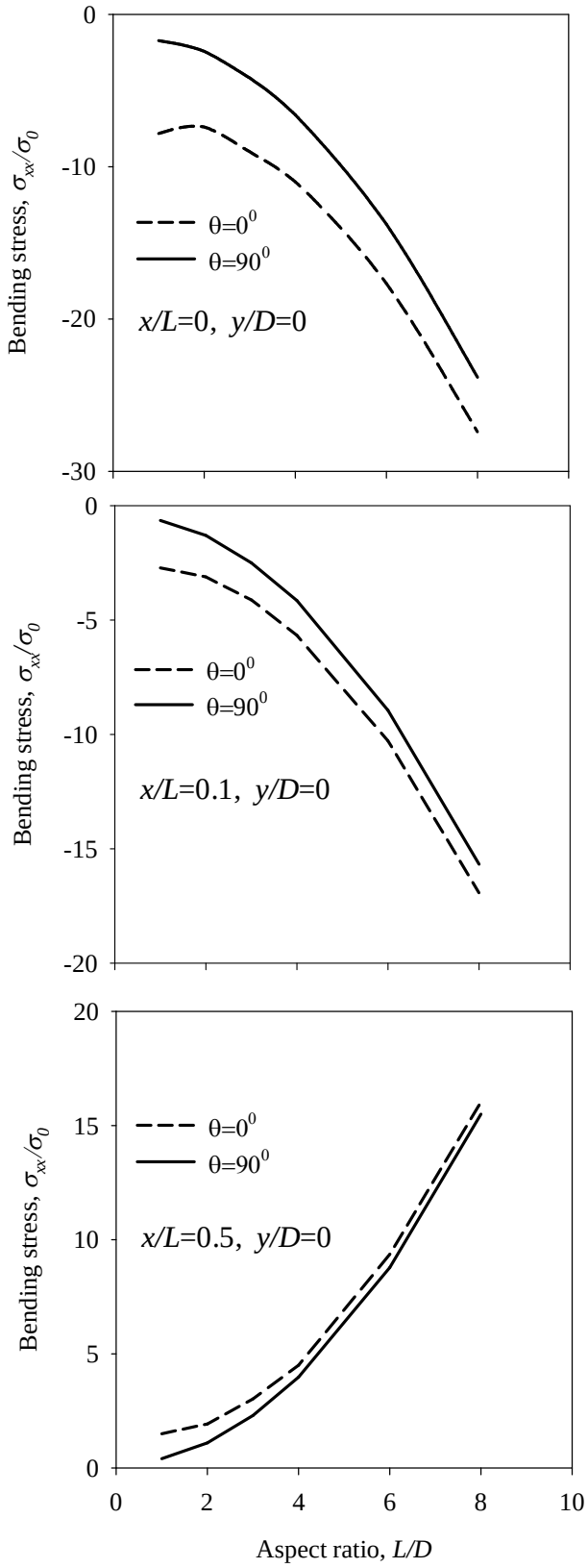

Fig.5.10 Influence of fiber orientation on bending stress components for the beam with axial stiffening condition at x/L= 0, 0.1 and 0.5

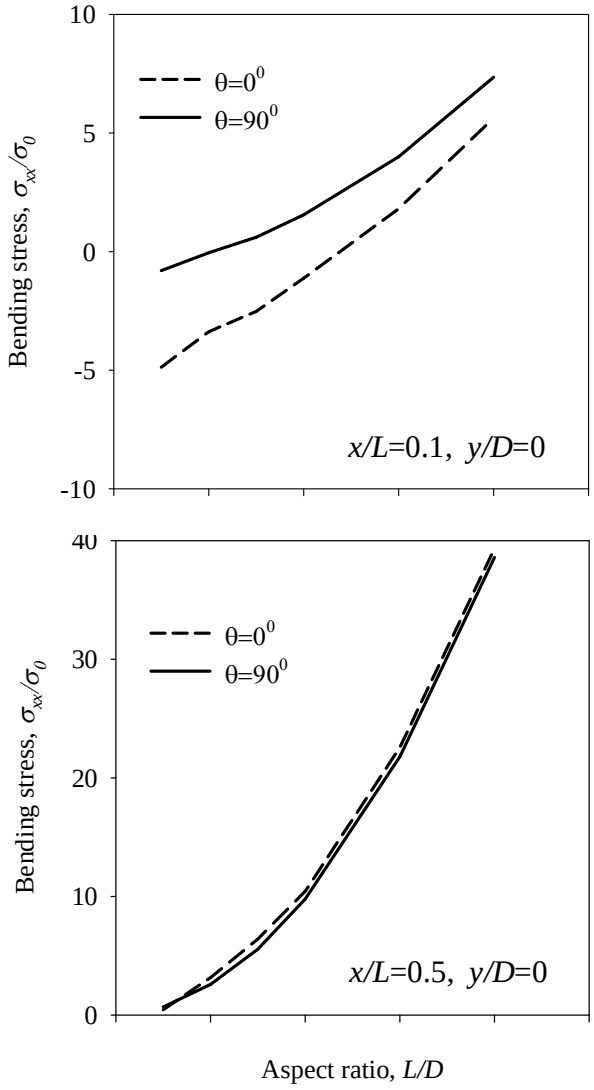

Fig.5.11 Influence of fiber orientation on bending stress components for the beam with lateral stiffening condition at x/L= 0.1 and 0.5

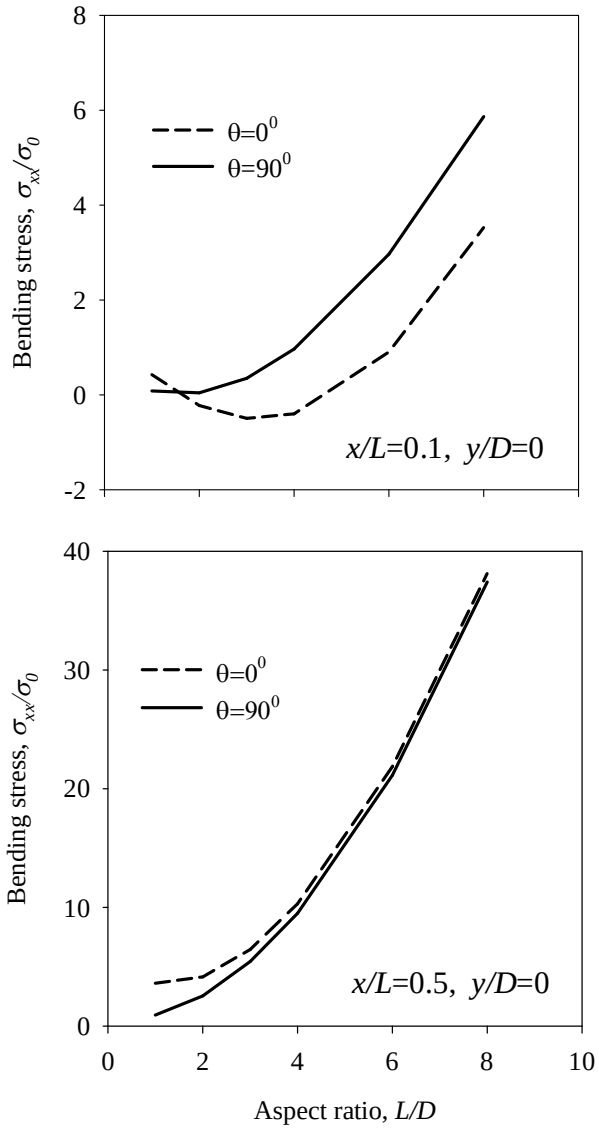

Fig.5.12 Influence of fiber orientation on bending stress components for the beam with no stiffening condition at *x/L*= 0.1 and 0.5

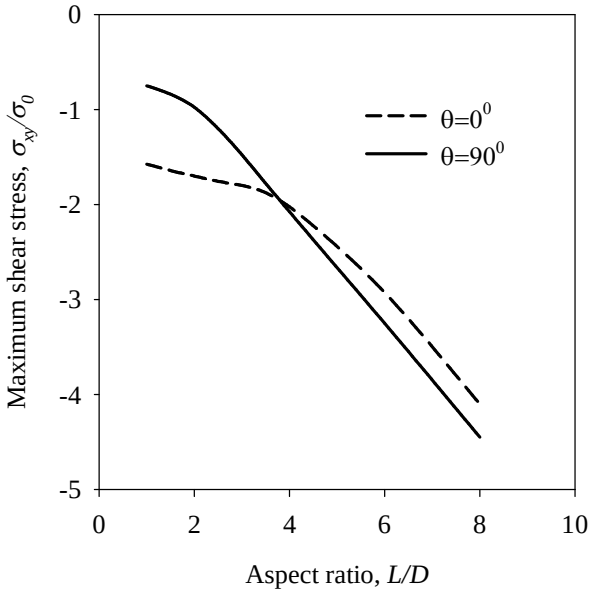

Fig.5.13 Influence of fiber orientation on shear stress components for the beam with axial stiffening condition at *x/L*= 0.1

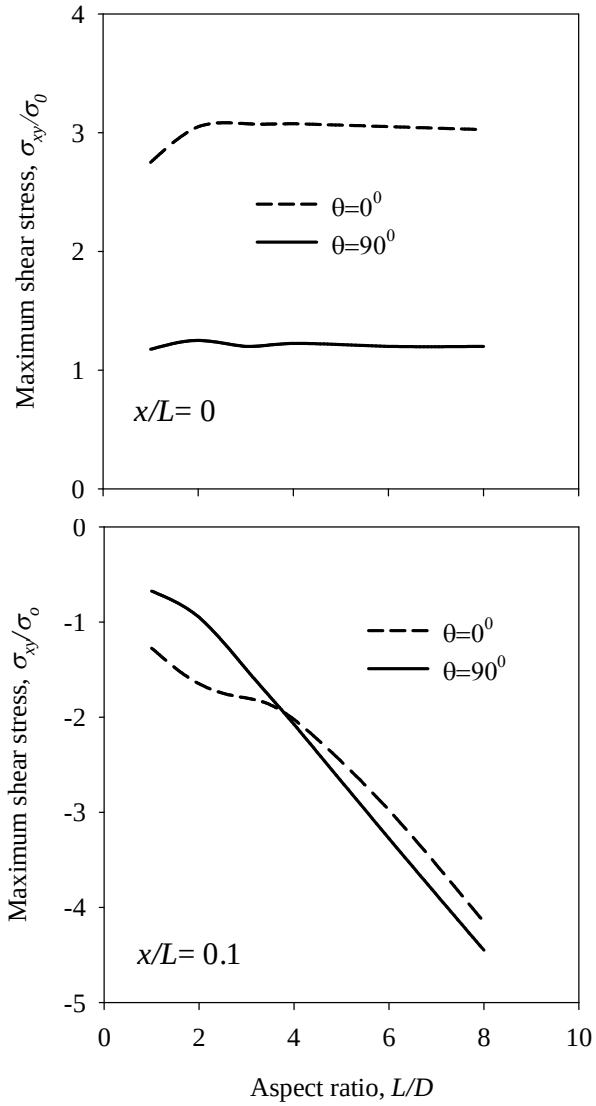

Fig.5.14 Influence of fiber orientation on shear stress components for the beam with lateral stiffening condition at *x/L*= 0 and 0.1

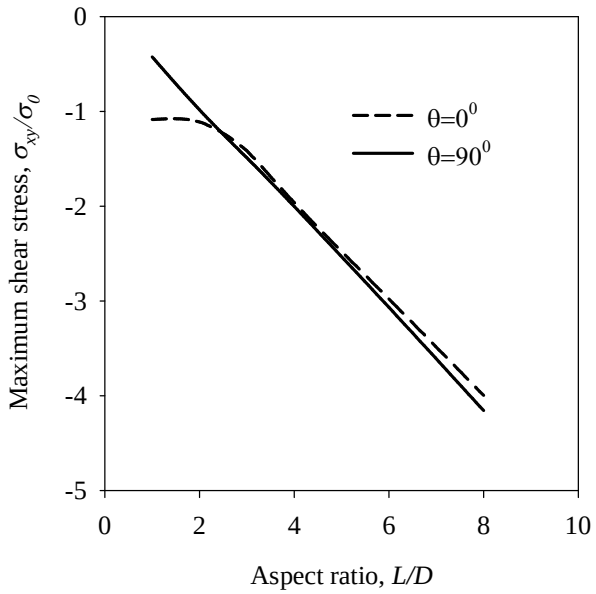

Fig.5.15 Influence of fiber orientation on shear stress components for the beam with no stiffening condition at *x/L*= 0.1

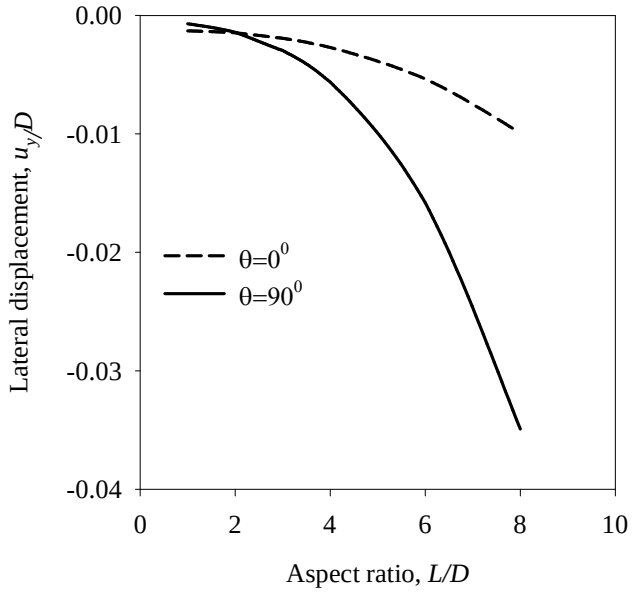

Fig. 5.16 Influence of fiber orientation on beam deflection components for the beam with axial stiffening condition at x/L=0.5 and y/D=0

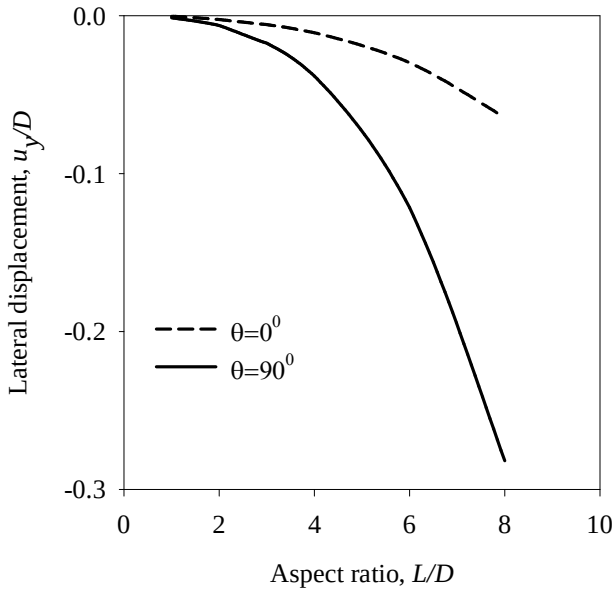

Fig. 5.17 Influence of fiber orientation on beam deflection components for the beam with lateral stiffening condition at x/L=0.5 and y/D=0

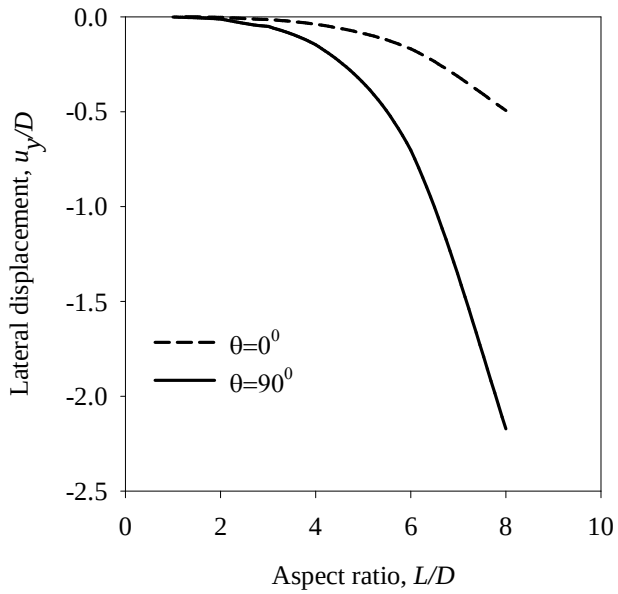

Fig. 5.18 Influence of fiber orientation on beam deflection components for the beam with no stiffening condition at x/L=0.5 and y/D=0

CHAPTER 6

COMPARISION AND VERIFICATION OF RESULTS

To verify the accuracy and reliability of the method proposed, a number of problems are analyzed. First, the results obtained for orthotropic materials by using potential function approach are now compared with the classical beam theory for both axial and lateral stiffening conditions. Then, the solutions verified with corresponding numerical results, i.e., FEM and FDM by considering fiber orientations $\theta=0^0$ and 90^0 for both axial and lateral stiffening conditions of same orthotropic materials. Finite difference formulation will be slightly discussed here for orthotropic material because it is not the major concern in this study that had been already formulated in several previous works [18-19]. Those works of FDM formulation have been used to find the solution of elastic field of all problems. Furthermore, as the analytical results have been discussed in details in the previous chapters, this chapter analyses basically the agreement of the results of the displacement potential method, classical beam theory and numerical methods without paying attention to the characteristics of the results.

6.1 Classical Beam theory

Although the classical beam theory may not be adequate for the analysis of stiffened short composite beams, the present potential-function solutions are compared with the classical simple beam theory in order to access the discrepancy of the solutions caused by attaching the stiffeners at the lateral ends. This simple beam theory basically gives the corresponding solutions of an unstiffened simply supported beam. Since the distribution of reaction at the bottom surface cannot be addressed appropriately using the elementary theory, the beam is considered here to be simply supported taking the resultant of the reaction forces. The solutions for the lateral displacement, bending stress and shear stress are obtained for the present model of the beam as shown in Fig. 4.1 without considering stiffeners at the lateral ends, which are given below as a ready reference for the interested readers.

$$u_y(x) = \frac{\sigma_0}{2E_1}\left(\frac{L}{D}\right)^3\left[2\left(\frac{x}{L}\right)^2 - \left(\frac{x}{L}\right)^3 - 1\right]x \tag{6.1}$$

$$\frac{\sigma_{xx}(x)}{\sigma_0} = \frac{24}{5}\left(\frac{L}{D}\right)^2\left(\frac{x}{L} - \frac{1}{20}\right)\left(\frac{1}{2} - \frac{y}{D}\right) \qquad [0 \le x/L < 0.1 \text{ and } 0.9 < x/L \le 1.0] \tag{6.2}$$

$$= 6\left(\frac{L}{D}\right)^2\left[\left(\frac{x}{L}\right)^2 - \left(\frac{x}{L}\right) + \frac{1}{25}\right]\left(\frac{1}{2} - \frac{y}{D}\right) [0.1 \le x/L \le 0.9] \tag{6.3}$$

$$\frac{\sigma_{xy}(x)}{\sigma_0} = 6\left(\frac{L}{D}\right)\left[\frac{1}{4} - \left(\frac{y}{D} - \frac{1}{2}\right)^2\right]\left(\frac{1}{2} - \frac{x}{L}\right) \qquad [0.0 \le x/L \le 1.0] \tag{6.4}$$

6.2 Finite Difference Method

Finite difference solutions are obtained on the basis of present displacement potential approach. The region of interest in which the potential function ψ is to be evaluated is divided into a desirable number of mesh points and the values of the function are sought only at these points. A uniform rectangular mesh network is used to discretize the beam domain. The number of meshes used in the x and y directions are 51 and 51 respectively. An imaginary boundary, exterior to the physical boundary of the beam, is considered for the present discretization. The fourth order partial derivatives of the governing differential equation (Eqns. 2.35, 2.37 and 2.41) are expressed by their corresponding central difference formulae whereas, in an attempt to avoid the inclusion of points exterior to the imaginary boundary, the second and third-order derivatives associated with the boundary expressions are replaced by their corresponding backward or forward difference formulae, keeping the order of local truncation error the same. The discrete values of the potential function ψ (x, y) are solved from the system of linear algebraic equations by the direct method of solution (triangular decomposition method). Since all the components of stress and displacements are expressed in terms of function ψ, the parameters of interest are readily calculated from the values of ψ obtained at the mesh points of the domain. The detailed computational scheme for the discretization of the domain,

management of boundary conditions, evaluations of the parameters of interest are given in references [6, 18-19].

6.3 Finite Element Method

Finite element method is widely used all over the world for various computational purposes in lab and commercial areas. In this study, ANSYS has been used to solve several problems in order to compare and verify the analytical results. The relevant boundary conditions used are the same as those used in the analytical solution. Four nodded rectangular plane elements are used to construct the corresponding mesh network of the beam. The total number of finite elements used to construct the element mesh network for all problems is 6400 (80x80). All the elements are of the same size and their distribution is kept uniform all over the domain. The convergence and accuracy of the solution has been verified by varying the number of finite elements used to model the beam.

6.4 Comparison of Solutions for Stiffened beam of Orthotropic Composite Material

The comparison of ψ-solutions with the corresponding solutions of the elementary beam theory is presented in Figs. 6.1-6.3 for both the cases of axial and lateral stiffeners. The simple beam theory is, however, found to be, to some extent, in contrast with the other solution, which is because of the fact that it does not take into account the influence of stiffener at the lateral ends. In general, the simple beam theory under predicts the lateral deflection of the beams, which is, however, found to be influenced by the type of stiffeners at the lateral ends. For the case of axial stiffeners, the prediction by the simple theory is reasonably close to the other solution, which is however not the case for lateral stiffeners at the ends.

Fig. 6.2 shows the comparison of the two solutions of bending stress at sections x/L= 0 and 0.5 of the beam for both the cases of axial and lateral stiffeners. The bending stress distributions obtained by the elementary theory show linear variations over the beam depth for both the

stiffener. Moreover, the agreement between the solutions are identified to be independent of section concerned, that is, the status of agreement remains unchanged for sections at or away from the stiffened ends. Another interesting observation is that the axial stiffeners cause the distribution of bending stress to deviate more from that of elementary solutions than the case of lateral stiffeners, in terms of both magnitude and nonlinearity. As a result, two solutions of bending stress distribution at the mid-span section of a simply-supported beam of L/D = 3 are found to be quite close to each other, which is however not the case with axial stiffeners.

The shear stress distributions at section x/L= 0.25 of the beam (L/D = 3) obtained by two different approaches for both the cases of axial and lateral stiffeners are presented in Fig. 6.3. For both the cases of stiffeners, two solutions are found to be in good agreement, which, in turn, reveals that the stiffeners at the lateral ends of the simply-supported beam do not make the actual distributions of shear stress, especially for sections away from the stiffened ends, much different from those predicted by simple beam theory.

6.5 Verification of Solutions for Stiffened Beam with Fiber Orientation $\theta=0^0$

An orthotropic composite (glass/epoxy) beam with fiber orientation $\theta=0^0$, beam aspect ratio L/D=3 and the uniform loading parameter σ_0=40 MPa has been chosen for the comparison. This comparison is figured out by considering stiffened end (x/L=0) or near to the stiffened end (x/L=0.1) and mid section (x/L=0.5) or near to the mid section (x/L=0.25) of the beam by considering both axial and lateral stiffening conditions. Here, near to the stiffened end (x/L=0.1) and near to the mid section (x/L=0.25) is considered for those particular cases where beam properties i.e. normalized displacement and normalized stresses are zero at the stiffened end and mid section of the beam. A good agreement between the analytical and numerical results can be realized from Figs. 6.4-6.6. These figures show the comparison of normalized lateral displacement (u_y/D), normalized bending stress (σ_{xx}/σ_0) and normalized shear stress (σ_{xy}/σ_0) components at different sections of the beam for both axial and lateral stiffening conditions. One can see that even at the stiffened end (x/L=0) or near to the stiffened end (x/L=0.1) the results are almost same. Slight discrepancies of the results of FEM with those of

the present analytical and FDM solutions can be attributed to the fact that the FDM solutions are obtained using a relatively lower mesh density compared to that of FEM solution. The result of the present analytical method exactly conforms to the results of FEM. The present ψ-solution is free from the limitation and provides reliable and accurate results at any section of the orthotropic material with fiber orientation $\theta=0^0$.

6.6 Verification of Solutions for Stiffened Beam with Fiber Orientation $\theta=90^0$

The parameters chosen for the comparison of the results of the present orthotropic composite (glass/epoxy) beam are: fiber orientation $\theta=90^0$, beam aspect ratio $L/D=3$ and the maximum intensity of the bending load $\sigma_0=$ 40 MPa. The comparison of normalized displacement component u_x/L and normalized stress components σ_{xx}/σ_0, σ_{xy}/σ_0 are displayed in Figs. 6.7-6.9 respectively at two different sections of the beam for both axial and lateral stiffening conditions of the beam. It is noted that all the results obtained by ψ-solution, FDM and FEM agree well within acceptable limits. The slight discrepancy associated with FDM, which was discussed in section 6.5, has also found in current problem.

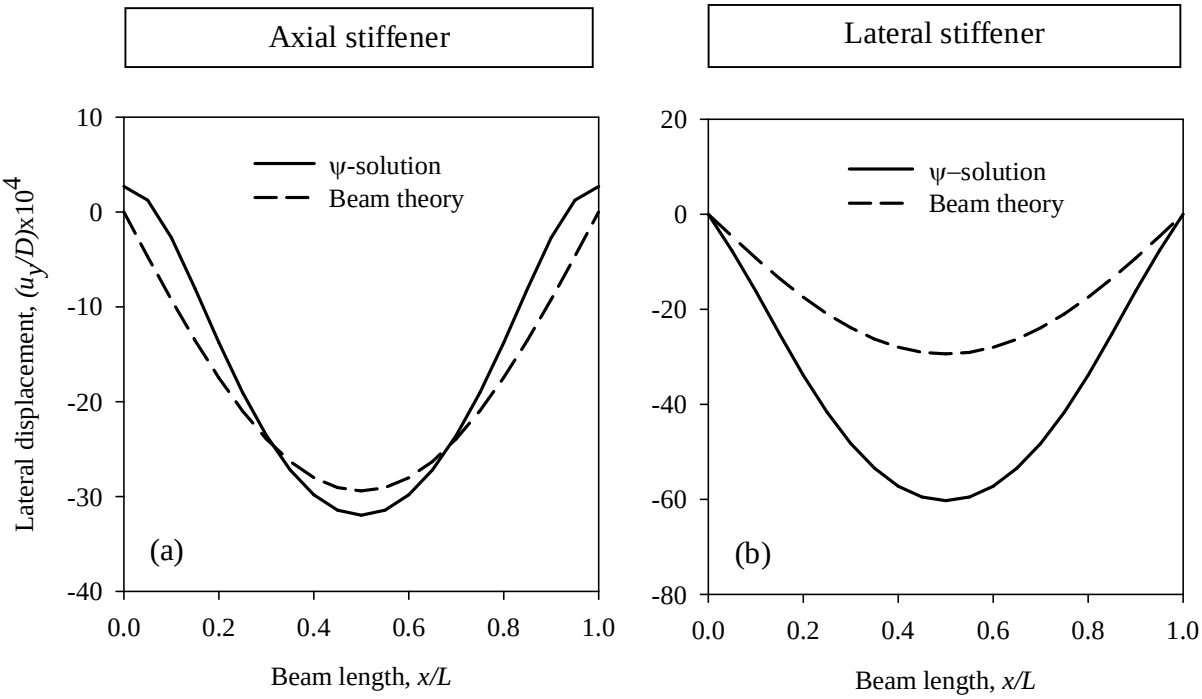

Fig. 6.1 Comparison of solutions for lateral displacements at section, $y/D = 0.5$ of the stiffened orthotropic composite beam, $L/D = 3$

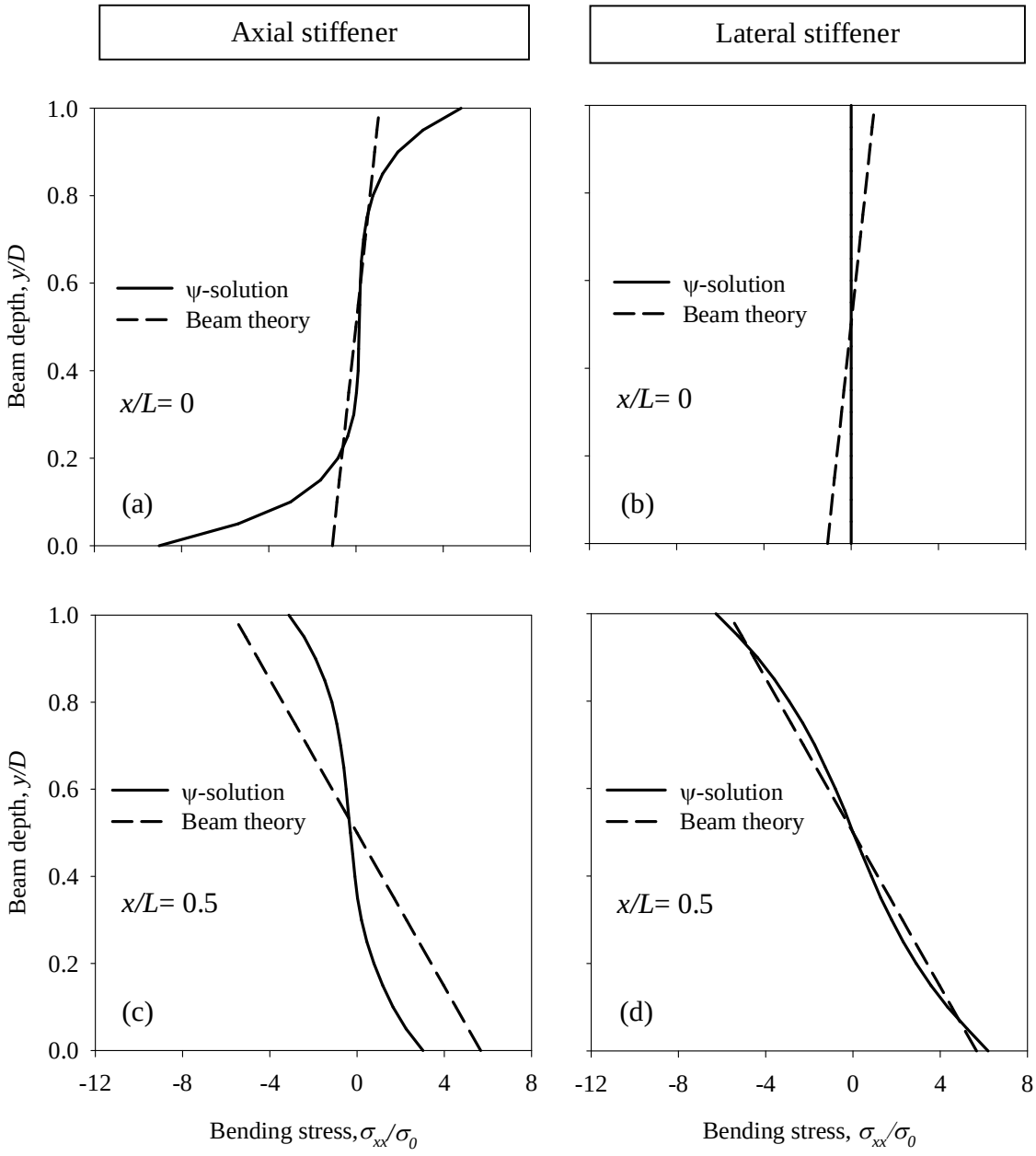

Fig. 6.2 Comparison of solutions for bending stresses at different sections of the stiffened orthotropic composite beam, L/D = 3

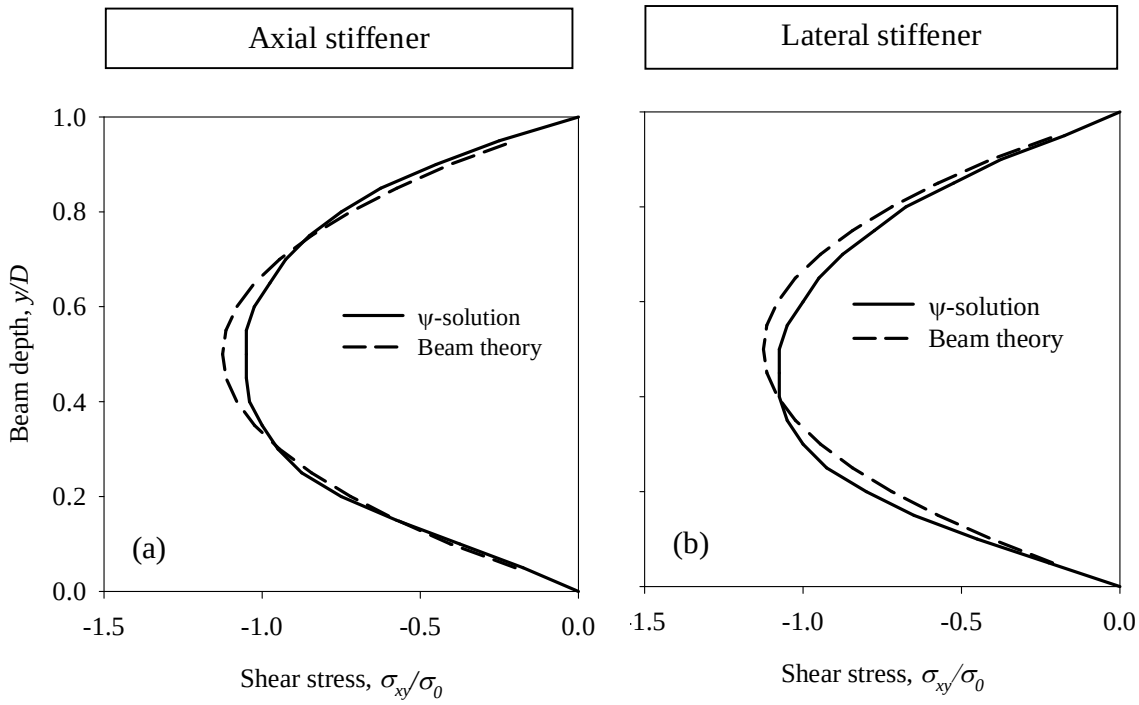

Fig. 6.3 Comparison of solutions for shear stresses at section, x/L= 0.25 of the stiffened orthotropic composite beam, L/D = 3

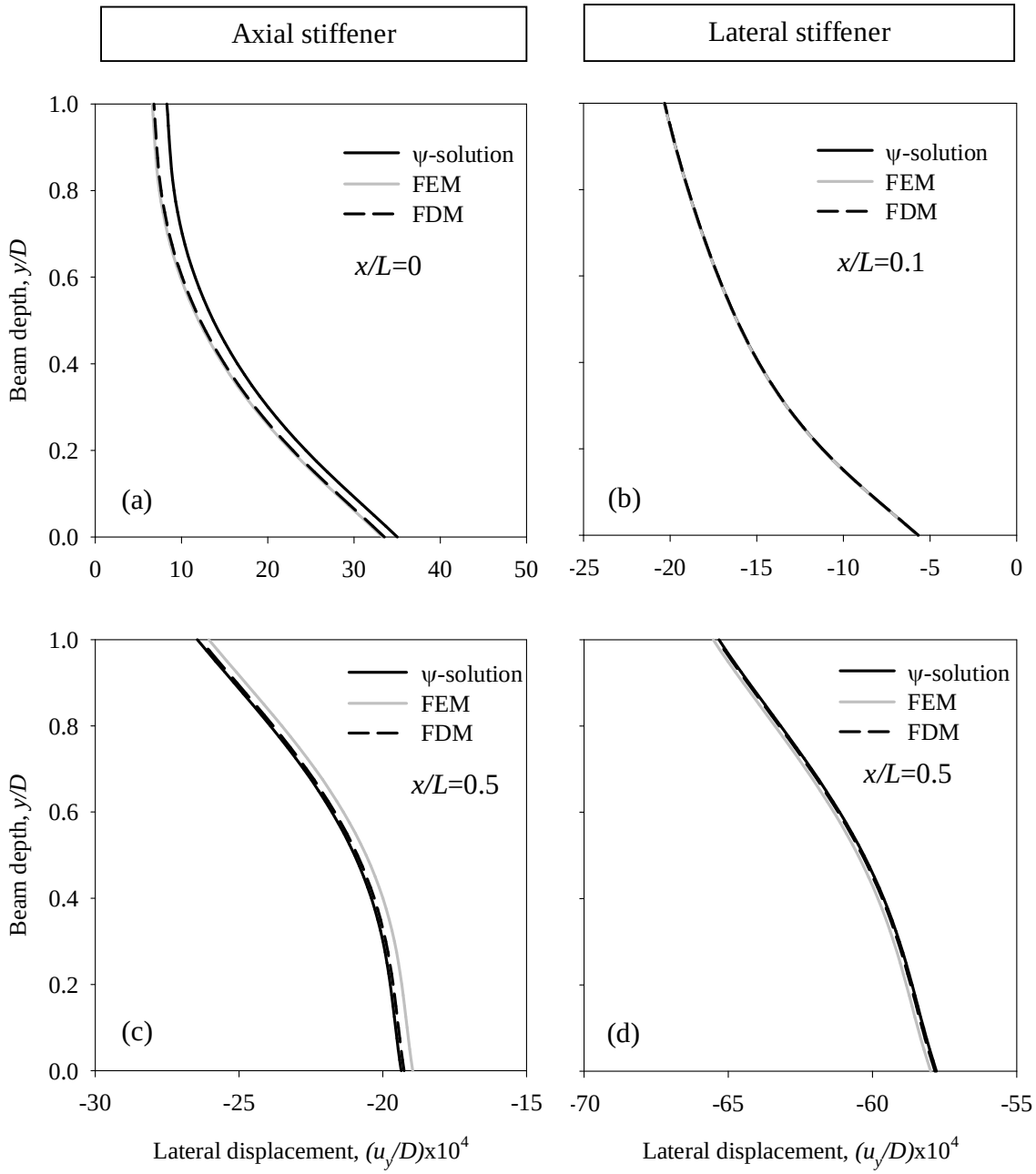

Fig. 6.4 Verification of normalized lateral displacements at different sections of the stiffened orthotropic composite beam for $\theta=0^0$ and L/D= 3

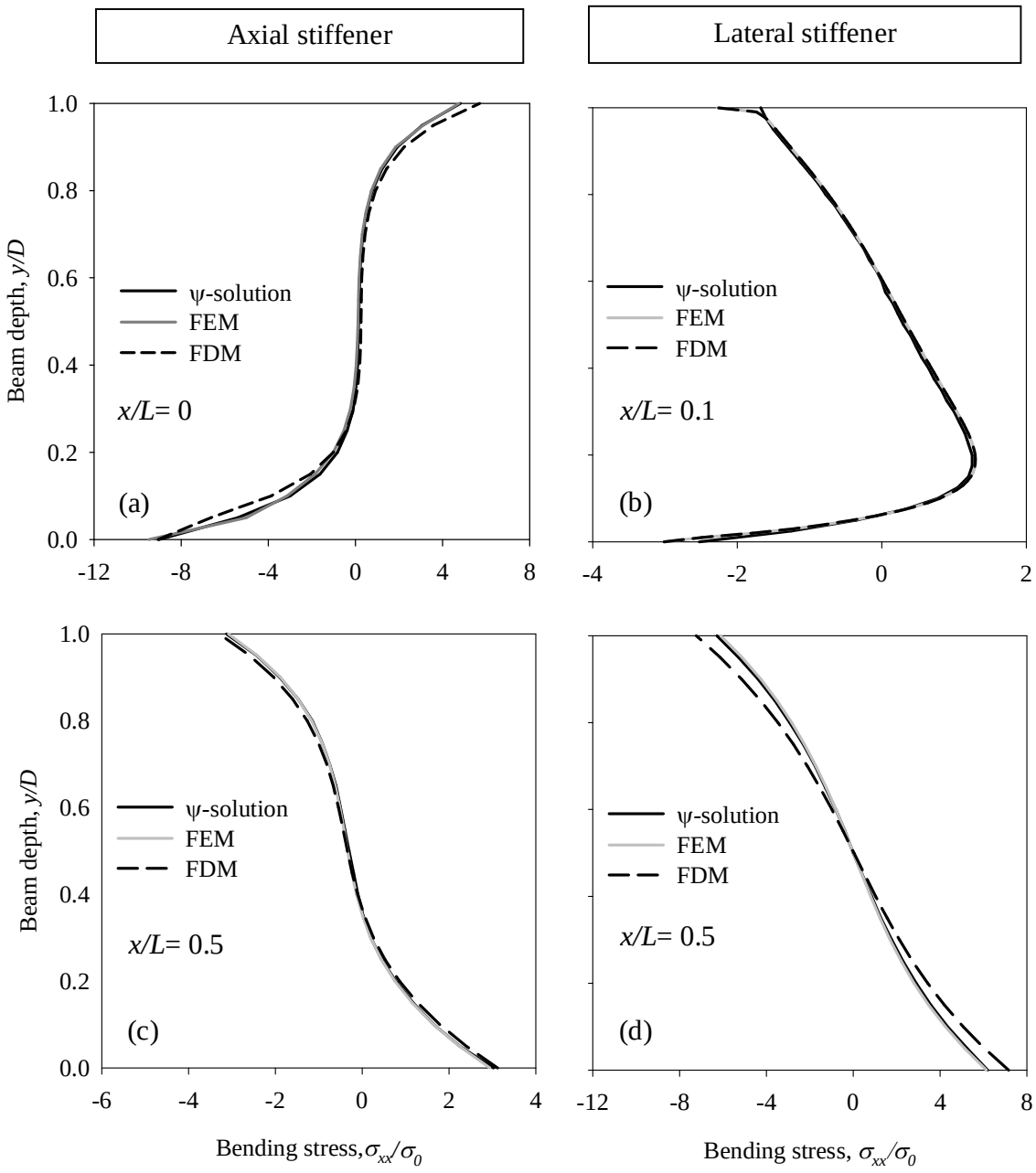

Fig. 6.5 Verification of normalized bending stresses at different sections of the stiffened orthotropic composite beam for $\theta=0^0$ and $L/D=3$

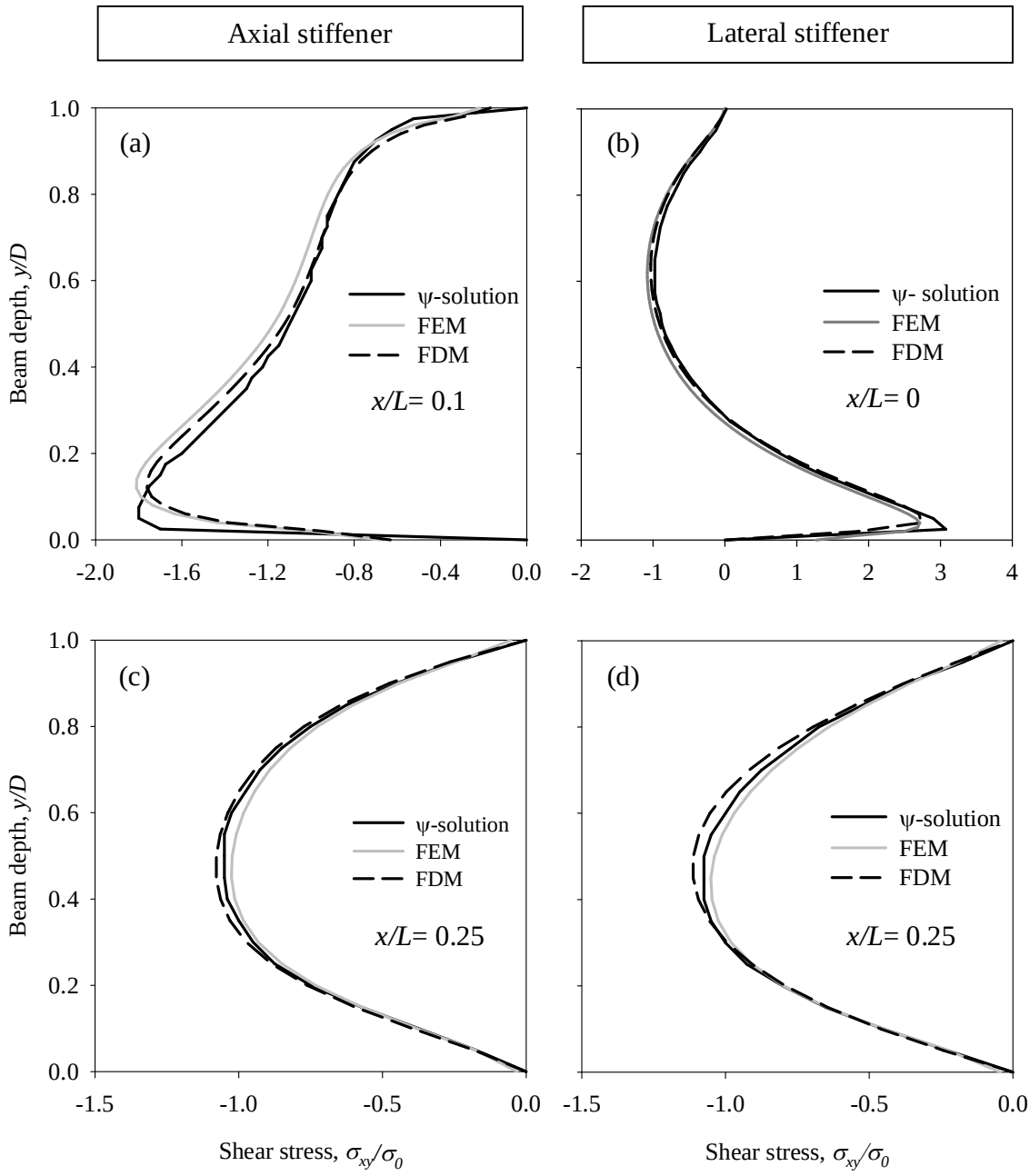

Fig. 6.6 Verification of normalized shear stresses at different sections of the stiffened orthotropic composite beam for $\theta=0^0$ and $L/D=3$

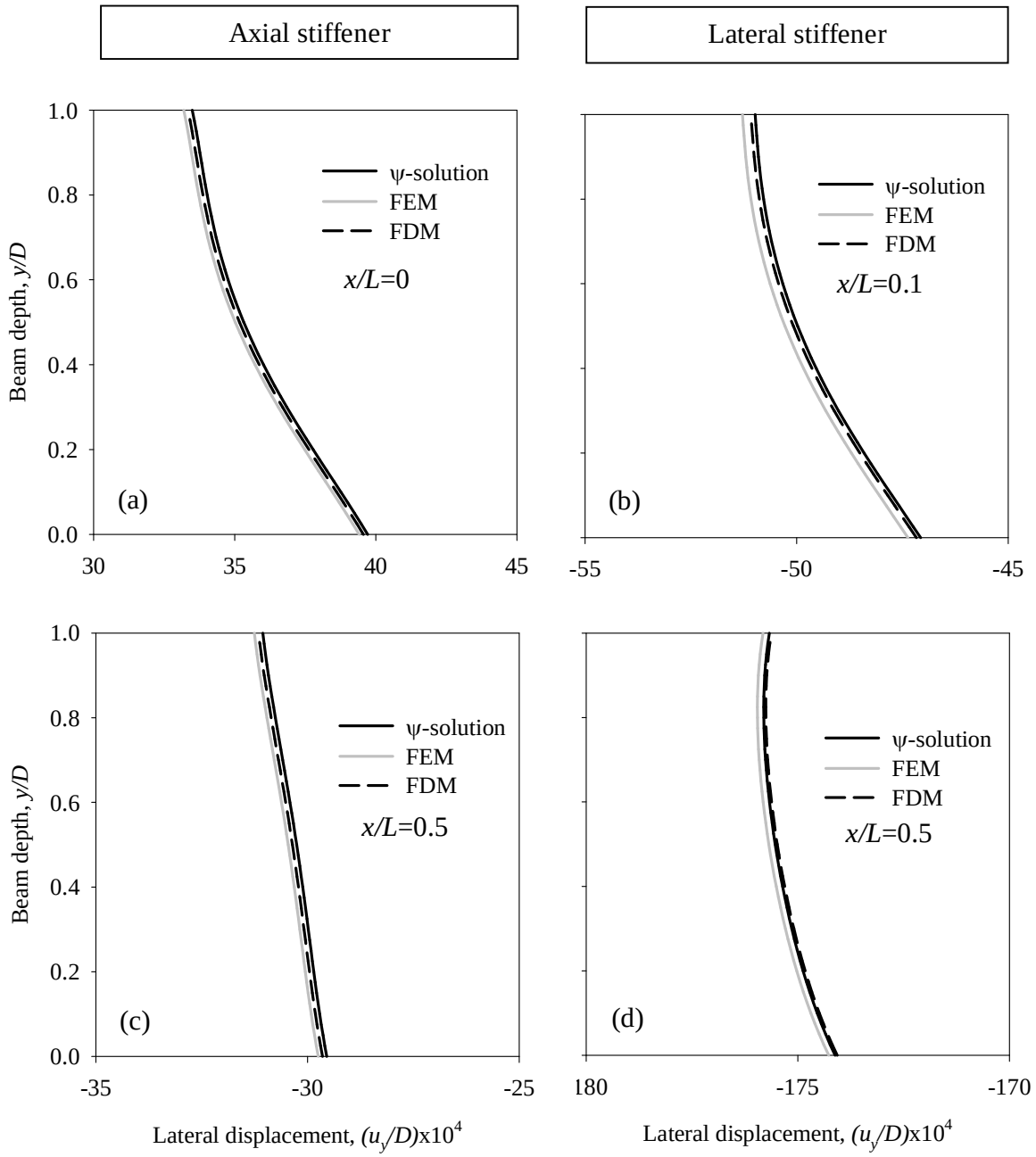

Fig. 6.7 Verification of normalized lateral displacements at different sections of the stiffened orthotropic composite beam for θ=90^0 and L/D= 3

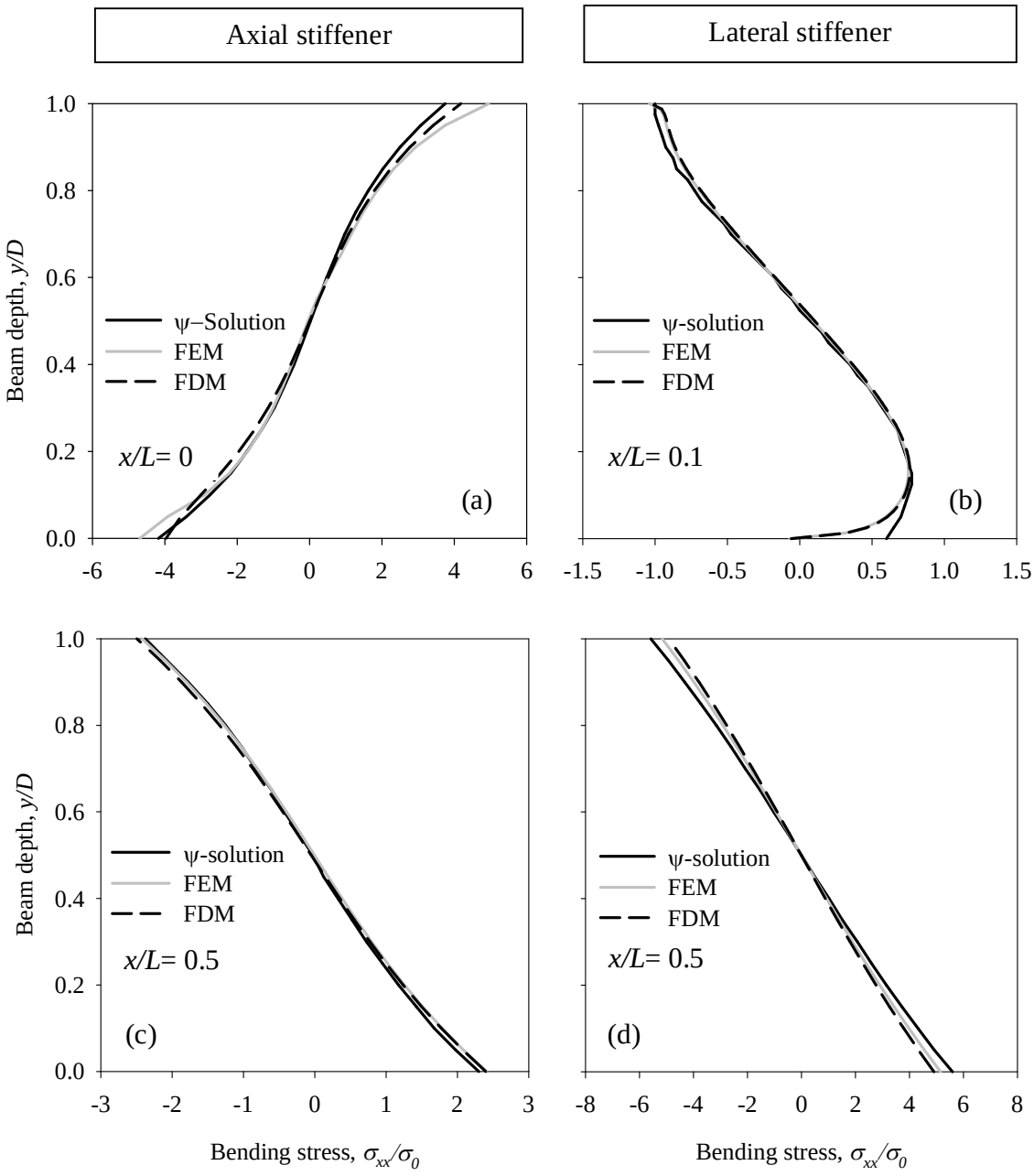

Fig. 6.8 Verification of normalized bending stresses at different sections of the stiffened orthotropic composite beam for θ=90^0 and L/D= 3

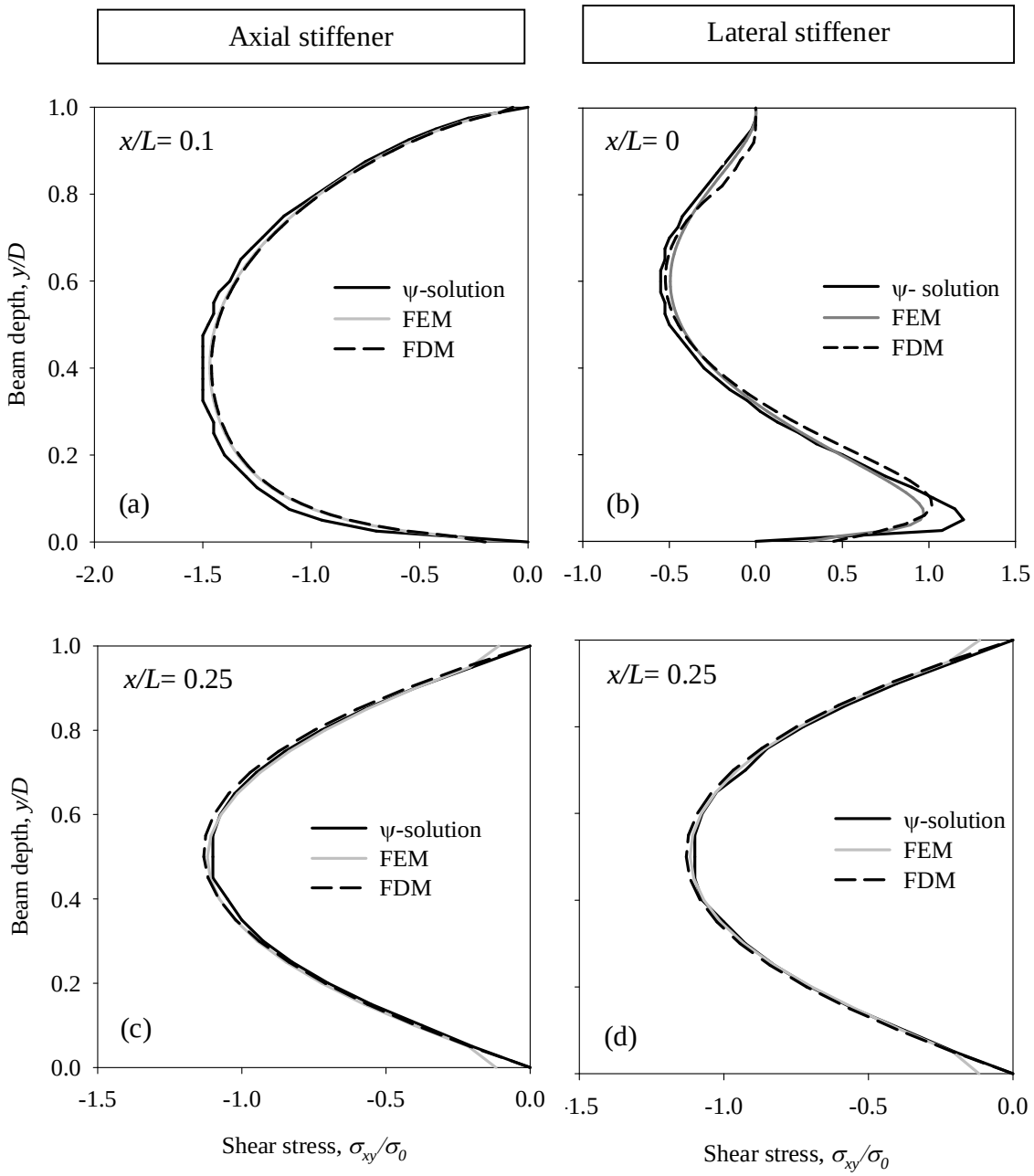

Fig. 6.9 Verification of normalized shear stresses at different sections of the stiffened orthotropic composite beam for θ=90^0 and L/D= 3

CHAPTER 7

CONCLUSIONS AND RECOMMENDATIONS

7.1 Conclusions

The analytical solution for the elastic field of a stiffened simply-supported composite beam subjected to a uniformly distributed loading has been successfully derived for both isotropic and orthotropic materials. Having appropriate analytical expressions for all the necessary boundary conditions, an efficient and accurate analytical scheme has been developed in terms of a potential function defined in terms of displacement components for the analysis of stiffened thick composite beam. The analytical scheme developed is not only limited to the problems of isotropic materials, but also equally applicable to orthotropic composite materials with all possible mixed modes of boundary conditions, whether they are prescribed in terms of displacements, strains or stresses or even any combination thereof. The superiority of the present modelling scheme over the existing approaches is that it reduces the solution of a plane problem to the determination of a single function satisfying a single differential equation of equilibrium. The capability of the method is demonstrated by solving a number of problems of stiffened composite beam of isotropic as well as orthotropic composite materials with different types of stiffeners as well as different types of fiber orientation.

The overall results of the stiffened simply supported composite beam under distributed loading reveals that the presence of stiffeners has a significant influence on the elastic behavior of the beam. This conclusion has been made evident when the results of elastic field are analyzed in a comparative fashion for axial, lateral and no stiffening conditions. The influence of beam aspect ratio also plays an important role in defining the state of displacement and stresses in the beam. The intensity of stress is found to decrease with increase of beam aspect ratio. Further from the comparison of results of fiber reinforced composite beam with three different types of stiffening conditions, it is revealed that the fiber orientation effect is critical shear stress in the

neighbourhood of to the stiffened ends, especially for lower aspect ratio. The lateral displacement however shows the dominating characteristics for the case of fibers oriented perpendicular to the direction of loading as well as also for all three stiffening conditions.

An analytical method usually provides exact solution whereas numerical methods give approximate solution. Exact analytical solution is always preferable over any numerical solution of a particular problem. But the practical fact is that the analytical methods of solutions are usually limited to only very ideal cases. That is why the analytical methods of solution could not gain popularity in the field of stress analysis of actual structures. An attempt is made to remove the limitation of the literature by developing a new analytical scheme for stress analysis of stiffened simply supported composite beam. In order to check the reliability and accuracy of the present analytical solutions, results are compared with the corresponding solution of approximate numerical methods, namely, Finite Element Method and Finite Difference Method. This is because of the fact that no other reliable solution is available in the literature that can be compared with the present solutions. From comparison of the results of different methods, it is observed that solutions are in excellent agreement with each other. More specially, the present analytical solutions are found to be almost identical to those of the FEM with few exceptions only at the stiffened ends. Finite difference solutions also compare well with the present solutions, but slight discrepancies are observed for some sections, especially at the stiffened end, which is probably because of low mesh density used to model the beam by Finite difference method.

7.2 Recommendations

This is completely a new analytical method to find out the stress and displacement filed of a stiffened simply-supported composite beam.

- The method has been investigated and instituted as capable to deal isotropic and orthotropic stiffened beams effectively for uniformly distributed load. The present approach needs to be expanded for the analytical solution of anisotropic materials.

- It also require to be investigated for a variety of loading configurations like three point bending, four point bending etc. in order to have its wide range of adoptability and versatility.

- The method can effectively and efficiently deal with the structures of unidirectional composite lamina. Further, even for a unidirectional lamina, the loading should be either in the direction of fibers or perpendicular to the fiber. Therefore, the method, at its present states, cannot be directly applied to laminated (multilayered) composites with fibers oriented in different directions. However, with minor modification in the formulations, the method can be made suitable for laminated composites without any limitation of the fiber direction.

REFERENCES

1. Timoshenko, S.P. and Goodier, J. N., Theory of Elasticity, -3rd Ed., McGraw Hill Book Co., New York, 1970.

2. Borg, S. F., Fundamentals of Engineering Elasticity, World Scientific, Singapore, 2nd ed., 1990.

3. Conway, H. D., Chow, L., and Morgan, G.W., "Analysis of deep beams," Journal of Applied Mechanics, Trans ASME 18(2), 163–172, 1951.

4. Chow, L., Conway, H. D., and Winter, G., "Stresses in Deep Beams", Trans ASCE, Paper No. 2557, 1952.

5. Conway, H. D., and Ithaca, N. Y., "Some problems of orthotropic plane stress," Journal of Applied Mechanics, Trans ASME, 52, 72–76, 1953.

6. Chapel, R. E., and Smith, H. W., "Finite-Difference solutions for plane stresses," AIAA Journal 6, 1156–1157, 1968.

7. Parker, D. F., "The role of Saint-Venant's Solutions in rod and beam theories," Journal of Applied Mechanics, Trans ASME 46, 861–866, 1979.

8. Horgan, C. O., and Knowels, J. K., "Recent developments concerning Saint-Venant's Principle," Advances in Applied Mechanics, 23, 179–269, 1983.

9. Horgan, C. O., and Simmonds, J. G., " Saint-Venant End Effects in Composite Structures," Composite Engineering, Vol 4, No 3, 279–286, 1994.

10. Uddin, M. W., “Finite Difference Solution of Two-dimensional Elastic Problems with mixed Boundary Conditions”, M. Sc. Thesis, Carleton University, Canada, 1966.
11. Durelli, A. J., and Ranganayakamma, B., “Parametric solution of stresses in beams,” Journal of Engineering Mechanics 115(2), 401–414, 1989.

12. Rehfield, L. W. and Murthy, L. N., “Toward a new engineering theory of bending: Fundamentals”, AIAA Journal, vol. 20. pp. 693-699, 1982.

13. Murty A. V. K., “Towards a consistent beam theory”, AIAA Journal, vol. 22. pp. 811-816, 1984.

14. Suzuki S., Stress analysis of short beams, AIAA Journal, vol.24. pp. 1396-1398, 1986.

15. Hardy S. J. and Pipelzadeh M. K., “Static analysis of short beams, Journal of strain analysis”, vol. 26, No. 1, pp.15-29, 1991.

16. Ahmed, S. R., Idris, A. B. M., and Uddin, M. W., “Numerical solution of both ends fixed deep beams,” Computers & Structures 61(1), 21–29, 1996.

17. Ahmed, S. R., Khan, M. R., Islam, K. M. S., and Uddin, M. W., “Investigation of stresses at the fixed end of deep cantilever beams,” Computers &Structures 69, 329–338, 1998.

18. Ahmed, S. R., Hossain, M. Z. and Uddin, M.W., “A general mathematical formulation for finite-difference solution of mixed-boundary-value problems of anisotropic materials,” Computers & Structures, 83, 35–51, 2005.

19. Akanda, M. A. S., Ahmed, S. R. and Uddin, M. W., “Stress analysis of gear teeth using displacement potential function and finite differences,” International Journal for Numerical Methods in Engineering, 53, 1629–1640, 2002.

20. Ahmed, S. R., Nath, S. K. D., and Uddin, M.W., “Optimum shapes of tire treads for avoiding lateral slippage between tires and roads,” International Journal for Numerical Methods in Engineering, 64, 729–750, 2005.

21. Nath, S. K. D., Afsar, A. M., and Ahmed, S. R., “Displacement potential solution of a deep stiffened cantilever beam of orthotropic composite material,” Journal of Strain Analysis, IMechE 2007; 42: 529-541

22. Nath, S. K. D. and Ahmed, S. R., “Displacement Potential Solution of Stiffened Composite Struts Subjected to Eccentric Loading,” Journal of Applied Mathematical Modelling 2009; 33(3): 1761-1775.

23. Rahman, H. “Stress analysis of cracked stiffened panels under flexural and axial loading,” M. Sc. Thesis, Bangladesh University of Engineering & Technology, 2013

24. Biswal, K. C., Ghosh, A. K., “Finite element analysis for stiffened laminated plates using higher order shear deformation theory,” Computers & Structures 1994;53 (1):161–71

25. Sadek, E, A., Tawfik, S. A., “A finite element model for the analysis of stiffened laminated plates,”. Computers & Structures 2000; 75(4):369–83.

26. Ranzi, G., Gara, F., Leoni, G., Bradford, M. A., “Analysis of composite beams with partial shear interaction using available modelling techniques: a comparative study,” Computers & Structures 2006; 84:930–41.

27. Nath, S. K. D., Ahmed, S.R., “A displacement-potential based numerical solution of orthotropic composite panels under end moment and shear loading,” Journal of Mechanics of Materials & Structures 2009; 4(6):987–1004.

28. Bernasconi, A., Davoli, P., Basile, A., Filippi, A., “Effect of fibre orientation on the fatigue behaviour of a short glass fibre reinforced polyamide-6”, International Journal of Fatigue, Volume 29, Issue 2, February 2007, Pages 199-208.

29. Kaman, M. O., “Effect of fiber orientation on fracture toughness of laminated composite plates $[0°/\theta°]_s$,” Engineering Fracture Mechanics, Volume 78, Issue 13, August 2011, Pages 2521-2534.

30. Majid, D.L., Abdullah, E.J., Harun, N.F., Lim, G.Y., Baharudin, B.T.H.T., “Effect of Fiber orientation on the structural response of a smart composite structure,” Procedia Engineering, Volume 50, 2012, Pages 445-452.

31. Vincent, T., Ozbakkaloglu, T., “Influence of fiber orientation and specimen end condition on axial compressive behavior of FRP-confined concrete,” Construction and Building Materials, Volume 47, October 2013, Pages 814-826.

32. Nath, S. K. D. and Wong, C. H., “Finite difference solution of a both end fixed orthotropic composite beam under uniformly distributed loading using displacement potential function formulation,” Journal of Engineering Mechanics, ASCE 2011; 137 (4): 258-267

33. Jones, R. M. Mechanics of composite materials, 1975 (McGraw-Hill, New York)

34. Kaw, A.K., Mechanics of Composite Materials, Taylor & Francis Inc., New York, 2006